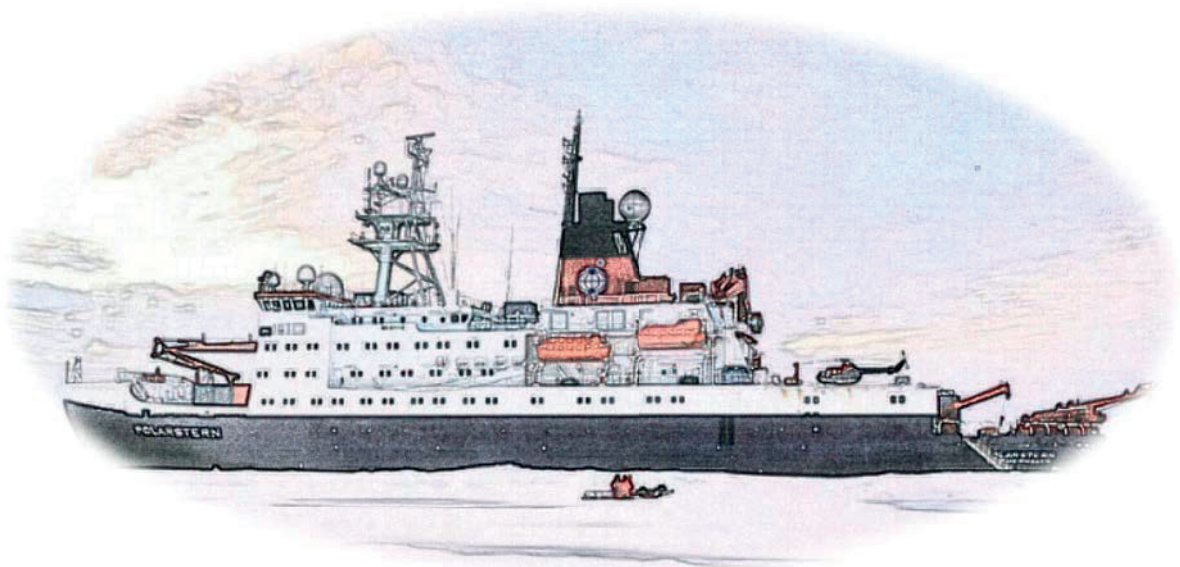


Paleobathymetric Reconstruction, Modeled Ocean Circulation, and Sedimentation History in the Weddell Sea, Antarctica



DISSERTATION

Zur Erlangung des Grades Dr. rer. nat.
Vorgelegt dem Fachbereich Geowissenschaften
der Universität Bremen
von

XIAOXIA HUANG

July 30, 2015



ALFRED-WEGENER-INSTITUT
HELMHOLTZ-ZENTRUM FÜR POLAR-
UND MEERESFORSCHUNG



Universität Bremen

Gutachter:

Dr. Wilfried Jokat, Professor für Geophysik der Polargebiete

Universität Bremen und Alfred-Wegener-Institut

Dr. Cornelia Spiegel, Professorin für Geodynamik der Polargebiete

Universität Bremen

Promotionskolloquium: 17 November 2015

EIDESSTATTLICHE ERKLÄRUNG

Xiaoxia Huang
Wuwei, Gansu
733307 China

Hiermit versichere ich, dass ich

1. die Arbeit ohne unerlaubte fremde Hilfe angefertigt habe,
2. keine anderen als die von mir angegebenen Quellen und Hilfsmittel benutzt habe und
3. die den benutzten Werken wörtlich oder inhaltlich entnommenen Stellen als solche kenntlich gemacht habe.

Bremerhaven, den 29. Jul. 2015

Xiaoxia Huang

Cover picture modified from Mario Hoppmann

Zusammenfassung

Das Weddellmeerbecken ist von besonderer Bedeutung für das Verständnis von Klimaprozessen, einschließlich der Erzeugung von Wassermassen im Ozean und deren Einflüsse auf die Ozeanzirkulation, sowie der Dynamik des antarktischen Eisschildes. Die Sedimentschichten im Becken dienen als Archiv der glazialen Entwicklung, der Meeresströmungen und der tektonischen Prozesse.

Diese Arbeit ist auf das Verständnis der Sedimentationsgeschichte, der Vorhersage der Paläo-Wassertiefen mit allen verfügbaren mehrkanalseismischen Linien und Bohrungen, sowie der Anwendung dieser Paläo-Wassertiefen für allgemeine Zirkulationsmodelle (GCM) des Weddellmeerbeckens ausgerichtet. Die erstellten Sedimentmächtigkeitsdaten (präglazial, Übergang, glazial) und paläobathymetrischen Daten dieser Arbeit leisten einen wesentlichen Beitrag für numerische Klima- und Ozeanzirkulationsmodellierungen.

Die sedimentären Mächtigkeitsdaten bieten die Voraussetzung, die Sedimentationsregime der präglazialen und glazial dominierten Entwicklungsstadien des Weddellmeeres zu vergleichen. Die präglazialen Ablagerung mit Mächtigkeiten bis zu 5 km wurden durch die tektonische Entwicklung und Meeresbodenspreizungsgeschichte des Weddellmeeres kontrolliert und zeigen primär den Einfluss terrigener Sedimentzufuhr. Die sedimentäre Übergangseinheit weist eine relativ hohe Sedimentationsrate und eine Mächtigkeit von bis zu 3 km auf, welche sich möglicherweise auf eine frühe Bildung des ostantarktischen Eisschildes, der teilweise bis zur Küste und teilweise bis zum inneren Schelf vordrang, zurückführen lässt. Das Hauptablagerungsgebiet der glazialen sedimentären Einheit liegt vor dem Filchner-Ronne-Eisschelf und zeigt Sedimentationsraten bis zu 140-200 m/Jahr auf. Daraus lässt sich folgern, dass der Eisschild im mittleren Miozän bis auf dem mittleren oder äußeren Schelf auf Grund aufsaß. Bodenwasserströmungen wirkten stark auf die Sedimentation der Tiefsee ein.

Die paläobathymetrischen Datensätze bei 15, 34 und 120 Millionen Jahren vor heute wurden durch eine strukturelle Restaurationstechnik (backstripping) rekonstruiert und auf paläoklimatische Modellparameter angewandt. Gekoppelte GCM-Modellierungen wurden mit den Randbedingungen eines globalen warmen Klimas im mittleren Miozän mit den neuen paläobathymetrischen Gittern des Weddellmeeres berechnet. Die Ergebnisse der GCM-Modellierung legen nahe, dass die Bildung des Tiefenwassers und die Ozeanzirkulation besonders empfindlich auf die Paläobathymetrie des Weddellmeeres reagieren. Die Rekonstruktionen zeigen, dass das Weddellmeer im mittleren Miozän durch eine Schelfkante charakterisiert wurde, welche wesentlich südlicher als heute oder in früheren paläobathymetrischen Modellen lag. Die südwärtige Verschiebung der Schelfkante im Weddellmeer führt zu dramatischen Veränderungen in der Tiefenlage der modellierten Mischwasserschicht und der Bildung des Bodenwassers. Die Intensivierung der Bodenwasserbildung spielt eine wichtige Rolle in der Sedimentverteilung und Erzeugung der Geomorphologie am Randes des Weddellmeeres, was sich durch die Entwicklung einer Reihe von mächtigen Sedimentdriftkörpern ausdrückt.

In Ergänzung zu den paläobathymetrischen Untersuchungen des Weddellmeeres sind zwei weitere Studien zur Interpretation seismischer Daten im südöstlichen Weddellmeer und entlang des Kontinentalrandes von Dronning Maud Land durchgeführt worden. Große Ablagerungszentren, der sogenannte Crary Trough

Mouth Fan und markante Sedimentrücken wurden als glaziale Ablagerungen im südöstlichen Weddellmeer interpretiert. Zwei großräumige, sinusförmige, nordost-südweststreichende Rücken können als turbiditische Konturite aufgrund von komplizierten Transportprozessen, welche parallel und senkrecht zum Kontinentalhang auftreten, interpretiert werden. Ein großes sedimentäres Einzugsgebiet mit einer ergiebigen Sedimentzufuhr, Veränderungen des Meeresspiegels und die Dynamik des Eisschildes liefern den größten Beitrag zur Sedimentation. Die bemerkenswerte Zunahme von Massentransportablagerungen im späten Miozän und mittlerem bis spätem Pliozän steht im Zusammenhang mit der starken Zunahme des Porendrucks während rascher Sedimentakkumulation und Veränderungen des Meeresspiegels. Möglicherweise sind diese Ablagerungen auch durch glazial-isostatisch bedingte Paläo-Erdbeben ausgelöst worden.

Auf Grundlage von reflexionsseismischen Daten und Bohrungsdaten, welche am Kontinentalrand des Dronning Maud Landes aquiriert worden sind, werden Sedimentationsprozesse von Ihrer Quelle bis zur Ablagerung untersucht. Meine Untersuchungen zeigen, dass das Jutul-Penck Grabensystem im Dronning Maud Land eine bedeutende Rolle in Hinblick auf Erosion, Transport und Ablagerung von Sedimenten spielt. Des Weiteren habe ich in dieser Region zum ersten Mal seismische Kamine Strukturen gefunden, deren Entstehung ich auf vulkanische Prozesse zurückführe.

Summary

The Weddell Sea basin is of particular significance for understanding climate processes, including the generation of ocean water masses and their influences on ocean circulation as well as the Antarctic ice sheets dynamics. The sedimentary record, preserved in the basin serves as an archive of the pre-glacial to glacial development, ocean circulation and tectonic evolution.

This thesis focuses on understanding the sedimentation history and reconstructing paleo-water depths, using all available multichannel seismic lines and existing drilling sites, with the aim to apply the paleo-water depths to General Circulation Models (GCM) of the Weddell Sea basin. A series of sedimentary thicknesses grids (pre-glacial, transitional, full-glacial) and paleobathymetric grids produced in this work are essential contributions for numerical climate simulations and ocean circulations.

These sedimentary thickness grids allow the comparison of sedimentary regimes of the pre-glacially dominated and glacially dominated stages of Weddell Sea history. The pre-glacial deposition with thicknesses of up to 5 km was controlled by the tectonic evolution and sea-floor spreading history interacting with terrigenous sediment supply. The transitional unit shows a relatively high sedimentation rate and has thicknesses of up to 3 km, which may be attributed to an early formation of the East Antarctic Ice Sheet having partly advanced to the coast or even inner shelf. The main deposition centre of the full-glacial unit lies in front of the Filchner-Ronne Ice Shelf and has sedimentation rates of up to 140-200 m/Myr, which infers that ice sheets grounded on the middle to outer shelf and that bottom-water currents strongly impacted the deep-sea sedimentation in the middle Miocene.

The paleobathymetric grids at 15, 34 and 120 Ma are reconstructed by using a backstripping technique and applied to constrain paleoclimate models. Coupled GCM runs are forced by global warm climatic boundary conditions of the Mid-Miocene and the new Weddell Sea paleobathymetry data. The GCM model results suggest that deep water formation and ocean circulation are especially sensitive to the paleobathymetric configuration of the Weddell Sea which is mainly characterized by a more southerly shelf break than at present or in previous paleobathymetric reconstructions for the Miocene. The southwards shifted shelf break of the Weddell Sea results in dramatic changes in simulated mixed layer depth and bottom water formation. Intensification of this bottom water plays a significant role in sediment distribution and the geomorphology of the Weddell Sea margin, e.g. through the build-up of a number of large sediment drifts.

In addition to the paleobathymetric study of the Weddell Sea, I carried out two seismic interpretation studies in the southeast Weddell Sea and along the Dronning Maud Land margin. Large deposition centers, the Crary Trough Mouth Fan and prominent sediment ridges, are interpreted as glacial deposits of the southeastern Weddell Sea. Two giant, sinuous, NE-SW-oriented sediment ridges are interpreted as turbidity-contourites, due to the complicated down-slope/along-slope processes occurring across their margins. The large catchment area, abundant sediment supply, fluctuating sea level and ice sheet dynamics are the major contributions for the sedimentation. The remarkable increase in mass-transport deposits during the Late Miocene and Middle to Late Pliocene is related to the build-up of pore overpressure during rapid sediment accumulation as well as changing sea level and may be triggered by glacio-isostatic paleoearthquakes.

Based on seismic reflection data and well data acquired on the continental margin offshore Dronning Maud Land, the sedimentation processes are investigated. My investigations reveal that the Jutul-Penck Graben system on the Dronning Maud Land plays a significant role in erosion, transport, and deposition of sedimentary material. I further found seismic chimney structures in this region for the first time and attribute their formation to volcanic processes

Table of Contents

1	Introduction.....	1
1.1	Weddell Sea	1
1.1.1	The evolution of the Weddell Sea basin	1
1.1.2	Ocean circulation	2
1.1.3	Antarctic glacial history	4
1.2	Motivation and scientific questions	7
2	Dataset and methods	9
2.1	Multichannel seismic reflection data	9
2.1.1	Data acquisition and equipment.....	9
2.1.2	data processing.....	12
2.2	Stratigraphic model, age correlation, time to depth conversion	12
2.3	Backstripping	13
2.4	GCM setup.....	13
3	Contributions to scientific journals.....	14
3.1	Variability in Cenozoic sedimentation and paleo-water depths of the Weddell Sea basin related to pre-glacial and glacial conditions of Antarctica	14
3.2	Middle Miocene to Present Sediment Transport and Deposits in the Southeast Weddell Sea, Antarctica.....	15
3.3	Intensification of Weddell Sea circulation in the Middle Miocene	15
3.4	Sedimentation and potential venting on the rifted continental margin of Dronning Maud Land.....	16
4	Variability in Cenozoic sedimentation and paleo-water depths of the Weddell Sea basin related to pre-glacial and glacial conditions of Antarctica.....	17
4.1	Abstract.....	17
4.2	Introduction.....	17
4.3	Regional setting and Antarctic glacial history	18
4.4	Dataset and Methods.....	20
4.4.1	Seismic dataset.....	20
4.4.2	Age information and age model.....	20
4.4.3	Time to depth conversion, sediment thicknesses	21
4.4.4	Backstripping	22
4.5	Results.....	23
4.5.1	Seismic characteristics and stratigraphy	23
4.5.2	Sediment thicknesses and rates	26
4.5.3	Backstripping and paleobathymetry	31
4.6	Discussion	33
4.6.1	Pre-glacial regime	33
4.6.2	Transitional phase	34
4.6.3	Full-glacial phase	36
4.6.4	Paleobathymetry	37
4.7	Conclusions.....	38
4.8	Acknowledgements.....	39
4.9	References.....	39
5	Intensification of Weddell Sea circulation in the Middle Miocene	46
5.1	Abstract.....	46
5.2	Introduction.....	46

5.3 Data and methods.....	48
5.4 Results.....	48
5.4.1 Contourite drifts	48
5.4.2 modeled SSTs, mixed layer depth, and ocean current velocities.....	50
5.5 Discussion.....	54
5.6 Conclusions.....	55
5.7 Acknowledgements.....	55
5.8 References.....	55
5.7 Supplementary information	57
6 Middle Miocene to Present Sediment Transport and Deposits in the Southeast Weddell Sea, Antarctica.....	62
6.1 Abstract.....	62
6.2 Introduction.....	62
6.3 Background and regional hydrographic settings.....	64
6.4 Data and methods.....	65
6.5 Results.....	66
6.5.1 stratigraphic ages	66
6.5.2 Levee and contourite deposits.....	66
6.5.3 Mass Transport Deposits.....	73
6.5.4 Shelf edge deposits	77
6.6 Discussion.....	78
6.6.1 Stratigraphic correlations	78
6.6.2 Depositional environment of turbidity-contourite	78
6.6.3 MTDs and associated trigger mechanisms	81
6.6.4 Possible implications for Antarctic ice sheets	83
6.7 Conclusions.....	83
6.8 Acknowledgements.....	84
6.9 References.....	84
7 Sedimentation and potential venting on the rifted continental margin of Dronning Maud Land.....	90
7.1 Abstract.....	90
7.2 Introduction.....	90
7.3 Geological setting	91
7.4 Data and interpretation constraints	93
7.5 Results and interpretation	94
7.5.1 Seismic structures	94
7.5.2 Total sediment thickness variations and basement topography.....	99
7.6 Discussion.....	101
7.6.1 Basin sedimentation processes.....	101
7.6.2 Indication for potential venting?.....	102
7.7 Conclusions.....	105
7.8 Acknowledgements.....	105
7.9 References.....	105
8 Conclusions and Outlooks	110
8.1 Conclusions.....	110
8.2 Outlooks.....	112
8.2.1 Paleobathymetry prospective	112
8.2.2 stratigraphic age model prospective.....	113
Bibliography	114

Acknowledgements.....	119
Curriculum Vitae	120

List of figures

Fig. 1.1 Overview map of the Weddell Sea	1
Fig. 1.2 Tectonic reconstructions	3
Fig. 1.3 Schematic of water masses and sediment drifts	7
Fig. 2.1 Existing seismic lines and ODP sites	10
Fig. 2.2 A sketch of seismic data acquisition.....	12
Fig. 4.1 General overview of the Weddell Sea basin with the network of seismic profiles and drilling sites.....	19
Fig. 4.2 ODP Sites 693, 697, and 694, and SHALDRIL drill core NBP0602A-3C....	22
Fig. 4.3 Porosity–depth information	24
Fig. 4.4 The compilation of the available age information.....	25
Fig. 4.5 Multichannel seismic reflection image of transect A	27
Fig. 4.6 Multichannel seismic reflection image of transect B	28
Fig. 4.7 Multichannel seismic reflection data of transect C.	29
Fig. 4.8 Gridded sediment thicknesses.	30
Fig. 4.9 Sedimentation rate grids	32
Fig. 4.10 Paleobathymetry at 15, 34, and 120Ma	33
Fig. 4.11 The role of plate-tectonic motion, ice sheet development, ocean circulation and sediment deposition center	35
Fig. 5.1 Paleobathymetry of the Weddell Sea.....	47
Fig. 5.2 Sediment drifts.....	49
Fig. 5.3 Sea Surface Temperature (SST in °C).....	51
Fig. 5.4 The simulated mixed layer depth (km)	52
Fig. 5.5 The simulated ocean velocities	53
Fig. 5.S1 preindustrial simulations.....	58
Fig. 5.S2 Horizontal barotropic streamfunction.	59
Fig. 5.S3 Wind stress	60
Fig. 6.1 Southeast Weddell Sea and multi-channel seismic lines.....	64
Fig. 6.2 The interpreted glacial key horizons of multi-channel seismic line	69
Fig. 6.4 Interpreted seismic profile AWI-92020.....	70
Fig. 6.5 The seismic profile BGR-86013	71
Fig. 6.6 Examples of the levee deposits	72
Fig. 6.7 A example of the channel-levee complex.....	73
Fig. 6.8 A example of mounded drift.....	74
Fig. 6.9 MTDs	75
Fig. 6.10. Examples of the MTDs.....	77
Fig. 6.12 global sea level curves, Antarctic ice volume, and sedimentation rates.....	80
Fig. 6.13. Simplified depositional models	81
Fig. 7.1 Dronning Maud Land margin and multichannel seismic lines	92
Fig. 7.2 ODP 690, 693 and the recovered dominant lithologies.....	93
Fig. 7.3 Examples of pipe-like features	94
Fig. 7.4 Interpreted large-scale debris flow deposits and slumps	96
Fig. 7.5 Multichannel seismic line BGR-96100	97
Fig. 7.6 A filled valley separating Maud Rise from Antarctica.....	98
Fig. 7.7 The interpreted multichannel seismic line BGR-78014	99
Fig. 7.8. Two types of canyons	100
Fig. 7.9 A: The basement depth and total sediment thickness.....	101
Fig. 7.10 Regional topographic changes along the DML margin, ice streams, canyons, debris flow deposits and depocenters	104

List of Tables

Table 2.1 Summary of seismic surveys	11
Table 4.1 Summary of the seismic stratigraphy	25
Table 4.2 Parameters used for the subsidence calculation	38
Table 5.1 Antarctic Bottom Water (AABW) index	61

Abbreviation:

SHALDRIL: Shallow Scientific Drilling
IODP: Integrated Ocean Drilling Program
ODP: Ocean Drilling Program
ACC: Antarctic Circumpolar Current
EAIS: East Antarctic Ice Sheet
WAIS: West Antarctic Ice Sheet
APIS: Antarctica Peninsula Ice Sheet
SDLS: Antarctic Seismic Data Library System
DML: Dronning Maud Land
AABW: Antarctic Bottom Water
WSBW: Weddell Sea Bottom Water
COT: Continent oceanic boundary
GCM: Global Circulation Models
SSTs: sea-surface temperatures
COSMOS: Community Earth System Models
MIOW: Mid-Miocene simulation with new Weddell Sea paleobathymetry
MIO: Mid-Miocene simulation with existing paleobathymetry
MMCO: Middle Miocene Climatic Optimum
CTMF: Crary Trough Mouth Fan
MTDs: Mass Transport Deposits
IRD: ice-rafted debris
SDRs: seaward dipping reflectors
MCS: multi-channel seismic

1 Introduction

1.1 Weddell Sea

The Weddell Sea region in the Atlantic sector of Antarctica (Fig. 1) plays an essential role in the global thermohaline circulation by mixing the abyssal world ocean in the Southern Hemisphere (Rahmstorf, 2002). The Weddell Sea basin (Fig. 1) experienced approximately 180 million years of tectonic, paleoceanographic and paleoclimate history, spanning from the Mesozoic Gondwana breakup to the present. The large sediment volume preserved in the Weddell Sea basin is of particular significance for understanding the interactions between sedimentation, Antarctic ice sheet dynamics, ocean circulation, and tectonic processes over this period.

The present Weddell Sea is bounded to the east by the high-elevation Dronning Maud Land (DML) and the East Antarctic Ice Sheet (EAIS), to the west by the mountainous Antarctic Peninsula and its ice sheet (Antarctic Peninsula Ice Sheet, APIS), and to the south by the vast Filchner-Ronne Ice Shelf, which is fed by large ice-streams from both the EAIS and the West Antarctic Ice Sheet (WAIS) (Fig. 1) (Dalziel 2007). (Fig. 1). At its widest, the Weddell Sea measures around 2,000 km across; its area is around 3.4 million km² (Halpern et al., 2008). The wild, remote Weddell Sea, its sea ice, the cold deep water that forms at its margins, and the ice sheets neighboring it all play crucial roles in determining the global climate and ecosystem.

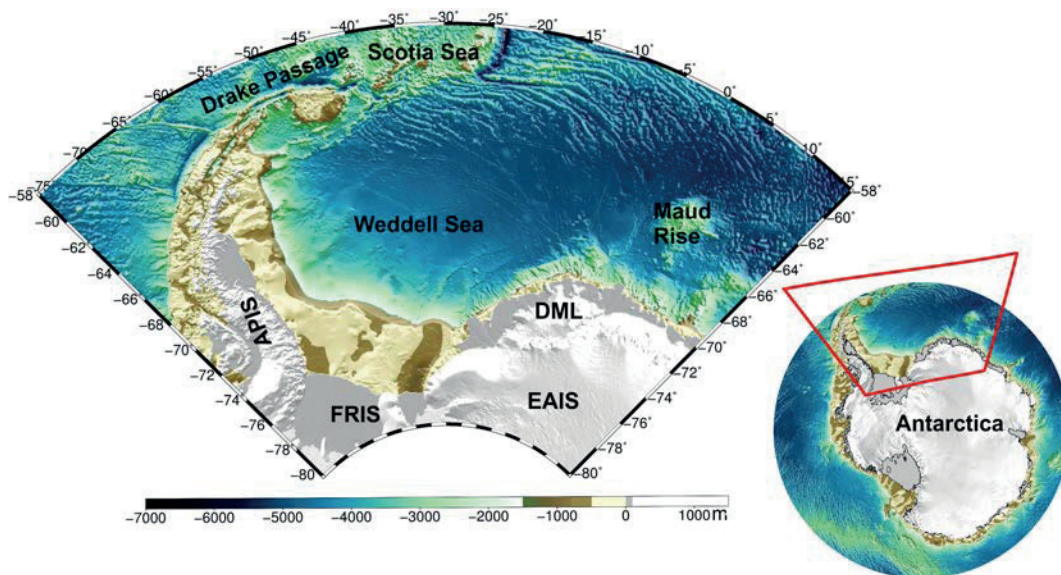


Fig. 1.1 Overview map of the Weddell Sea, showing the shelf bathymetry, extent of ice shelves (grey), and the ice-sheet surface elevation. APIS: Antarctic Peninsula Ice Sheet; EAIS: East Antarctic Ice Sheet; FRIS: Filchner-Ronne Ice Shelf; DML: Dronning Maud Land.

1.1.1 The evolution of the Weddell Sea basin

Antarctica formed the central parts of the late Proterozoic supercontinent Rodinia and the Paleozoic/Mesozoic supercontinent Gondwana. The initial breakup of

Gondwana in the Weddell Sea was tentatively dated as 160-180 Ma in earlier tectonic models (Labrecque and Barker, 1981, Studinger and Miller, 1999, Jokat et al., 2003). More recent refined plate tectonic models and magnetic anomalies suggest that the initial stretching and extensional movements took place in a basin comprising continental crust of the Filchner-Ronne Shelf at 167 Ma (König and Jokat, 2006) (Fig. 2A). The scenario of Gondwana breakup starting in the southern/southwestern Weddell Sea and propagating clockwise around Antarctic from Jurassic times to present has also been supported by magnetic anomalies (Lawver et al., 1991, 2003). The first ocean floor in the Weddell Sea was formed as a direct result of the separation of South America (SAM) from Antarctica (ANT) from 147-122 Ma (Livermore and Woollet, 1993; Livermore et al., 2005, König and Jokat, 2006) (Fig. 2B).

The divergence of the South American and Antarctic plates finally led to the complete development of an east-west oriented spreading system facing the coast of western Dronning Maud Land by about 131 Ma (Jokat et al., 2003a; König and Jokat, 2006) (Fig. 2C). Seaward dipping reflector sequences (SDRs), seen in seismic records across the passive volcanic margins of SAM and Africa (AFR) indicate that this accompanied the onset of seafloor spreading in the southern South Atlantic Ocean (Hinz et al., 2004). By about 118.0 Ma (Fig. 2D, D'), the divergence of South America and Africa from Antarctica had given rise to a deep-water connection between the South Atlantic and the southwest India Ocean (Lawver et al., 1992).

Drake Passage, lying just north of the Weddell Sea, is the key oceanographic gateway between the Pacific and the Atlantic oceans. Along with declining atmospheric CO₂, the gateway's opening has long been hypothesized to have had profound effects on global circulation and climate (Kennett, 1977; Livermore et al., 2005, 2007; De Conto and Pollard, 2003; Kartz et al., 2011; Dalziel, 2014). Opening is suggested to have removed the last barrier to the wind-driven Antarctic Circumpolar Current (ACC), the largest current in the world's oceans. There is little agreement on how wide or deep Drake Passage needs to have been to exert a global influence (Huber and Nof, 2005). The timing of opening is also a subject of discussion. Using tectonic reconstructions, Eagles and Jokat (2014) suggested that a continuous shallow gateway was produced after 50 Ma, perhaps with the 42 Ma onset of seafloor spreading in small basins in the southern Scotia Sea (Eagles et al., 2006). Consistent with this, Nd isotopic evidence in core samples from Pacific and Atlantic oceans indicate that the exchange of significant water from the Pacific to Atlantic by 41 Ma (Scher and Martin, 2006). A deeper (>2.5 km) gateway opened by 30 Ma (Lawver et al., 1998; Eagles et al., 2005; Livermore et al., 2007; Eagles and Jokat, 2014).

1.1.2 Ocean circulation

The breakup of Gondwana and subsequent opening of the Southern Ocean basins significantly impacted global ocean circulation, climatic conditions, and the pattern of marine sedimentation (Brown et al., 2006). Changes in the widths and depths of oceanic gateways, and in regional bathymetry influenced ocean current transport and overturning circulation (Orsi et al., 1999). Deep circulation of the ACC must have been established by about the late Oligocene (25-23 Ma), after both the Tasman gateway (between Antarctica and Australia) and Drake Passage (between Antarctica and South America) opened, as suggested by paleoceanographic studies using observations in sediment core materials (Pfuhl and McCave, 2005; Lyle et al., 2007). The ACC is considered to have caused or stabilised Antarctic glaciation (Barker and

Thomas, 2003). Later, in Miocene times, invigorated oceanic/atmospheric circulation associated with internal climate feedbacks are suggested to have acted to further isolate Antarctica from low-latitude heat/moisture sources (Shevenell et al., 2008).

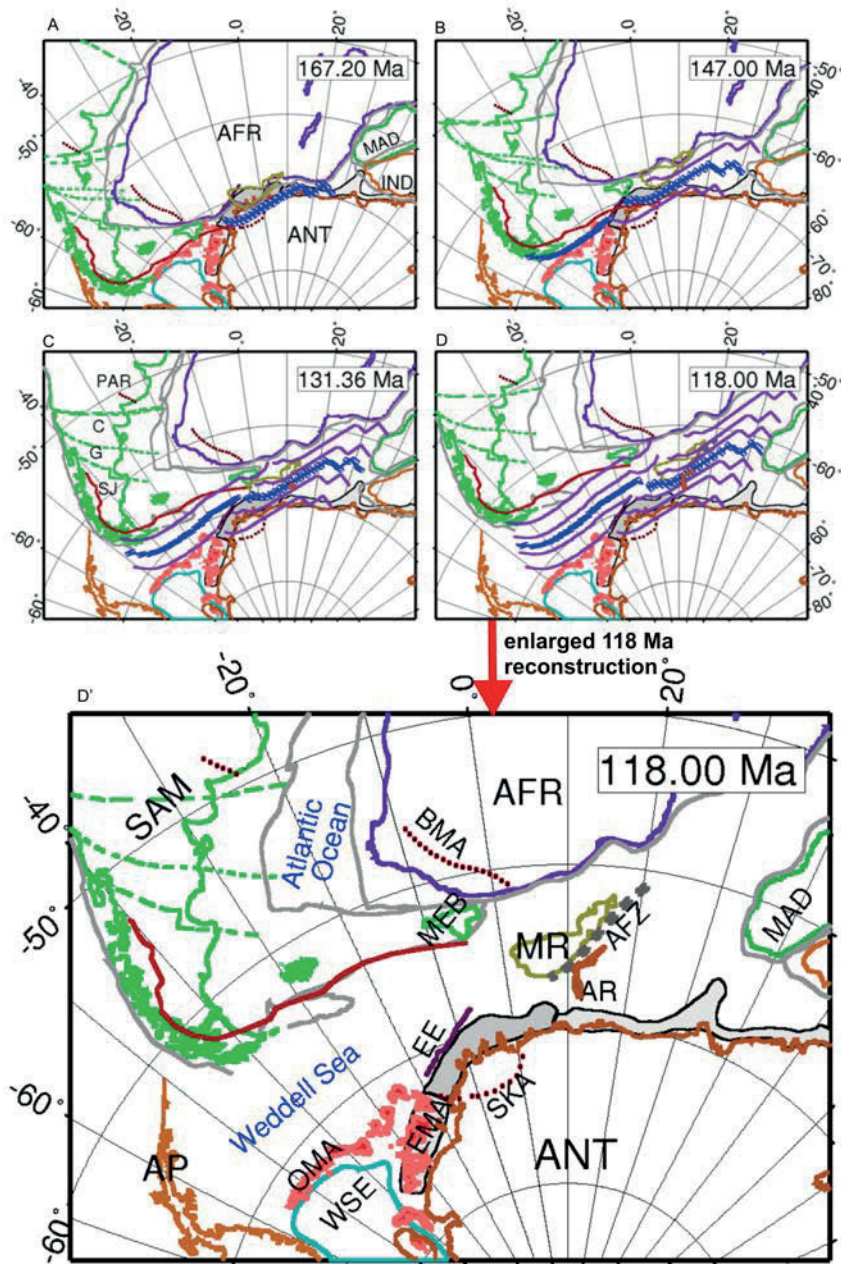


Fig. 1.2 Tectonic reconstructions showing Gondwana breakup and dispersal, modified after König and Jokat, 2006 and Ghidella et al., 2007. Grey lines: estimated present continent-ocean boundary in SAM and AFR. Grey polygons: East ANT continental-ocean transition. Dark red line: NE limit of area altered by post-breakup tectonics at the Pacific margin of SAM. Ma: Magnetic Anomaly; FZ: Fracture Zone; ANT: Antarctica; AFR: Africa; AP: Antarctic Peninsula; AR: Astrid Ridge; BMA: Beattie MA; EE: Explora Escarpment; EMA: Explora MA; MEB: Maurice Ewing Bank; MFZ: Mozambique FZ; MR: Mozambique Ridge; OMA: Orion MA; WSE: Weddell Sea Embayment; SAM: South America.

At present, ocean circulation in the Weddell Sea is dominated by the cyclonic Weddell Gyre, which is responsible for the exchange and mixing of Circum-Deep Water with the global circulation and controls the dynamics of the southern portion of the Atlantic sector of the southern Ocean (Gordon et al., 1981; Orsi et al., 1993; Fahrbach et al., 1995) (Fig. 3A). The Weddell Gyre is the result of interaction between the ACC and the Antarctic continental shelf (Weppernig et al., 1996; Orsi et al., 1999, Foldvik et al., 2004). The gyre's influence extends globally as it is one of few places in the world where deep and bottom water, the drivers of global thermohaline circulation, form (Beckmann et al., 1999; Fahrbach et al., 2011). Sea water that comes into contact with sea ice and the ice shelves on the Weddell Sea continental shelf, cools and sinks to produce dense cool precursor water masses for Antarctic Bottom Water (AABW), which goes on to flood the deep Southern Ocean and spread equatorwards into the deep-sea basins of the Atlantic, Indian and Pacific Oceans (Foldvik et al., 2004; Nicholls et al., 2009, Ohshima et al., 2013). The ice shelf water spills over at an average transport rate of 1.6 Sv ($10^6 \text{ m}^3/\text{s}$) to make a significant contribution to the production of Weddell Sea Bottom Water (WSBW) and AABW (Gordon et al., 1993, Fahrbach et al., 1995; Foldvik et al., 2004). Around 50-70% of AABW is formed in the Weddell Sea Basin (Orsi, 1999).

The sedimentary record, preserved below the basin floor, serves as an archive of the pre-glacial to glacial development, as they act in accompaniment to tectonic processes and ocean circulation. Since the pioneering work of McCave and Tucholke (1986) and Faugères et al. (1993), contourites have been described mainly in the North and South Atlantic basins. Here, these sediment bodies are predominantly associated with deep water masses (e.g. AABW). Later work has identified contourites in the Mediterranean, Indian, Pacific, Arctic, and Antarctic realms (Rebesco et al., 1997, Maldonado et al., 2006; Hernández-Molina et al., 2009 Uenzelmann-Neben and Gohl, 2012). In its simplest terms, the contourite concept is that bottom currents, acting along submarine slopes, are capable of building thick and extensive sediment bodies, termed sediment drifts, often with a noticeably mounded geometry, by winnowing fine-grained sediments (Stow et al., 2002, 2009; Rebesco et al., 2014) (Fig. 3B and C). From this concept, it follows that the history of sediment drift development as interpreted from marine geophysical data can be used to diagnose the evolution of bottom currents on geological timescales. The Weddell Sea, with its numerous sediment drifts and channel-levee deposits that can be attributed to the abundant deep-water masses (e.g. AABW, WSBW, Weddell Gyre), is no exception to this approach to paleoceanography.

1.1.3 Antarctic glacial history

The modern Antarctic ice sheets cover the entire continent, leaving only 0.3% of the land area exposed. It reaches a thickness exceeding 4500 m in places and has a total volume of 25.4 million km^3 (Lythe et al., 2001). The Antarctic Ice Sheet currently discharges 90% of its ice and entrained sediment load via ice streams. Ice streams are corridors of ice within an ice sheet that flow orders of magnitude faster than their surroundings (Rignot et al., 2011).

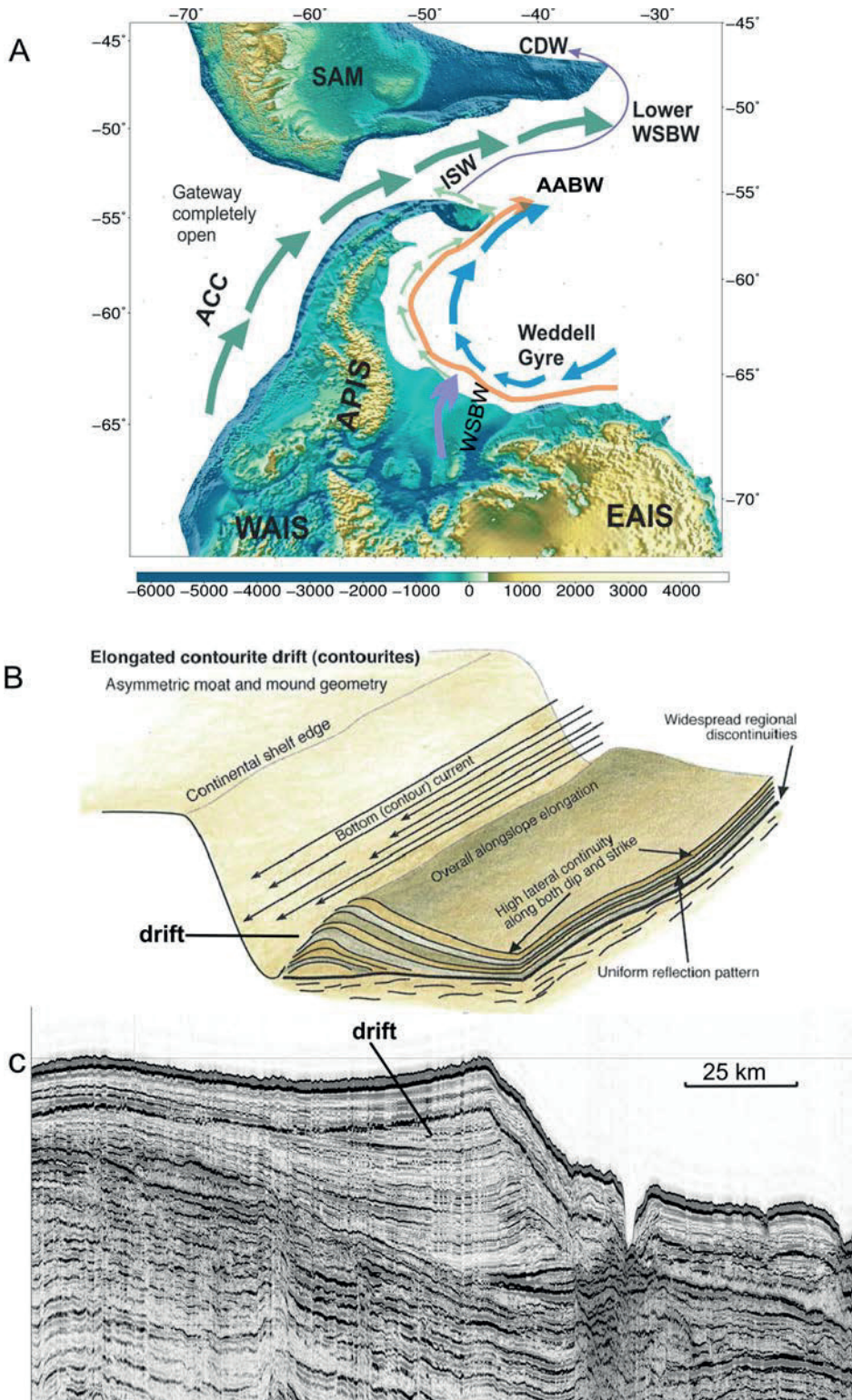


Fig. 1.3 A) Schematic of water masses in the Weddell Sea region after the complete opening of Drake Passage. ACC: Antarctic Circumpolar Current; AABW: Antarctic Bottom Water; ISW: Ice Shelf Water; CDW: Circum Deep Water. B) conceptual sketch of the relationship between a sediment drift and bottom current, modified after Rebesco et al. (2014). C) example of a sediment drift from the study region.

In spite of its polar position, Antarctica is thought to have remained mostly ice-free, vegetated, and with mean annual temperatures above freezing until the latter half of the Cenozoic (around 34 million years ago) (Kennett, 1977). From fossil foraminifera recovered from the deep ocean floor surrounding Antarctica, a stepwise cooling trend is recognizable during the Eocene, during which time Antarctic climate appears to have deteriorated enough to form small, ephemeral ice sheets (Liu et al., 2009; Scher et al., 2011). At the Eocene/Oligocene boundary, a sudden, widespread glaciation of Antarctica occurred, accompanying a shift towards colder temperatures from a warm, ice-free greenhouse world. This is recognized as one of the most fundamental reorganizations of global climate known from the geologic record (Lear et al., 2000; Zachos et al., 2008; Liu et al., 2009) (Fig. 4). A stable cold dry climate was established in Antarctica and most of East Antarctica became glaciated by a perennial large ice sheet at about 34 Ma.

Reasons for the initial growth of the EAIS near the Eocene/Oligocene boundary are under debate. Kennett (1977) and Exxon et al. (2000) attributed it to the tectonic opening of ocean gateways (Tasmania Passage and Drake Passage), which led to reduced south poleward heat transport by establishment of the ACC and, hence, the thermal isolation of Antarctica. Testing this by arbitrarily reducing southward heat transport by 20% in coupled global climate and ice sheet models, DeConto and Pollard. (2003) gateway opening is unlikely to have influenced Antarctic glaciation in exactly this way. In contrast, their model suggested, declining atmospheric CO₂ led to the conditions under which ice-climate feedbacks and orbital forcing permitted the Eocene/Oligocene climate transition.

Between 34 and 15 million years ago, global temperature was around 3-4 °C warmer than present day. Oxygen isotopes measured in fossil foraminifera taken from deep-sea sediment cores suggest fluctuations in global temperatures and high-latitude continental ice volumes were influenced by orbital cycles (Zachos et al., 2007; Paul et al., 2000, Naish et al., 2001). Interpretation of deep-sea isotopic records and observations made in geological data from all over the world suggest that the middle Miocene saw a period of change from a warm climatic optimum, approximately 17-15 million years ago, to a major cooling event at 14.5-13.5 million years ago. Oxygen isotope studies suggest that the volume of Antarctic ice grew and global temperature cooled (Shackleton and Kennett, 1975; Matthews and Poore, 1980; Prentice and Matthews, 1991; Zachos et al., 2008), conclusions that seem to be confirmed by the increase in ice rafted debris (Kennett and Barker, 1990), and evidence for large fluctuations in sea level (Haq et al., 1987; Miller et al., 2011). The permanent ice sheet on East Antarctica expanded out to the continental margins during this cooling period (Anderson, 1999; Lewis et al., 2007). West Antarctica, a smaller block of low-lying continental crust and volcanic highlands, remained substantially ice-free until the latest Miocene (Kennett and Barker, 1990, Anderson, 1999, Cooper et al., 2008). However, detailed seismic stratigraphic studies demonstrate that the West Antarctic Ice Sheet encroached into and grounded on the outer continental shelf in the Ross Sea on several occasions in the Middle Miocene (Anderson et al., 1990; Santis et al., 1995; Bart et al., 2001; Naish et al., 2001). The Antarctica Peninsula is considered to be the last region of Antarctica to have been fully glaciated as a result of Cenozoic climate cooling and the long cooling history of the peninsula is consistent with the extended timescales of tectonic evolution of the Antarctic margin, involving the opening of ocean passageways and associated establishment of circumpolar circulation (Anderson et al., 2011; DoConto et al., 2007). The transition from

temperate, alpine glaciation to a dynamic, polyether moist ice sheet took place during the middle Miocene (Davies et al., 2012).

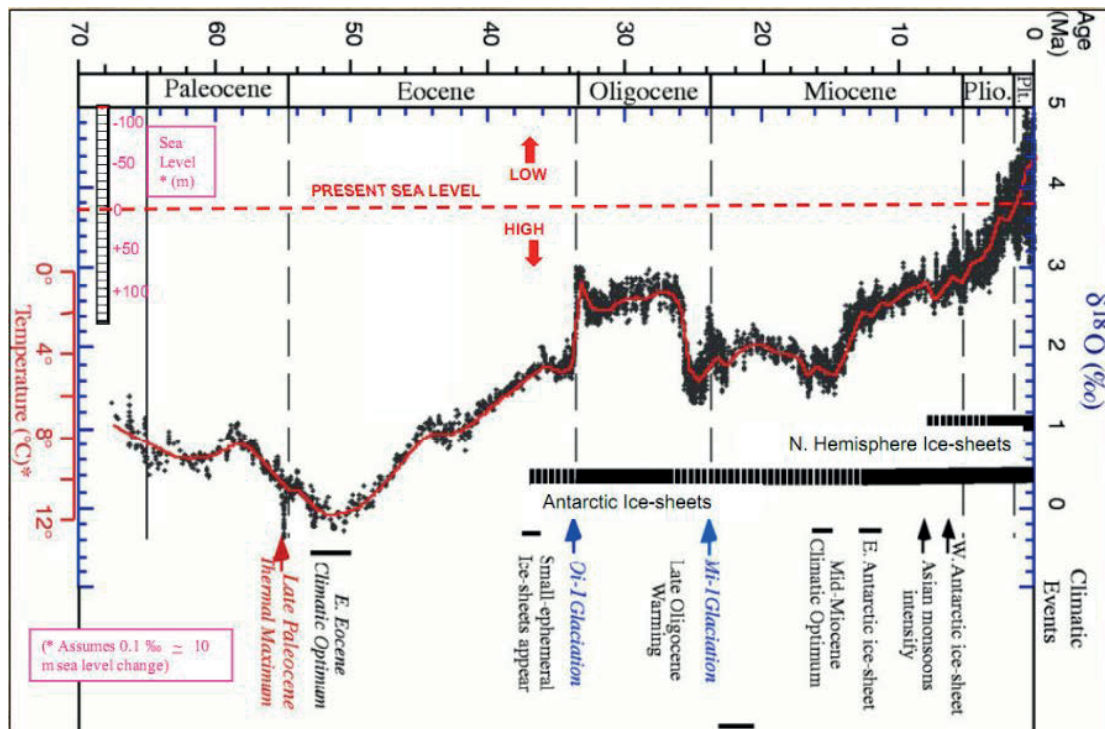


Fig. 1.4 Global sea level change and ice sheet evolution from Antarctica and the Arctic, figure from Zachos et al. (2008).

During late Miocene to Pliocene times, increased biogenic silica deposition and massive discharges of debris-rich icebergs, implying significant terrigenous flux from the Weddell Sea, Wilkes and Adélie coasts and Antarctic continental rise, imply further changes in ice sheet dynamics (Barker, Kennett et al., 1990; Grütznier et al., 2004; Naish et al., 2001; Williams et al., 2009; DeConto et al., 2009). Global ice volume and sea level were strongly influenced by orbital forcing at this time, leading to intense fluctuations of ice sheets in the northern hemisphere. Marine glacial deposits of this age consequently often exhibit regular glacial-interglacial cycles (Leisiecki and Raymo, 2005; Nasish et al., 2009; Miller et al., 2011; Patterson et al., 2014).

1.2 Motivation and scientific questions

The first part of this thesis is focused on analyzing seismo-stratigraphic records in order to create a digital sediment thickness map and a series of paleobathymetric models for the greater Weddell Sea from pre-glacial times to the present. One of these paleobathymetric maps is incorporated as a boundary condition into a Global Climate Model (GCM) for simulating paleoceanographic circulation and paleoclimate. This work is presented in chapters 3 and 4.

The second part of the thesis is focused on seismic interpretation and interpretation of the Weddell Sea's sedimentation history by close investigation of a number of depositional/erosional features in the southeast Weddell Sea and DML margin. The interaction of sedimentation, ice sheet dynamics, along-slope/down-slope

processes, sea level changes is considered in great detail. This work is presented in chapter 5 and 6.

The following questions will be addressed:

1. How has the depth and shape of the Weddell Sea basin changed over the past 100 million of years, since the opening of the Southern Ocean gateways, since the onset of the Antarctic glaciations, and during the transition from the greenhouse to icehouse world? **(Chapter 3)**

2. What is the distribution of sedimentary depocentres within the Weddell Sea basin, and how does it compare to the distribution of ice stream catchment areas on the adjacent Antarctic margins? **(Chapter 3)**

3. How did bathymetry influence ocean circulation in the Weddell Sea during the Middle Miocene? **(Chapter 4)**

4. What factors control, or have controlled, glacial sedimentation patterns in the southeast Weddell Sea? **(Chapter 5)**

5. What are and were the sources and transport patterns of sediment off the DML margin and in the Lazarev Sea? **(Chapter 6).**

2 Dataset and methods

This PhD thesis is based on multichannel seismic datasets that were gathered by several countries, including Germany, the UK, Norway and Spain over the period between 1978 and 2002. The seismic surveys from Germany were mostly collected by several RV Polarstern cruises (e.g. ANT V-4 (1987), ANT VIII-5 (1990) and ANT X-1/2 (1992), ANT XII/3 (1995), ANT XIV/3(1997), ANT XVIII/2 (2002)) (Table 1). All of the data are archived in the Antarctic Seismic Data Library System (SDLS; Wardell et al., 2007) and AWI database. In total, up to 900 seismic lines are incorporated in this study (Fig. 5).

2.1 Multichannel seismic reflection data

2.1.1 Data acquisition and equipment

The general principle of seismic reflection in the oceans is to cause sound waves to propagate through the solid earth, and to record those products of them that find their way back up to the surface. The seismic source can be a dynamite explosion or a pulse of compressed air released into the sea water. A large part of the seismic energy that reaches back up to the surface does so as echoes, which are reflections that happen at acoustic impedance contrasts. The seismic receiver used is an array of hydrophones towed behind the ship in a floating chain, a so-called streamer (Rosaire and Adler, 1934; Sheriff and Geldart, 1995)

Various acquisition equipments have been used during the course of several RV Polarstern cruises, which were undertaken by the Alfred Wegener Institute (AWI) over the past three decades. In 1986/87 and 1989/1990, an 8-litre array consisting of 3 Prakla Seismos compressed air pulsers, operating at 14 MPa, was used as the seismic source. The active length of the 24-channel hydrophone streamer was 600 m. In 1991/92, a 24-litre array, operating at 14 MPa, was used with a 2400 m-long streamer (96 channels). During the experiment in 1994/95, one or two large volume BOLT pulsers (32 l each) were used as seismic sources. Shots were fired every 60 s providing a shot point spacing of about 150 m. The airguns were towed at depths of 10 to 20 m to create a low frequency (~5 Hz) bubble signature. The recording units were REFTEK instruments with 400 to 1000 Mb disks or DAT tapes as storage media. Geophone strings (6 geophones each, 4.5 Hz frequency) were used to receive the seismic signals (Jokat et al., 1997). During the austral summer seasons 1996/1997 and 2001/2002, the ANTXIV/3 and ANT XVIII/2 expeditions aboard RV Polarstern were carried out to complement the existing data sets in the western Weddell Sea (Jokat and Oerter 1998). Multichannel seismic (MCS) and seismic refraction data were acquired by using a 24-litre pulser cluster and an 800 m, 96 channel streamer. The length of the streamer limited the ability to model seismic velocities from the MCS data, especially in the abyssal plain of the Weddell Sea where the water depth ranges from 3 to 4 km. More details regarding the other cruises are listed in Table 1.

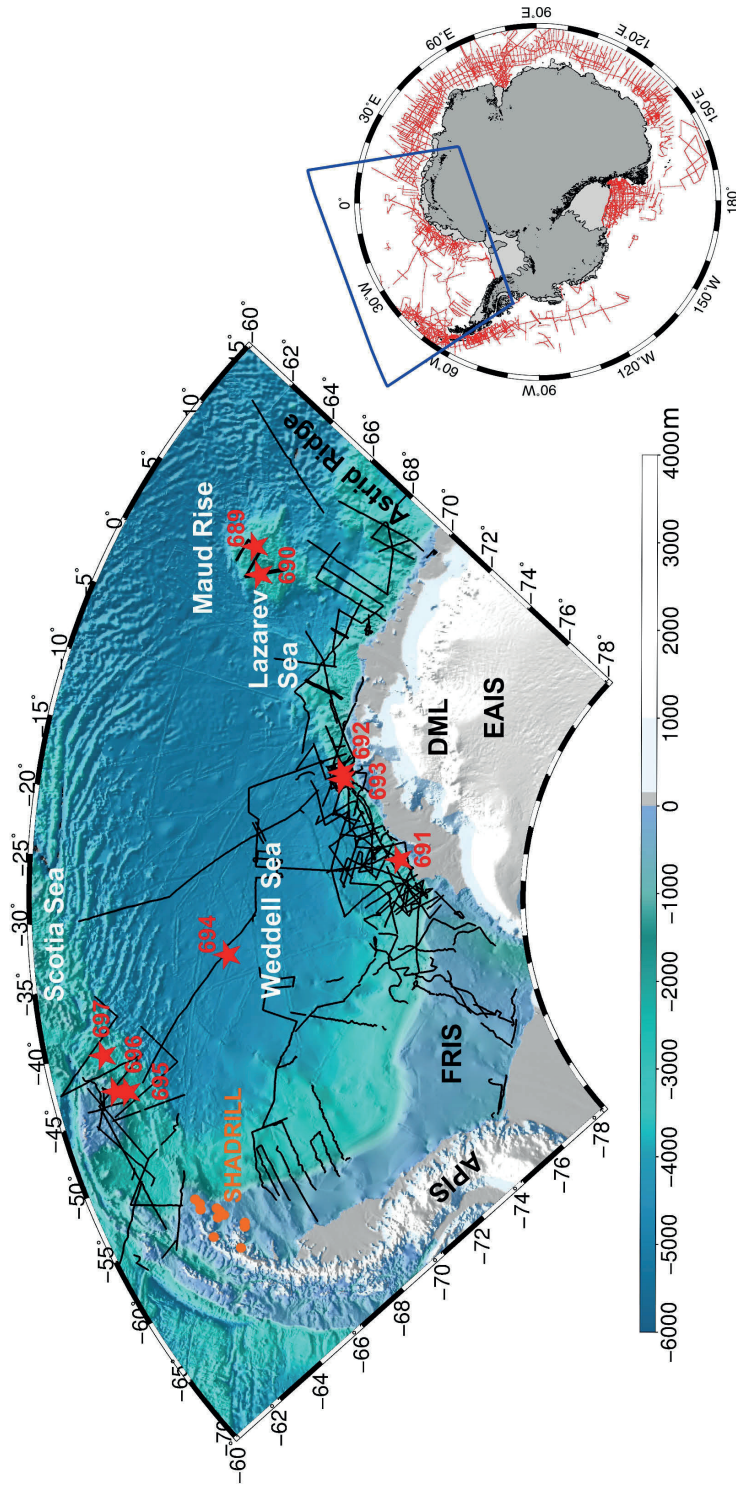


Fig. 2.1 Existing seismic lines (black) in the Weddell Sea basin and environs. The red stars represent ODP sites; orange circles represent SHADRILL sites. Inset: red lines represent all of the available seismic lines around the margins of Antarctica.

Table 2.1 Summary of seismic surveys

Year	Institute	Vessel	Seismic volume (l)	No. of pulsers	Streamer (m)	No. of Channels	Sample rate (ms)	Total survey (km)
1977	NARE	Polarsirkel	3	1	800	16	4	1000
1978	BGR	S.V. Explora	24	24	2400	48	4	5854
1979	NARE	Polarsirkel	5	1	900	18	4	1012
1985	NARE	Andenes	13	2	1200	24/28	4	2600
1985	BAS	James Clark Ross	8.5	4	2400	24	4	1940
1986	BGR	Polarstern	25	10	1500	30	4	6263
1987	AWI	Polarstern	5	2	600	24	2	2800
1990	AWI	Polarstern	6	3	600	24	2	4100
1990	BGR	Polarstern	25	10	2400	48	4	3000
1992	AWI	Polarstern	24	8	600/2400	96	2	3900
1995	AWI	Polarstern	24	8	600/2400	96	2	2063
1996	BGR	A. Nemchinov	53	8	3000	120	2	3836
1996	AWI	Polar Queen	90	2	2400	96	2	723
1997	R	IACT/CSIC/UG	22.14	5	2400	96	2	
1997	AWI	Polarstern	24	8	600/2400	96	2	4418
2002	AWI	Polarstern	24	8	800	96	2	2932

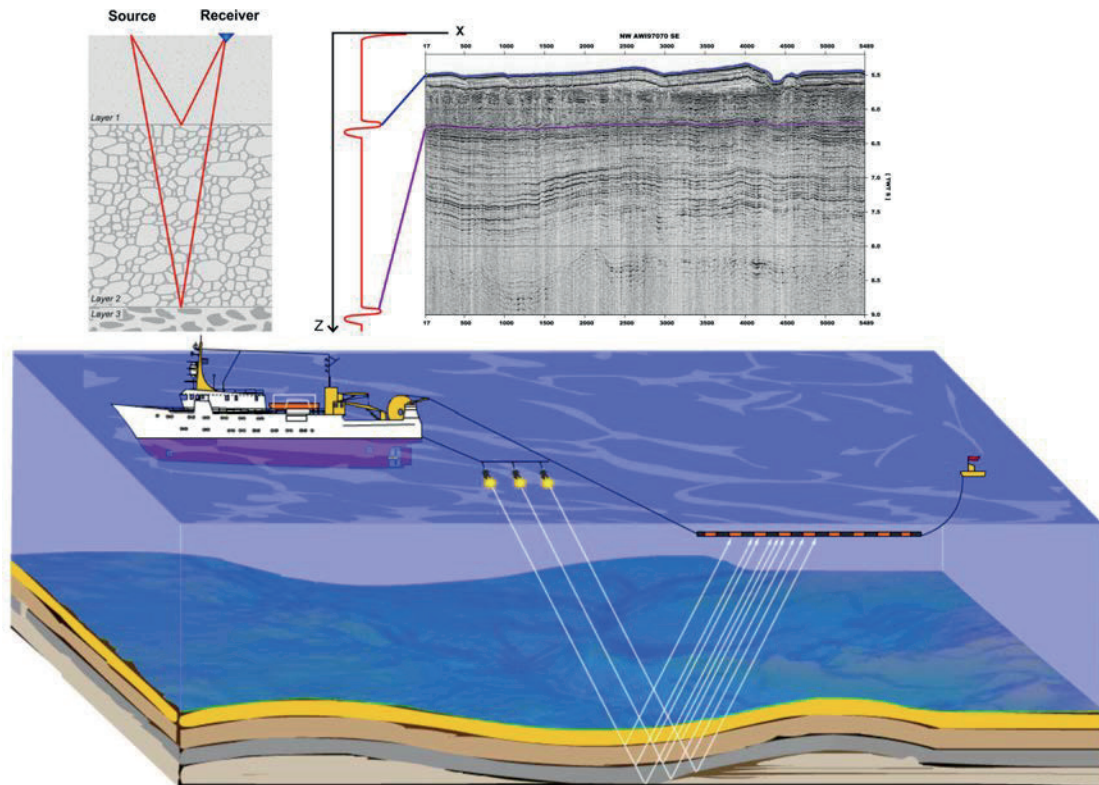


Fig. 2.2 A sketch describing the acquisition of multichannel seismic reflection data (modified from Mjelde, 2009), and an example seismic profile collected in 1997 from the Weddell Sea.

2.1.2 data processing

Various processing steps were applied subsequent to acquisition. The exact processing sequence used for each survey depends on the survey aims. Commonly used procedures include demultiplexing, geometry definition, sorting, velocity analysis, normal move out, f-k filtering, stacking, frequency filtering, muting, and multiple suppression. Details of the processing steps can be found in the publications and and cruise reports related to the various measurement campaigns (Oszkó, 1996; Rogenhagen, 2000).

2.2 Stratigraphic model, age correlation, time to depth conversion

A basin wide seismic stratigraphic framework is set up using by tying the lithostratigraphy known at ODP and SHADRILL sites into the network of all available multichannel seismic lines in the Weddell Sea (Fig. 5). ODP Sites 693 and 692 are located on a mid-slope bench on the Weddell Sea margin. Site 693, with 483.9 m penetration, reached down to Albian – Early/Lower Cretaceous sediments, separated by a hiatus, which ended around 34 Ma, from the overlying early Oligocene clayey-mudstones and diatomaceous oozes of a transitional unit. Site 694 in the central Weddell Sea was drilled 391.3 m into middle Miocene sediments at the lower boundary of the full glacial unit. The oldest sediments encountered at Site 697 in Jane Basin, at the northern edge of the Weddell Sea, are of early Pliocene age (Barker, 1988). SHALDRIL core NBP602A-3C reached a depth of 20 m below sea floor from the Antarctic Peninsula (Smith et al., 2011), and returned Eocene and late Oligocene sediments (Fig. 6). These sites allow us to interpret four major sequences, which

provide age control on Cenozoic deposition in the periods 0-3 Ma, 3-7 Ma, 7-15 Ma, and 15-34 Ma.

In order to convert seismic travel time to depth, we applied a velocity model that is built from all published velocity-depth functions (Kudryavtzev, 1987; Hübscher, 1994; Hübscher et al., 1996; Rogenhagen et al., 2004). P-wave velocities derived from sonobuoy recordings (Hübscher, 1994; Hübscher et al., 1996) were used to constrain time-to-depth conversions. We interpreted the key horizons and completed the depth conversion procedure using the seismic interpretation system and TDQTM package in LANDMARK. Finally, sediment thicknesses were obtained and used to predict the paleobathymetry of Weddell Sea basin.

2.3 Backstripping

The backstripping technique was used to reconstruct the paleobathymetry of the Weddell Sea for use as one of the boundary conditions in the General Climate Model. The use of high-resolution paleobathymetric models in climatically sensitive areas like the Weddell Sea is expected to significantly improve the accuracy of numerical climate models. The purpose of backstripping is to use the stratigraphic record to quantitatively estimate the depth of the seafloor and basement in the absence of sediment and water loading (Watts and Ryan, 1976; Alan and Aland, 2005). The technique involves stepwise removal of sediment loads and decompaction of the remaining underlying sequence, and isostatic correction for the replacement of the sedimentary load by water or air. In this study, we include five steps: 1) Removal of the top sedimentary layer; 2) Flexural unloading of the lithosphere; 3) Decompaction of the remaining sediments (Suckro, 2013); 4) Thermal subsidence; 5) Sea-level correction. More details will be presented in Chapter 3.

2.4 GCM setup

In order to understand the interactions between regional paleobathymetry, ocean circulation, and sedimentation patterns, we implemented the paleobathymetry grids in a GCM to simulate mid-Miocene ocean circulation. The GCM is the fully coupled global atmosphere-ocean-sea ice-vegetation Earth System Model COSMOS, which was originally developed at the Max Planck Institute in Hamburg (JungCLAUS et al., 2010). The standard early to middle Miocene model setup (MIO; 20–15 Ma) applies global paleobathymetry, orography and ice-sheet adjustments (Herold et al., 2008) and has been updated by a regional paleobathymetry dataset comprising the North Atlantic/Nordic Seas sector (Ehlers and Jokat, 2013). The work described in this thesis describes the effect of further embellishing the model using our new Weddell Sea sector paleobathymetry in the MIO setup. More details are presented in Chapter 4.

3 Contribution to scientific journals

3.1 Variability in Cenozoic sedimentation and paleo-water depths of the Weddell Sea basin related to pre-glacial and glacial conditions of Antarctica

Xiaoxia Huang*, Karsten Gohl, Wilfried Jokat
Alfred Wegener Institute, Helmholtz-Centre for Polar and Marine Research
Am Alten Hafen 26, D-27568 Bremerhaven, Germany
Submitted to Global and Planetary Change on 22 August 2013
Received in revised form 21 March 2014
Accepted 26 March 2014
Available online 3 April 2014, Volume 118, pages 25-41

In this paper, we present a uniformed seismic stratigraphic age model and sediment thicknesses, sedimentation rates, and paleobathymetric grids from preglacial to full glacial times. We expand this initial stratigraphy model to the greater Weddell Sea region through a network of more than 200 additional seismic lines. Information from few boreholes are used to constrain sediment ages in this stratigraphy, supported by magnetic anomalies indicating decreasing oceanic basement ages from southeast to northwest. Using these constraints, we calculate grids to depict the depths, thicknesses and sedimentation rates of pre-glacial (145 - 34 Ma), transitional (34 - 15 Ma) and full-glacial (15 Ma to present) units. These grids allow us to compare the sedimentary regimes of the pre-glacially dominated and glacially dominated stages of Weddell Sea history. The pre-glacial deposition with thicknesses of up to 5 km was controlled by the tectonic evolution and sea-floor spreading history interacting with terrigenous sediment supply. The transitional unit shows a relatively high sedimentation rate and has thicknesses of up to 3 km, which may attribute to an early formation of the East Antarctic Ice Sheet, which was partly advanced to the coast or even inner shelf. The main deposition centre of the full-glacial unit lies in front of the Filchner-Ronne Ice Shelf and has sedimentation rates of up to 140 - 200 m/Myr, which infers that ice sheets grounded on the middle to outer shelf and that bottom-water currents strongly impacted the sedimentation. We further show paleobathymetric grids at 15 Ma, 34 Ma, 120 Ma by using a backstripping technique. Our results provide constraints for an improved understanding of the paleo-ice sheet dynamics and paleoclimate conditions of the Weddell Sea region.

I interpreted the key horizons and expanded the stratigraphic model to the entire Weddell Sea. I calculated the sediment thicknesses, sedimentation rates, and paleobathymetric grids. I also wrote the initial manuscript. Dr. Karsten Gohl and Prof. Wilfried Jokat supervised this work and helped to revise the manuscript.

3.2 Middle Miocene to Present Sediment Transport and Deposits in the Southeast Weddell Sea, Antarctica

Xiaoxia Huang*, Wilfried Jokat
Alfred Wegener Institute, Helmholtz-Centre for Polar and Marine Research
Am Alten Hafen 26, D-27568 Bremerhaven, Germany
Submitted to Global Planetary Change on 6th January 2015, under review with the revised version

In this study, we describe a series of sedimentary features along the continental margin of the southeast Weddell Sea to constrain glacial-influenced sedimentation processes from the Middle Miocene to the present. The Crary Trough Mouth Fan (CTMF), channel systems, Mix-system turbidity-contourites are investigated by using seismic reflection, sub-bottom profiler, and results from ODP Site 693. The sinuous, NE-SW-oriented turbidity-contourites are characterized by bathymetric highs that are more than 150 km wide, 700 km long, and have a sediment thickness of up to 2 km. The unique sedimentation environment of the southeast Weddell Sea is controlled by a large catchment area and its fast (paleo-) ice streams feeding the Filchner Ronne Ice Shelf, turbidity/bottom currents as well as sea level changes. A remarkable increase in mass transport deposits (MTDs) in the Late Miocene and Early Pliocene strata has been related to, ice sheet loading, eustatic sea level fall, earthquakes, and overpressure of rapid sediment accumulation. Our seismic records also imply that fluctuations of East Antarctic ice sheet similar to those that occurred during the last glacial cycle might have been typical for southern Weddell Sea during glacial periods since the Late Miocene or even earlier.

I selected the seismic data and interpreted the sedimentary features on the southeast Weddell Sea margin. I wrote the initial manuscript. Prof. Wilfried Jokat supervised this work and helped to improving the manuscript with several discussions.

3.3 Intensification of Weddell Sea circulations in the Middle Miocene

Xiaoxia Huang, Michael Stärz, Karsten Gohl, Gerrit Lohmann
Alfred Wegener Institute, Helmholtz-Centre for Polar and Marine Research
Am Alten Hafen 26, D-27568 Bremerhaven, Germany
Submitted to Geophysical Research Letter on 20th May 2015, under review.

Here we present circulation model results that suggest the deep water formation and ocean circulation are especially sensitive to the paleobathymetric configuration of the Weddell Sea, which our recent work has shown to be characterized by a more southerly shelf break than at present or in previous paleobathymetric data. The southerly-replaced shelf break of the Weddell Sea results in dramatic changes in simulated mixed layer depth. The modeled parameters further indicate that paleobathymetric configuration impacts water mixing, sea surface temperature changes, and bottom water formation. Bottom water plays a significant role in sediment distribution and constructing geomorphology of the continental rise via developing a number of sediment drifts.

In this work, I supplied the paleobathymetric grids to Dr. Michael Stärz and Prof. Gerrit Lohmann. Dr. Michael Stärz carried out the General Circulation Model experiments based on my data and other boundary conditions. I wrote the manuscript. Dr. Karsten Gohl and Prof. Gerrit Lohmann supervised the work. All of the authors revised the manuscript and contributed to the results in several discussions.

3.4 Sedimentation and potential venting on the rifted continental margin of Dronning Maud Land

Xiaoxia Huang, Wilfried Jokat
This work is in still in preparation for submission.

In this work, we present the sedimentation history on the Dronning Maud Land (DML) margin. We suggest that the relief of Dronning Maud Land (DML), formed by Middle and Late Mesozoic tectonic activity, had a strong spatial control on both early fluvial and subsequent glacial erosion and deposition. The sources, process, and products of sedimentation along the DML margin and in the Lazarev Sea have been barely studied. The onshore mountain belt parallel to the coast of the DML margin acts as a barrier to the transport of terrigenous sediments from the east Antarctic interior to the margin and Lazarev Sea. The Jutul-Penck Graben system allows for local transport across the old mountain belt. Ice streams formed along this pre-existing tectonic fluvial system and controlled glacial sediment transport and deposition. Offshore, we attribute repeated large-scale debris flow deposits to instability of sediments deposited locally on the steep gradient of the DML margin by high sediment flux ice streams. Two types of canyons are defined based on their axial dimensions and sedimentary processes. They arise from turbidity currents and slope failures during glacial/fluvial transport. For the first time, we report pipe-like seismic structures in this region and suggest that they occurred as consequences of volcanic processes.

I interpreted the sedimentary features and wrote the initial manuscript. Prof. Wilfried Jokat has been supervising the work and helping to improve the manuscript.

4 Variability in Cenozoic sedimentation and paleo-water depths of the Weddell Sea basin related to pre-glacial and glacial conditions of Antarctica

Xiaoxia Huang*, Karsten Gohl, Wilfried Jokat
Alfred Wegener Institute, Helmholtz-Centre for Polar and Marine Research
Am Alten Hafen 26, D-27568 Bremerhaven, Germany

4.1 Abstract

The Weddell Sea basin is of particular significance for understanding climate processes, including the generation of ocean water masses and their influence on ocean circulation as well as the dynamics of the Antarctic ice sheets. The sedimentary record, preserved below the basin floor, serves as an archive of the pre-glacial to glacial development of these processes, which were accompanied by tectonic processes in its early glacial phase. Three multichannel seismic reflection transects, in total nearly 5000 km long, are used to interpret horizons and define a seismostratigraphic model for the basin. We expand this initial stratigraphy model to the greater Weddell Sea region through a network of more than 200 additional seismic lines. Information from few boreholes are used to constrain sediment ages in this stratigraphy, supported by magnetic anomalies indicating decreasing oceanic basement ages from southeast to northwest. Using these constraints, we calculate grids to depict the depths, thicknesses and sedimentation rates of pre-glacial (145 - 34 Ma), transitional (34 - 15 Ma) and full-glacial (15 Ma to present) units. These grids allow us to compare the sedimentary regimes of the pre-glacially dominated and glacially dominated stages of Weddell Sea history. The pre-glacial deposition with thicknesses of up to 5 km was controlled by the tectonic evolution and sea-floor spreading history interacting with terrigenous sediment supply. The transitional unit shows a relatively high sedimentation rate and has thicknesses of up to 3 km, which may attribute to an early formation of the East Antarctic Ice Sheet, which was partly advanced to the coast or even inner shelf. The main deposition centre of the full-glacial unit lies in front of the Filchner-Ronne Ice Shelf and has sedimentation rates of up to 140 - 200 m/Myr, which infers that ice sheets grounded on the middle to outer shelf and that bottom-water currents strongly impacted the sedimentation. We further calculate paleobathymetric grids at 15 Ma, 34 Ma, and 120 Ma by using a backstripping technique. Our results provide constraints for an improved understanding of the paleo-ice sheet dynamics and paleoclimate conditions of the Weddell Sea region.

4.2. Introduction

The breakup of Gondwana and the subsequent opening of the Southern Ocean basins coincided with changes in global ocean circulation and climatic conditions (Jokat et al., 2003a), and first-order changes in water mass distribution and marine sedimentation pattern (Brown et al., 2006). Changes in the widths and depths of oceanic gateways, and in regional bathymetry influenced ocean current transport and overturning circulation. At present, the Weddell Sea Embayment, at the very southern part of the Atlantic sector of the Southern Ocean, is of particular significance for the generation of deep and bottom-water masses (Orsi et al., 1999, Foldvik et al., 2004). The clockwise rotating Weddell Gyre is responsible for the exchange and mixing of Antarctic Deep Water with the global circulation system as well as for the transport of

Antarctic ice to the Atlantic Ocean through the so-called iceberg alley (Andersen and Andrews, 1999).

Various studies have shown that sedimentary processes in the Weddell Sea basin were strongly influenced by ice sheet dynamics and by ocean circulation (e.g., Jokat et al., 1996; Rogenhagen and Jokat, 2000). At its southern margins, repeated ice advances and retreats sculpted the landscape of the continental shelf, and transported sediments to the continental slope and rise (Anderson, 1999). Farther offshore, ocean-current related sedimentation transport processes have produced extensive contourite channel-levee deposits (Michels et al., 2002, Weber et al., 1994). Previous seismostratigraphic studies of the Weddell Sea focused mostly on local scales. Miller et al. (1991) proposed a seismostratigraphic model for the eastern margin of the Weddell Sea. They introduced seven horizons (Fig. 2C). A large hiatus was found at Ocean Drilling Project (ODP) site 693 at the Eocene-Oligocene boundary. Kristoffersen (1991) studied the Crary Fan and its channel-levee complex in the southern Weddell Sea. Maldonado et al. (2003, 2005) worked on contourite drifts that result from the interaction of the ACC and Weddell Gyre in the northwestern Weddell Sea. Rogenhagen et al. (2005) improved and expanded Miller et al.'s (1990) study area to the southeastern Weddell Sea by adding new seismic data and calculated sediment thicknesses. Anderson (2010) focused on the James Ross Basin and Joinville Plateau in the northwestern Weddell Sea and provided constraints on the ice sheet evolution of the eastern margin of the Antarctic Peninsula based on seismic profiles and shallow boreholes (SHALDRIL). Lindeque et al. (2013) interpreted a long northwest-southeast seismic transect across the southern Scotia Sea and Weddell Sea (Fig. 1, transect B) and proposed a modified seismic horizon stratigraphy based on it.

In this study, we analyze all existing seismic profiles of the Weddell Sea region and attempt to synthesize a unified stratigraphic model by integrating previously published local models with modifications in some cases. We calculate sediment depth, isopach and sedimentation rate grids for the entire basin from pre-glacial to full glacial times. Sediment thicknesses and volumes are estimated from basin-wide seismic horizon correlations using drill sites for stratigraphic control. We applied a backstripping method in order to analyze the subsidence history and paleobathymetry. The gridded maps are then used to discuss sediment transport and deposition processes corresponding to terrigenous sediment supply, as well as past ice sheet dynamics and ocean circulation of the Weddell Sea basin.

4.3. Regional setting and Antarctic glacial history

The Weddell Sea basin experienced more than 180 million years of tectonic, paleoceanographic and paleoclimate history, spanning from its rifting as part of Mesozoic Gondwana break-up to the present (Dalziel and Grunow, 1992; Dalziel, 2007; König and Jokat, 2010). It is bounded to the east by the high-elevation Dronning Maud Land and the East Antarctic Ice Sheet (EAIS), to the west by the mountainous Antarctic Peninsula and its ice sheet (APIS), and to the south by the vast Filchner-Ronne Ice Shelf, which is fed by large ice-streams from both the EAIS and the West Antarctic Ice Sheet (WAIS) (Fig.1).

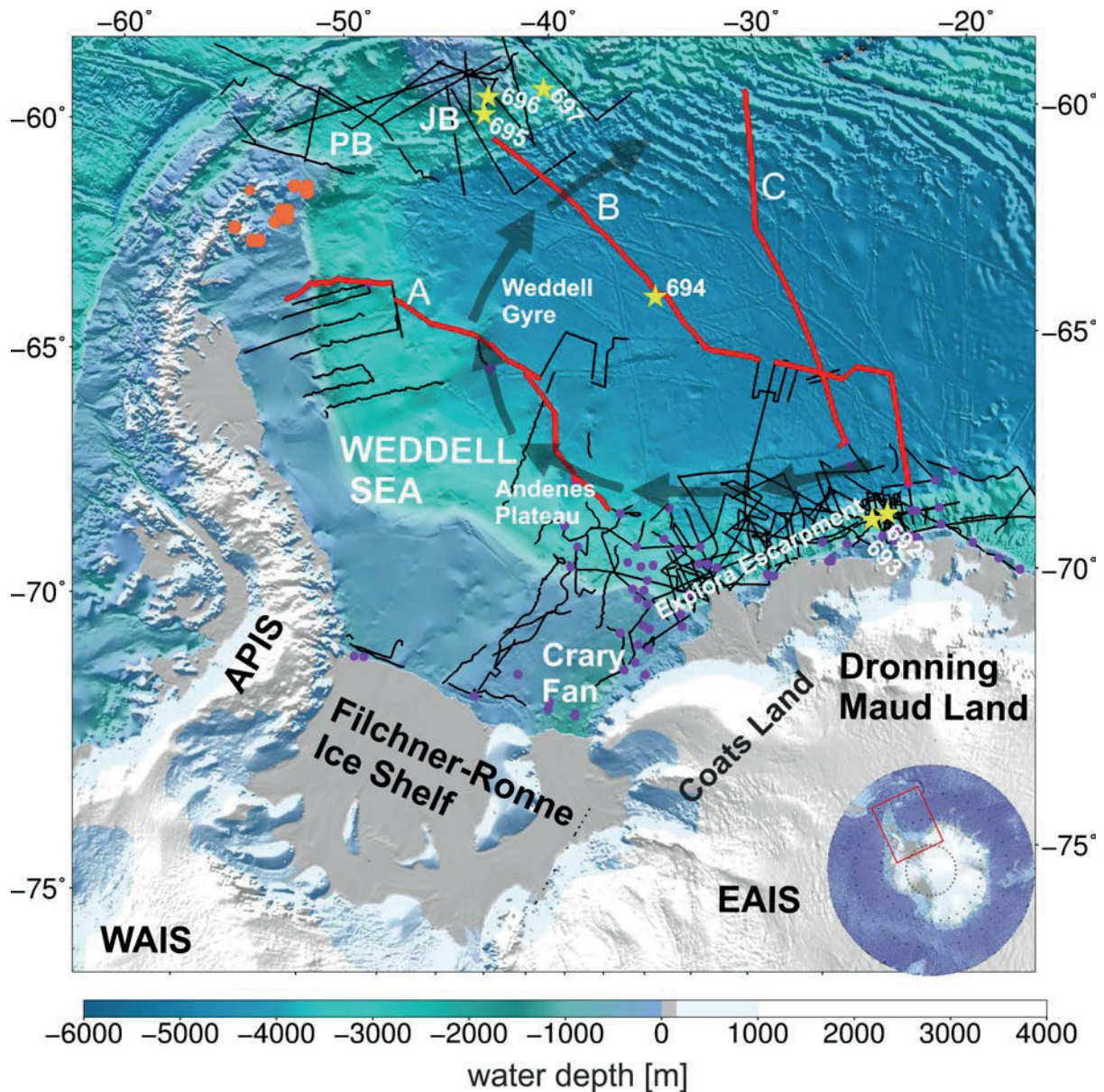


Fig. 4.1 General overview of the Weddell Sea basin with the network of seismic profiles from the Antarctic Seismic Data Library System (SDLS) and three long transects (thick red lines, marked A, B, C) initially used and described in the text. Background image: global seafloor topography grid (Arndt et al., 2013) merged with ETPO1 Global Relief Model (Amante and Eakins, 2009). APIS: Antarctica Peninsula; WAIS: West Antarctic Ice Sheet; EAIS: East Antarctic Ice Sheet; DML: Dronning Maud Land. Three red thick lines are the long transects, black lines are other multichannel seismic reflection data; yellow stars= ODP Leg 113 boreholes; orange circles = SHALDRIL boreholes. Purple circles are the locations of refraction seismic experiments of various expeditions, which were used in setting up the velocity model of the region.

Antarctica's glacial history has been investigated using seismic and coring/drill records of marine sediments, glaciomorphological studies, ice cores, and numerical models of paleoclimate and ice sheet dynamics (e.g., Naish et al., 2001; Zachos et al., 2001; DeConto et al., 2003a,b; Pollard and DeConto, 2005). DeConto et al. (2003a, b)

proposed that rapid Cenozoic glaciation of Antarctica was induced by declining atmospheric CO₂. Results from the Integrated Ocean Drilling Program (IODP) Leg 318 off Wilkes Land have shown that a long-term cooling can be observed between the Early Eocene Climatic Optimum (~54-52 Ma) and the Middle Miocene (~15-13 Ma) with the onset of transient cooling episodes in the middle Eocene at ~46-45 Ma (Passchier et al., 2013). There is no evidence that significant ice sheet volumes developed during the middle to late Eocene (~45-37 Ma). Localized glaciation, predominantly in the form of mountain glaciers and ice caps, occurred in West Antarctica at the early Eocene, although the existence of a larger WAIS in the region cannot be ruled out (Anderson, 1999). A recent paleotopographic reconstruction infers that an early ice sheet covered a larger area of West Antarctica at the Eocene-Oligocene transition than previously thought (Wilson et al., 2012, 2013). Observations from the ANDRILL sediment core recovered from beneath the Ross Ice Shelf document frequent and extended occurrences of open marine conditions in the Ross Sea embayment during the early Pliocene, suggesting that WAIS collapses were common (e.g., Naish et al., 2009). Modeled WAIS variations range from full glacial extents with grounding zones near the continental shelf break, to intermediate states similar to the modern situation, and brief but dramatic retreats, leaving only small isolated ice caps on West Antarctic high lands. Transitions between full-glacial, intermediate and collapsed states are relatively rapid, taking one to several thousand years (Pollard and DeConto, 2009).

4.4 Daraset and Methods

4.4.1 Seismic dataset

Our study is based on multichannel seismic datasets that were collected by Germany, the UK, Norway and Spain between 1984 and 2002, and which are archived in the Antarctic Seismic Data Library System (SDLS; Wardell et al., 2007). In total, up to 250 seismic lines are incorporated in this study (Fig. 1). Furthermore, we added five seismic lines (SM01, SM02, SM03, SM04, and SM05) to the database, which were acquired in the northwestern Weddell Sea by a Spanish survey in 1997 (Maldonado et al., 2003). P-wave velocities derived from sonobuoy recordings (Hübscher, 1994; Hübscher et al., 1996) were used to constrain time-to-depth conversions.

Three long transects (4900 km in this study) of seismic reflection data, labelled A, B and C, were used to set up the initial basin-wide seismostratigraphy (Fig. 1). Those profiles were selected to portray the southern continental rise, the central Weddell Sea, and the northeastern Weddell Sea, and thus cover nearly the entire basin. We interpreted two Cenozoic unconformities, which can be traced on all three transects, albeit only tentatively in places owing to data gaps and varying data quality. We use Lindeque et al.'s (2013) nomenclature for these two unconformities. WS-u5 and WS-u4 are the boundaries of our three main seismic units, which we label as pre-glacial, transitional, and full glacial.

4.4.2 Age information and age model

Magnetic isochron data were compiled from various studies by Ghidella et al. (2002), König and Jokat (2006), and Maldonado et al. (2007) to provide constraints on basement ages. These isochrons show that the oceanic basement of the Weddell Sea ranges in age from late Jurassic to early Miocene (Livermore and Woollett, 1993; Livermore and Hunter, 1996). The oldest magnetic spreading anomaly runs sub-

parallel to the Explora Escarpment, and has an interpreted age of 145-137 Ma (Jokat et al., 2003a). Further west and north, the western, northern and central Weddell Sea adjacent to the south dates from the period ~118 Ma to -83 Ma (König and Jokat, 2009). The Powell Basin and Jane Basin opened as back-arc basins behind a northwestward directed subduction zone that resulted from the subduction of the Weddell Sea crust beneath the South Orkney block (Lawver and Gahagan, 1998). Subsequent to the rifting of the Mesozoic continental crust with associated break-up volcanism in the northwestern Weddell Sea, the Powell Basin formed between 29.7 and 21.1 Ma, but the age of the adjacent Jane Basin is controversial, dating either from 17.4 to 14.4 Ma or the period before 30 Ma (Lawver et al., 1991; Eagles and Livermore, 2002; Bohoyo et al., 2007). In summary, the overall ocean spreading of the Weddell Sea ranged from 145 Ma in the southeast to 14.4 Ma in the northwest.

ODP Sites 693 and 692 are located on a mid-slope bench on the Weddell Sea margin. Site 693 with 483.9 m penetration was drilled down to Albian – Early/Lower Cretaceous sediments, separated by a hiatus of 34 Ma from the overlying early Oligocene clayey-mudstones and diatomaceous oozes of our transitional unit (Fig. 2C) (Barker, 1988). These sites, thus, provide age control on Cenozoic deposition down to WS-u5 (15 Ma) and WS-u4 (34 Ma). Site 694 (Fig. 2B) in the central Weddell Sea was drilled 391.3 m to middle Miocene sediments at the lower boundary of the full glacial unit. The oldest sediments encountered at Site 697 (Fig. 2A) in Jane Basin are of early Pliocene age (Barker, 1988). SHALDRIL core NBP602A-3C reached a depth of 20 m below sea floor (Fig. 2D) from the Antarctic Peninsula (Smith et al., 2011), returned Eocene and late Oligocene sediments, and so allowed us to interpret the ages of WS-u4 and WS-u5 in the northwestern Weddell Sea.

4.4.3 Time to depth conversion, sediment thicknesses

In order to convert seismic travel time to depth, we applied a velocity model that is built from all published velocity-depth functions (Kudryavtzev, 1987; Hübscher, 1994; Hübscher et al., 1996). The regional velocity-depth functions are similar to that used by Rogenhagen et al. (2005). They incorporated 135 velocity-depth functions (Figs. 1, 3), a bathymetry of more than 50,000 data points and calculated with the general velocity-depth (d_s, V_{av}) $V_{av} = 0.17 \cdot d_s (km) + 2.02 (km / s)$ (Hübscher, 1994, V_{av} = average velocity, d_s = sediment thickness). This step is necessary due to the variability of the bathymetry in the Weddell Sea. We completed the depth conversion procedure using the TDQTM package in LANDMARK. To convert a time data point x, y, t to depth, TDQTM triangulates the x, y locations of the nearest time-depth functions, calculating the depth at each corner of the triangle, and then working for t by linear interpolation between them. However, the distribution of the velocity-depth functions is generally sparse and uneven in the Weddell Sea. Most of the depth-velocity functions are generated in the southeastern Weddell Sea, which means the estimated depth calculations are likely to be more reliable in the southeast than other regions. In the southern Weddell Sea, the profiles are of variable spacing, length and orientation due to the remoteness and harsh ice conditions. Here, we supplemented our data set with published seismic refraction results indicating that the southern Weddell Sea hosts a basin containing up to 10-13 km thick sediments (Kudryavtzev, 1987; Hübscher, 1994; Hübscher et al., 1996; Hübscher et al., 1998). From these results, we assumed 12 km as the maximum sediment thickness in front of Filchner-Ronne ice shelf. We subdivided the sediment column into 3 - 5 km of pre-glacial, 2 km of transitional, and 3 - 5 km of full-glacial sediments based on proportional

relative thicknesses of the seismo-stratigraphic sequences and their correlated ages just to the north.

Gridded isopach maps of the total sedimentary deposit as well as their pre-glacial, transitional and full glacial units were produced by using GMT software. A grid spacing of 0.2×0.1 min and a low-tension factor of 0.25 was applied in order to interpolate between the widely-spaced data profiles. We set the sediment thickness to zero along at the Antarctic coastline where the exposure of igneous and metamorphic basement rocks is known. The volumes of the sedimentary units were calculated by applying the GMT routines `grdvolume` and `grdmask` to our thickness grids.

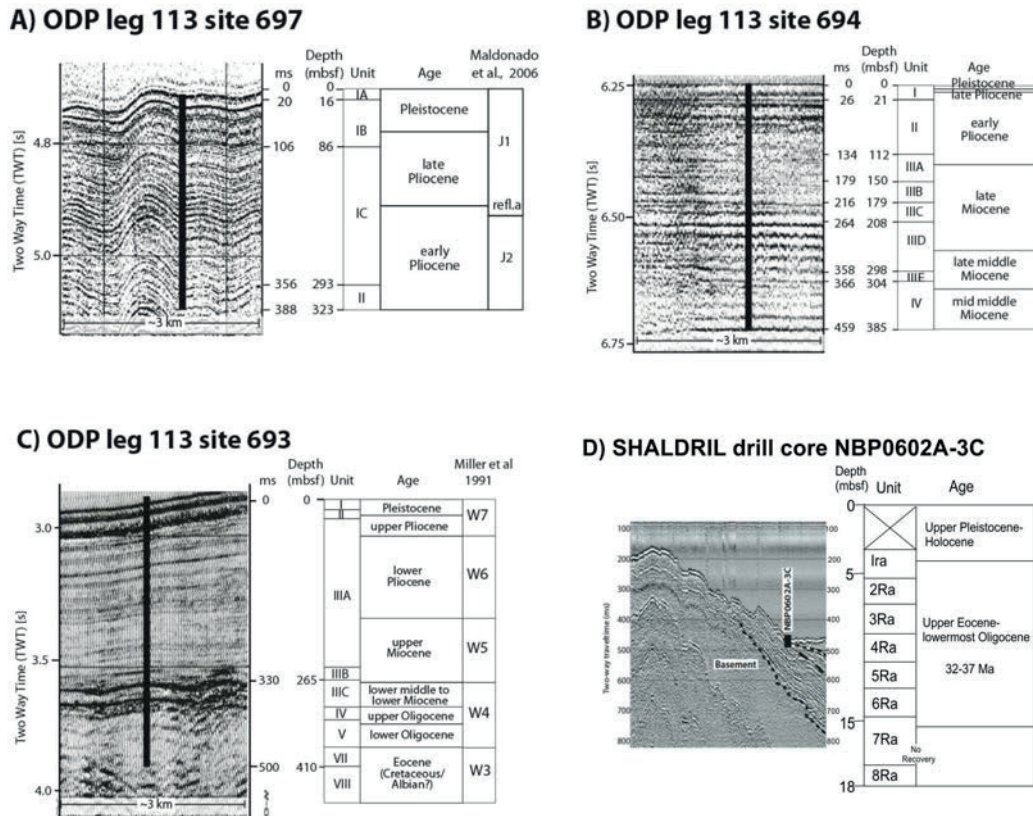


Fig. 4.2 ODP Sites 693, 697, and 694, and SHALDRIL drill core NBP0602A-3C with age information.

4.4.4 Backstripping

The backstripping technique involves the stepwise removal of sediment loads and applies decompaction of the remaining underlying sequence as well as isostatic correction for the replacement of the sedimentary load by water or air. In this study, for each step five main calculations are applied as below:

1. Removal of the top sedimentary layer:

The respective top sedimentary unit of each downward backstripping step is removed using the calculated thicknesses.

2. Flexural unloading of the lithosphere:

The effects of the sedimentary load on basement subsidence are calculated from the density and thickness of the sedimentary units at the time they were deposited. We calculate the flexural response of a lithosphere approximated as an elastic beam to loading using functions by Watts (2011).

3. Decompaction of the remaining sediments:

We used a single porosity-depth relationship from ODP Leg 113 (Barker, 1988; Fig. 3). This relationship is best stated as an exponential function $\phi(y) = \phi_0 \exp(-c \cdot d)$, in which ϕ_0 is the porosity at the top of the sediment column, d is depth in the column, and c is a constant.

4. Thermal subsidence:

The bathymetric effects of thermal contraction, densification, and isostatic equilibration of cooling lithosphere are added to the corrections from the backstripped model from estimates of oceanic crustal age, crustal stretching factor and rift age. The cooling of oceanic lithosphere causes its bathymetric surface to deepen in proportion to the square root of its age (Parsons and Sclater, 1977). In the southernmost areas, the stretched continental lithosphere will have subsided in a similar way as its geotherm returned to a pre-stretching state. This subsidence can be approximated with an exponential age-relation (McKenzie, 1978). The age information for the Weddell Sea basin (Fig. 4) is based on a new compilation of magnetic isochrons and age grids (Livermore and Woollett, 1993; Livermore and Hunter, 1996; Müller et al, 2008). Fixed parameters applied in the calculations are listed in Tab2. We use an average stretching factor of 2.5 for the extended continental lithosphere as estimated by Hübscher et al. (1996), Jokat et al. (1996) and König and Jokat (2006).

5. Sea-level correction:

Sea-level changes have the same isostatic effects as loading or unloading by sediments. We corrected for this effect from the difference in the sea-level height between the present and the time when the sediment unit was deposited, using the global sea-level curve of Miller et al. (2005).

4.5. Results

4.5.1 Seismic characteristics and stratigraphy

The acoustic basement itself is very rugged in the northwestern Weddell Sea with several seamounts breaking through to the seafloor (Fig. 6, 7), whereas the basement in the central Weddell Sea is less rugged (Fig. 6, between 600 and 1100 km). The acoustic basement of transect A, along the southern and southwestern continental rise, is rather gentle (Fig. 5). Most of the seismic profiles in the Weddell Sea show three clearly distinguishable sedimentary units (Tab. 1) above the acoustic basement.

The first unit is characterized by these features: sub parallel wavy reflectors, lower amplitude sequences with partly strong discontinuous reflections and horizontal, spaced transparent zones (Figs. 5, 6, 7). Early Cretaceous organic-rich mudstones from this unit were drilled at ODP Site 693 off the southeastern Weddell Sea margin (Barker, 1988). Following Lindeque et al. (2013), we interpret it as pre-glacial unit. We follow Lindeque et al's (2013) stratigraphic model for this unit in the central Weddell Sea along transect B (Fig. 6) and expand it to the wider region by correlating the seismic characteristics with those of transects A and C. Our unconformity WS-u4 marks the upper boundary of the pre-glacial unit and is consistent with unconformity W4 of Miller et al (1991). They interpreted the unconformity as the product of a major erosional event.

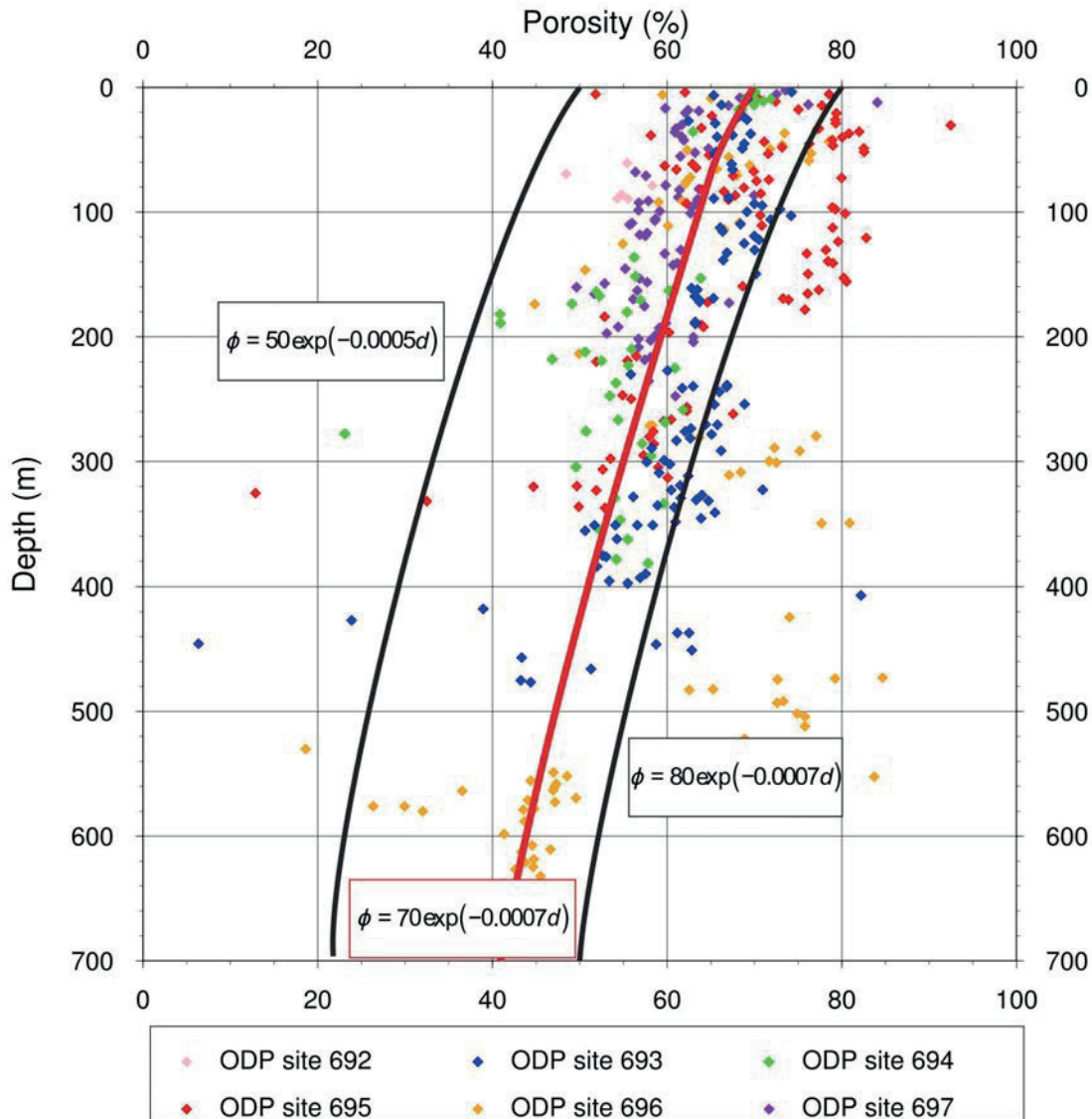


Fig. 4.3 Porosity–depth information from ODP Leg 113 reports (Barker et al., 1988) in the Weddell Sea. The thick red line is the porosity–depth relation, which was used for decompaction in this study $\phi_0 = 70$, $c = 0.0007$. Another two porosity–depth relations showed by two black thick lines, which were used for error estimation.

The second unit is characterized by medium acoustic response and laminated reflections. Chaotic facies are separated by thin draping layers of medium reflectivity and by partly semi-transparent zones (Fig. 5, 6). Early Oligocene silty and clayey mud and sandy mudstones from this unit were drilled at ODP Sites 693 and 696 (Barker, 1988). We interpret it as the transition unit, which is separated from the upper unit by an unconformity mapped as WS-u5, which represents a prominent and widespread unconformity corresponding to reflector W5 of Miller et al. (1990). This reflector is also coincident with ‘Reflector c’, the most prominent unconformity in the northwestern Weddell Sea (Maldonado et al., 2005). In the southern Weddell Sea, WS-u5 coincides with the horizon W4 of Rogenhagen et al. (2005) and is interpreted to represent the onset of glacially-dominated sedimentation processes.

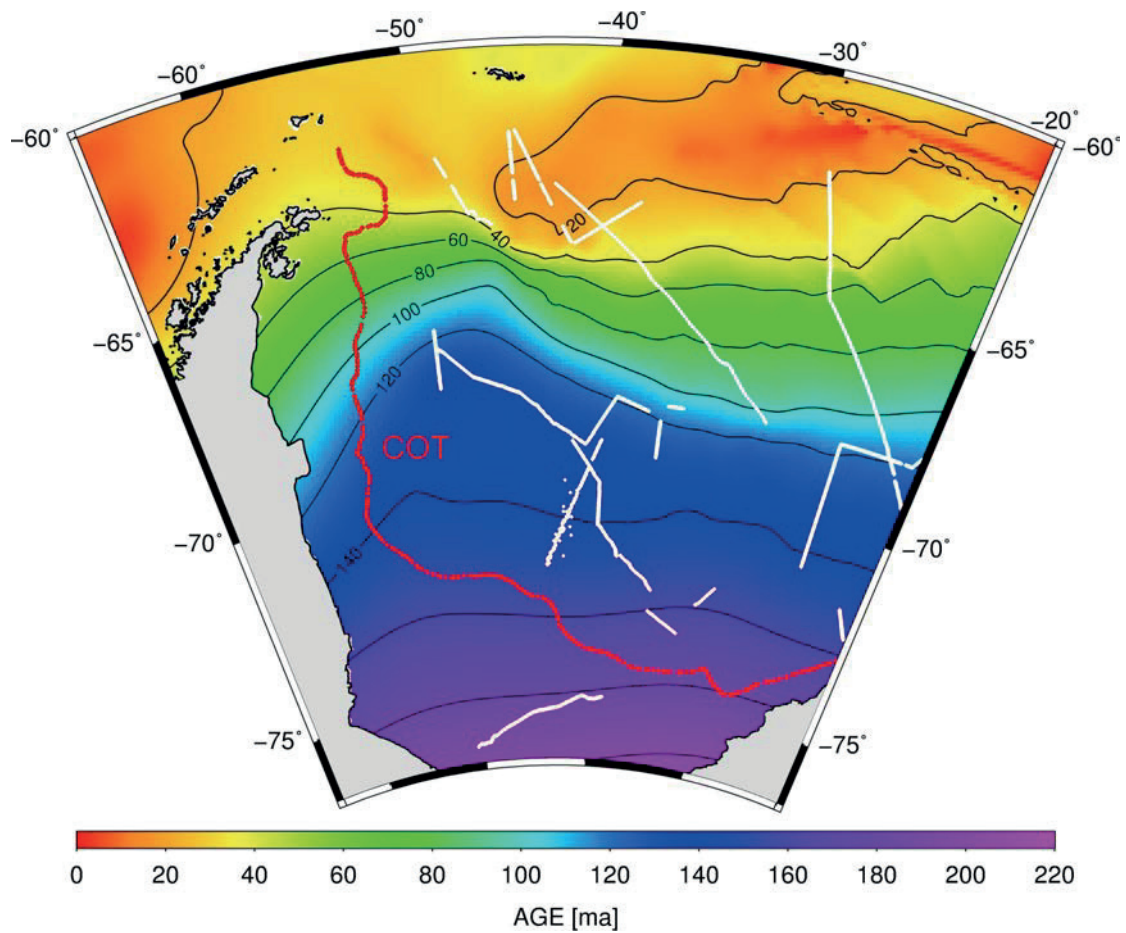
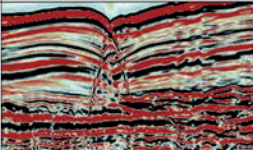
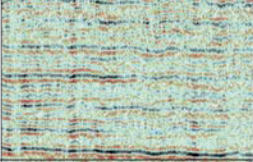
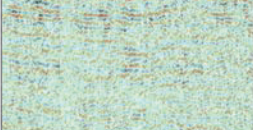


Fig. 4.4 The compilation of the available age information in the Weddell Sea basin, which is applied for thermal subsidence calculation. The red line is continental–ocean transition (COT). The white lines are the seismic lines, which were applied by backstripping.

Table 4.1 Summary of the seismic stratigraphy of the deposition sequences and major paleoceanography events.

Sediment units	Dominant unconformities	Seismic Characteristics	Seismic examples	Major events
Full-Glacial 15 Ma - Now	WS-u5	Drift, channel and basin fill in, finely laminated, high amplitude reflections, unconformities, parts are chaotic reflections with lower reflectivity due to debris flows.		Grounding cycles of EAIS and WAIS on the continental; WAIS brings terrigenous sediments to margin; Early expansions of APIS onto the continental shelf in the south.
Transitional 34 - 15Ma	WS-u4	Medium reflectivity, discontinuous and horizontal reflections higher amplitude close to bottom of pre-glacial.		Earliest glacial event on the AP; EAIS & WAIS formation; Onset of the ACC; Abrupt Eocene-Oligocene cooling.
Pre-Glacial 145 - 34 Ma	Basement	Lower amplitude sequence with strong discontinuous reflections in parts, horizontal, spaced, transparent zones.		Drake Passage open, SAM -AP separation complete; AABW forms; Weddell Sea spreading.

The third unit is generally characterized by a regular and thinly bedded pattern of parallel, continuous high-amplitude reflections. Locally, this pattern is interrupted by chaotic reflections with lower reflectivity in the southern Weddell Sea (Fig. 5). We interpret this unit as full glacial, which is bounded by seafloor and WS-u5. Abundant drifts and channel-levee systems are present on the southern continental rise (Michels et al., 2002). The sediment drifts show semi-transparent, continuous, sub-parallel or irregular, wavy to discontinuous as well as moderate to low amplitude reflectors (Fig. 5). The acoustic facies of the channel-levee systems vary greatly between the drifts. Some channel floors are characterized by high-amplitude, discontinuous reflectors, and surrounded by transparent facies. Levees are shown by relatively well-stratified deposits that abruptly wedge out at the side of channels (Fig. 5). Glacial turbidites are recorded at ODP Site 694 as well as in the significant Ice Rafted Debris (IRD) of Miocene sequences at ODP Site 693 (Barker, 1988).

4.5.2 Sediment thicknesses and rates

The total sedimentary thickness was interpolated between seismic lines and clipped where no sufficient data coverage exists (Fig. 8A). Generally, the grid shows a trend of decreasing total sediment thicknesses from the continental margin to the abyssal plain of the Weddell Sea. Most sediment was deposited on the continental shelf and slope, with large depocentres in front of the Filchner-Ronne Ice Shelf and along the southern continental rise of the Weddell Sea. Here, interpretations of seismic refraction data suggested up to 12 km of sedimentary infill. The Crary Fan occupies a large depression filled with more than 8 km thick sediments in the southeastern Weddell Sea (Fig. 8A). Haugland (1985) identified the fan from multichannel seismic data and interpreted it as an accumulation of glacially-transported material. Kuvaas and Kristoffersen (1991) also described the structure of the fan in detail. Another major sediment depocentre with 5 km of sediment exists off the continental slope of the eastern Antarctica Peninsula. The sedimentary deposits of the northern Weddell Sea reach a maximum thickness of only 2 km, partly reflecting the much younger crust in this region. Only thin (<3 km) sedimentary sequences were deposited on the Explora Escarpment off the Dronning Maud Land margin.

Following the observed trend from the total sedimentary thickness grid, the thickness of the pre-glacial unit also decreases from the continental margin towards the deep sea (Fig. 8B). Its greatest thickness, of 5 km, is found in front of the Filchner-Ronne Ice Shelf. The continental margin of the western Weddell Sea seems host a series of small depocentres with a maximum thickness of 4 km. In the northern and eastern Weddell Sea, the pre-glacial sediment thickness is only about 0.5 km.

According to our stratigraphic model, the transitional unit started being deposited at about 34 Ma, and its deposition lasted about 5 million years in the northeast and 20 million years in the southwest. As is the case for the pre-glacial unit, the main depocentres lie in the southern Weddell Sea, where the maximum sediment thickness of this unit reaches 2.5 km (Fig. 8C).

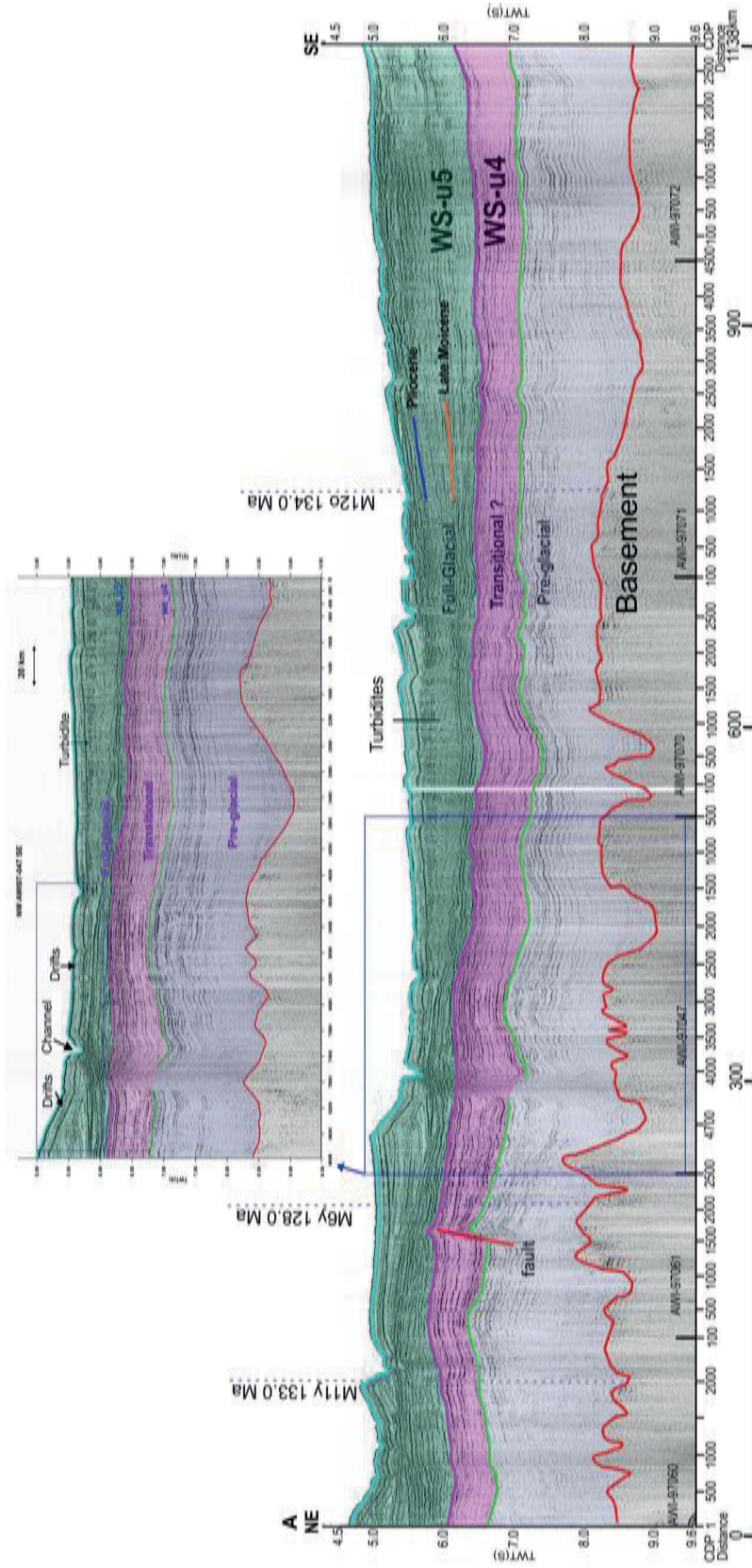


Fig. 4.5 Multichannel seismic reflection image of transect A and interpretation (AWI-97060, AWI-97061, AWI-97047, AWI-97070, AWI-97071, AWI-97072), located at southern continental margin. Drifts and channels are very abundant, the basement is relative gentle. Interpretation of multichannel seismic reflection image AWI-97047. Large drifts with aggradational deposition and partly or fully infilled channels are observed in the northwest, and turbidite flows appear in the southeast in the fullglacial unit.

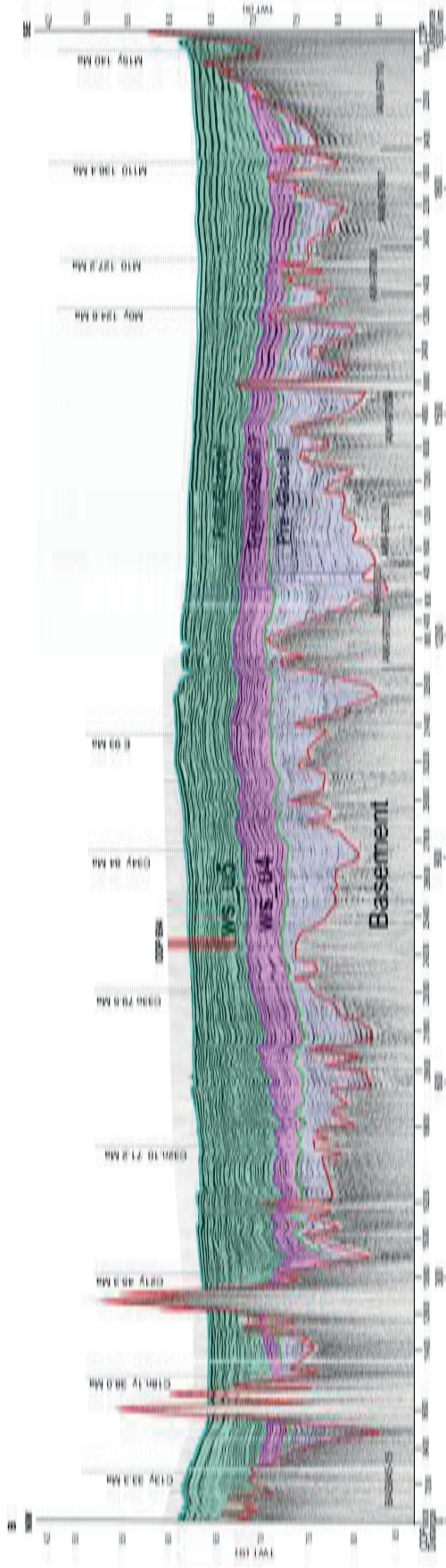


Fig. 4.6 Multichannel seismic reflection image of transect B and interpretation (BAS845-15, AWI97032, AWI97031, AWI97029, AWI97009, AWI97008, AWI97007, AWI96110), crossed the central Weddell Sea and linked the southeastern Weddell Sea.

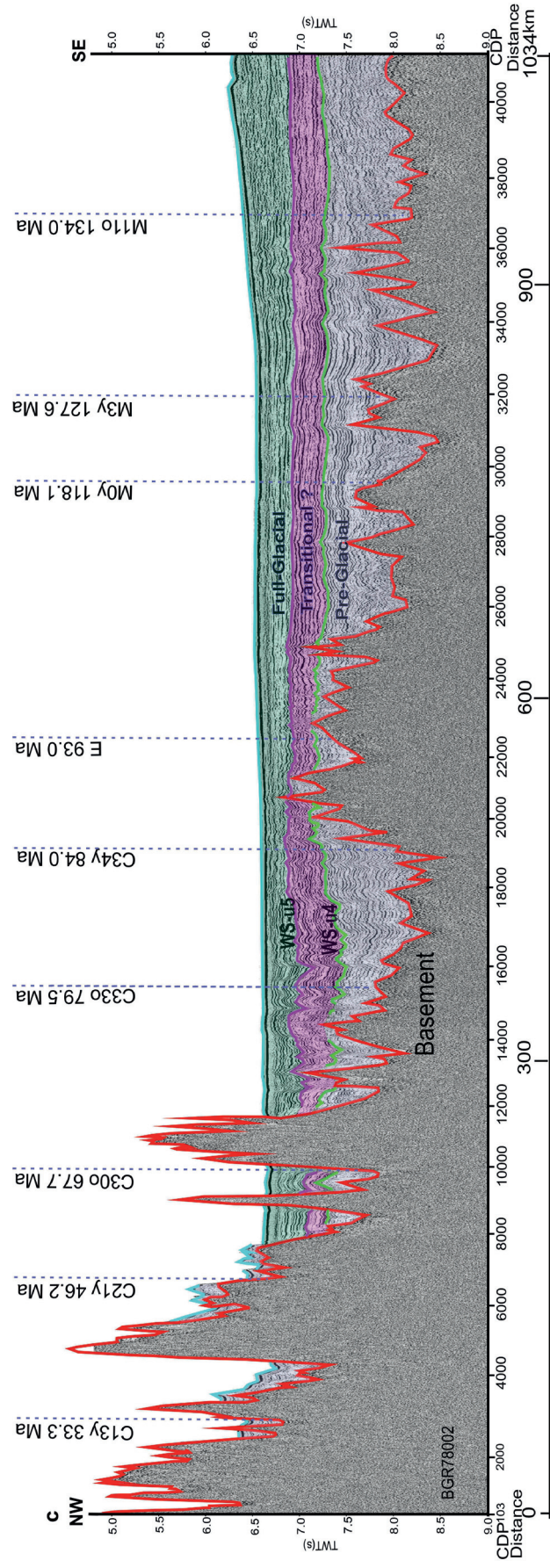


Fig. 4.7 Multichannel seismic reflection data of transect C (BGR78002) crossing the eastern and northeastern region of the Weddell Sea. Very rugged basement and seamounts were found in the north.

The thicknesses of the full-glacial unit range from 0 to 5 km. The main depocentre overlies those of the pre-glacial and transitional units (Fig. 8D). With respect to the number of the seismic lines, small separate depocentres are observed within this unit, e.g. in the northwestern Weddell Sea. Some medium-sized depocentres with maximum thicknesses of about 3 km are found at the eastern Antarctica Peninsula margin and along the margin off Dronning Maud Land, which correspond to the small sedimentary basins on the seismic profile we observed.

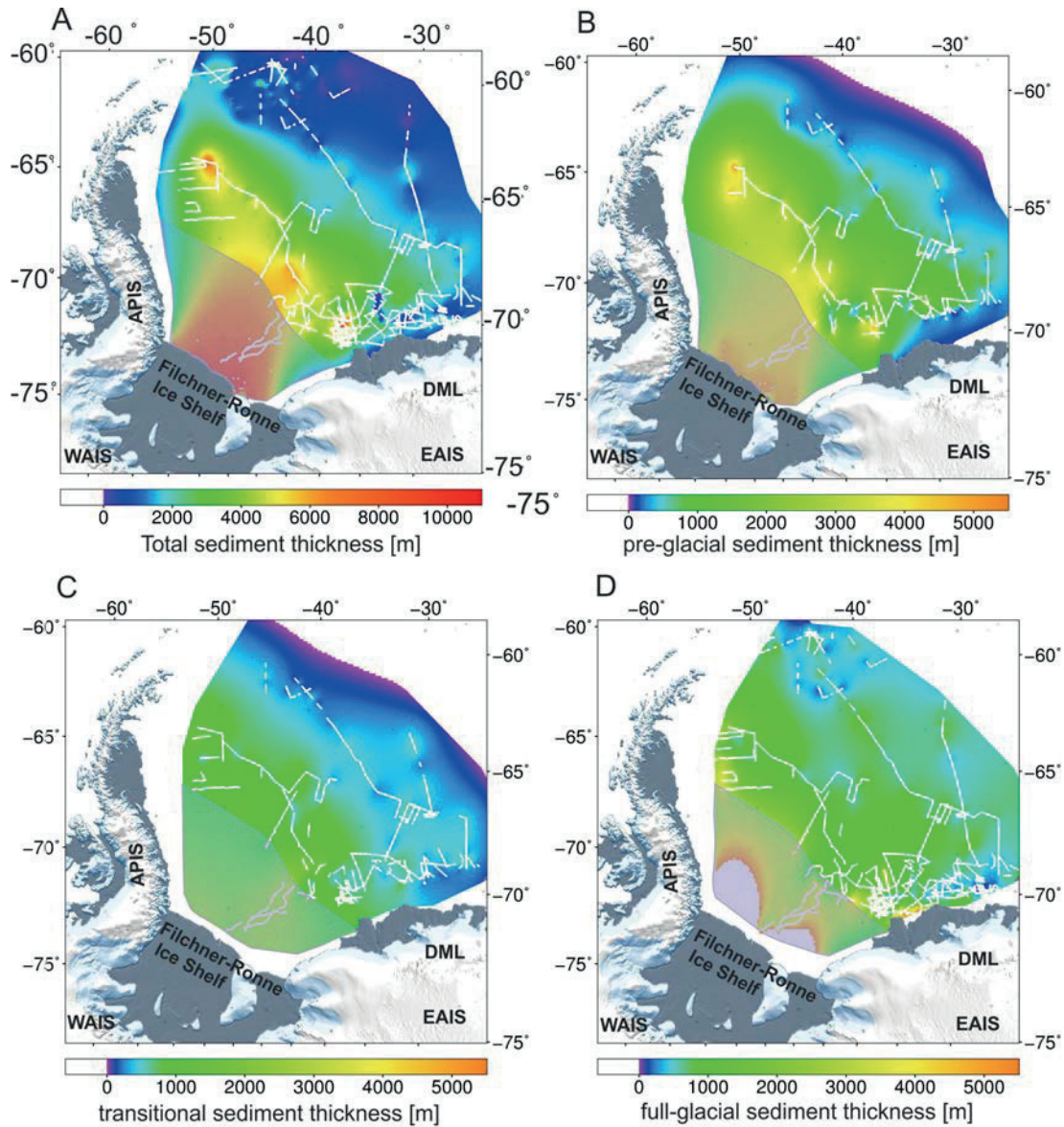


Fig. 4.8 Gridded sediment thicknesses of the Weddell Sea basin. A: total sediment thickness; B: pre-glacial sediment thickness calculated as the difference between the depth of horizon WS-u4 and the top of basement; C: transitional sediment thickness calculated as the difference between the depth of horizon WS-u5 and WS-u4; D: full-glacial sediment thickness calculated as the difference between the depth of the seafloor and horizon WS-u5. The masked areas are assumptions based on seismic refraction experiments.

The total sedimentary volume for the Weddell Sea can be calculated to be $3.89 \times 10^6 \text{ km}^3$ with contributions by the pre-glacial unit of $1.60 \times 10^6 \text{ km}^3$, the transitional unit of $0.51 \times 10^6 \text{ km}^3$ and the full-glacial unit of $2.0 \times 10^6 \text{ km}^3$.

Sedimentation rates were derived on the basis of the age ranges and gridded sediment thicknesses of the pre-glacial, transitional, and full-glacial units. We used sites along the three long transects A, B, C and sites from seismic profiles in various other locations in order to obtain a roughly regular point grid to calculate the sedimentation rates. We gridded the calculated sedimentation rates for each unit in order to show temporal and spatial trends in sediment deposition processes in the Weddell Sea (Fig. 9). The pre-glacial unit deposited at relatively slow sedimentation rates, in particular in the southeastern and northeastern Weddell Sea, where the rates vary from 10 to 25 m/Myr, compared to about 40 m/Myr in front of the Filchner-Ronne Ice Shelf. In some of the small basins of the northwestern Weddell Sea, the value increases up to 80 m/Myr. In contrast to the pre-glacial unit, higher sedimentation rates are found for the transitional unit, particularly in the southern Weddell Sea, where the rate is 100-160 m/Myr. In the central Weddell Sea, the rate varies from 40 to 80 m/Myr. During full-glacial times, sediments were deposited with rates from 120 to 200 m/Myr.

4.5.3 Backstripping and paleobathymetry

The backstripping calculations in steps 1-3 are completed along seismic profiles for horizons aged 15 Ma (lower boundary of full glacial), 34 Ma (lower boundary of transitional), and 120 Ma (none deposition), which are based on the interpretation of Miller et al. (1990), Rogenhagen et al. (2004) and Lindeque et al. (2013) (Fig. 10). The horizon at 120 Ma was selected to represent an early opening stage of the Weddell Sea basin in the Cretaceous, 34 Ma represents the dominant Eocene-Oligocene transition from the Cenozoic greenhouse to the icehouse world with suggested onset of the ACC, and 15 Ma represents the middle Miocene for which paleoclimate records indicate a major intensification of Antarctic glaciation (Anderson and Andrews, 1999). The resulting backstrip corrections are gridded to produce a gradually-varying field from deeper to shallower across the Weddell Sea. The thermal and paleobathymetric corrections are calculated directly from the age grid. A set of paleobathymetric models is generated by adding all of the corrections to the present-day bathymetry.

The models (Fig. 10) yield a consistent trend of deepening in the regional evolution of the Weddell Sea basin. This is consistent with the overall dominance of thermal subsidence effects. At 120 Ma, the basement, which currently lies beneath as much as 12 km of sediments, is restored to a level of only ~ 3 km below seafloor. At the Eocene-Oligocene boundary (34 Ma), the grids show that the basin is about 0.5 - 1 km shallower compared with that of the present in the northwestern Weddell Sea, which is mainly due to the fact that relative young oceanic crust yields remarkable effect of the thermal subsidence. However, the paleowater depth of the central Weddell Sea is nearly consistent with today and the Middle Miocene. The small elevation difference is probably caused by the mantle rebound and decompaction of the remaining sediments after removal 5 - 6 km sediment layers, which were mostly deposited during glacial time (Fig. 8). The effect of the thermal subsidence is nearly neglectable in the central Weddell Sea for the period from 15 Ma to present day.

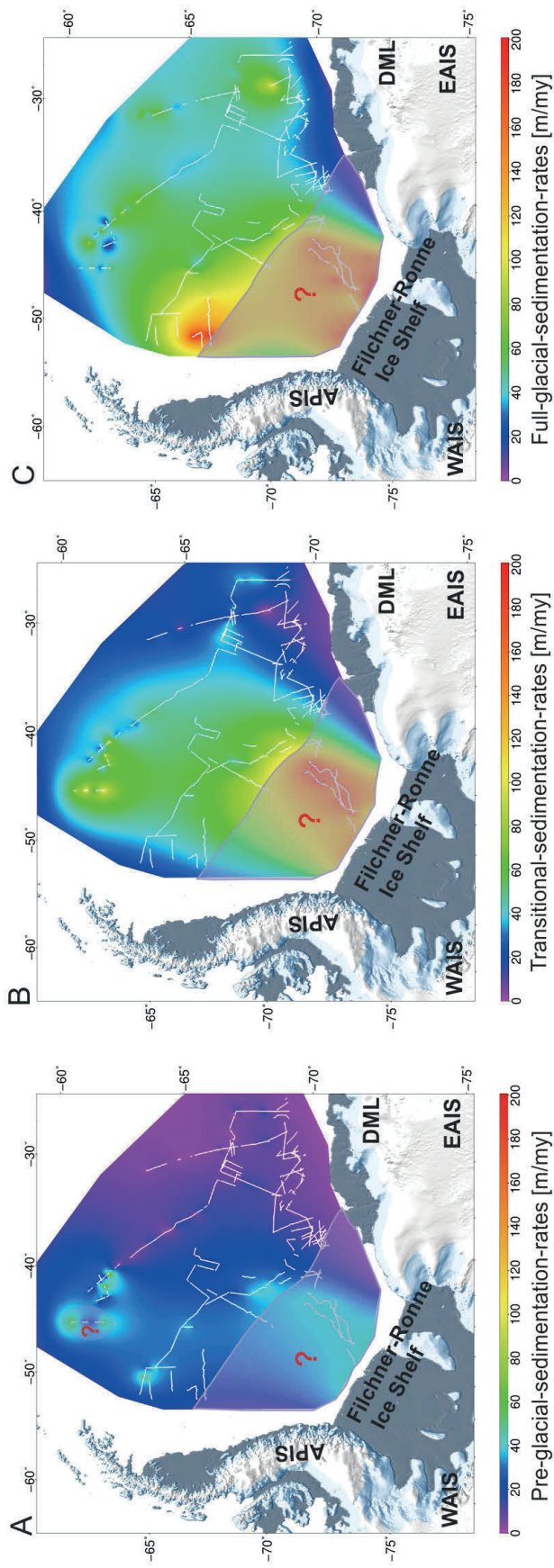


Fig. 4.9 Sedimentation rate grids for the pre-glacial, transitional and full-glacial. Calculations are based on the sediment thickness and our age model. Mask regions with question marks are uncertain due to insufficient data and bad data quality.

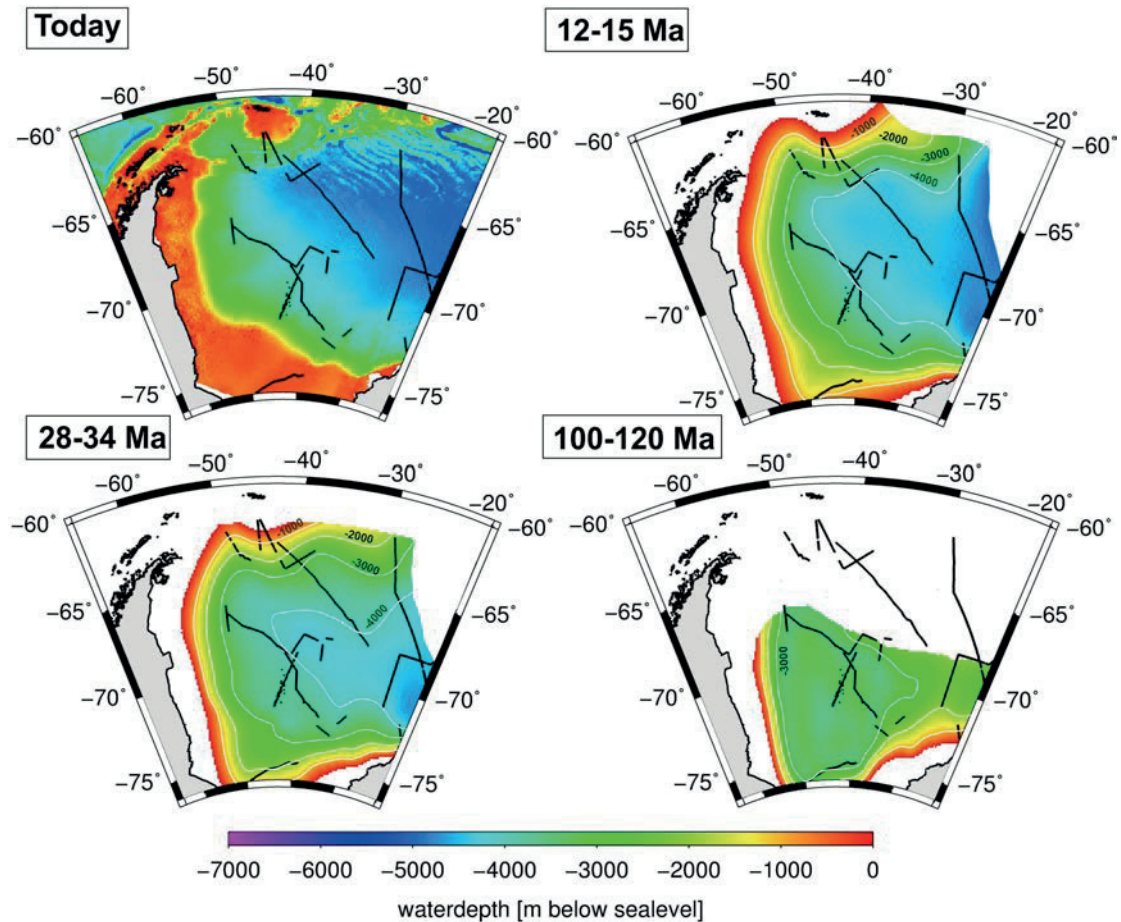


Fig. 4.10 Paleobathymetry reconstruction. Today's bathymetry is from the ETPO1 Global Relief Model (Amante and Eakins, 2009). Paleobathymetry at 15, 34, and 120Ma is calculated in this study. The coastline plotted at 120 Ma is to give a general orientation, not the true coastline at that time.

4.6. Discussion

The development of the Weddell Sea basin witnessed the interplay of complex seafloor spreading and tectonic processes with the deposition of large amounts of sediments since the Jurassic. For instance, as reported from seismic refraction experiments in the southernmost Weddell Sea in front of the Filchner-Ronne Ice Shelf, 10 - 12 km of sediments overlie a basement of stretched continental crust (Hübscher et al., 1996; Kudryavtzev et al., 1987; Leitchenkov et al., 2000). Here, pre-glacial sedimentation processes were likely dominated by thermal lithospheric subsidence and variations in terrigenous sediment supply. Later, the developing and fluctuating Antarctic ice sheets have supplied sediments which interacted with intensified ocean circulation in the Weddell Sea to play a significant role in transporting and distributing sediments, particularly after the opening of Drake Passage/Scotia Sea gateway and intensification of the ACC.

4.6.1 Pre-glacial regime

The pre-glacial unit contains sediments deposited within a large time range of up to 116 million years, spanning from Mesozoic deposits on the oldest oceanic basement in the southwestern Weddell Sea (about 145 Ma) to the Eocene-Oligocene transition (about 34 Ma). The long history of thermal lithospheric subsidence in the southern and southeastern Weddell Sea and the proximity to terrigenous sediment supply have resulted in the large deposit thicknesses along the continental margin of Dronning Maud Land and the Filchner-Ronne shelf (Fig. 9B, Fig 11). Plate-kinematic reconstructions (König and Jokat, 2006) demonstrate that the Weddell Sea rift evolved into a large basin already in the Early Cretaceous, creating the wide embayment of the Filchner-Ronne Basin between the elevated regions of the southern Antarctic Peninsula, the Ellsworth-Whitmore Mountains of West Antarctica and Dronning Maud Land of East Antarctica. King (2000) proposed that the Weddell Sea embayment is likely to have been a major depocentre since the Jurassic. The reconstructed Antarctic paleotopography of Wilson et al. (2012) suggests the continued presence of a low-lying basin in this region in the late Eocene. As most of the period of sediment deposition during pre-glacial times falls into the Cretaceous and early Cenozoic global 'greenhouse' climate (e.g. (Zachos, 2008)), we can rule out any role for glacially-controlled transport processes. During late Eocene times, temperate alpine-style glacial conditions have been suggested for the northern Antarctic Peninsula region by analyses of shallow sediment drill cores from the northwestern Weddell Sea shelf (Smith and Anderson, 2010, Anderson et al., 2011), but it can be expected that their contribution to the pre-glacial sediments in the entire Weddell Sea basin is relatively small (Fig. 9A).

It can therefore be assumed that the bulk of the sediment transport was carried out by continental-scale river systems, transporting sediments from the Antarctic interior through the Filchner-Ronne rift basin and depositing most of it in the evolving southern Weddell Sea (Weber et al., 1994; Michael et al., 2002) (Fig. 11). It can be speculated that erosion of the subduction-related orogen of the Antarctic Peninsula supplied sediments to the western Weddell Sea margin.

4.6.2 Transitional phase

In our stratigraphic age model, deposition of the transitional unit begins at the Eocene-Oligocene boundary (~34 Ma) in the southern Weddell Sea and between 10 and 15.5 Ma in the northwestern Weddell Sea. Compared to the pre-glacial unit, the sediment thickness is relatively thin, but it accumulated at much higher rates (up to 140 m/Myr), particularly in the southern Weddell Sea depocentre (Fig. 8C, Fig. 9B). The change of sedimentation rate can be related to marked changes in transport and depositional environment, for instance the onset of coast-proximal ice sheet grounding that would increase the quantity of sediments delivered into the basin. The shift to a cool-temperate climate with perennial sea-ice in Antarctica is evident in the global deep-sea oxygen isotope signature at the Eocene-Oligocene boundary (Zachos et al., 2001, 2008; Liu et al., 2009). Gravel- and pebble-grade IRDs have been observed in middle to lower Oligocene sediments of ODP Leg 113 Site 693 (Barker, 1988). This implies that glaciers were grounded close to the coast or on the inner shelf at that time (Barker et al., 2005).

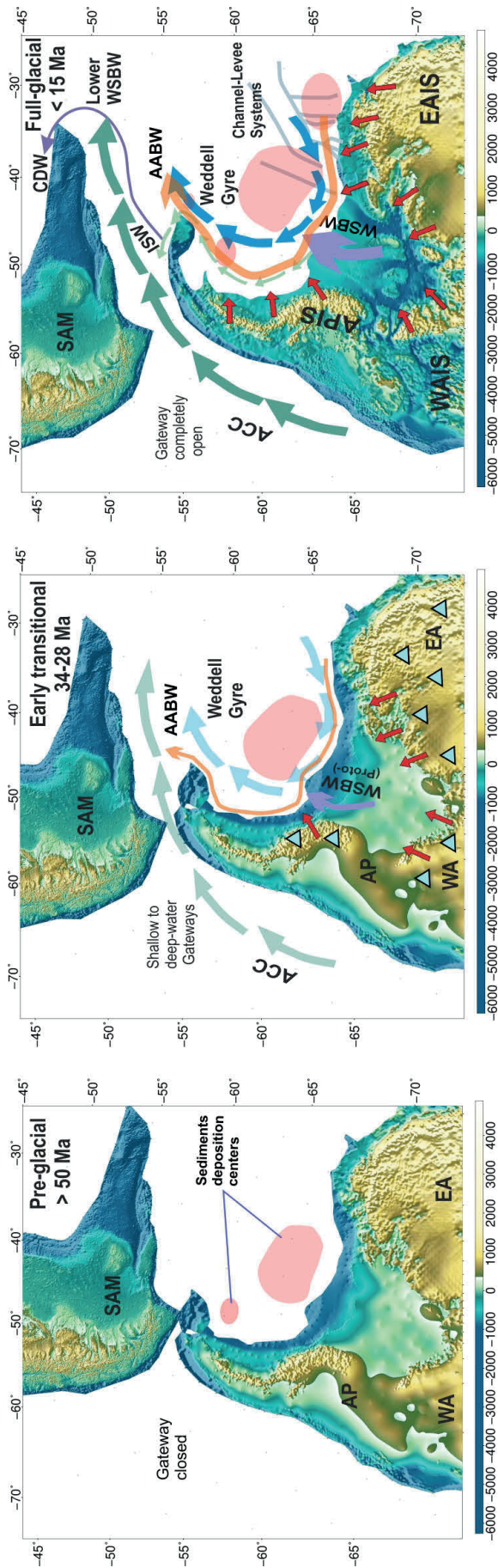


Fig. 4.11 Model showing the role of plate-tectonic motion, ice sheet development, ocean circulation and sediment deposition center in the greater Weddell Sea region. The South American Plate is from ETOPO1 (Amante and Eakins, 2009), the rotation angles for the full-glacial, transitional and pre-glacial are from Eagles and Jokat (2014). Present-day Antarctic bed topography is from BEDMAP2 (Fretwell et al., 2013). The reconstruction topographies of Antarctica are taken from Wilson et al., 2012. (A) Pre-glacial regime, SAM: South American Plate, AP: Antarctica Peninsula, WA: West Antarctica, EA: East Antarctica. Yellow bars: pre-glacial sediment deposition centers, Green lines: river system. (B) Transitional regime. ACC: Antarctic Circumpolar Current. Triangles: ice-caps. Red arrow: the direction of ice movement. (C) Full-glacial regime.

Sediments of the transitional unit are about 1-km thick off the eastern Antarctic Peninsula margin, and decrease to 0.5 km thickness in the northwestern Weddell Sea (Fig. 8C). Our calculations show that sedimentation rates are in the range of 60-100 m/Myr (Fig. 9C) and compare to those determined for the region by Maldonado et al. (2003) (70 - 108 m/Myr) and Lindeque et al. (2013) (110 m/Myr). The variable sedimentation rates and thicknesses during the transitional phase may be related to varying onset times for the various sectors of the Antarctic Peninsula Ice Sheet. Anderson et al. (2011) and Smith and Anderson (2010) argued for the presence of local glaciers and ice caps during the middle Eocene-early Oligocene (49 - 32 Ma) and early Oligocene at the northern Antarctica Peninsula. We see no obvious evidence to conclude that a major WAIS was grounded on the inner shelf of the Weddell Sea in the Oligocene. What if, we would expect to have a significant higher sedimentation rate than we observe as well as erosional features occurred during the deposition processes. This confirms earlier studies showing that continental ice of West Antarctica consisted of isolated ice caps in the Oligocene that amalgamated and advanced onto the continental shelves not earlier than at Late Miocene times (Anderson et al., 2010).

The development of the Antarctic Circumpolar Current (ACC) would not only have enhanced Antarctic ice sheet growth but also changed the way that the Weddell Gyre, which may have affected the sediment deposition and erosion in the Weddell Sea, interacted with the global ocean. In particular, Antarctic Bottom Water (AABW) and Warm Saline Deep Water, as shown by Diester-Hass and Zahn (1996), may have been integrated to the general ocean circulation during the transitional regime (Fig. 11).

4.6.3 Full-glacial phase

The full-glacial unit of the Weddell Sea has been deposited since the middle Miocene (15 Ma) according to our stratigraphic model. A large amount of sediments (up to 5 km thickness) were deposited (Fig. 8D) at very high sedimentation rates (up to 180 m/Myr) in the main depocentre in front of the Filchner-Ronne Ice Shelf. The resulting Crary Fan is not mapped completely in the full glacial unit due to the limited seismic data in the southern Weddell Sea. Despite the lack of data, it is evident that the fan was formed by glacial sediments supplied from western Dronning Maud Land as inferred in earlier studies. Kuvaas (1991) argue that this would have occurred after the EAIS advanced to the coastline, triggering enormous down-slope transport to the continental rise in the middle Miocene (Bart et al. 1999). The time since the middle Miocene is the period in which the major Antarctic ice sheets have been built (e.g., Lear, 2000; Shevenell et al., 2004; Zachos et al., 2001) and played a dominant role in sedimentation processes. The first significant observations of IRDs and turbidite units are reported from the middle Miocene of ODP sites 693 and 694, indicating the presence of ice sheets grounding on the shelves and generating a large influx of sediments to the Weddell Sea basin (Barker, 1988; Kennett, 1990).

Our data reveal another depocentre off the western Weddell Sea margin east of the Antarctica Peninsula with about 3 km sediment thickness and relatively high sedimentation rates (Fig. 8D, 9C). Shelf sediment progradation observed in seismic profiles east of the Antarctic Peninsula and depositional lobes in the northwestern Weddell Sea imply phases of an APIS advancing to the outer shelf (Barker, 2002; Bart et al., 2005). From this marine evidence, it is possible to infer that significant ice

sheet growth in West Antarctica and on the Antarctic Peninsula occurred and impacted the sedimentation during the full-glacial time in the Weddell Sea region.

Contourite studies have identified ocean-bottom current directions around the Antarctic Peninsula and at the southern continental margin of the Weddell Sea (Michels et al., 2001; Maldonado et al., 2005). They also infer increased bottom current intensity along the entire Antarctic margin of the Weddell Sea in the period from ~15 to 5 Ma. The Weddell Gyre and a fully developed ACC interacted with other water masses to influence the deposition pattern (Fig. 11). The distribution of contourite drifts was mainly controlled by the physiography of the basin and bottom current flow directions (Maldonado et al., 2005). As illustrated by Fig. 6, abundant sediment drifts and channel-levee systems occur on the continental margin in the full-glacial unit. Younger sediments are mostly drift deposits that reach a thickness of more than 1 km and accumulated at rates of more than 80 m/Myr, particularly during the late Miocene (Fig. 5, Fig. 9C). These drift bodies developed during the transport of sediments by a combination of contour currents and/or turbidity flows (Michels et al., 2001; Kuhn et al., 2001; Uenzelmann-Neben et al., 2006), fed by an abundance of glacial sediments brought to the basin margin cycles of ice sheet advanced and retreat.

4.6.4 Paleobathymetry

Possible sources of error in the paleobathymetric estimates are uncertainties in the modelled lithospheric thickness, stretching factor, porosity-depth relationship, and distributions of crustal nature and age. Seismic data from the edge of the Filchner-Ronne Ice Shelf suggest a continental crustal stretching factor between 1.5 and 3.0 (Hübscher et al., 1996; Jokat et al., 1996). Following König and Jokat (2006), we use a relatively large stretching factor of 2.5 for the rifted continental crust and lithosphere, which they adopted for reconstructing the initial position of the Antarctic Peninsula with respect to East Antarctica at the Filchner-Ronne Ice Shelf. Stretching factors of 1.5 - 3.0 lead to differences of 0.2 - 2.0 km in thermal subsidence. A large source of uncertainty consists of the lack of knowledge on the extent of the continent-ocean transition of the Weddell Sea embayment. We used the simplified continent-ocean transition (COT) proposed by König and Jokat (2006) and applied a simple boundary between regions modeled with continental and oceanic thermal subsidence. For instance, at 120 Ma, the effect of thermal subsidence varies from 1.6 km to 2.5 km based on the oceanic crust model. However, the continental crustal subsidence model results in about 3 km sinking close to the COT, which means the relative error can be as high as 95%.

Available drill sites in the Weddell Sea basin only provide local porosity-depth relationships to a maximum sedimentary penetration depth of 700 m. Our adoption of these porosities for the entire basin is an oversimplification. For instance, as Fig. 3 shows if we apply a top porosity ϕ_0 and constant c as 50%, 0.0005 or 80%, 0.0007 instead of 70%, 0.0007, which was obtained from ODP Leg 113, this leads to relative errors around -30% and +16% of $\phi_0=70\%$ and -33% for $c=0.0007$.

Further sources of uncertainty arise from processes and parameters that we have not taken into account. Oceanic crustal thickness variations lead to areas of shallower and deeper bathymetry. Long wavelength changes result from the transmission of viscous stresses to the lithosphere from the underlying mantle. This dynamic topography may affect large areas with amplitudes of ± 1 km (Steinberger et al, 2001). Negative dynamic topography accompanies subduction, which was ongoing along the Antarctic Peninsula with an eastward subducting plate throughout Cretaceous and Cenozoic times. Positive dynamic topography accompanies the action of mantle

plumes, which are thought to have accompanied the earliest stages of breakup in the Weddell Sea and to have affected the Maud Rise region in Albian times.

Table 4.2 Parameters used for the subsidence calculation of rifted crust.

parameter	name	value
a	Lithosphere thickness	125 km
ρ_w	density of sea water	1.03 g/cm ³
ρ_m	density of mantle	3.3 g/cm ³
α	thermal expansion coefficient	3.1*10 ⁻⁵ 1/°C
T1	asthenosphere temperture	1365 °T
τ	thermal time constant	62.8 Ma

However, by taking into account all presently available geophysical and geological information and considering the existing large uncertainties, we are confident to deliver a first estimate of the paleobathymetric evolution of the Weddell basin, which will improve the testing of paleoceanographic and paleoclimatic scenarios through model simulations.

4.7. Conclusions

1. We extended existing local and sub-regional stratigraphic models to the entire Weddell Sea basin. Two seismic unconformities (WS-u4, WS-u5) and three seismic units (pre-glacial, transitional, full glacial) were mapped and served as a base to calculate for the first time basin-wide grids of sediment depths, thicknesses, rates and paleobathymetries.
2. The distribution of the total sediment thickness shows a decreasing trend northward. The maximum sediment thickness of up to 12 km is found in the southern Weddell Sea in front of the Filchner-Ronne Ice Shelf.
3. The pre-glacial unit has the thickest sediments owing to its long sedimentation period of 80 - 100 m/Myr, but was deposited with a relatively low rate. The tectonic evolution and seafloor spreading history of the Weddell Sea interacted with terrigenous sediment supply processes to control its distribution.
4. The transitional unit accumulated at a relatively high sedimentation rate. Its thickness varies in the range of 0 - 3 km. A relatively strong sediment supply from a growing EAIS grounded to the coast or even inner shelf could be the main contributor to sedimentation on the continental rise.
5. The high sedimentation rate at the full glacial period generated depocentres near the margins of the southern, southeastern and western Weddell Sea. Here, the

maximum sediment thickness is 4 - 5 km for this period. Sedimentation rates varied from 0 to 200 m/Myr. The large amount of sediments, and their deposition at high sedimentation rates in the southern Weddell Sea imply an increase of glacial advances of grounded EAIS, WAIS and APIS to the middle or outer shelf since the middle Miocene. Large sedimentary drifts and channel-levee complexes are abundant close to the continental margin, suggesting turbidity currents and other mass-flow processes redistributing the sediments.

6. We derived a grid series of the paleobathymetric evolution of the Weddell Sea basin for 120 Ma, 34 Ma and 15 Ma, which will improve the testing of paleoceanographic and paleoclimatic scenarios through model simulations.

4.8 Acknowledgements

The authors would like to thank the masters, crews and seismic teams of the many ship expeditions to the Weddell Sea who made the acquisition of the data used in this study possible. The British Antarctic Survey (BAS), the German Federal Institute of Geosciences and Resources (BGR) as well as research institutes in Norway and Spain are gratefully acknowledged for their contribution of the used seismic data to the Antarctic Seismic Data Library System (SDLS). We used the GMT graphics software (Smith and Wessel, 1990) for gridding routines and map productions. Many thanks to Graeme Eagles for his careful reading of the manuscript before submission. X.H. has been receiving a PhD scholarship from the Chinese Scholarship Council. This study has primarily been supported through institutional funds of the Alfred Wegener Institute through Work Package 3.2 of its research program PACES.

4.9 References

- Abreu, V.S., and Anderson, J.B., (1998). Glacial eustasy during the Cenozoic: Sequence stratigraphic implications. *Am. Assoc. Petrol Geol. Bulletin*, 82, 1385–1400.
- Anderson, John B., Andrews, John T (1999): Radiocarbon constrains on ice sheet advance and retreat in the Weddell Sea, Antarctica. *Geology*, 27(2), 179-182, doi:10.1130/0091-7613(1999)027<0179:RCOISA>2.3.CO;2
- Anderson, J.B., Wellner, J.S. (Eds.), (2011). *Tectonic, Climatic, and Cryospheric Evolution of the Antarctic Peninsula*. American Geophysical Union, Washington, D. C., <http://dx.doi.org/10.1029/SP063> (218 pp.).
- Anderson, J.B., (1999). *Antarctic Marine Geology*. Cambridge University Press, 289 pp.
- Anderson, J.B., and S.S. Shipp, (2001). Evolution of the West Antarctic Ice Sheet. *Antarctic Res. Series*, 77, 45-57.
- Anderson, J.B., Warny, S., Askin, R., Wellner, J., Bohaty, S., Smith, T., 2011. Cenozoic cryosphere expansion and the demise of Antarctica's last refugium. *Proc. Natl. Acad. Sci.*, 108, 11299–11726.
- Amante, C. and B. W. Eakins, ETOPO1 1 Arc-Minute Global Relief Model: Procedures, Data Sources and Analysis. NOAA Technical Memorandum NESDIS NGDC-24, 19 pp, March 2009.
- Arndt, J.E., H. W. Schenke, M. Jakobsson, F. Nitsche, G. Buys, B. Goleby, M. Rebesco, F. Bohoyo, J.K. Hong, J. Black, R. Greku, G. Udintsev, F. Barrios, W. Reynoso-Peralta, T. Morishita, R. Wigley, "The International Bathymetric Chart of

the Southern Ocean (IBCSO) Version 1.0 - A new bathymetric compilation covering circum-Antarctic waters", *Geophys Res Lett.*, doi: 10.1002/grl.50413.

Allen, P. A. and Allen, J. R., 2005. *Basin Analysis: Principles and Applications*, second edition, Blackwell Publishing, 549pp.

Bart, P.J., D. E. Batist and Jokat, W., 1999. Interglacial collapse of Crary Trough Mouth Fan, Weddell Sea, Antarctica: implications for Antarctic glacial history analysis. *J. Sediment Res.*, 69(6), 1276-1289.

Bart, P.J., Egan, D.E., Warny, S.A., 2005. Direct constraints on Antarctic Peninsula Ice Sheet grounding events between 5.12 and 7.94 Ma. *J. Geophys. Res.*, 110, F04008, doi:10.1029/2004JF000254.

Barker, P.F., Camerlenghi, A., (2002). Glacial history of the Antarctic Peninsula from Pacific margin sediments. In: Barker, P.F., Camerlenghi, A., Acton, G.D., Ramsay, A.T.S. (Eds.), *Proceedings of the Ocean Drilling Program, Scientific Results*, 178. 1–40. Available from: Ocean Drilling Program, College Station, TX, 77845-9547, USA.

Barker, P.F., Kennett, J.P., et al, (1988). *Proceedings of the Ocean Drilling Program, Scientific Results Leg 113. Ocean Drilling Program: 774.* doi:10.2973/odp.proc.ir.113.1988.

Barker, P.F., Thomas, E., (2004). Origin, signature and palaeoclimate influence of the Antarctic Circumpolar Current. *Earth Sci Rev.*, 55, 1–39. doi:10.1016/j.earscirev.2003.10.003.

Brown, B., Gaina, C., Mueller, R. D., (2006). Circum-Antarctic palaeobathymetry: Illustrated examples from Cenozoic to recent times. *Paleogeogr. Paleoclimatol, Paleocol.*, 231, 158-168. doi:10.1016/j.palaeo.2005.07.033.

Bohoyo, F., Galindo-Zaldívar, J., Jabaloy, A., Maldonado, A., Rodríguez-Fernández, J., Schreider, A., Suriñach, E., (2007). Extensional deformation and development of deep basins associated with the sinistral transcurrent fault zone of the Scotia–Antarctic plate boundary. *Geological Society, London, Special Publications* 290, 203–217. <http://dx.doi.org/10.1144/SP290.6>.

DeConto, R.D., Pollard, D., 2003a. Rapid Cenozoic glaciation of Antarctica triggered by declining atmospheric CO₂. *Nature* 421, 245– 249.

DeConto, R.D., Pollard, D., 2003b. A coupled climate–ice sheet modeling approach to the early Cenozoic history of the Antarctic ice sheet. *Palaeogeogr. Palaeoclim. Palaeocol.* 198, 39– 52.

Dalziel, I.W.D., 2007. The Ellsworth Mountains: Critical and enduringly enigmatic, in: Copper, A.K., Raymond, C.F. (Eds.), *Antarctica: A Keystone in a Changing World-Online Proceedings of the 1-th ISAES*. USGS Open-File Report 2007-1047, Short Research Paper 004, 5p.; doi: 10.3133/of2007-1047.srp004.

Dalziel, I.W.D., Grunow, A., 1992. Late Gondwanide tectonic rotations within Gondwanaland. *Tectonics* 11, 603-606.

Diester-Haass, L. and Zahn, R. (1996). The Eocene-Oligocene transition in the Southern Ocean: history of water masses, circulation, and biological productivity inferred from high resolution records of stable isotopes and benthic foraminiferal abundances (ODP Site 689). *Geology*, vol.26, p.163-166.

Eagles, G., and Livermore, R. A. (2002). Opening history of Powell Basin, Antarctic Peninsula. *Mar. Pet Geol.*, 185(3-4), 195-205. [http://dx.doi.org/10.1016/S0025-3227\(02\)00191-3](http://dx.doi.org/10.1016/S0025-3227(02)00191-3).

Eagles, G., Livermore, R.A., Morris, P., (2006). Small basins in the Scotia Sea: the Eocene Drake Passage gateway. *Earth Planet. Sci. Lett.* 242, 343–353. <http://dx.doi.org/10.1016/j.epsl.2005.11.060>.

Eagles, G. Jokat, W. (2014). Plate tectonic reconstructions for studies in Drake Passage, *Tectonophysics*, 611, 28-50, doi: 10.1016/j.tecto.2013.11.021

Fretwell, P. , Pritchard, H. , Vaughan, D. G. , Bamber, J. L. , Barrand, N. , Bell, R. , Bianchi, C. , Bingham, R. , Blankenship, D. D. , Casassa, G. , Catania, G. , Callens, D. , Conway, H. , Cook, A. , Corr, H. F. J. , Damaske, D. , Damm, V. , Ferraccioli, F. , Forsberg, R. , Fujita, S. , Furukawa, T. , Gogineni, P. , Griggs, J. , Hamilton, G. , Hindmarsh, R. , Holmlund, P. , Holt, J. , Jacobel, R. , Jenkins, A. , Jokat, W. , Jordan, T. , King, E. C. , Krabill, W. , Riger-Kusk, M. , Tinto, K. , Langley, K. , Leitchenkov, G. , Luyendyk, B. P. , Matsuoka, K. , Nixdorf, U. , Nogi, Y. , Nost, O. , Popov, S. , Rignot, E. , Rippin, D. , Riviera, A. , Ross, N. , Siegert, M. J. , Shibuya, K. , Smith, A. , Steinhage, D. , Studinger, M. , Sun, B. , Thomas, R. , Tabacco, I. , Welch, B. , Young, D. , Xiangbin, C. and Zirizzotti, A. (2013): Bedmap2: improved ice bed, surface and thickness datasets for Antarctica , *The Cryosphere*, 7 , pp. 375-393 . doi: 10.5194/tc-7-375-2013.

Foldvik, A., T. Gammelsrød, S. Østerhus, E. Fahrback, G. Rohardt, M. Schroder, K. Nicholls, L. Padman, and R. Woodgate (2004), Ice Shelf Water overflow and bottom water formation in the southern Weddell Sea, *J. Geophys. Res.*, 109, C02015, doi:10.1029/2003JC002008.

Ghidella, M. E., G. Yañez, and J. L. LaBrecque (2002), Revised tectonic implications for the magnetic anomalies of the western Weddell Sea, *Tectonophysics*, 347, 65– 86. [http://dx.doi.org/10.1016/S0040-1951\(01\)00238-4](http://dx.doi.org/10.1016/S0040-1951(01)00238-4).

Hübscher, C., (1994). Krustenstrukturen und Verlauf des Kontinentalrandes im Weddell-Meer/Antarktis. *Ber. Polarforsch.* 147, 233.

Hübscher, C., Jokat, W., Miller, H., (1996). Structure and origin of southern Weddell Sea crust: results and implications. In: Storey, B.C., King, E.C., Livermore, R.A. (Eds.), *Weddell Sea Tectonics and Gondwana Break-up*. Geol. Soc., London, Spec Publ. 108, 201-212.

Hübscher, C., Jokat, W., King, E., Kudryavtzev, G., Leitchenkov, G., 1998. The Weddell Sea basin between Nerkner Island and Antarctic Peninsula. *Terra Antarctica*, 5(195-198).

Hambrey, M. J. , Ehrmann, W. and Larsen, B. (1991). Cenozoic glacial record of the Prydz Bay continental shelf, East Antarctica , In: Barron, J; Larsen, B, et al. (eds.), *Proc. ODP, Sci. Results*, College Station, TX. (Ocean Drilling Program), 119, 77-132, 119 , pp. 77-132 . doi: 10.2973/odp.proc.sr.119.200.1991.

Haugland, K., Kristoffersen, Y. and Velde, A. 1985: Seismic investigations in the Weddell Sea embayment. *Tectonophysics* 114, 293-313. [http://dx.doi.org/10.1016/0040-1951\(85\)900018-6](http://dx.doi.org/10.1016/0040-1951(85)900018-6).

Jokat, W., C. Hübscher, U. Meyer, L. Oszko, T. Schöne, W. Versteeg, and H. Miller (1996), The continental margin off East Antarctica between 10°W and 30°W, in *Weddell Sea Tectonics and Gondwana Break up*, edited by B. C. Storey, E. C. King, and R. A. Livermore, *Geol. Soc. Spec. Publ.*, 108, 129–141.

Jokat, W., Boebel, T., König, M., Meyer, U., (2003). Timing and geometry of early Gondwana breakup. *J. Geophys. Res.*, 108 (B9), 2428. <http://dx.doi.org/10.1029/2002JB001802>.

Kudryavtzev, G.A., Smirnova, E.A., Schumilov, V.A., Poselov, V.A., (1987). Deep structure of the earth crust in the southern part of the Weddell Sea (by data of the DSS line (in Russian). In: Ivanov, V.L., Grikurov, G.E. (Eds.), *The Geological and Geophysical Research in Antarctica*. Sevmorgeologia, Leningrad, pp. 99-108.

Kennett, J. P., and D. A. Hodell. (1995). Stability or instability of Antarctic ice sheets during warm climates of the Pliocene? *GSA Today* 5, 10-13.

Kennett, J.P.a.B., P, F., (1990). Climatic and oceanographic developments in the Weddell Sea, Antarctica, since the latest Cretaceous: An ocean-drilling Program. *Ocean Drilling Program scientific results*, 113: 865-880.

King, E. C, (2000). The crustal structure and sedimentation of the Weddell Sea embayment: implication for Gondwana reconstructions. *Tectonophysics* 327, 195-212.

König, M., Jokat, W., (2006). The Mesozoic breakup of the Weddell Sea. *J. Geophys. Res.*, 111, B12102. doi: 10.1029/2005JB004035.

König, M., Jokat, W., (2010). Advanced insights into magmatism and volcanism of the Mozambique Ridge and Mozambique Basin in the view of new potential field data. *Geophys. J. Int.*, 180, 158-180. doi: 10.1111/j.1365-246X.2009.04433.x.

Kovacs, L.C., Morris, P., Brozena, J., Tikku, A., (2002). Seafloor spreading in the Weddell Seas from magnetic and gravity data. *Tectonophysics* 347, 43–64. doi: 10.1016/S0040-1951(01)00237-2.

Kuvaas, B., Kristoffersen, Y., (1991). The Crary Fan: a trough-mouth fan on the Weddell Sea Continental Margin, Antarctica. *Mar. Geol.*, 97, 345–362. [http://dx.doi.org/10.1016/0025-3227\(91\)90125-N](http://dx.doi.org/10.1016/0025-3227(91)90125-N).

Kristoffersen, Y., Haugland, K., (1986). Geophysical evidence for East Antarctic plate boundary in the Weddell Sea. *Nature* 322, 538–541. doi:10.1038/322538a0.

Kadmina, I.N., Kurinin, R.G., Masolov, V.N., Grikurov, G.E, (1983). Antarctic crustal structure from geophysical evidence: a review. *Antarctic Earth Science*: 498-502.

Leitchenkov, G., Guseva, J., Gandyukhin, V., Grikurov, G., Kristoffersen, Y., Sand, M., Golynsky, A., Aleshkova, N., 2008. Crustal structure and tectonic provinces of the Riiser-Larsen Sea area (East Antarctica): results of Geophysical studies. *Mar. Geophys. Res.*, 29, 135–158. <http://dx.doi.org/10.1007/s11011-008-9051-z>.

Lear, C. H., H. Elderfield, and P. A. Wilson (2000), Cenozoic deep-sea temperatures and global ice volumes from Mg/Ca in benthic foraminiferal calcite, *Science*, 287 269–272. doi: 10.1126/science.287.5451.269.

Lindeque, A., Martin, Y., Gohl, K., Maldonado, A. (2013): Deep sea pre-glacial to glacial sedimentation in the Weddell Sea and southern Scotia Sea from a cross-basin seismic transect. *Mar. Geol.*, 336, 61-83. <http://dx.doi.org/10.1016/j.margeo.2012.11.004>.

Liu, Z, Pagani, M, Zinniker, D, Deconto, R, Brinkhuis, H, Shah, R. S, Leckie, M, Pearson, A. (2009): Global Cooling During the Eocene-Oligocene Climate Transition. *Science* 323, 1187-1190. doi: 10.1126/science.1166368.

Lawver, L. A., and L. M. Gahagan (1998), Opening of Drake Passage and its impact on Cenozoic ocean circulation, in *Tectonic Boundary Conditions for Climate Reconstructions*, edited by T. J. Crowley, and K. C. Burke, pp. 212–223, Oxford Univ. Press, New York.

Lawver, L. A., J.-Y. Royer, D. T. Sandwell, and C. R. Scotese, Crustal development: Gondwana break-up - Evolution of the Antarctic continental margins, in *Geological Evolution of Antarctica*, edited by M. R. A. Thompson, J. A. Crame, and J. Thompson, Cambridge Univ., 533-540, 1991.

Livermore, R.A. & Woollett, R. W (1993): Seafloor spreading in the Weddell Sea and southwest Atlantic since the Late Cretaceous. - *Earth Planet. Sci. Letters* 117,475-495.

Livermore, R.A., Hunter, R.J., (1996). Mesozoic seafloor spreading in the southern Weddell Sea. In: Storey, B., King, E.C., Livermore, R.A. (Eds.), *Weddell*

Sea Tectonics and Gondwana Break-up: *Geol. Soc. Spec. Publ.*, 108, pp. 227–241 (London). doi: 10.1144/GSL.SP.1996.108.01.17.

Livermore, R., Nankivell, A., Eagles, G., Morris, P., 2005. Paleogene opening of Drake Passage. *Earth Planet. Sci. Lett.*, 236, 459–470. <http://dx.doi.org/10.1016/j.epsl.2005.03.027>.

Maldonado, A., Barnolas, A., Bohoyo, F., Galindo-Zaldívar, J., Hernández-Molina, J., Lobo, F., Rodríguez-Fernández, J., Somoza, L., Vázquez, J.T., (2003). Contourite deposits in the central Scotia Sea: the importance of the Antarctic Circumpolar Current and Weddell Gyre flows. *Paleogeogr. Paleoclimatol. Paleoecol.*, 198, 187–221. doi:10.1016/S0031-0182(03)00401-2.

Maldonado, A., Barnolas, A., Bohoyo, F., Escutia, C., Galindo-Zaldívar, J., Hernández-Molina, F.J., Jabaloy, A., Lobo, F.J., Nelson, C.H., Rodríguez-Fernández, J., Somoza, L., Vázquez, J.T., (2005). Miocene to recent contourite drifts development in the northern Weddell Sea (Antarctica). *Global Planet Change* 45, 99–129. <http://dx.doi.org/10.1016/j.gloplacha.2004.09.013>.

Maldonado, A., Bohoyo, F., Galindo-Zaldívar, J., Hernández-Molina, F.J., Lobo, F.J., Shreyder, A.A., Suriñach, E., 2007. Early opening of Drake Passage: regional seismic stratigraphy and paleoceanographic implications, in Antarctica: A Keystone in a Changing World. Extended Abstract EA57, online Proceedings of the 10th International Symposium on Antarctic Sciences (ISAES). In: Cooper, A.K., Raymond, C.R., et al. (Eds.), USGS Open-File Report (<http://pubs.usgs.gov/of/2007/1047/ea/of2007-1047ea057.pdf>).

Michels, K.H., Rogenhagen, J., Kuhn, G., (2001). Recognition of contour-current influence in mixed contourite–turbidite sequences of the western Weddell Sea, Antarctica. *Mar. Geophys. Res.*, 22, 465–485. doi: 10.1023/A:1016303817273.

Michels, K.H., Kuhn, G., Hillenbrand, C.-D., Diekmann, B., Fütterer, D.K., Grobe, H., Uenzelmann-Neben, G., (2002). The southern Weddell Sea: combined contourite–turbidities sedimentation at the southeastern margin of the Weddell Gyre. In: Stow, D.A.V., Pudsey, C., Howe, J.C., Faugères, J. C., Viana, A.R. (Eds.), *Geological Society of London, Memoirs*, 22, pp. 305–323. <http://dx.doi.org/10.1144/GSL.MEM.2002.022.01.32>.

Miller, H., Henriot, J.P., Kaul, N., Moons, A., (1990). A fine-scale stratigraphy of the eastern margin of the Weddell Sea. In: Bleil, U., Thiede, J. (Eds.), *Geological History of the Polar Oceans: Arctic Versus Antarctic*. Kluwer Academic Publishers, pp. 131–161. doi: 10.1007/978-94-009-2029-3_8.

McKenzie, D.P. 1978. Some remarks on the development of sedimentary basins. *Earth and Planetary Science Letters*, 40, 25–32.

Miller, K., 2005. The Phanerozoic Record of Global Sea-Level Change, *Science*, 310, doi: 10.1126/science.1116412.

Naish, T., Powell, R., Levy, R., Henrys, S., Krissek, L., Niessen, F., Pompilio, M., Scherer, R. & Wilson, G.S. (2007), "Synthesis of the initial scientific results of the MIS Project (AND-1B core), Victoria Land Basin, Antarctica", *Terra Antarctica*, vol. 14, no. 3, pp. 317-327.

Naish, T., Powell, R., Levy, R., Wilson, G., Scherer, R., Talarico, F., Krissek, L., Niessen, F., Pompilio, M., Wilson, T., Carter, L., DeConto, R., Huybers, P., McKay, R., Pollard, D., Ross, J., Winter, D., Barrett, P., Browne, G., Cody, R., Cowan, E., Crampton, J., Dunbar, G., Dunbar, N., Florindo, F., Gebhardt, C., Graham, I., Hannah, M., Hansraj, D., Harwood, D., Helling, D., Henrys, S., Hinnov, L., Kuhn, G., Kyle, P., Läufer, A., Maffioli, P., Magens, D., Mandernack, K., McIntosh, W., Millan, C., Morin, R., Ohneiser, C., Paulsen, T., Persico, D., Raine, I., Reed, J.,

Riesselman, C., Sagnotti, L., Schmitt, D., Sjunneskog, C., Strong, P., Taviani, M., Vogel, S., Wilch, T. & Williams, T. 2009, "Obliquity-paced Pliocene West Antarctic ice sheet oscillations", *Nature*, vol. 458, no. 7236, pp. 322-328.

Nicholls, K. W., S. Østerhus, K. Makinson, T. Gammelsrød, and E. Fahrback (2009). Ice-ocean processes over the continental shelf of the southern Weddell Sea, Antarctica: A review, *Rev. Geophys.*, 47, RG3003, doi:10.1029/2007RG000250.

Orsi, A., G. Johnson, and J. Bullister (1999), Circulation, mixing, and production of Antarctic Bottom Water, *Prog. Oceanogr.*, 43, 55–109.

Passchier, S., Bohaty, S.M., Jiménez-Espejo, F., Pross, J., Röhl, U., van de Flierdt, T., Escutia, C., and Brinkhuis, H., 2013. Early Eocene to middle Miocene cooling and aridification of East Antarctica. *Geochem., Geophys., Geosyst.*, 14(5):1399–1410. doi:10.1002/ggge.20106.

Pfuhl, H.A, and I Nicholas M., (2007), The Oligocene-Miocene boundary – cause and consequence from a Southern Ocean perspective, in *Deep time perspectives on climate change - marrying the signal from computer models and biological proxies*, The Micropalaeontological Society Special Publications, edited by Mark Williams, Alan M Haywood, F J Gregory and Daniela N Schmidt, pp. 389-407, The Micropalaeontological Society, London, ISBN: 978-1-86239-240-3.

Pollard, D. and R.M. DeConto. 2005. Hysteresis in Cenozoic Antarctic ice sheet variations. *Glob. Planet. Change*, 45, 9-21, doi: 10.1016/j.gloplacha.2004.09.011.

Pollard, D., DeConto, R.M., (2009). Modelling West Antarctic ice sheet growth and collapse through the past five million years. *Nature* 458, 320–323. <http://dx.doi.org/10.1038/nature07809>.

Parsons, B., Sclater, J.G., 1977. An analysis of the variation of ocean floor bathymetry and heat flow with age. *J. Geophys. Res.* 82, 803–827.

Rebesco, M., Camerlenghi, A., (2008). Late Pliocene margin development and mega debris flow deposits on the Antarctic continental margins: evidence of the onset of the modern Antarctic Ice Sheet? *Paleogeogr. Paleoclimatol, Paleoecol.*, 260, 149–167. doi: 10.1016/j.palaeo.2007.08.009.

Rebesco, M., Camerlenghi, A., Geletti, R., Canals, M., (2006). Margin architecture reveals the transition to the modern Antarctic ice sheet ca. 3 Ma. *Geology* 34, 301–304. <http://dx.doi.org/10.1130/G22000.1>.

Rogenhagen, J., Jokat, W., (2000). The sedimentary structure in the western Weddell Sea. *Mar. Geol.*, 168, 45–60. [http://dx.doi.org/10.1016/S0025-3227\(00\)00048-7](http://dx.doi.org/10.1016/S0025-3227(00)00048-7).

Rogenhagen, J., Jokat, W., (2002). Origin of the gravity ridges and Anomaly-T in the southern Weddell Sea. In: Gamble, J.A., Skinner, D.N.B., Henrys, S. (Eds.), *Antarctica at the Close of a Millennium, Proceedings of the 8th International Symposium on Antarctic Earth Sciences*. Royal Society of New Zealand, Wellington, pp. 227–231.

Rogenhagen, J., Jokat, W., Hinz, K., Kristoffersen, Y., (2004). Improved seismic stratigraphy of the Mesozoic Weddell Sea. *Mar. Geophys. Res.*, 25, 265–282. <http://dx.doi.org/10.1007/s11001-005-1335-y>.

Smith, R.T., Anderson, J.B., (2010). Ice-sheet evolution in James Ross basin, Weddell Sea margin of the Antarctic Peninsula: the seismic stratigraphic record. *Geological Society of America Bulletin* 122 (5/6), 830–842. <http://dx.doi.org/10.1130/B26486.1>.

Smith, R.T., Anderson, J.B., (2011). Seismic stratigraphy of the Joinville Plateau: implications for regional climate evolution. In: Anderson, J.B., Wellner, J.S. (Eds.), *Tectonic, Climatic, and Cryospheric Evolution of the Antarctic Peninsula*. Geopress,

American Geophysical Union, Washington DC, USA, pp. 51–61.
<http://dx.doi.org/10.1029/2010SP000980>.

Steinberger, B., Schmelting, H., Marquart, G., 2001. Large-scale lithospheric stress field and topography induced by global mantle circulation. *Earth Planet. Sci. Lett.* 186, 75–91.

Stein, C. and S. Stein, A model for the global variation in oceanic depth and heat flow with lithospheric age, *Nature*, 359, 123–128, 1992.

Siegert, J. Martin., (2008). Antarctic subglacial topography and ice-sheet evolution. *Earth Surface Processes and Landforms* 33, 646–660. doi: 10.1002/esp.1670.

Shevenell, A.E., Kennett, J.P. and Lea, D.W., (2004). Middle Miocene Southern Ocean cooling and Antarctic cryosphere expansion. *Science*, 305(5691): 1766–70. doi: 10.1126/science.1100061.

Sclater, J. G., and P. A. F. Christie, 1980, Continental stretching: an explanation of the post-mid-Cretaceous subsidence of the central North Sea basin: *Journal of Geophysical Research*. V. 85, p. 3711–3739.

Storey, B.C., A.P.M. Vaughan, and I.L. Millar, Geodynamic evolution of the Antarctic Peninsula during Mesozoic times and its bearing on Weddell Sea history, in *Weddell Sea Tectonics and Gondwana Break-up*, edited by B.C. Storey, E.C. King, and R. Livermore, *Geol. Soc. Spec. Publ.*, 108, 87–103, 1996.

Scher, H. D., and E. E. Martin, 2006: Timing and climatic consequences of the opening of Drake Passage, *Science*, 312, 428–430. doi: 10.1126/science.1120044.

Smith, W. and Wessel, P. (1990). Gridding with continuous curvature splines in tension. *Geophysics*, 55(3), 293–305. doi: 10.1190/1.1442837.

Uenzelmann-Neben, G., (2006). Depositional patterns at Drift 7, Antarctic Peninsula: along- slope versus down-slope sediment transport as indicators for oceanic currents and climatic conditions. *Mar. Geol.*, 233, 49–62. <http://dx.doi.org/10.1016/j.margeo.2006.08.008>.

Wardell, N., Childs, J.R., Cooper, A.K. (2007). Advances through collaboration: sharing seismic reflection data via the Antarctic Seismic Data Library System for Cooperative Research (SDLS). In: Cooper, A.K., Raymond, C.R. (Eds.), *Antarctica: A Keystone in a Changing World—Online Proceedings of the 10th ISAES: USGS Open-File Report 2007-1047, Short Research Paper 001*. <http://dx.doi.org/10.3133/of2007-1047.srp001> (4 pp.).

Whittaker, J. and Müller, R.D., (2006), Seismic Stratigraphy of the Adare Trough Area, Antarctica, *Mar. Geol.*, 230, 179–197, doi:10.1016/j.margeo.2006.05.

Wilson, D. S., Jamieson S. R., Barrett, J. P., Leitchenkov, G., Gohl, K., Later, D, R. (2012). Antarctic topography at the Eocene-Oligocene boundary. *Paleogeogr. Paleoclimatol., Paleoecol.*, 335–336, 24–34. <http://dx.doi.org/10.1016/j.palaeo.2011.05.028>.

Watts, A., 2001. *Isostasy and Flexure of the Lithosphere*, Cambridge University Press.

Zachos, C. J, Dickens, R. Gerald, Zeebe, E. Richard., (2008). An early Cenozoic perspective on greenhouse warming and carbon-cycle dynamics. *Nature* 451, 279–283. doi:10.1038/nature06588.

Zachos, J.C., Breza, J.R., and Wise, S.W., 1992. Early Oligocene ice-sheet expansion on Antarctica: stable isotope and sedimentological evidence from Kerguelen Plateau, southern Indian Ocean. *Geology*, 20:569–573.

5 Intensification of Weddell Sea circulation in the Middle Miocene

Xiaoxia Huang, Michael Stärz, Karsten Gohl, Gerrit Lohmann

Alfred Wegener Institute, Helmholtz-Centre for Polar and Marine Research
Am Alten Hafen 26, D-27568 Bremerhaven, Germany

5.1 Abstract

As the Weddell Sea is the quasi global powerhouse of bottom water formation and, thus, significant driver of global ocean circulation, we select this region for a thorough study on the effects that changes in paleobathymetry have on Mid-Miocene water mass formation. Here we present circulation model results that suggest the deep water formation and ocean circulation are especially sensitive to the paleobathymetric configuration of the Weddell Sea, which our recent work has shown to be characterized by a more southerly shelf break than at present or in previous paleobathymetric data. The southerly-replaced shelf break of the Weddell Sea results in dramatic changes in simulated mixed layer depth. The modeled parameters further indicate that paleobathymetric configuration impacts water mixing, sea surface temperature changes, and bottom water formation. Bottom water plays a significant role in sediment distribution and constructing geomorphology of the continental rise via developing a number of sediment drifts.

5.2 Introduction

The Weddell Sea embayment of Antarctica (Fig. 1) of the Southern Ocean is crucial for global ocean circulation as one of the main sites of deep and bottom water production (Nicholls et al., 2009). The general ocean circulation is dominated by the cyclonic Weddell Gyre, which moves water from the surface down to the seafloor (Orsi et al., 1993; Fahrbach et al., 1995). Changes in the geometry and distribution of ocean gateways due to changes of bathymetry can be expected to have had significant impacts on the Weddell Gyre circulation and paleoceanography, sedimentation pattern and in the process inhibiting or enhancing the mixture and transport of water from different regions (Bice et al., 1998, Sykes et al., 1998). Ocean circulation in turn affects climate through the transport of salt, heat and moisture (Bice et al., 1998). Unfortunately, Global Circulation Models (GCM) that couple atmospheric and oceanic circulation tends to lack realistic detailed paleobathymetric constraints (Hayes et al., 2009).

In this study, the Miocene ocean circulation in the Weddell Sea has been simulated by means of implementing a paleobathymetry setup into the GCM applying elevated CO₂ concentration (450 ppmv and 278 ppmv) and ice sheet heights, ocean gateways. The improved Weddell Sea paleobathymetry (Huang et al., 2014) is characterized by a shelf break placed farther south than present, which results in more pronounced changes in sea-surface temperatures (SSTs) (Fig. 3), mixed layer depth (Fig. 4), and Weddell Gyre circulation (Fig. 5) in our GCM runs compared to the previous low-resolution paleobathymetry (Herold et al., 2008). The deeper Middle Miocene mixed layer and increased Antarctic Bottom Water (AABW) formation may have enhanced primary production and sediments distribution.

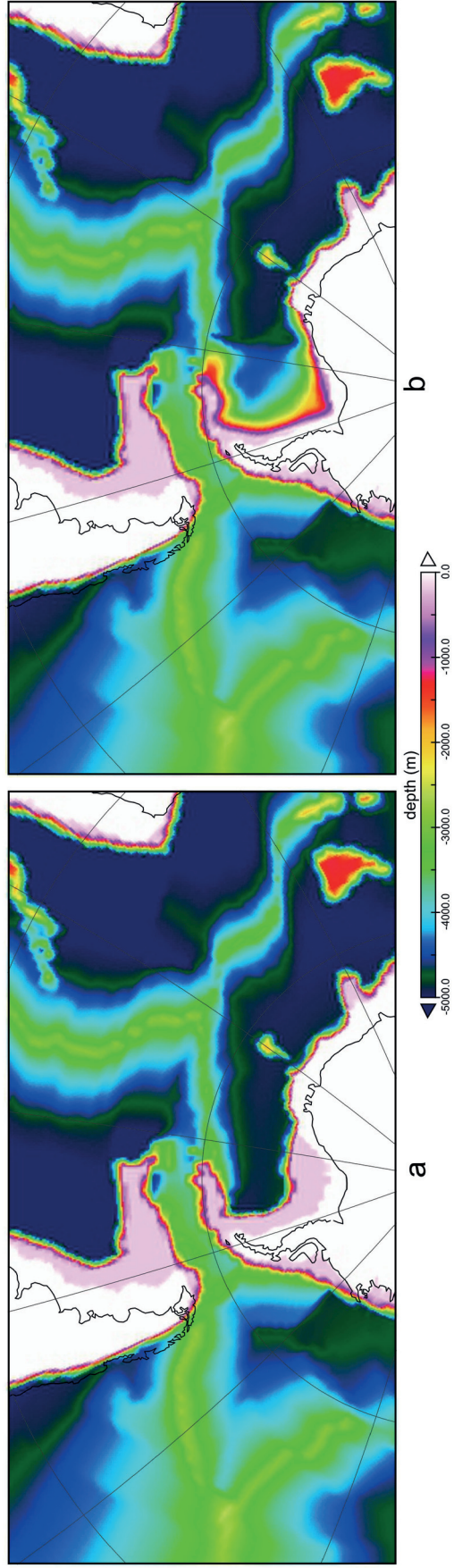


Fig. 5.1 Paleobathymetry reconstruction of the Weddell Sea during the Middle Miocene (15 Myrs ago). MIO- previous paleobathymetry and MIOW- with implementing the improved paleobathymetry, respectively.

5.3 Data and methods

The Miocene climate and ocean circulation is investigated by means of the fully coupled global atmosphere-ocean-sea ice-vegetation Earth System Model COSMOS, originally developed at Max Planck Institute in Hamburg (Jungclauss et al., 2010). The standard early to middle Miocene model setup (MIO; 20–15 Ma) applies global paleobathymetry, orography and ice-sheet adjustments (Herold et al., 2008) and has been updated by a regional paleobathymetry dataset comprising the North Atlantic/Nordic Seas sector (Ehlers and Jokat., 2013). We further embed a high-resolution paleobathymetry of the Weddell Sea sector (Huang et al., 2014) into the standard Miocene model setup (MIOW). The effect of CO₂ on Miocene boundary conditions is investigated in both paleobathymetric setups, MIO and MIOW, by performing model studies at preindustrial CO₂ (278 ppm CO₂; MIO_278, MIOW_278) and at 450 ppm CO₂-levels (MIO_450, MIOW_450), respectively, which is in line with CO₂ constraints throughout the Neogene (Beerling and Royer, 2011).

We use a comprehensive fully coupled Earth System Model, COSMOS (ECHAM5-JSBACH-MPIOM) for this study. The atmospheric model ECHAM5 (Roeckner et al., 2003), complemented by a land surface component JSBACH (Brovkin et al., 2009), is used at T31 resolution (~3.75°), with 19 vertical layers. The ocean model MPI-OM (Marsland et al., 2003), including sea ice dynamics that is formulated using viscous-plastic rheology, has a resolution of GR30 (3° × 1.8°) in the horizontal, with 40 uneven vertical layers. The climate model has already been used to simulate the last millennium (Jungclauss et al., 2010), the Miocene warm climate (Knorr et al., 2011; Knorr and Lohmann, 2014).

5.4 Results

5.4.1 Contourite drifts

Miller et al. (1990)' seismic stratigraphic study of the Weddell Sea dates a basin-wide unconformity, named WS-u5, to the Middle Miocene via ties to sediment cores of Ocean Drilling Project (ODP) Sites (Fig. 2). Drastic changes in seismic facies at WS-u5 are interpreted to represent an increased role of glacial-marine depositional processes after the Middle Miocene (Miller et al., 1990). We observe mounded, elongate sediment bodies with asymmetric shapes adjacent to channels have been observed at the continental rise of the south and west Weddell Sea (Fig. 2b, d). Their internal reflectivity shows continue parallel or subparallel reflectors and mounded geometry, which, by following the classifications (Faugères et al., 1990, Stow et al., 2002), allows us to interpret these features as sediment drifts (contourites). A further large-scale chaotic, semi-transparent unit can be identified above the unconformity WS-u5 and is interpreted as mass transport deposits (Fig. 2a, c). Sediment drifts are constructed by the action of bottom currents over long time scales, and are widely considered to indicate AABW flow in Middle Miocene strata (Rebesco et al., 1997; Uenzelmann-Neben, 2002; Hernández-Molina et al., 2009). In turn, the distribution of sediment drifts delimits the extent of the proto-AABW (Sykes et al., 1998). The Middle Miocene onset of a number of sediment drifts (Fig. 2) in the Weddell Sea indicates a major shift in deposition processes, which therefore link to changes in ocean circulation and ice sheet expansion.

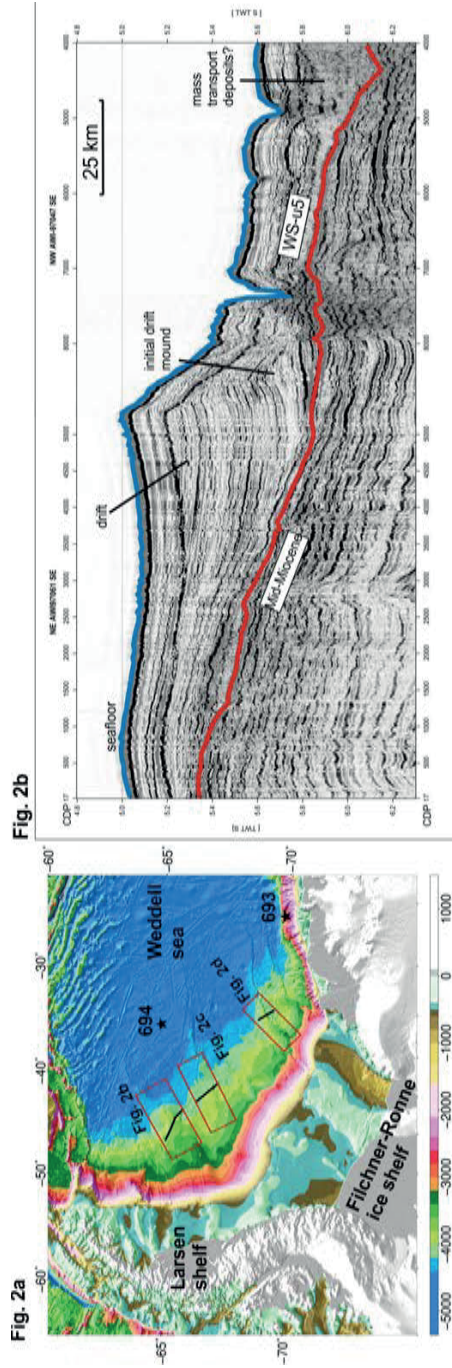


Fig. 5.2 Sediment drifts resolved by multichannel seismic reflection data on the continental rise of the Weddell Sea (Fig. 2b, d). Fig.2c shows a large mass transport deposits.

5.4.2 modeled SSTs, mixed layer depth, and ocean current velocities

Our Miocene model studies at preindustrial atmospheric CO₂-level of 278 ppmv, MIO_278 (without implementing improved Weddell Sea paleobathymetry) and MIOW_278 (with implementing Weddell Sea paleobathymetry), both reveal global warming of +2.4°C. The warming is accompanied by major reductions in seasonal and perennial sea ice when compared to modern ice extents (Fig. 3a,b, Fig. S1 of supplementary material), as much of the Weddell Sea surface warms above the freezing point (-1.9°C). Global mean surface air temperature is 6.7°C warmer than preindustrial and governs further increase in SST and concomitant sea ice reduction. However, in the experiment with a previous low-resolution paleobathymetry (Bice et al., 1998; Hayes et al., 2009; Herold et al., 2008), MIO_450, freezing point temperatures are reached and perennial sea ice forms at the southern margin of the Weddell Sea (Fig. 3c). In contrast, our improved paleobathymetric constraints in MIOW_450 induce additional warming at the sea surface and a complete absence of perennial sea ice in the southern Weddell Sea. The eastern sector of the Weddell Sea is characterized by SSTs of up to 6°C warmer than in preindustrial times (Fig. 3d).

The mixed layer depth provides an insight into the vertical structure of the ocean. It is very sensitive to the locations and morphologies of the shelf breaks in the two paleobathymetric models (Fig. 1 and Fig. 4c, d). Our improved paleobathymetry permits development of a mixed layer that extends all the way to the Weddell seafloor under MMCO conditions (Fig. 4d). The global paleobathymetric model (Herold et al., 2008), on the other hand, permits a much shallower mixed layer (Fig. 4c).

Generally, the Weddell Gyre, as a consequence of wind stress, reveals a similar circulation pattern throughout the water column (barotropic mode) as at present (Fig. 5 and Fig. S1). The western part of the modern Weddell Gyre is limited by perennial sea ice at the Antarctic Peninsula continental shelf (Hayes et al., 2009; Sykes et al., 1998) (Fig. S1 of supplementary material). The reduced Middle Miocene sea ice allows for increased transfer of wind stress towards the ocean surface, which in turn results in stronger surface velocities in the Weddell Gyre (Fig. 5). The most pronounced gyre circulation is observed in MIOW_450, in which the centre of the Weddell Gyre, defined by the minimum of dynamic topography (Hayes et al., 2009), is shifted polewards by ~6° (pre-industrial: 61.5°S; MIO_450: 60.5°S; MIOW_450: 66.5°S) (Figs. 1 and 5). Here, too, the choice of paleobathymetry is important for understanding regional water circulation in the Miocene Weddell Sea. The experiment with the previous low-resolution paleobathymetry implies the Weddell Gyre to be weak or absent in deeper water layers (Fig. 5b, MIO_450). In contrast, with the improved paleobathymetry, strong deep-water currents are modeled parallel to the ocean margins (Fig. 5d, MIOW_450).

The southward displacement of the Weddell Gyre during the MMCO facilitates the entrainment of northeastern sourced warm waters into the southern Weddell Sea embayment, leading to the ultimate loss of perennial sea ice (Fig. 3d). Pronounced barotropic flow and mixing in the Weddell Gyre governs the vertical water mass transport fostering local deep water (Fig. 5d) and remote circulation, for instance in the Atlantic abyss (Tab.1 of supplementary material). In addition, our new paleobathymetric constraints effectively steer the wind stress induced barotropic stream function of the Weddell Gyre (Fig. S2 of supplementary material). In turn, the clockwise gyre circulation favors distinct vertical mixing via Ekman transport (pumping) as shown in the mixed layer depth (Fig. 4b,d) and in AABW formation in the Southern Ocean (60–80°S) (Tab. 1 of supplementary material).

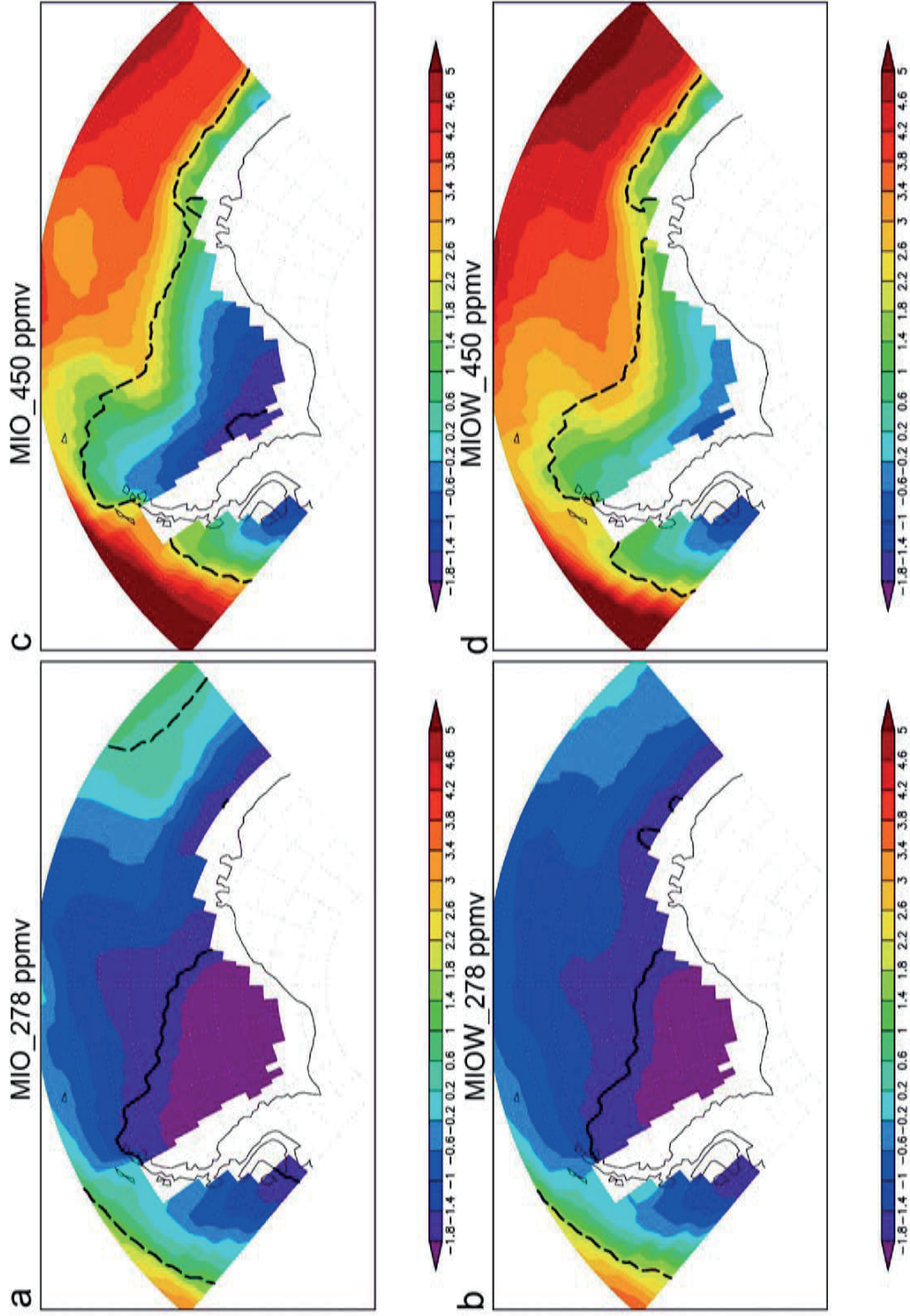


Fig. 5.3 Sea Surface Temperature (SST in °C), Fig. 3a: MIO-278 (CO₂-278 ppmv, with previous paleobathymetry); Fig. 3b: MIO-278 (CO₂-278 ppmv, with the improved paleobathymetry); Fig. 3c: MIO-450 (CO₂-450 ppm, with previous paleobathymetry); Fig. 3d: MIO-450 (CO₂-450 ppm, with the improved paleobathymetry). Dashed line represent seasonal sea ice extent, solid line represents perennial sea ice extent, see more details of the model boundary conditions in the methods.

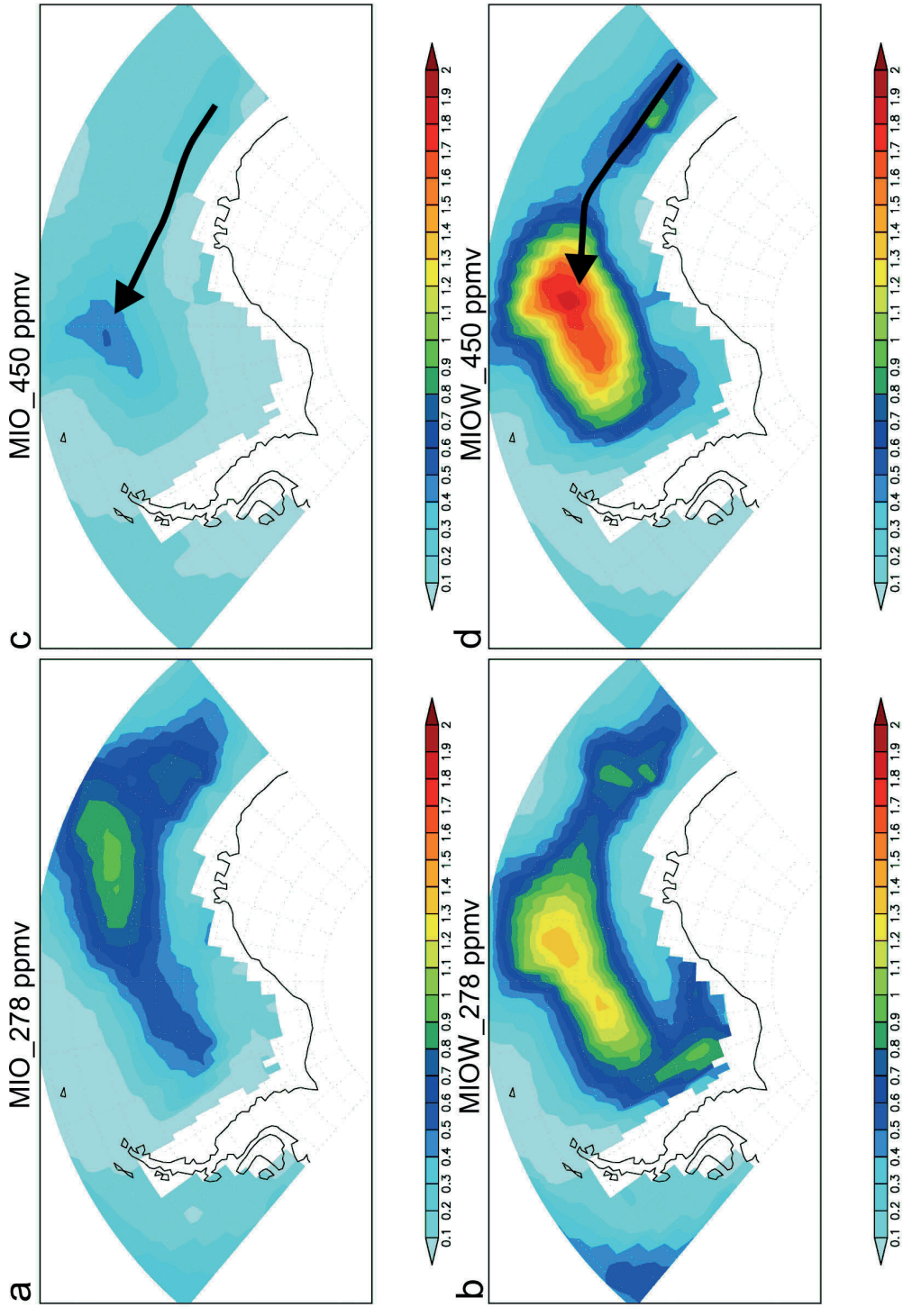


Fig. 5.4 The simulated mixed layer depth (km) with different paleobathymetry and CO₂ levels (similar to Fig. 3).

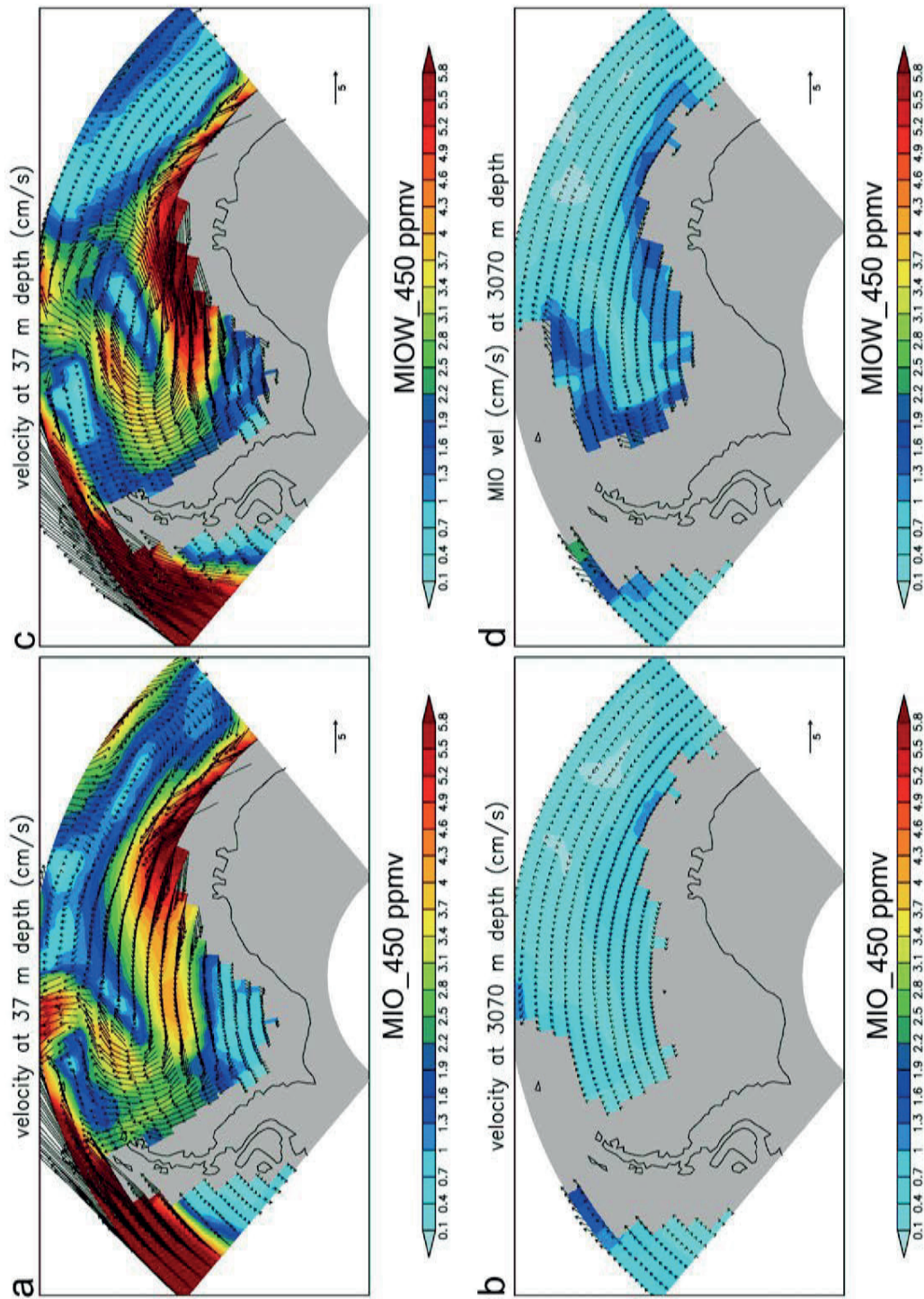


Fig. 5.5 The simulated ocean velocities ($\text{cm} \cdot \text{sec}^{-1}$) in the Weddell Sea at surface and deep water for the Middle Miocene times based on the previous paleobathymetry (MIO-450) and implementing the improved paleobathymetry (MIO-450).

5.5 Discussion

The model results consistently confirms that a higher than present-day CO₂ concentration is necessary to reproduce Middle Miocene warmth in the model (You et al., 2009) (Fig. 3c, d). The increase of the atmospheric CO₂ concentration to 450 ppmv, combined with the improved Weddell Sea paleobathymetry, produces the warmest sea surface in the Weddell Sea (Fig. 3d.). It is important to notice that the wind stress is relative the same between MIO_450 and MIO_278 (as well as between MIO_278 and MIO_278 in Fig. S3 of supplementary material), which further confirms that the additional SST warming is a consequence of the improved paleobathymetry. The model scenarios further indicate that MMCO ended under the influence of the decline CO₂ and a major increase of AABW formation (Fig. 3b, Tab 1 of supplementary). Today's AABW forms as a result of brine injection during sea ice formation, which requires a cold climate and cold SSTs (Ohshima et al., 2013). Compared to the simulations under other boundary conditions, the low CO₂ concentrations and with the improved paleobathymetry increase AABW formation to 10.12 Sv (MIO_278, Tab 1 of supplementary material). This scenario enhances the contribution of the AABW formation in the Weddell Sea by cooling of surface water to form more sea ice as well as drawing warmer, saltier water from the surrounding oceans (e.g., Indian Ocean sector). An increased sea-ice cover in cold climate could have reduced outgassing of CO₂ from upwelling, therefore reducing the atmospheric CO₂ (Marshall et al., 2012).

We argue that the AABW originating in the Weddell Sea significantly influenced the evolution and present morphology of the continental rises of the Weddell Sea, via the production of a number of sediment drifts (Fig. 2). The drift deposits document stages of particularly dynamic bottom current conditions (Faugères et al., 1999; Stow et al., 2002; Rbesco et al., 1997; Uenzelmann, 2002; Hernández-Molina et al., 2009; Uenzelmann-Neben and Gohl, 2012). Unfortunately, no drill sites exist on the sediment drifts in the Weddell Sea to preserve a directly-dateable record for the proto-AABW. However, Barker et al. (1988) suggested that strong bottom currents produced the terrigenous siliceous mud sequences drilled by ODP Leg 113 (Sites 693 and 694) on the mid-slope of Dronning Maud Land margin and in the central Weddell Sea (Barker et al., 1988) (Fig. 2). Fast paleo-ice streams on the Filchner-Ronne and Larsen shelves would have transported these sediments to the shelf edge and continental rise. The well-preserved sediment drifts in the southern and western Weddell Sea (Fig. 2b,d) can thus be directly correspond to locations of the strong Mid-Miocene AABW formation.

Compared to preindustrial times, the main process in water column stratification in the Weddell Sea during the MMCO is considered to be freshwater input from sea ice melting (Fig. 3c,d). The new paleobathymetry results in pronounced deepening of the mixed layer at the same high CO₂ level of the warm climate background (Fig. 4c,d). Under reduced atmospheric CO₂ conditions, deepening of the mixed layer in the southwest Weddell Sea demonstrates that upward displacement of more saline waters from depth and their partial mixing with surface water along the Antarctic continental margin could have contributed to the higher densities required for the production of the AABW as well (Figs. 4a, b). In the warm climate, and with the more southerly shelf break of the new paleobathymetry, the dramatically deeper mixed layer (Fig. 4c, d) permits intrusion of warm water from the Indian Ocean sector

to the Weddell Sea. The broad shallow shelf from previous paleobathymetry models (Fig. 1a) most likely acts to isolate basinal water and prevent mixing (Fig. 4c).

5.6 Conclusions

Our study provides robust evidence that paleo-ocean circulation is extremely sensitive to regional changes in paleobathymetry. The Weddell Gyre shifts poleward after applying an improved Mid-Miocene paleobathymetric grid. The higher-than present CO₂ level and the improved paleobathymetry together induce the warmest SSTs in the Weddell Sea as well as global climate associated to the MMCO. A low CO₂ level and with the improved paleobathymetry simulate the major AABW formation for the Atlantic sector. As a consequence, abundant AABW production and large sediment drifts developed and modified the margin geomorphology along the western and southern Weddell Sea continental rise and the regions with AABW flow. Globally, the dramatic deepening of the mixed layer may have influenced the evolution of deep ocean temperature and has potential consequences for carbon cycling by an increase in primary biomass production. Our study sheds light on how the shelf break significantly interacts with regional ocean circulation of the Weddell Sea. A similar test in the Ross Sea and other Antarctic embayment would therefore be of great interest to improve understanding of paleoclimate and the mechanisms of AABW formation in the Southern Ocean.

5.7 Acknowledgements

The authors would like to thank the masters, crews and seismic teams of the many ship expeditions to the Weddell Sea who made the acquisition of the data used in this study possible. X.H. has been receiving a PhD scholarship from the Chinese Scholarship Council (CSC).

5.8 References

- Barker, P.F., Kennett, J.P., et al, (1988). Proceedings of the Ocean Drilling Program, Scientific Results Leg 113. Ocean Drilling Program: 774. doi:10.2973/odp.proc.ir.113.1988.
- Bice, K.L., Barron, E.J., Peterson, W.H., 1998. Reconstruction of realistic early Eocene paleobathymetry and ocean GCM sensitivity to specified basin configuration. In: Crowley Thomas, J., Burke Kevin, C. (Eds.), Tectonic Boundary Conditions for Climate Reconstructions. Oxford University Press, Oxford, United Kingdom, pp. 227–247.
- Bice, K.L., Scotese, C.R., Seidov, D., Barron, E.J., 2000. Quantifying the role of geographic change in Cenozoic ocean heat transport using uncoupled atmosphere and ocean models. *Palaeogeography, Palaeoclimatology, Palaeoecology* 161 (3-4), 295–310.
- Beerling, D. J., & Royer, D. L. (2011). Convergent cenozoic CO₂ history. *Nature Geoscience*, 4(7), 418-420.
- Ehlers, B. M., & Jokat, W. (2013). Paleo-bathymetry of the northern North Atlantic and consequences for the opening of the Fram Strait. *Marine Geophysical Research*, 34(1), 25-43.
- Fahrbach, E., G. Rohardt, N. Scheele, M. Schröder, V. Strass, an A. Wisotzki (1995), Formation and discharge of deep and bottom water in the northwestern

Weddell Sea, *Journal of Marine Research*, 53, 515–538.

Faugères, J.C., Stow, D.A.V., Imbert, P., Viana, A.R., (1999). Seismic features diagnostic of contourite drifts. *Marine Geology*, 162, 1–38.

Herold, N., M. Seton, R. D. Müller, Y. You, and M. Huber (2008), Middle Miocene tectonic boundary conditions for use in climate models, *Geochem. Geophys. Geosyst.*, 9, Q10009, doi:10.1029/2008GC002046.

Hernández-Molina, F. J., Paterlini, M., Violante, R., Marshall, P., de Isasi, M., Somoza, L., & Rebesco, M. (2009). Contourite depositional system on the Argentine Slope: an exceptional record of the influence of Antarctic water masses. *Geology*, 37(6), 507-510.

Hayes, D. E., Zhang, C., & Weissel, R. A. (2009). Modeling paleobathymetry in the Southern Ocean. *Eos, Transactions American Geophysical Union*, 90(19), 165-166.

Huang, X., Gohl, K., Jokat, W., (2014) Variability in Cenozoic sedimentation and paleo-water depths of the Weddell Sea basin related to pre-glacial and glacial conditions of Antarctica, *Global and Planetary Change*. DOI: 10.1016/j.gloplacha.2014.03.010.

Jungclauss, J. H. et al. Climate and carbon-cycle variability over the last millennium. *Clim. Past* 6, 723–737 (2010)

Knorr, G., Butzin, M., Micheels, A. & Lohmann, G. A warm Miocene climate at low atmospheric CO₂ levels. *Geophys. Res. Lett.* 38, 1–5 (2011)

Knorr, G. & Lohmann, G. Climate warming during Antarctic ice sheet expansion at the Middle Miocene transition. *Nature Geosci.* 7, 2–7 (2014)

Miller, H., Henriot, J.P., Kaul, N., Moons, A., (1990). A fine-scale stratigraphy of the eastern margin of the Weddell Sea. In: Bleil, U., Thiede, J. (Eds.), *Geological History of the Polar Oceans: Arctic Versus Antarctic*. Kluwer Academic Publishers, pp. 131–161. doi: 10.1007/978-94-009-2029-3_8.

Marsland, S. J., Haak, H., Jungclauss, J. H., Latif, M. & Röske, F. The Max-Planck-Institute global ocean/sea ice model with orthogonal curvilinear coordinates. *Ocean Model.* 5, 91–127 (2003).

Marshall, J., & Speer, K. (2012). Closure of the meridional overturning circulation through Southern Ocean upwelling. *Nature Geoscience*, 5(3), 171-180.

Uenzelmann-Neben, G., & Gohl, K. (2012). Amundsen Sea sediment drifts: Archives of modifications in oceanographic and climatic conditions. *Marine Geology*, 299, 51-62.

Nicholls, K. W., Østerhus, S., Makinson, K., Gammelsrød, T., & Fahrbach, E. (2009). Ice-ocean processes over the continental shelf of the southern Weddell Sea, Antarctica: A review. *Reviews of Geophysics*, 47(3).

Orsi, A. H., Nowlin Jr, W. D., & Whitworth III, T. (1993). On the circulation and stratification of the Weddell Gyre. *Deep Sea Research Part I: Oceanographic Research Papers*, 40(1), 169-203.

Ohshima, K. I., Fukamachi, Y., Williams, G. D., Nihashi, S., Roquet, F., Kitade, Y., ... & Wakatsuchi, M. (2013). Antarctic Bottom Water production by intense sea-ice formation in the Cape Darnley polynya. *Nature Geoscience*, 6(3), 235-240.

Rebesco, M., Larter, R.D., Barker, P.F., Camerlenghi, A., Vanneste, L.E., 1997. History of sedimentation on the continental rise west of the Antarctic Peninsula. In: Cooper, A.K., Barker, P.F. (Eds.), *Geology and Seismic Stratigraphy on the Antarctic Margin: 2*. American Geophysical Unions. Antarctic Research Series, vol. 71, pp. 29–49.

Roeckner, E. et al. The Atmospheric General Circulation Model ECHAM5. Part 1. Model Description (Max-Planck-Institut für Meteorologie report no. 349, 2003)

Brovkin, V., Raddatz, T., Reick, C. H., Claussen, M. & Gayler, V. Global biogeophysical interactions between forest and climate. *Geophys. Res. Lett.* **36**, 1–5 (2009)

Stow, D.A.V., Faugères, J.C., Howe, J.A., Pudsey, C.J., Viana, A.R., (2002). Bottomcurrents, contourites and deep-sea sediment drifts: current state-of-the-art. In: Stow, D.A.V., Pudsey, C.J., Howe, J.A., Faugeres, J.C., Viana, A.R. (Eds.), *Deep-water contourite systems: Modern drifts and ancient series*. Memoir. Geological Society of London, London, pp. 7–20.

Sykes, T. J. S., Ramsay, A. T. S., & Kidd, R. B. (1998). Southern hemisphere Miocene bottom-water circulation: a palaeobathymetric analysis. *Geological Society, London, Special Publications*, 131(1), 43-54.

Uenzelmann-Neben, G. (2002). Contourites on the Agulhas Plateau, SW Indian Ocean: indications for the evolution of currents since Palaeogene times. *Geological Society, London, Memoirs*, 22(1), 271-288.

You, Y., M. Huber, R. D. Müller, C. J. Poulsen, and J. Ribbe (2009), Simulation of the Middle Miocene Climate Optimum, *Geophys. Res. Lett.*, 36, L04702, doi:10.1029/2008GL036571.

5.7 Supplementary information

This supporting information provides additional figures about the preindustrial simulations, horizontal barotropic streamfunction and wind stress as well as a table with Antarctic Bottom Water index.

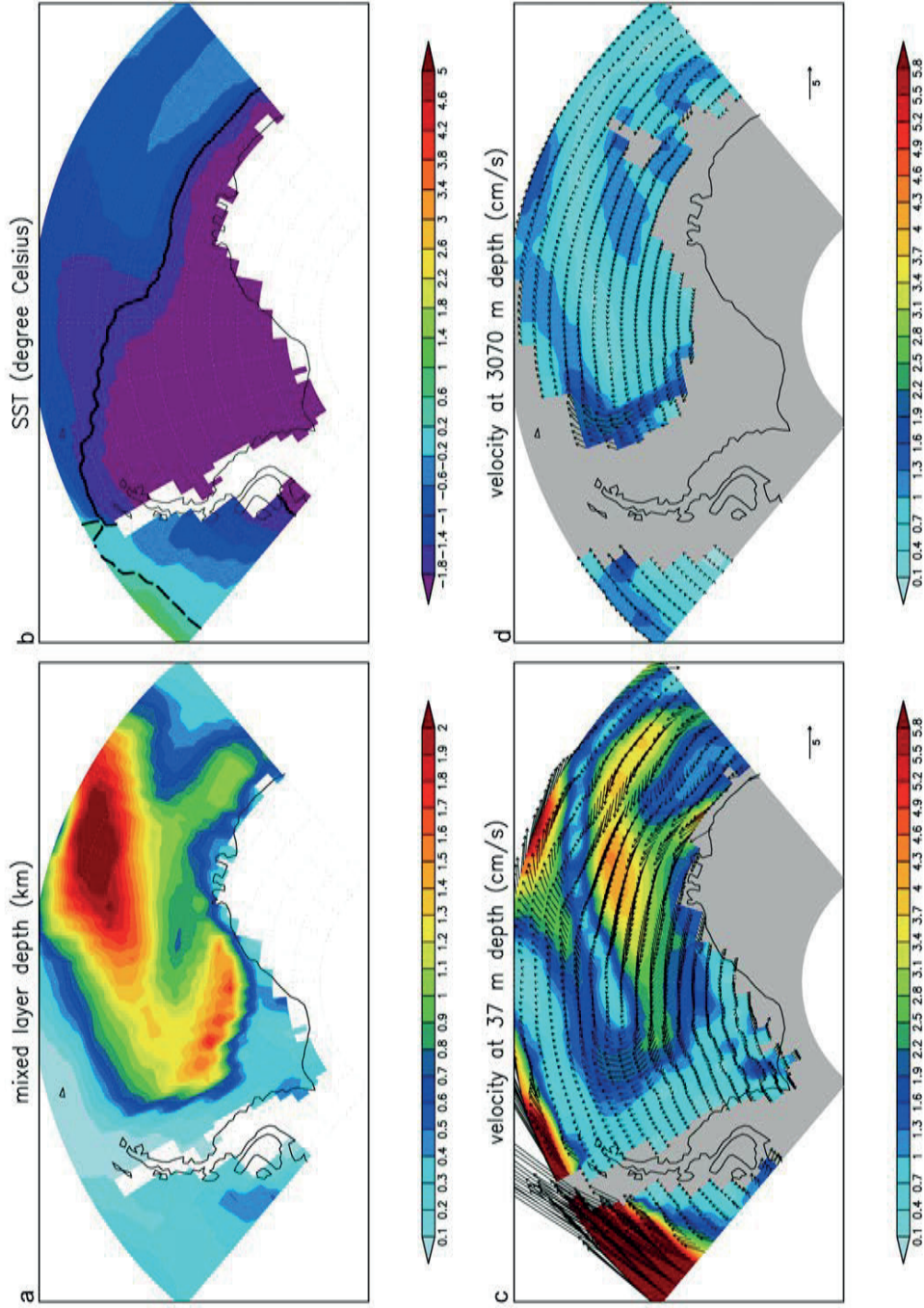


Fig. 5.S1 preindustrial simulations. a): mixed layer depth reaches to the maximum deepening compared to the simulations with other boundary conditions. b): Sea Surface Temperature, the surface waters of the study region are near freezing point temperature ($-1.9\text{ }^{\circ}\text{C}$), and the entire Weddell Sea is covered by perennial (multi-year) sea ice, whereas seasonal sea ice cover reaches up to -50° latitude (not shown). Pre-industrial SSTs beyond the perennial ice cover extent are warmer and range between -1° and 0°C . c, d): are the simulated current velocities of the Weddell Gyre at 37m and 3070m.

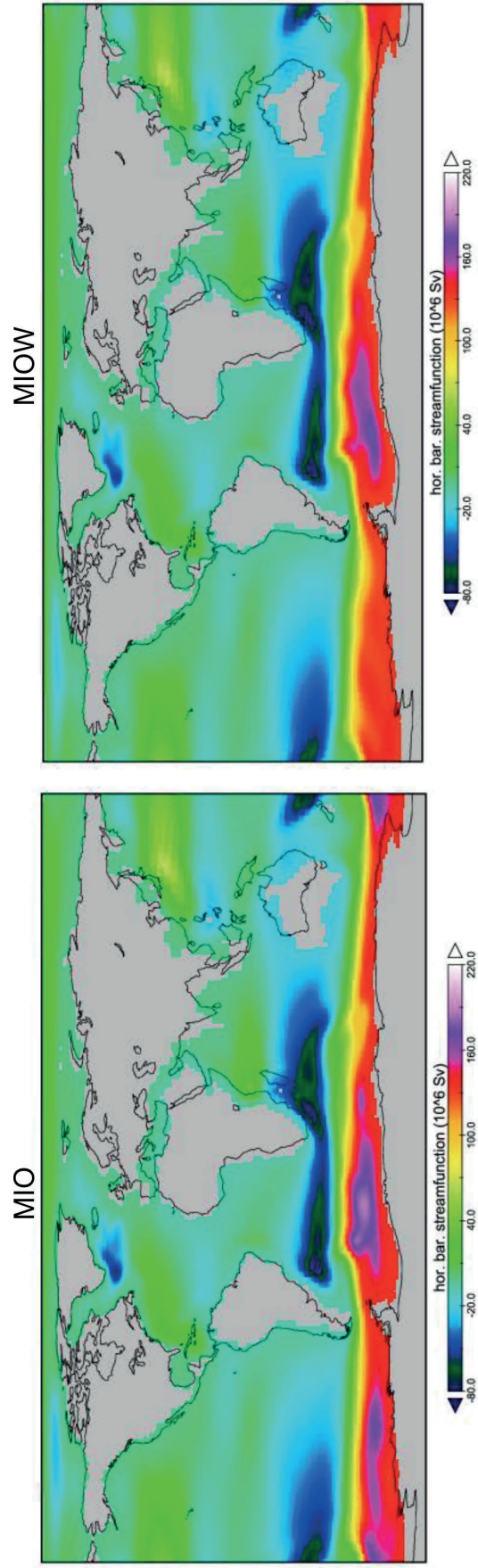


Fig. 5.S2 Horizontal barotropic streamfunction (vertically integrated water mass flux, $1\text{Sv} = 1 \times 10^6 \text{ m}^3 \cdot \text{sec}^{-1}$) for (a) the Miocene model run without the improved Weddell Sea bathymetric dataset (MIO); (b) the Miocene model run including a improved bathymetric dataset of the Weddell Sea (MIOw).

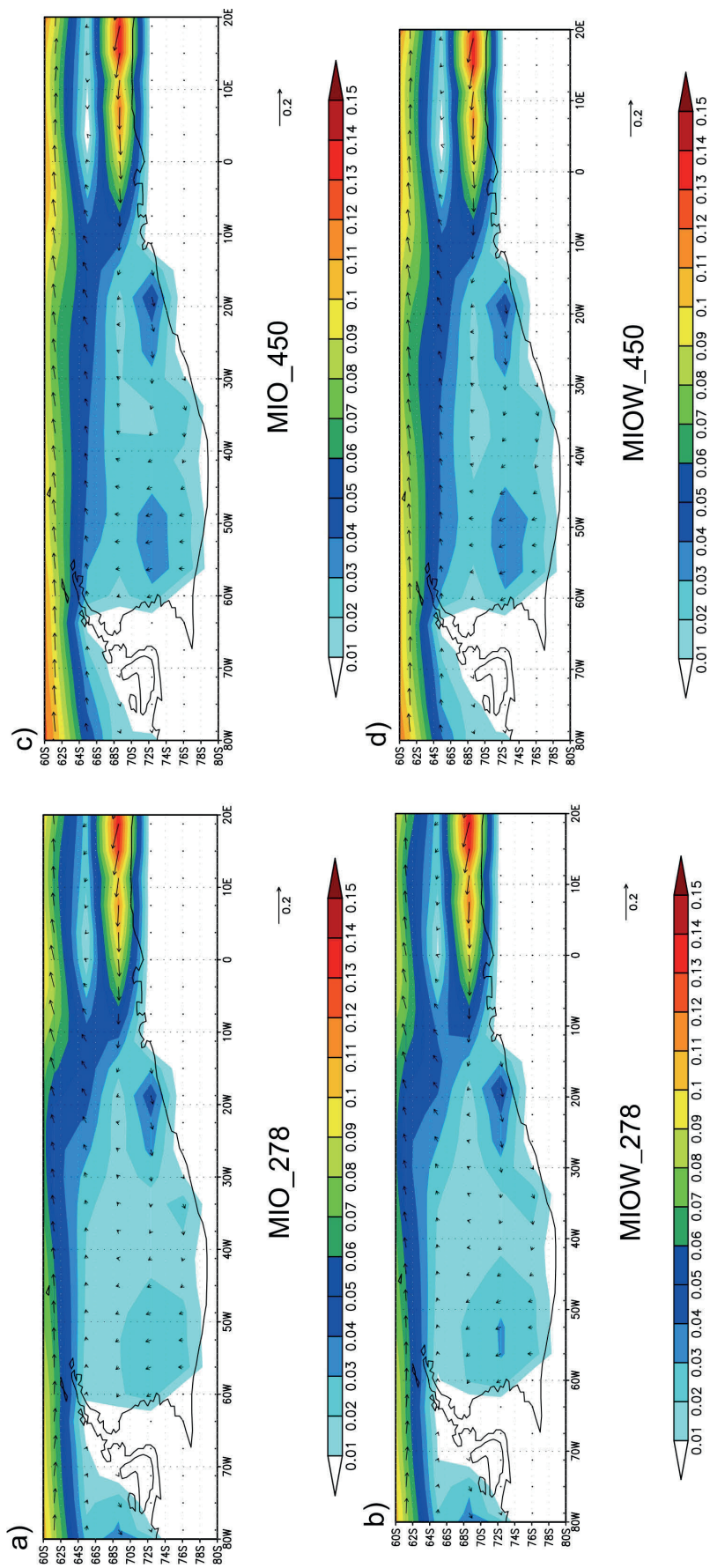


Fig. 5.S3: a, b represent the wind stress with CO₂ level 278 ppmv and different paleobathymetric grids; c, d represent the wind stress with CO₂ level 480 ppmv and different paleobathymetry grids. The calculated wind stress under different boundary conditions is similar, which conforms that the changes of the Weddell Gyre is resulted by the changes of the paleobathymetry.

Table 5.1 Antarctic Bottom Water (AABW) index, in the Atlantic sector as defined by the minimum in the Atlantic Meridional Overturning Circulation between 30-60°N and a global AABW index, defined by the meridional circulation in the Southern Ocean between 60-80°S.

model runs	global AABW index (60-80°S, Sv)	AABW index (-30-60°N)
PI	-8.76	-2.86
MIO_450 ppmv	-2.44	-0.46
MIO_278 ppmv	-6.9	-1.83
MIOW_450 ppmv	-4.05	-1.66
MIOW_278 ppmv	-10.12	-1.97
MIOW_PI	-12.42	-3.46

6 Middle Miocene to Present Sediment Transport and Deposits in the Southeast Weddell Sea, Antarctica

Xiaoxia Huang*, Wilfried Jokat

Alfred Wegener Institute, Helmholtz-Centre for Polar and Marine Research
Am Alten Hafen 26, D-27568 Bremerhaven, Germany

6.1 Abstract

Understanding the transport and deposition of sediments along the Antarctic continental shelves helps to provide constraints on past ice sheet dynamics. Seismic stratigraphic and scientific drilling data from the Antarctic continental margins have provided much direct evidence concerning ice sheet evolution and sedimentation history. In this study, we describe a series of sedimentary features along the continental margin of the southeast Weddell Sea to constrain glacial-influenced sedimentation processes from the Middle Miocene to the present. The Crary Trough Mouth Fan (CTMF), channel systems, Mix-system turbidity-contourites are investigated by using seismic reflection, sub-bottom profiler, and results from ODP Site 693. The sinuous, NE-SW-oriented turbidity-contourites are characterized by bathymetric highs that are more than 150 km wide, 700 km long, and have a sediment thickness of up to 2 km. The unique sedimentation environment of the southeast Weddell Sea is controlled by a large catchment area and its fast (paleo-) ice streams feeding the Filchner Ronne Ice Shelf, turbidity/bottom currents as well as sea level changes. A remarkable increase in mass transport deposits (MTDs) in the Late Miocene and Early Pliocene strata has been related to, ice sheet loading, eustatic sea level fall, earthquakes, and overpressure of rapid sediment accumulation. Our seismic records also imply that fluctuations of East Antarctic ice sheet similar to those that occurred during the last glacial cycle might have been typical for southern Weddell Sea during glacial periods since the Late Miocene or even earlier.

Keywords: Seismic interpretation, Weddell Sea, turbidity-contourites, Mass transp

6.2 Introduction

Glacially derived depositional and erosional features dominate the seafloor and upper sedimentary strata of the continental margin of the southwestern Weddell Sea, Antarctica (Fig. 1). Interactions between down-slope and along-slope sedimentary processes are common at all continental margins and the along-slope processes can create various depositional features (drifts) (Hernández-Molina et al., 2010). Bottom currents (along-slope processes) are capable of building thick and extensive sediment deposits, often with a noticeable mounded geometry by winnowing fine-grained sediments, which are interpreted as mounded drifts (Stow et al., 2002, 2009; Rebesco et al., 2014). Turbidity currents (down-slope processes) are responsible for crafting the morphology of continental margins by forming channels and levee deposits (Straub, 2007). Therefore, sediment drifts and levee deposits reported on the Antarctic continental rise may host valuable records on the past ocean circulation, current velocities, ice-sheet stabilities and sea-ice coverage.

The mounded drifts have been reported along Antarctic margins. Several elongate-mounded drifts have been investigated in great detail at Antarctic Peninsula Pacific Margin (Drift 6, 7). Drift 7 is an elongate body about 200 km long, 70 km wide and up to 1 km thick. It has been interpreted as having formed by turbidity currents flowing in deep-sea channels extending from the margin to the abyssal plain, and redistributed by the SW-following boundary current derived from AABW (Rebesco et al., 1996; Hernández-Molina et al., 2006). Similar in the northern Weddell Sea and Scotia Sea, extensive contourite drifts are suggested to be originated from AABW and Weddell Gyre flows (Maldonado et al., 2003, 2006). Uenzelmann-Neben and Gohl (2012) proposed that the flows of the proto-AABW and intensified southwest-flowing bottom currents are the main factors in the development of elongate-mounded drifts with lengths of 30 km in the Amundsen Sea. Kuvaas and Leitchenkov (1992) identified 20-30 km wide mounded sediment ridges in Prydz Bay and attributed their formation to a westward flowing bottom current activity interacted with overbank flow from turbidity currents within the channel.

Large-scale down-slope movement has left mass transport deposits (MTDs) as common occurrences on the Antarctic continental slopes. e.g. Scotia Sea (Ruano et al., 2014), the Amundsen Sea (Uenzelmann-Neben and Gohl, 2012), Wilkes Land margin (Donda et al., 2008) and Weddell Sea margin (this study). The gentle gradient of 1° in the southeast Weddell Sea will have permitted increased deposition and preservation of MTDs on the more distal middle to lower continental slope (Fig. 1). Sediment loading, crustal rebound, sea level changes, earthquakes, active tectonics and fluids and/or gas hydrate dissociation are common triggers of MTDs (Bart et al., 1999; Shanmugan, 2006; Nelson et al., 2011; Piper et al., 2012; Vargass et al., 2012).

Trough-mouth fans are shelf-edge and upper-slope depocentres adjacent to the mouths of paleo-ice streams (broad zones of fast-flowing ice) that existed along formerly-glaciated continental shelves at high latitudes (Vorren and Laberg, 1997; Ó Cofaigh et al., 2003; Dowdeswell et al., 2004). Examples are the Belgica Fan on the continental margin of the Bellingshausen Sea, the Prydz Channel Fan on the upper continental slope, the Scoresby Sund Fan off East Greenland, and the CTMF at the southeastern Weddell Sea continental margin (Kuvass and Kristoffersen, 1991; O'Brien et al., 2004; Dowdeswell et al., 2008; Laberg et al., 2013, this study). The associated CTMF formed when grounded ice repeatedly reached the continental shelf edge as fast-flowing ice streams, delivering large volumes of sediments directly to the upper slope. The CTMF is one of the largest high-latitude deep sea fans and comprises a thick, prograding slope (Kuvaas and Kristoffersen, 1991; Ó Cofaigh et al., 2003).

In this contribution, we bring new constraints to the interpretation of sedimentary structures in the Weddell Sea and their relationship to regional and global change by correlating those interpretations to the regional stratigraphic model of Miller et al. (1990) from ODP site 693. To do this, we tie the drill site to the network of seismic surveys ANT V-4 (1987), ANT VIII-5 (1990) ANT X-1/2 (1992) in the southern Weddell Sea. We concentrate on the description on the depositional history of the key elements such as turbidity-contourites and MTDs on the CTMF off Filchner Trough and their formation mechanisms. Age control of the significant sedimentary features is of great help in understanding the margin evolution history of study region from the Middle Miocene to the present day.

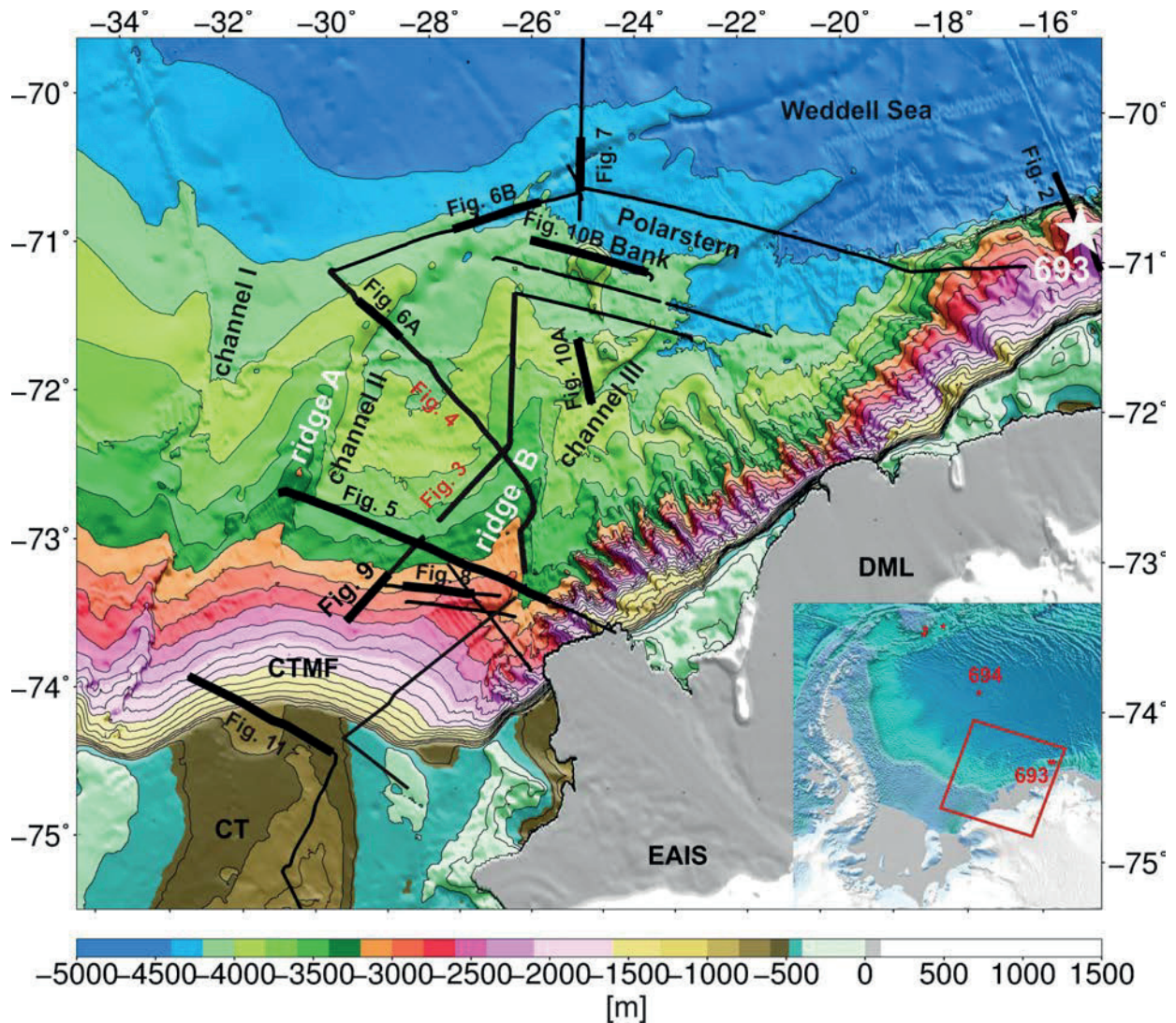


Fig. 6.1 Bathymetry map with locations of multi-channel seismic lines. Heavy red and black lines shows the portions, which were displayed in the paper. Background image: global seafloor topography grid (Arndt et al., 2013) EAIS: East Antarctic Ice Sheet; DML: Dronning Maud Land; FT: Filchner Trough; CTMF: Cray Trough Mouth Fan; Black lines: multi-channel seismic lines; white stars = ODP 693 site.

6.3 Background and regional hydrographic settings

Three large channels, referred to as I, II, and III, cross the CTMF from SW to NE, steering around a series of basement highs that are interpreted as a chain of volcanic seamounts, including Polarstern Bank (Jokat et al., 1996) (Fig. 1). The development of the channels has been related to an advance of Antarctic ice in Middle Miocene times (~14-10 Ma; Kuvass and Kristoffersen, 1991). This advance, and another in Late Pliocene times (~3.3-2.4 Ma), is known from large-amplitude shifts of benthic $\delta^{18}\text{O}$ and eustatic sea level measured in cored sediments globally (Zachos et al., 2008; Tripathi et al., 2009, Miller et al., 2011). The Middle Miocene event is thought to have controlled sedimentation process all along the continental margins of Antarctica and the Southern Ocean (e.g., Anderson, 1999; Lear and Wilson, 2000; Zachos et al., 2008; Shevenell et al., 2004). In the Weddell Sea, this notion is supported by the first occurrence of abundant ice-rafted debris (IRD) and turbidite units in Middle and Late Miocene strata at Sites 693 and 694 (Barker et al., 1988).

Paleo-ice streams played a significant role in delivering a great quantity of glacial sediments from the continent to the shelf edge. Submarine slope channels (kilometers wide and hundreds of meters deep) on continental margins acted as conduits for the transfer of large volumes of coarse-grained sediment from these streams to the deep oceans. A huge depocentre with up to 5 km of glacial sediments exists in the southern Weddell Sea (Huang et al., 2014). The sediments were transported by paleo-ice streams and subsequently reworked by gravitational flows, which led to the production of seaward prograding clinoforms at the margin (Cooper et al., 2008). Joughin and Bamber (2005) examined the mass balance of the ice-stream catchments feeding the Filchner Ronne Ice Shelf, which comprise approximately 22% of Antarctica's grounded ice sheets. The total area of the drainage basins associated with the Filchner-Ronne Ice Shelf is about 2,681,000 km² with accumulation flux about 230 Gton/year. The remarkable, unique, large catchment basins that drain to the Filchner Ronne Shelf are responsible for the large quantity of the glacial sediments in the southern Weddell Sea compared to other parts of the Antarctic margin.

From lithofacies analysis of material recovered in gravity cores, Weber et al. (1994) and Michels et al. (2002) reported on the existence of extensive contourite/channel-levee deposits in the Weddell Sea. The margin slope of the southeastern Weddell Sea is dominated by gullies and channels eroded by turbidity currents (Gales et al., 2014). These currents can be related to the Weddell Sea Embayment's importance in global ocean circulation; it is here that a significant proportion of global deep and bottom water is generated (Weppernig et al., 1996). This occurs as part of the regional ocean circulation in the Weddell Sea, which is dominated by the cyclonic, wind-driven Weddell Gyre that moves surface water down to the seafloor (Gordon et al., 1993; Orsi et al., 1993; Fahrbach et al., 1995). Cold downslope-flowing Weddell Sea Bottom Water (WSBW) is a precursor to Antarctic Bottom Water (AABW), which originates as dense shelf water (Gordon et al., 1993, Fahrbach et al., 1995). The dense shelf water forms on the continental shelf by regionally varying combinations of brine rejection from sea-ice growth and ocean/ice shelf interactions (Ohshima et al., 2013). It spills over the Filchner Trough in the southeastern Weddell Sea at an average transport rate of 1.6 Sv (10⁶ m³/s) (Foldvik et al., 2004). About 50-70% of the AABW is formed in the Weddell Sea Basin (Orsi, 1999). AABW is an important component of the global thermohaline circulation as it is the source for most of the world ocean's cold bottom water (Fahrbach et al. 1995; Orsi et al. 1999).

6.4 Data and methods

The bathymetric, sediment echosounding and seismic surveys presented in this study were acquired during RV Polarstern cruises ANT V-4 (1987), ANT VIII-5 (1990) and ANT X-1/2 (1992). In 1986/87 and 1989/1990, an 8-litre array operating at 14 MPa consisting of 3 Prakla Seismos air pulsers was used as the seismic source. The active length of the 24-channel hydrophone streamer was 600 m. In 1991/92, a 24-litre pulser array operated at 14 MPa was used with a 2400 m-long streamer (96 channels). These expeditions acquired over 25,000 km of multichannel seismic data in the southern Weddell Sea. Technical details of the data acquisition and special problems encountered in ice-covered regions are discussed in Jokat et al. (1997).

Sub-bottom profiling surveys were carried out using a conventional 3.5 kHz sediment echosounder system during the first expedition ANTV-4. Later, an Atlas Hydrographic Parasound parametric sediment echosounder was used, recording the

data on paper. Bathymetric surveys were carried out using a Hydrosweep DS-2 system, based on 15 kHz signals. ODP Site 693, with 483.9 m penetration (Fig. 2), provides age control for the shallow seismic sequences of the Weddell Sea. The site is located on a mid-slope bench close to 15.5°W on the Weddell Sea margin (Barker et al., 1988) (Fig. 1; white star).

In essence, we use the stratigraphic model of Miller et al. (1990) at ODP site 693 for constraining our interpretation of the upper three units. To support our interpretation we correlate the stratigraphic information into the seismic network around the CTMF and Polarstern Bank (Fig. 1). For consistency with recent publications by Lindeque et al. (2013) and Huang et al. (2014), however, we use a slightly different nomenclature, referring to key seismic horizons as WS-u5, WS-u6, WS-u7 (these correspond to W5, W6, and W7 of Miller et al. 1990).

6.5 Results

Three depositional units and a number of different types of sedimentary features are recognized along the southeastern continental margin of the Weddell Sea based on seismic reflection data and sub-bottom profiles. The details will be presented in this section.

6.5.1 stratigraphic ages

Unit 1 is bounded by the prominent unconformities WS-u6 and WS-u5. WS-u5 can be traced along all seismic profiles in the study area. This lowermost unit shows partly high amplitude, subparallel reflectors with intervening transparent zones (Fig. 3, CDP 17 to 2700) (Fig. 4, CDP 500-2500). Partly chaotic acoustic response with high amplitudes was observed on profiles AWI-90140 (CDP 17-5000, Fig. 3) and AWI-90020, CDP 17-2700, Fig. 4). The middle unit (Unit 2) is bounded by reflectors WS-u6 and WS-u7 and overlies Unit 1. Stratified strong parallel reflectors, as well as wavy reflectivity, characterize the sediment ridge between Channels II and III (Fig. 1, Fig. 3, AWI-90140, CDP 17-4800). Acoustically transparent zones or discontinuous reflections are often observed (Fig. 3, AWI-90140, CDP 6400-7958; AWI-90160, CDP: 17-2000; Fig. 4, CDP 17-2500) within this unit. Such transparent, opaque and chaotic reflection patterns can be associated with mass transport events. Growth faults or fractures are observed in this unit. Unit 3 is characterized by parallel or subparallel stratified reflectors with strong acoustic response, and irregularly-spaced transparent zones. Locally, reflectors are truncated or terminate at the seafloor (Fig. 4, CDP 3500-4500).

6.5.2 Levee and contourite deposits

The most prominent linear ridge-shaped sediment accumulations are the two elongate sediment ridges (ridge A and ridge B, Figs. 1 and 5), which were deposited at the distal part of CTMF in the southern Weddell Sea (Fig. 1). These sediment ridges occur as distinct linear and segmented seafloor relief running almost perpendicular to the continental margin of DML (Figs.1, 5). Levee and contourite deposits are observed in the two ridges.

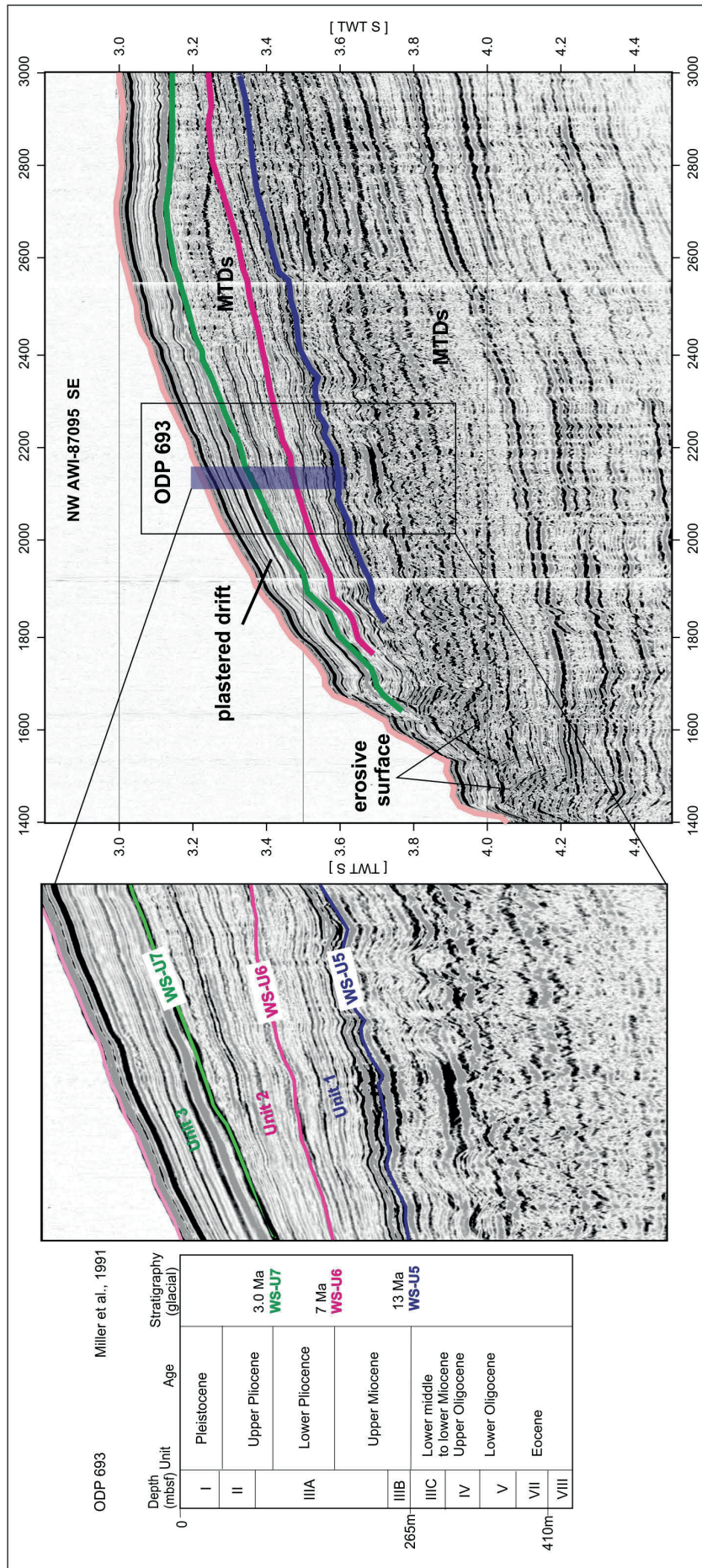


Fig. 6.2 The interpreted glacial key horizons of multi-channel seismic line from the ODP drilling site 693, and correlated it to the seismic network used in this study

6.5.2.1 Ridge A

Together with seismic reflection profiles, the bathymetric pattern constrains ridge A to be more than 80 km wide and 700 km long. Ridge A (Fig. 5 CDP: 1-1000) accumulated at the northwestern flank of Channel II, which was filled by sediment at the CTMF. The ridge terminates at about 70° S 23° W. Its maximum sediment thickness is about 2 km. In the interior of the ridge, levee deposits are extensively observed and characterized by stratified, semi-transparent acoustic units overlying chaotic seismic facies (Fig. 6A). The maximum thickness of levee deposits on the northwestern side of Channel II is around 1 km; on the southeastern side the levee sediments are significantly thinner. Within Unit 1, levee deposits have developed with subparallel reflectors on the top of partly chaotic reflections (Fig. 6A). Levee deposits continue to be present in Unit 2, in which divergent reflectors are observed (Fig. 6A CDP: 9700-10500). Unit 3 consists of well-stratified reflectors lying subparallel to the present seafloor. The channel infill is characterized by chaotic facies with very high amplitudes. A similar levee deposit with asymmetric geometry is observed associated with Channel II on the distal part of the CTMF (Fig. 6B).

Pairs of slightly asymmetrical, clear levee deposits with moderate- to low-amplitude or transparent reflectors on both flanks of the channel II are observed at the distal part of the CTMF (Fig. 1, Fig. 7 in unit 1), where they are interpreted as a channel levee complex. This part of channel II apparently originated during the deposition of Unit 2 and was filled by sediment characterized by chaotic facies with strong amplitude. However, the west flank of channel II (Fig. 7, CDP: 5400-6400) is characterized by a variable reflection pattern that includes well-stratified reflectors, mostly likely a buried drift (Unit 1). Hummocky to chaotic reflection are observed in Unit 2, and levee deposits dominate the Unit 3 with occasionally sediment waves. The total sediment thickness of the levee is about 0.5 km.

6.5.2.2 Ridge B

Ridge B is bounded by channels II and III, is more than 150 km wide and 700 km long, and terminates at about 70° S 22° W (Figs. 1, 4, 5). The maximum sediment thickness of ridge B is about 4 km. A mounded depositional body is observed at the western flank of Channel III (Fig. 5) on the slope of the southern Weddell Sea margin (Fig. 1). The ridge shows prograding reflection configurations, generated by strata that were deposited by lateral outbuilding or progradation to form gently sloping depositional surfaces. The reflection configurations change from sigmoid (Unit 1) to oblique (Unit 2) (Fig. 5, CDP: 3000-7500). A prominent mounded body (in Unit 3) displays strong amplitudes in reflectors that are truncated towards the flank of channel III. Small-scale slumps with chaotic reflectivity are present at the channel wall (Fig. 5).

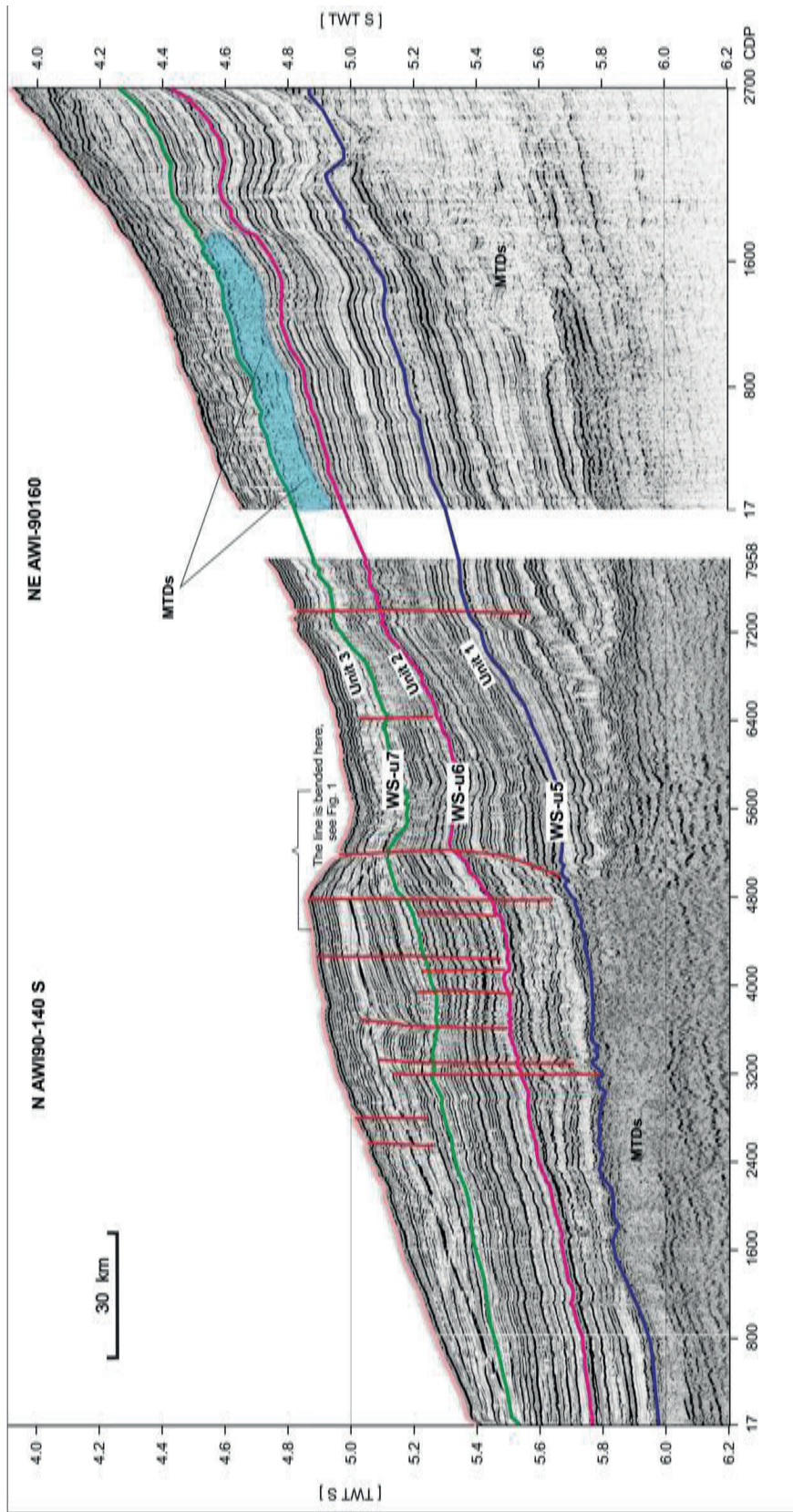


Fig. 6.3 A combined long interpreted seismic profile (AWI-90140 AWI-90160) from the continental slope of the southeast Weddell Sea. Red lines represent the growth faults.

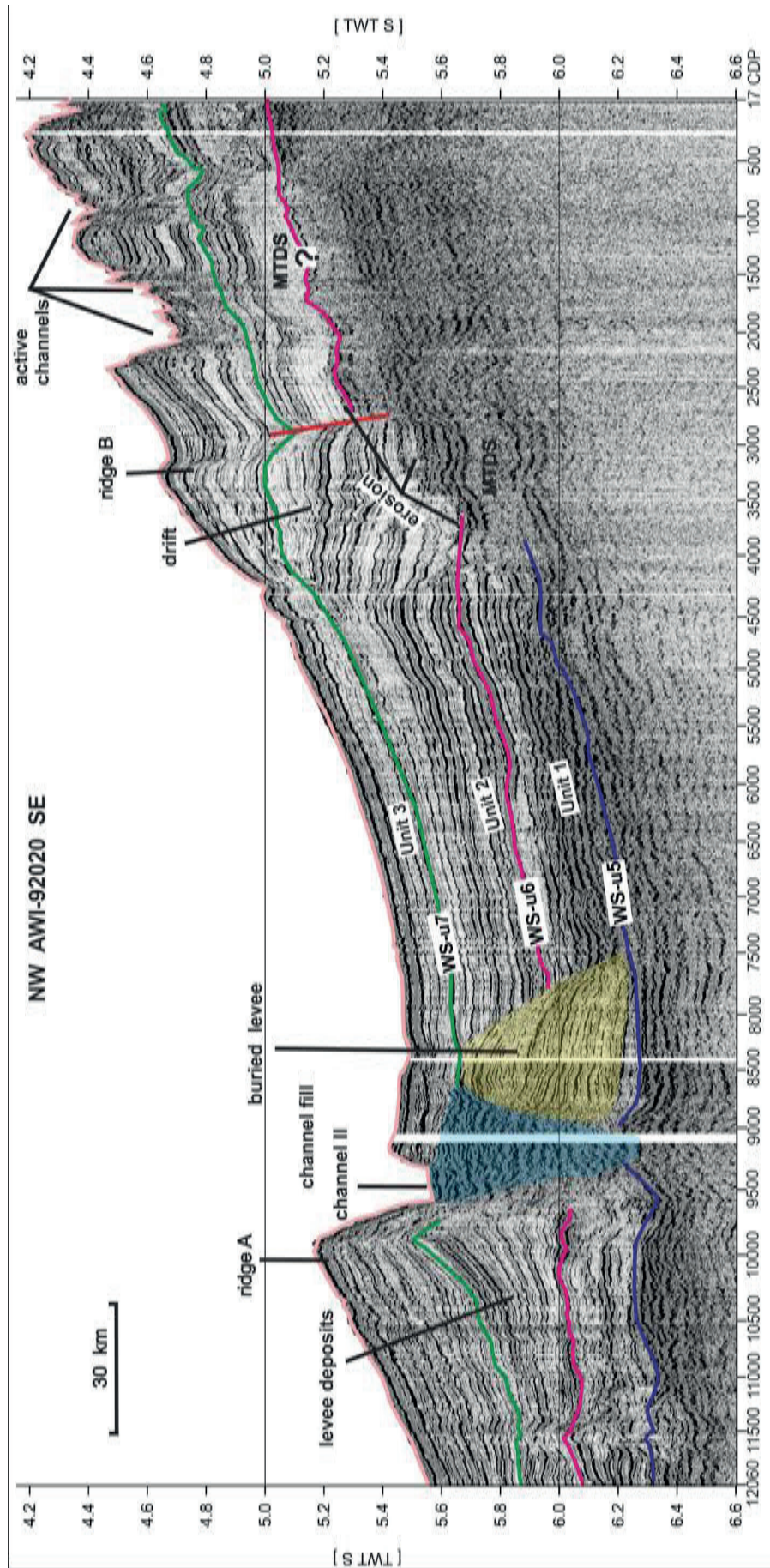


Fig. 6.4 Interpreted seismic profile AWI-92020, which crossed the two large sediment ridges and the channel II. Note the levee deposits and the buried old eastern levee deposits are observed on the west side of the channels.

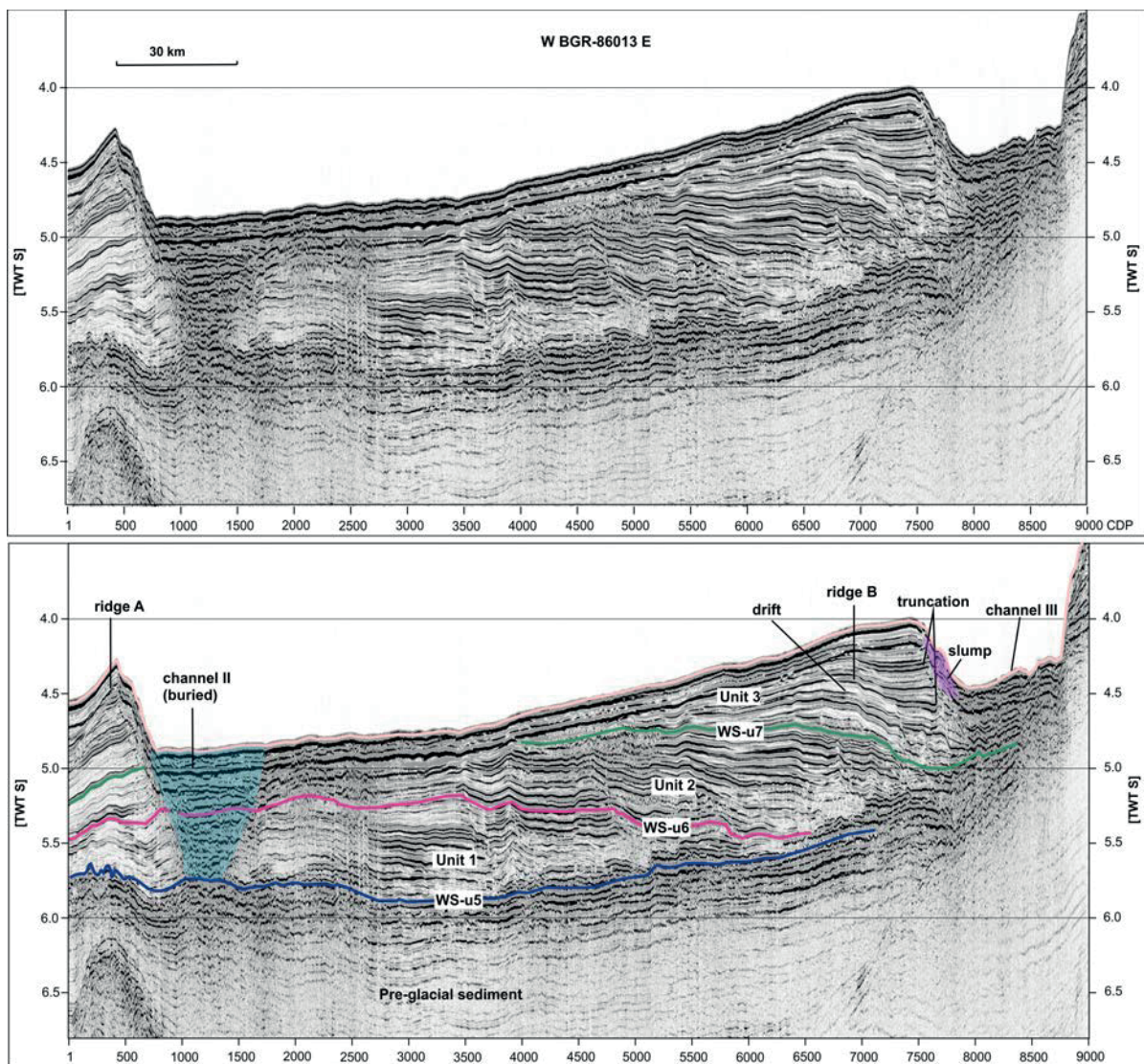


Fig. 6.5 The seismic profile BGR-86013, which gives an overview for the cross section of the sediment ridges A and B as well as Channel II and III.

Figure 8 shows data from the NW margin of Channel III on the CTMF, around 30 km basinward of the profile BGR-86013 (Fig. 5). The sedimentary body is asymmetric in shape, with a steeper and rougher eastern slope and a gentler, smoother western slope. Its steep side is characterized by relatively high amplitude reflectors that terminate at the seafloor (Fig. 8, CDP2300-2450). In contrast, the more gentle side shows parallel or sub-parallel internal reflectivity, which is sub-parallel to the sea floor above WS-u7. Hummocky or chaotic reflectivity is observed both sides of the mound and is interpreted to show buried channels above unconformity WS-u6. It appears that the mound migrated to the west during the deposition of Unit 1 to Unit 2, perhaps due to headward erosion on the steeper flank. Figure 8 shows overall along-slope elongation with asymmetric channel and mounded geometry, according to the classification of Rebeco et al., (1997) and Stow et al., (2002), the ridge B (Figs. 5, 8) is most likely a mounded drift. Two buried channels at both sides of the mound are observed at the flank of channel III.

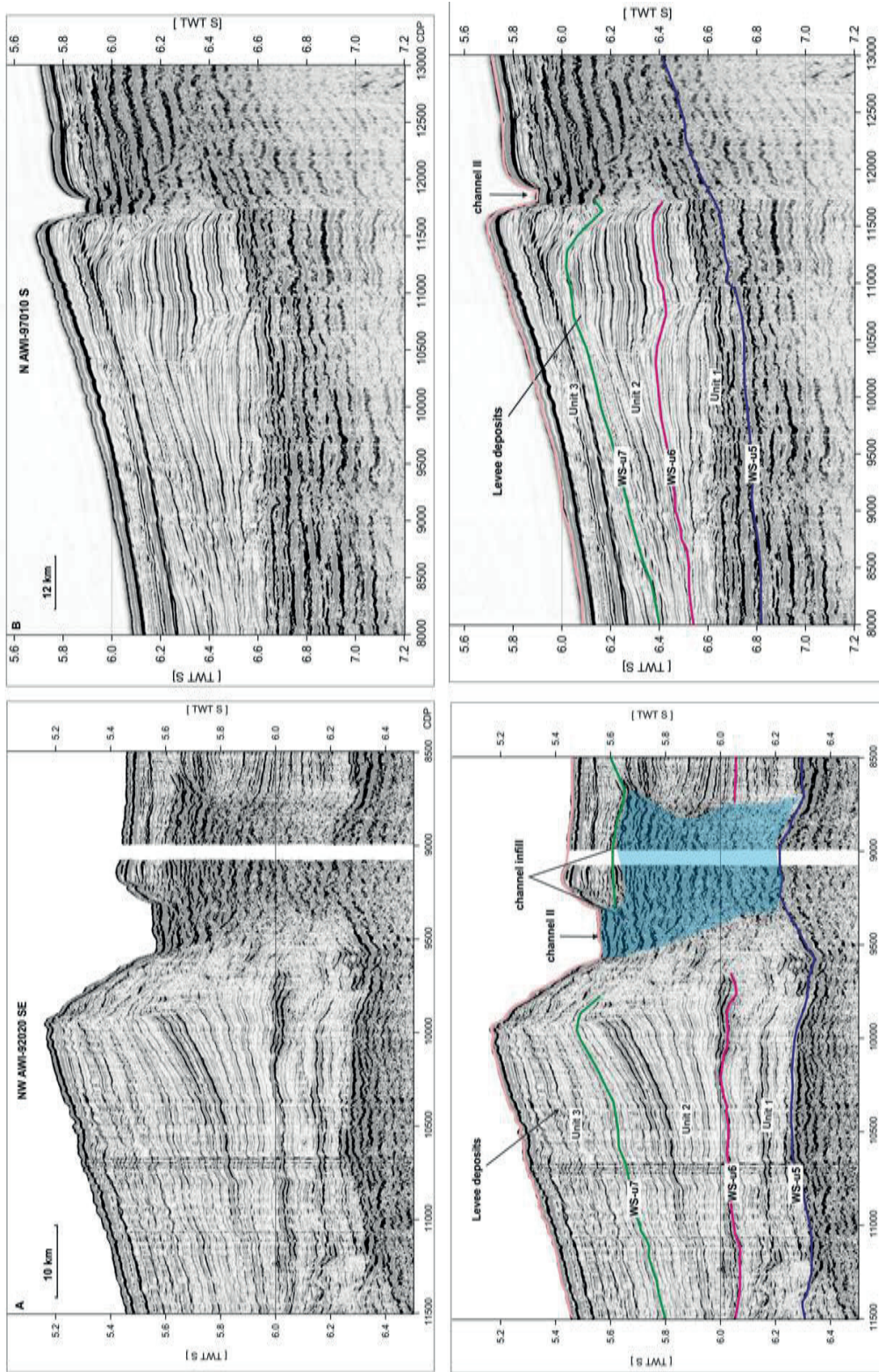


Fig 6.6 Examples of the levee deposits on the flanks of Channel II, see the locations at the Fig. 1.

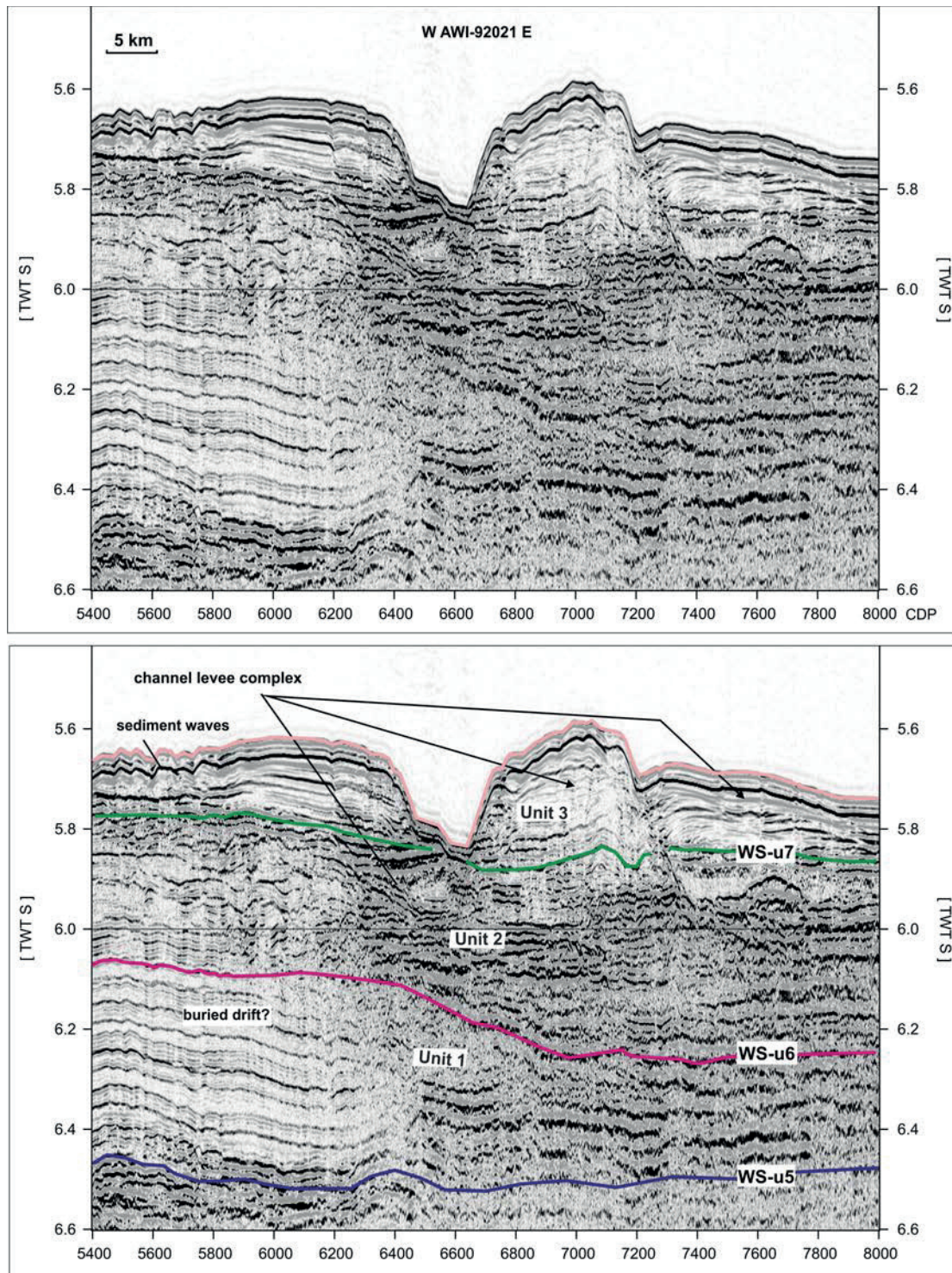


Fig 6.7 A example of the channel-levee complex, which shows several different elements, including the channel, channel infill, levee deposits sediment waves, and a buried drift in Unit 1, the location can be found in Fig. 1.

6.5.3 Mass Transport Deposits

The interpretation of MTDs followed previously-established criteria, helping the identification of packages of chaotic and/or disrupted strata (e.g. Hampton et al., 1996, Frey-Martínez et al., 2006; Bull et al., 2009). MTDs are extensively observed at the upper/lower slope transition on the CTMF close to the DML margin (Figs. 1, 9), and show a remarkable increase in frequency in Unit 2 at the west side of the

Polarstern Bank (above WS-u6) (Figs. 10A, B). Such deposits are represented by broadly tabular to lenticular, internally chaotic to semi-transparent bodies, underlain by a laterally continuous reflector, which corresponds to a strongly eroded surface. The thickness of the MTDs varies between 50 and 300 m (Figs. 9, 10). In the sub-bottom profiler, the echo-facies comprises a high-amplitude, occasionally rough surface reflector, low penetration, and an absence of internal reflections, which are Glacigenic Debris Flow (Fig. 9, A-B). Glacigenic debris flow deposits is a type of MTDs, often occurs on the glaciated margins (Mulder and Alexander, 2001).

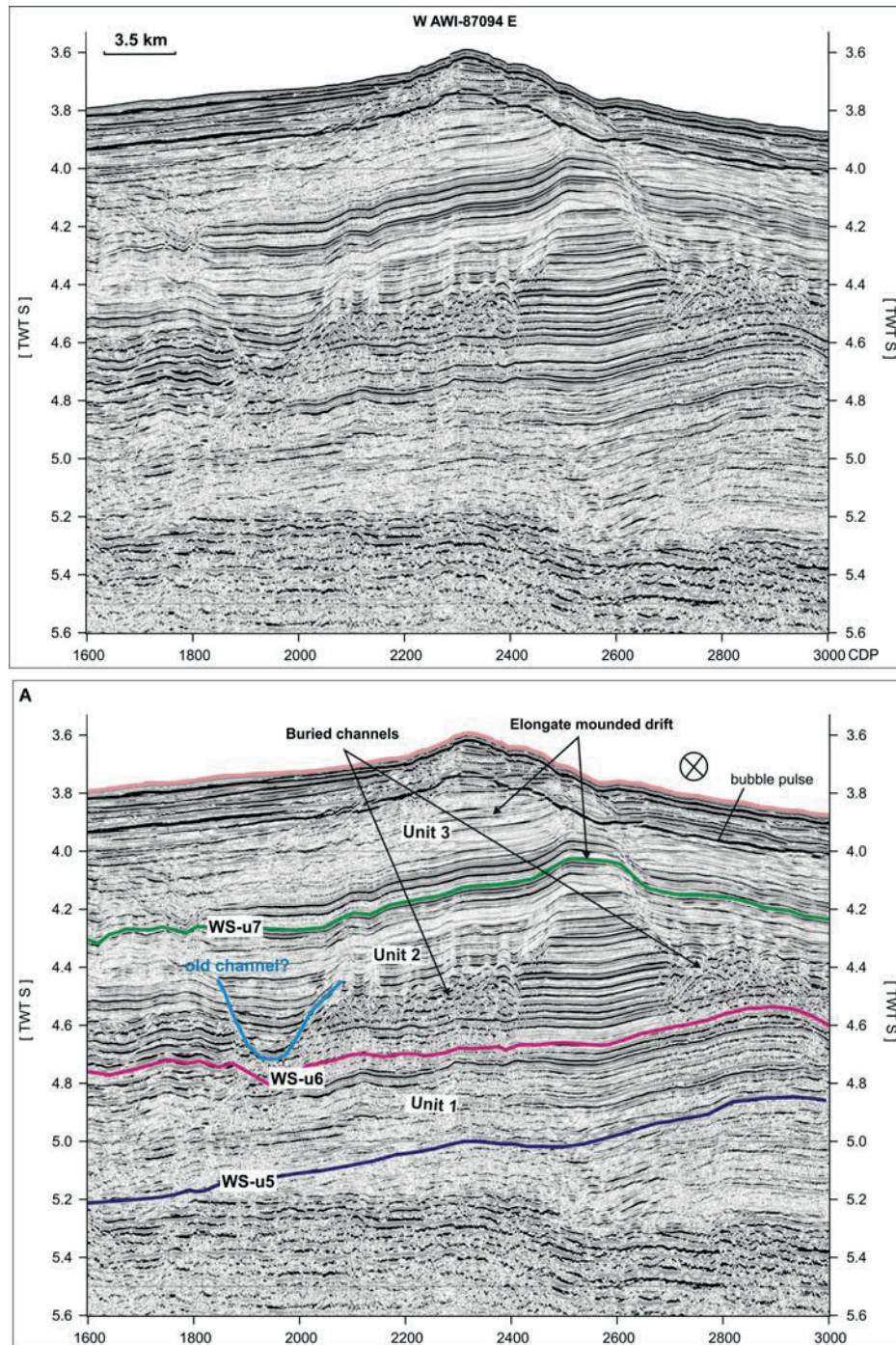


Fig. 6.8 A example of mounded drift formed from the Ridge B at the channel III, see the locations at the Fig. 1. There is a bubble pulse at about 4s TWT.

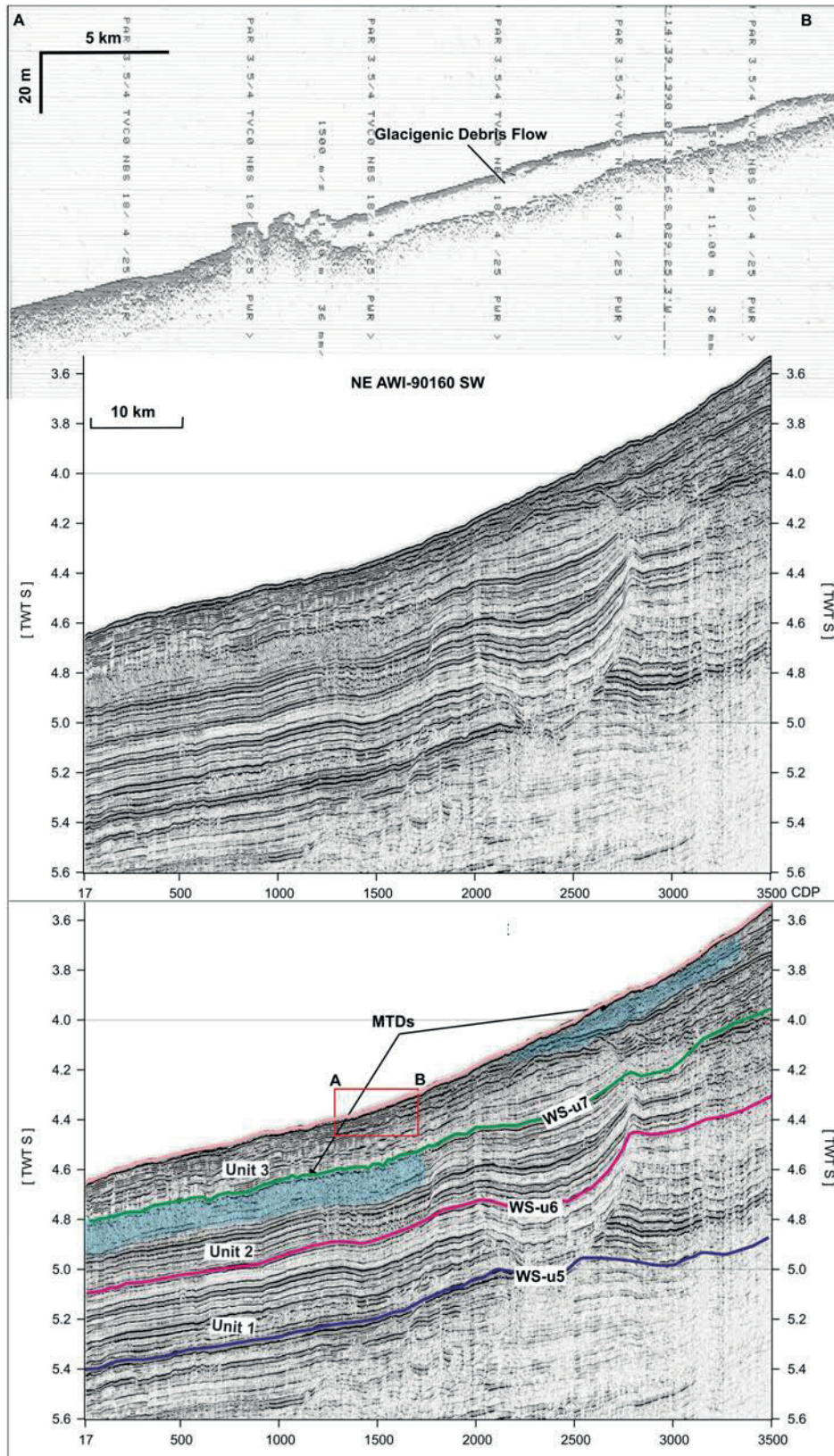


Fig. 6.9 MTDs are observed on seismic profile AWI-90160, which is located at the CTMF, see the location of the Fig. 1. AB is the scanned subbottom profilers. MTDs repeatedly occurred in Unit 2.

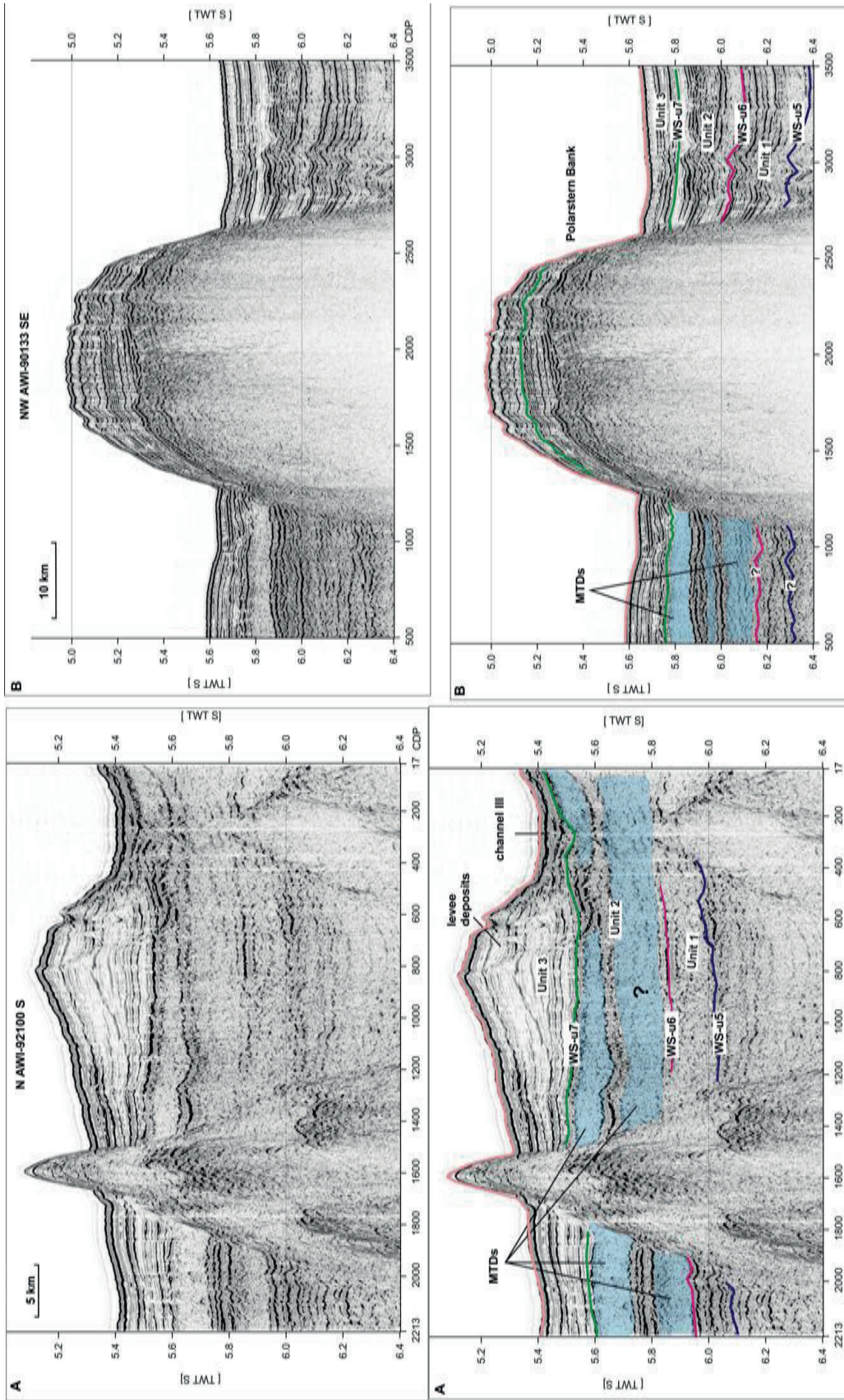


Fig. 6.10. Examples of the MTDs on the seismic profiles AWI-92100 and AWI-90133, which are around Polarstern Bank, see the locations on the Fig. 1.

6.5.4 Shelf edge deposits

The most prominent glacial trough in the Weddell Sea region is the 100-150 km wide Filchner Trough, which extends from beneath the Filchner Ice Shelf to the continental shelf edge (Fig. 1). On the outer shelf the trough is up to 500 m deep, and increases to about 1200 m water depth close to the ice shelf front in the south. The CTMF formed at the mouth of the Filchner Trough as a consequence of the transport of vast quantities of glacial sediments (Fig. 1). Figure 11 displays a seismic profile that crosses the outermost continental shelf, shelf edge and slope of the CTMF. A number of truncations and toplaps are observed on this profile. The tentatively interpreted WS-u5 shows a strong erosional, convex surface, and similar sub-parallel reflectors are observed above it. Reflectors in Unit 2 are less convex and Unit 1 is characterized by relatively chaotic reflectivity. The extensive progradation has resulted in the outer shelf building out over the slope (Fig. 11).

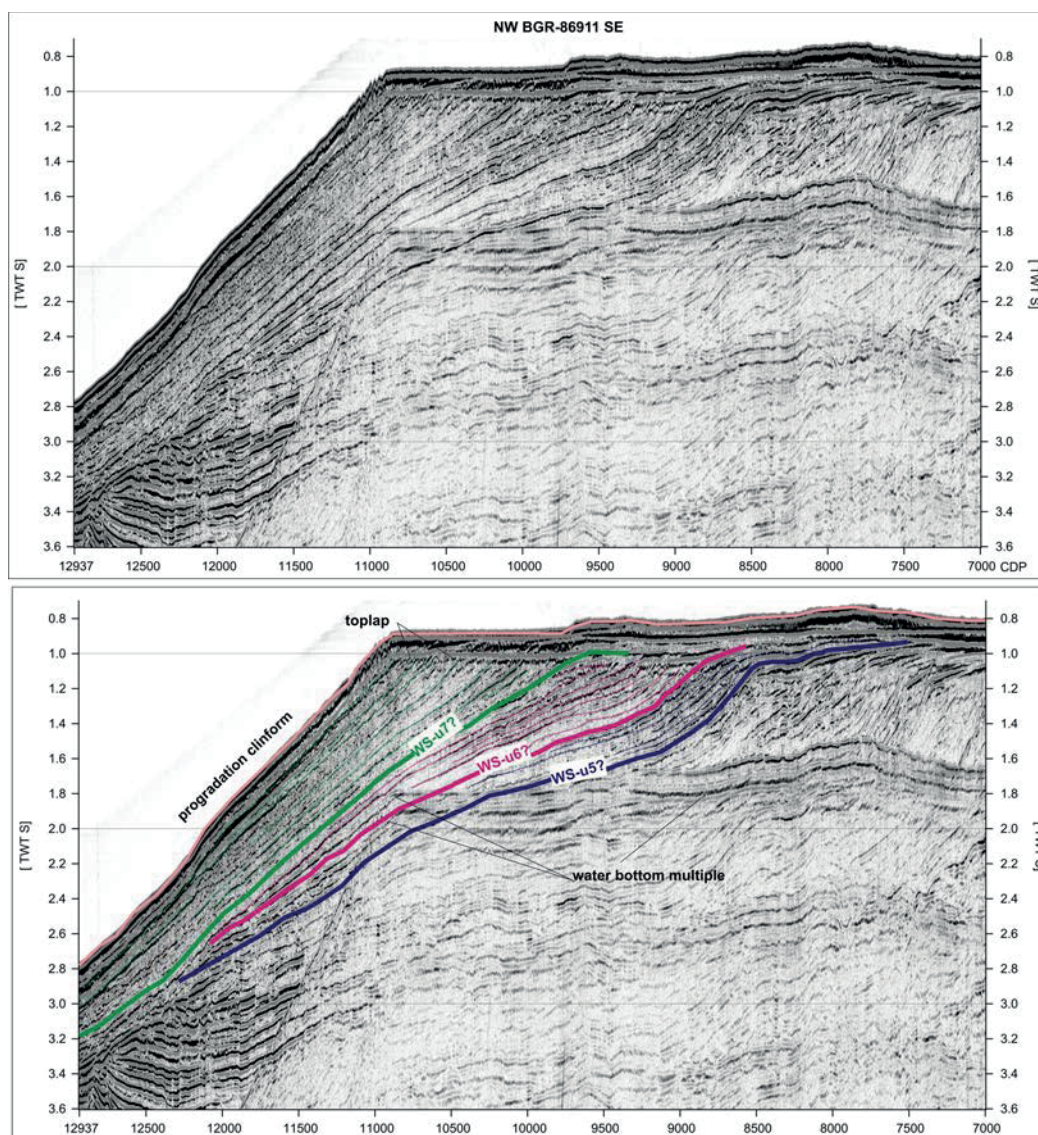


Fig. 6.11 Interpreted and non-interpreted seismic profile BGR-86011, which crossed the continental shelf edge, see the location on the Fig. 1.

6.6 Discussion

6.6.1 Stratigraphic correlations

A tentative stratigraphic correlation has been made based on the sampling at ODP Site 693, seismic expression of the used seismic network in this study, and previous age model studies (Miller et al., 1990; Rogenhagen et al., 2004; Huang et al., 2014). WS-u5 is a prominent reflector that can be recognized basin-wide, and which marks a shift of seismic facies from chaotic or discontinuous reflections to more irregular and transparent patterns (Fig. 2). We interpret WS-u5 to represent the beginning of a full-glacial regime in the Middle Miocene. Consistent with this, Unit 1 (~13-7 Ma) above WS-u5, is associated with glacial turbidites and IRD of Middle Miocene age at ODP Site 693 (Barker et al., 1988).

WS-u6 in our age model marks the Miocene/Pliocene boundary at ~7 Ma, based on magnetostratigraphic and biostratigraphic analysis of ODP Site 693 (Barker and Kennett, et al., 1990). Unit 2, overlying it, has been assigned a Late Miocene to Early Pliocene (7-3 Ma) age. During this period, a short phase of climatic warmth occurred (4.9-4.1 Ma) with surface water temperatures warmer than at the present day based on benthic Mg/Ca, corresponding to high sea level and partial Antarctic ice sheet retreat (Barker and Kennett, et al., 1990; Passchier, 2011).

Unconformity WS-u7 separates Unit 3 from Unit 2 and is assigned to the Late Pliocene (3.0 Ma), based on the drilling constraints of ODP 693 (Barker et al., 1988). This unit is dominated by a draping, continuous sequence of relatively constant thickness (Fig. 2). During this period, Antarctic cooling intensified and a major ice sheet expansion occurred, resulting in strengthened westerly winds and invigorated ocean circulation (Naish et al., 2009; McKay et al., 2012). This occurred as part of a global cooling that also saw sea level falls due to the expansion of Northern Hemisphere ice sheets (Miller et al., 2011; Zachos et al., 2008).

6.6.2 Depositional environment of turbidity-contourite

The two sediment ridges, A and B, show a complex of both extensive levee deposits (Figs. 6, 7) and elongate mound drifts (Figs. 5, 8). As described below, we tentatively interpret them (Figs. 5, 6, 7) as turbidity-contourites, mixed-system consequences of the interplay between turbidity and bottom currents. In general, the trend and degree of progradation of turbidity-contourites can vary with respect to sediment supply, margin morphology, bottom current intensity, and sea level and ice volume changes (Rebesco et al., 1997; Uenzelmann-Neben, 2006; Miller et al., 2011).

6.6.2.1 Bottom/turbidity currents

In Ridge A, the levees alongside deep-sea channels I and II developed by overbank deposition (Figs. 1, 6, 7). Overbank deposits are well developed on the western sides and less developed on the eastern sides of channels in the southern hemisphere because the Coriolis force deviates turbidity currents flowing along the channels (Figs. 6A). Pronounced growth, indicated by the divergent reflectors in the levee deposits, suggests a period of high sediment supply lasting from the Late Miocene to the Late Pliocene (Unit 2) (Fig. 6). This is consistent with the increased sedimentation rate (50 m/m.y.) reported for the period at ODP site 693 (Golovchenko et al., 1990). The semi-transparent, stratified reflectors inside levee deposits indicate the presence of fine-grained turbidites and hemipelagic and pelagic sediments, as sampled at ODP drill site 694 in the abyssal plain (Barker et al., 1988). Some fine-grained sediment were reworked by episodic turbidity currents to generate well-sorted deposits, which were transported over long run-out distances and deposited as large

levee or channel levee complexes over the past 15 Myr (Fig. 7) (Emery and Myers, 1996; Faugères et al., 1999; Michels et al., 2001, 2002).

Ridge B is bounded on one side by the non-depositional or erosional channel III (Figs. 5, 8). Its large mounded elongated sedimentary geometry is parallel to the deep bottom-current flow of WSBW. The channel's levees, like those described above, are the results of turbidity flow. These interpretations allow the diagnosis of Ridge B as consisting of a NE-SW trending turbidity-contourite. The position and geometry of turbidity-contourites are controlled by pre-existing seafloor morphology, which directs the various branches of the bottom currents. The direction of the bottom currents interacts, in turn, interact with the geometries of contourite bodies. Thus, we affirm the NE-SW trends of the turbidity-contourites were probably associated with the northeast flow direction of WSBW, which is as least as old as Ridge B in this region. AABW and the Weddell Gyre circulate along the continental margin and flow toward the west in the southeast Weddell Sea, where they have contrived the asymmetric geometry of the turbidity-contourites. The levee deposits in Ridge B are truncated at their margin with channel III (Figs. 5, 8). The truncated reflectors (Fig. 5, CDP 7500-8000) seem to have been eroded due to slope instability resulting from the elevation difference between the levee and the channel, which developed through the progressive aggradation of the former.

6.6.2.2 Sea level and ice sheet evolution

Continuous deposition occurred throughout the Miocene, Pliocene and Pleistocene (Barker and Kennett, 1988). Owing to their location on the CTMF (Figs. 1, 3, 4), a major depocentre for terrigenous sediment brought to the continental margin by paleo-ice streams, the large turbidity-contourite bodies described above will also have been affected by ice sheet advances/retreats that occurred in response to eustatic sea level change and climate change. In the seismic records, the reflection pattern in the lower part of Unit 1 shows a great variability of amplitudes (Figs. 5, 6, 7). This can be related to the onset of Antarctic glaciation in the Middle Miocene (Fig. 12). We suggest that sea level fall (between 54-69 m) (Miller et al., 2011), as a consequence of full Antarctic glaciation in the Middle Miocene, led to sediment starvation or erosion on the shelf, and an increase in deposition in the deep sea (Figs. 11, 12) This is supported by an increase in sedimentation rates at ODP site 693 from 2.5 m/m.y. in the Early Miocene to 8 m/m.y. in the Middle Miocene (Barker, Kennett et al., 1990) (Fig. 12).

A faster sedimentation rates with 24 m/m.y. and 50 m/m.y. have been seen in the late Miocene and early Pliocene (Unit 2) (Golovchenko et al., 1990) (Fig. 12), at ODP Site 693. In the seismic records, the divergent reflectors in the levee deposits of Unit 2 (Fig. 6A CDP: 9700-10500) also suggest a high sediment supply. Abundant MTDs are observed in this unit (Figs. 9, 10). We may suspect that Weddell Sea shelf margin have been severely glaciated as the ice sheets advanced, in order to continuously supply sediment during this period. However, the model studies suggested that the EAIS is thought to have experienced large-scale mass loss during the early Pliocene (Pollard and DeConto, 2009) (Fig. 12). Therefore, the southeast Weddell Sea margin was probably under a condition that lack of large-scale glaciation. The high voluminous terrigenous sediments supply could be attributed to the river system or deep canyons with filled local glaciers (Barker et al., 1992). We consider that a relatively sea level fall in this Unit is ascribed to the Pliocene intensification of Northern Hemisphere glaciating (Fig. 12).

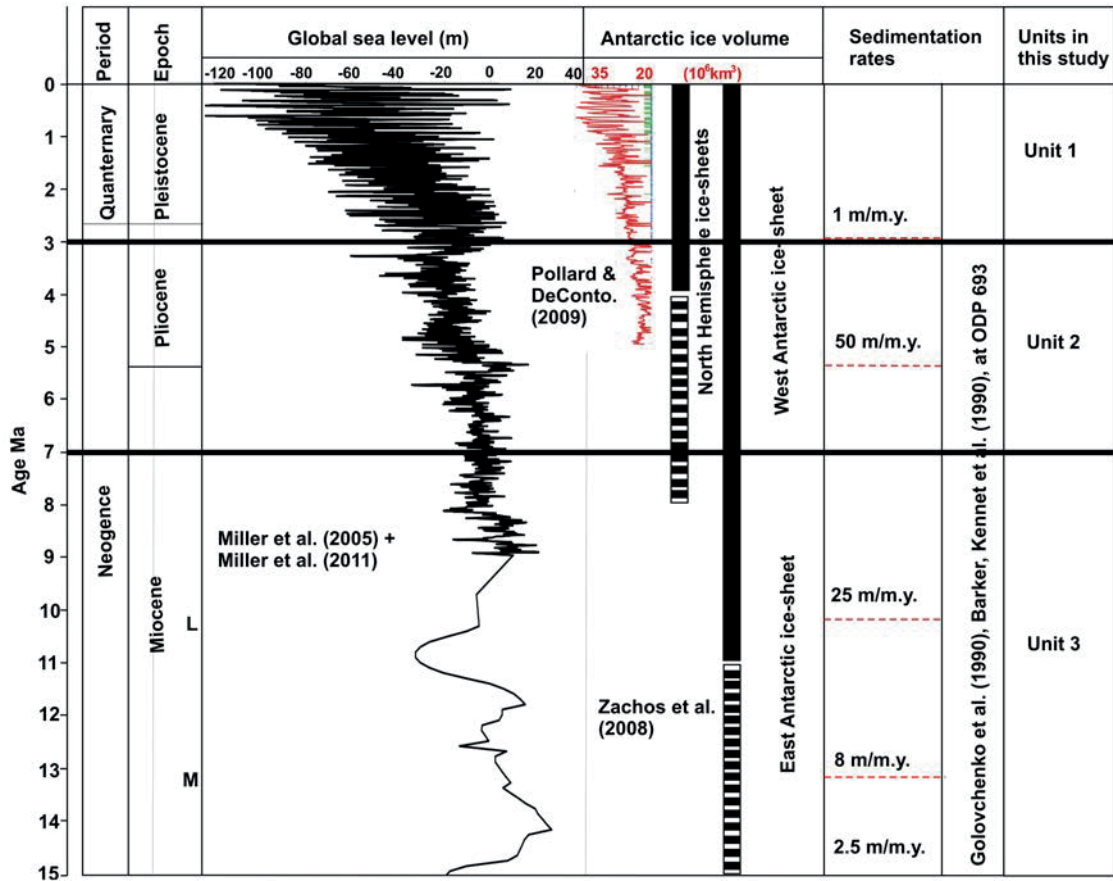


Fig. 6.12 A smoothed global sea level curves for the past 15 Myrs from Miller et al. (2006) and (2011). The red curve is the modeled Antarctic ice volume from Pollard and DeConto (2009). Solid bars indicate strong evidence for ice-sheet existence, and dashed lines indicate early phase of ice-sheet development. Sedimentation rates are adopted from the IODP report and the relevant publication. The last section is the distinguished units in this study.

A regional decrease in sedimentation rates (1 m/m.y.) beginning at about 3 Ma at ODP site 693 (Fig. 12) has been attributed to a reduction in the supply of terrigenous sediments to the Weddell Sea margin and the permanent grounding of the ice shelf along the Antarctic margin (Barker, Kennet et al., 1990). Global ice volume and sea level during the early Pliocene and Pleistocene were strongly influenced by orbital forcing, and marine glacial deposits of this age consequently often exhibit regular glacial-interglacial cycles (Leisiecki and Raymo, 2005; Miller et al., 2011; Patterson et al., 2014). In the seismic records, the widespread presence of levees in Unit 3 across the continental slope, rise, and abyssal plain (Fig. 6) suggests that turbid-water production and associated down-slope sediment gravity flows at former ice-sheet and ice-stream margins were probably the more significant processes in the formation and development of the levee deposits (Fig. 13).

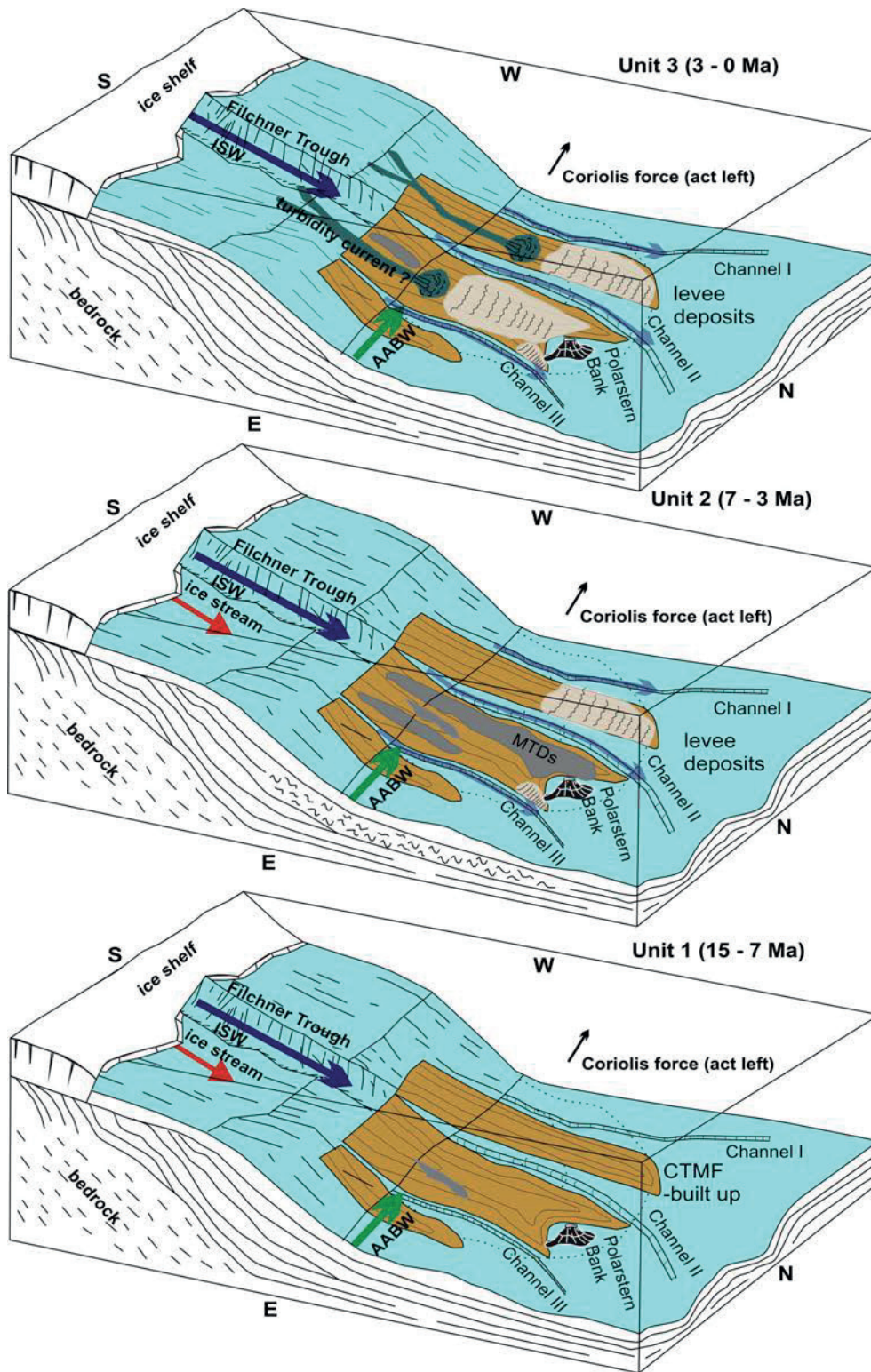


Fig. 6.13. Simplified depositional models for the observed seismic units off the Filchner Shelf. Unit 1 (15-7 Ma): CTMF started to build up by ice sheets advance. Unit 2 (7-3 Ma): increased MTDs are featured in this unit. Unit 3 (3-0 Ma): Levee deposits are dominated on the continental slope and rise.

6.6.3 MTDs and associated trigger mechanisms

MTDs have been extensively reported on the CTMF and around Polarstern Bank in the southeast Weddell Sea (Figs. 9, 10). Several trigger mechanisms for the

occurrence of the MTDs have been suspected in this study, including sediment loading, sea level change, earthquakes, active tectonics and fluids and/or gas hydrate dissociation (Masson et al., 1996; Reeder et al., 2000; Talling et al., 2007; Nelson et al., 2011; Piper et al., 2012; Ruano et al., 2014). However, fluid and/or gas hydrate dissociation is unlikely to be the trigger of MTDs in our study region due to lack of direct evidence for fluid flow in the seismic records.

Numerous MTDs in Unit 2 apparently rest on the prominent sequence boundaries WS-u6 and WS-u7 on the continental slope and rise (Figs. 9, 10), indicating they date from the Late Miocene to Late Pliocene. These correlations suggest a common cause with the formation of the major erosional unconformities, which have been correlated with sea-level changes, particularly in the early and Mid-Pliocene warm period when sea level fell by as much as 65 m (Dwyer and Chandler, 2008; Miller et al., 2011). Sea level fall plays a significant role in supplying fluvial sediments directly to deep water areas where they can form large volume gravity-flow deposits (Posamentier and Kolla, 2003).

Elsewhere, the seismic records imply that MTDs accumulated rapidly on the outer shelf and upper continental slope in the southeast Weddell Sea (Figs. 9, 10, 13). This is the case particularly in front of the Filchner Trough (Fig. 1, MTDs), where large amounts of sediment were rapidly delivered to the upper slope by ice streams in glacial times or deep canyons with local glaciers (Barker, Kennet et al., 1990, Huang et al., 2014). A high sediment supply, implied by the up to 50 m/m.y. sedimentation rate on the continental slope (Golovchenko et al., 1990), may have promoted subsequent down-slope remobilization. Inferred MTDs overlie thick successions of inferred hemipelagic and pelagic sediments of Unit 1 (Figs. 9, 10) and were possibly triggered by sediment loading leading to overpressure at the shelf break during rapid sediment accumulation. In addition, the steep topographic gradient (up to 7.5°) of the slope off the DML margin is likely to have promoted frequent mass transport as well (Figs. 1, 11). The steeper the slope, the greater the velocity of sediment gravity flows and, therefore, the greater the sediment discharge to the slope.

Lithospheric stress, induced by glacial loading and/or active tectonics, can trigger instabilities and generate MTDs (James and Ivins, 1998; Maslin et al., 2004, Shanmugan, 2006). Many studies show a strong linkage between MTDs and earthquakes induced by active intraplate deformation and volcanism (Ferentinos et al., 1988; Shanmugam, 2006; Argnani et al., 2012; Vargas et al., 2012). Abundant MTDs in the southern Scotia Sea have been attributed to active tectonics and earthquakes in the Scan and Dove basins, close to the active Antarctic-Scotia plate boundary (Ruano et al., 2014). However, monitoring at Neumayer station reveals modern-day seismic activity in the southeast Weddell Sea to be only slight to moderate (Reading, 2002; Fütterer et al., 2006). This is because plate boundary tectonics ceased to operate in the southeast Weddell Sea after 122 Ma (König and Jokat, 2006). This leaves only the very largest regional plate boundary earthquakes, for example at the South Sandwich Trench, as earthquake triggers for the region's MTDs. Glacial loading contrasts, on the other hand, might be more plausibly related to mass transport events in the southeast Weddell Sea. Yamane et al. (2015), for example, modeled a thicker Pliocene EAIS resulting from enhanced moisture transport and increased snowfall.

6.6.4 Possible implications for Antarctic ice sheets

Because of the numerous glacial unconformities on the shelf and the absence of a deep drill core penetrating these strata, it is challenging to establish a detailed prograding-slope stratigraphy of the CTMF to interpret the history of ice sheets advances/retreats and grounding events on the continental shelf. The observed changes of depositional style in the southeast Weddell Sea can be interpreted in terms of paleo-climate changes and glacial history (Fig. 13). The CTMF deposits and the initial giant turbidity-contourites are a composite product of multiple episodes of ice sheet advances/retreats during the deposition of three units under the region's glacial bottom current (alongslope processes) regime and turbidity flow (downslope processes). Later, as seen in units 2 and 3, extensive mass transport events (Figs. 9, 10, 13) occurred as slopes steepened beyond critical angles at some locations during the progradation and/or basinward tilting of platform strata near the shelf edge, to which ice sheets periodically advanced due to orbital forcing (Patterson et al., 2014).

The seismic reflection data most likely represent several million years of glacial history. The truncations and toplaps indicate temporary periods of erosion within an environment in which there has been net deposition over the past several million years (Fig. 11). The seismic reflection data most likely represent several million years of glacial history. During major glacial periods, an ice sheet may advance far into the marine realm as grounded ice. This will lead to large quantity of sediments delivered through transport at the base of a paleo-ice stream and subsequent reworking by gravitational flows, which led to the production of appreciable seaward prograded clinoforms at the margin (Figs. 11, 13).

6.7 Conclusions

Two giant, sinuous, NE-SW-oriented sediment ridges are the most prominent sedimentary features of the southeast Weddell Sea. The bathymetric expressions of the ridges are more than 150 km wide and 700 km long. Sediment thicknesses in the ridges reach as much as 2 km. We interpreted these ridges as turbidity-contourites, due to the complicated down-slope/along-slope processes occurring across their margins with channels at their flanks. The turbidity-contourites are formed by along slope process (e.g. AABW, WSBW), and significantly modified and conditioned by downslope process (turbidity flow) to form extensive levees in the study region. In addition, the seismic data allow us to interpret the influences over time of the region's unique large catchment area, fast (paleo-) ice streams, abundant sediment supply, fluctuating sea level, and advancing and retreating ice sheets, on the development of the giant turbidity-contourites.

Other, related, changes in depositional style are visible in our offshore seismic data from the Late Miocene to Late Pliocene in this study. The remarkable increase in MTDs during the Late Miocene and Middle to Late Pliocene (between WS-u6 and WS-u7) is related to the build up of overpressure during rapid sediment accumulation, changing sea-level, and possibly also glacial-isostatic paleoearthquakes. Our stratigraphic studies may indicate that fluctuations of Antarctic ice sheets similar to those occurring during late Quaternary glacial cycles have been typical for the region during glacial periods since the Late Miocene or even earlier. However, the details of the ice sheet dynamics can only be constrained by deep scientific drilling.

6.8 Acknowledgements

The authors would like to thank the masters, crews and seismic teams of the many ship expeditions to the Weddell Sea, who made the acquisition of the data used in this study possible. The German Federal Institute of Geosciences and Resources (BGR) as well as research institutes in Norway are gratefully acknowledged for their contribution of the used seismic data to the Antarctic Seismic Data Library System (SDLS). Many thanks to Dr. Graeme Eagles his careful reading and discussions of the manuscript before submission and the constructive comments from reviewers. X.H. has been receiving a PhD scholarship from the Chinese Scholarship Council (CSC).

6.9 References

Anderson, J.B., 1999. Antarctic Marine Geology. Cambridge University Press (289 pp).

Arndt, J.E., H. W. Schenke, M. Jakobsson, F. Nitsche, G. Buys, B. Goleby, M. Rebesco, F. Bohoyo, J.K. Hong, J. Black, R. Greku, G. Udintsev, F. Barrios, W. Reynoso-Peralta, T. Morishita, R. Wigley, (2013). "The International Bathymetric Chart of the Southern Ocean (IBCSO) Version 1.0 - A new bathymetric compilation covering circum-Antarctic waters", *Geophys Res Lett.*, doi: 10.1002/grl.50413.

Argnani, A., Armigliato, A., Pagnoni, G., Zaniboni, F., Tinti, S., & Bonazzi, C. (2012). Active tectonics along the submarine slope of south-eastern Sicily and the source of the 11 January 1693 earthquake and tsunami. *Natural Hazards and Earth System Science*, 12(5), 1311-1319.

Barker, P.F., Kennett, J.P., et al, (1988). Proceedings of the Ocean Drilling Program, Scientific Results Leg 113. Ocean Drilling Program: 774. doi:10.2973/odp.proc.ir.113.1988.

Bart, P.J., DeBatist, M., and Jokat, W., (1999), Interglacial collapse off Crary Trough Mouth Fan, Weddell Sea, Antarctica: Implications for Antarctic glacial history: *Journal of Sedimentary Research*, v. 69, p. 1276–1289.

Bart, P.J., J.B., Anderson, F. Trincardi, and S.S. Shipp. 2000. Seismic data from the Northern Basin, Ross Sea, record extreme expansions of the East Antarctic Ice Sheet during the late Neogene. *Marine Geology* 166:31–50, [http://dx.doi.org/10.1016/S0025-3227\(00\)00006-2](http://dx.doi.org/10.1016/S0025-3227(00)00006-2).

Barker, P. F., & Kennett, J. P. (1988). Leg 113. In Proc. Ocean Drill. Program Initial Rep (Vol. 113, p. 1033).

Barker, P.F., Kennett, J.P., et al., 1990. Proc. ODP, Sci. Results, 113: College Station, TX (Ocean Drilling Program). doi:10.2973/odp.proc.sr.113.1990.

Barker, P. F. (1992). The sedimentary record of Antarctic climate change. *Philosophical Transactions of the Royal Society B: Biological Sciences*, 338(1285), 259-267.

Cooper, A. K., Brancolini, G., Escutia, C., Kristoffersen, Y., Larter, R., Leitchenkov, G., ... & Jokat, W. (2008). Cenozoic climate history from seismic reflection and drilling studies on the Antarctic continental margin. *Developments in Earth and Environmental Sciences*, 8, 115-234.

Dowdeswell, J.A., Ó Cofaigh, C., Pudsey, C.J., (2004). Continental slope morphology and sedimentary processes at the mouth of an Antarctic palaeo-ice stream. *Marine Geology*.204, 203–214.

Dowdeswell J.A., O' Cofaigh C., Noormets R, et al. (2008). A major trough mouth fan on the continental margin of the Bellingshausen Sea, West Antarctica: the

Belgica Fan. *Marine Geology*, 252, 129–140.

Donda, F., O'Brien, P.E., De Santis, L., Rebesco, M., Brancolini, G., 2008. Mass wasting processes in the Western Wilkes Land margin: possible implications for East Antarctic glacial history. *Palaeogeogr., Palaeoclimatol., Palaeoecol.* 260, 77–91 (this issue). doi:10.1016/j.palaeo.2007.08.008.

Dwyer, G. S., & Chandler, M. A. (2009). Mid-Pliocene sea level and continental ice volume based on coupled benthic Mg/Ca palaeotemperatures and oxygen isotopes. *Philosophical Transactions of the Royal Society A: Mathematical, Physical and Engineering Sciences*, 367(1886), 157-168.

Emery, D., Myers, K., (1996). *Sequence Stratigraphy*. London: Blackwell Science, 297 pp.

Foldvik, A., Gammelsrød, T., & Tørresen, T. (1985). Circulation and water masses on the southern Weddell Sea shelf. *Oceanology of the Antarctic continental shelf*, 5-20.

Foldvik, A., T. Gammelsrød, S. Østerhus, E. Fahrbach, G. Rohardt, M. Schröder, K. Nicholls, L. Padman, and R. Woodgate (2004), Ice Shelf Water overflow and bottom water formation in the southern Weddell Sea, *Journal of Geophysical Research*, 109, C02015, doi:10.1029/2003JC002008. Fahrbach, E., G. Rohardt, N. Scheele, M. Schröder, V. Strass, and A. Wisotzki (1995), Formation and discharge of deep and bottom water in the northwestern Weddell Sea, *Journal of Marine Research*, 53, 515–538.

Faugères, J.C., Stow, D.A.V., Imbert, P., Viana, A.R., (1999). Seismic features diagnostic of contourite drifts. *Marine Geology*, 162, 1–38.

Ferentinos, G., Papatheodorou, G., & Collins, M. B. (1988). Sediment transport processes on an active submarine fault escarpment: Gulf of Corinth, Greece. *Marine Geology*, 83(1), 43-61.

Fütterer, D. K., Damaske, D., Kleinschmidt, G., Miller, H., & Tessensohn, F. (Eds.). (2006). *Antarctica: Contributions to Global Earth Sciences*. Springer Science & Business Media.

Gales, J. A., Leat, P. T., Larter, R. D., Kuhn, G., Hillenbrand, C. D., Graham, A. G. C., ... & Jokat, W. (2014). Large-scale submarine landslides, channel and gully systems on the southern Weddell Sea margin, Antarctica. *Marine Geology*, 348, 73-87.

Gordon, A. L. (1993). Weddell Sea exploration from ice station. *Eos, Transactions American Geophysical Union*, 74(11), 121-126.

Golovchenko, X., O'Connell, S.B., and Jarrard, R., 1990. Sedimentary response to paleoclimate from downhole logs at Site 693, Antarctic continental margin. In Barker, P.F., Kennett, J.P., et al., *Proc. ODP, Sci. Results*, 113: College Station, TX (Ocean Drilling Program), 239–251. doi:10.2973/odp.proc.sr.113.191.1990.

Huang, X., Gohl, K., Jokat, W., (2014) Variability in Cenozoic sedimentation and paleo-water depths of the Weddell Sea basin related to pre-glacial and glacial conditions of Antarctica, *Global and Planetary Change*. DOI: 10.1016/j.gloplacha.2014.03.010.

Howat, I.M., and Domack, E.W., (2003). Reconstructions of western Ross Sea palaeo-ice stream grounding lines from high resolution acoustic stratigraphy. *Boreas*, 32, 56-75.

Hernández-Molina, F.J., Paterlini, M., Somoza, L., Violante, R., Arecco, M.A., de Isasi, M., Rebesco, M., Uenzelmann-Neben, G., Neben, S., Marshall, P., 2010. Giant mounded drifts in the Argentine Continental Margin: origins, and global implications for the history of thermohaline circulation. *Marine and Petroleum*

Geology 27, 1508–1530.

Jokat, W., C. Hübscher, U. Meyer, L. Oszko, T. Schöne, W. Versteeg, and H. Miller (1996), The continental margin off East Antarctica between 10°W and 30°W, in *Weddell Sea Tectonics and Gondwana Break up*, edited by B. C. Storey, E. C. King, and R. A. Livermore, Geological Society London Special Publications, 108, 129–141.

Jokat, W., Fechner, N., & Studinger, M. (1997). Geodynamic models of the Weddell Sea embayment in view of new geophysical data. *The Antarctic region: geological evolution and processes*, 453-460.

Joughin, I. and Bamber, J.L. (2005). Thickening of the ice stream catchments feeding the Filchner–Ronne Ice Shelf, Antarctica. *Geophysical Research Letters* 32: doi: 10.1029/2005GL023844. issn: 0094-8276.

James, T.S. and Ivins, E.R. (1998) Predictions of Antarctic crustal motions driven by present-day ice sheet evolution and by isostatic memory of the Last Glacial Maximum, *J. Geophys. Res.*, B, 103, 4993-5017.

John, C. M., Karner, G. D., Browning, E., Leckie, R. M., Mateo, Z., Carson, B., & Lowery, C. (2011). Timing and magnitude of Miocene eustasy derived from the mixed siliciclastic-carbonate stratigraphic record of the northeastern Australian margin. *Earth and Planetary Science Letters*, 304(3), 455-467.

König, M., & Jokat, W. (2006). The Mesozoic breakup of the Weddell Sea. *Journal of Geophysical Research: Solid Earth* (1978–2012), 111(B12).

Kuvaas, B., Kristoffersen, Y., (1991). The Crary Fan: a trough-mouth fan on the Weddell Sea Continental Margin, *Antarctica Marine Geology*, 97, 345–362. [http://dx.doi.org/10.1016/0025-3227\(91\)90125-N](http://dx.doi.org/10.1016/0025-3227(91)90125-N).

Kuvaas, B., and Leitchenkov, G., 1992. Glaciomarine turbidite and current-controlled deposits in Prydz Bay, Antarctica *Marine Geology*, 108: 365-381.

Kennett, J.P., and Barker, P.F., 1990. Latest Cretaceous to Cenozoic climate and oceanographic developments in the Weddell Sea, Antarctica: an ocean-drilling perspective. In Barker, P.F., Kennett, J.P., et al., *Proc. ODP, Sci. Results*, 113: College Station, TX (Ocean Drilling Program), 937–960. doi:10.2973/odp.proc.sr.113.195.1990

Lear, C. H., H. Elderfield, and P. A. Wilson (2000), Cenozoic deep-sea temperatures and global ice volumes from Mg/Ca in benthic foraminiferal calcite, *Science*, 287 269–272. doi: 10.1126/science.287.5451.269.

Lindeque, A., Martin, Y., Gohl, K., Maldonado, A., 2013. Deep sea pre-glacial to glacial sedimentation in the Weddell Sea and southern Scotia Sea from a cross-basin seismic transect. *Mar. Geol.* 336, 61–83. <http://dx.doi.org/10.1016/j.margeo.2012.11.004>.

Laberg, J. S., Forwick, M., Husum, K., & Nielsen, T. (2013). A re-evaluation of the Pleistocene behavior of the Scoresby Sund sector of the Greenland Ice Sheet. *Geology*, 41(12), 1231-1234.

Lisiecki, L. E., & Raymo, M. E. (2005). A Pliocene–Pleistocene stack of 57 globally distributed benthic $\delta^{18}\text{O}$ records. *Paleoceanography*, 20(1).

Michels, K.H., Rogenhagen, J., Kuhn, G., (2001). Recognition of contour-current influence in mixed contourite–turbidite sequences of the western Weddell Sea, Antarctica *Marine Geophysical Research*, 22, 465–485. doi: 10.1023/A:1016303817273

Michels, K.H., Kuhn, G., Hillenbrand, C. -D., Diekmann, B., Fütterer, D.K., Grobe, H., Uenzelmann-Neben, G., (2002). The southern Weddell Sea: combined contourite–turbidities sedimentation at the southeastern margin of the Weddell Gyre.

In: Stow, D.A.V., Pudsey, C., Howe, J.C., Faugères, J. C., Viana, A.R. (Eds.), Geological Society of London, Memoirs, 22, pp. 305–323. <http://dx.doi.org/10.1144/GSL.MEM.2002.022.01.32>.

Miller, H., Henriot, J.P., Kaul, N., Moons, A., (1990). A fine-scale stratigraphy of the eastern margin of the Weddell Sea. In: Bleil, U., Thiede, J. (Eds.), Geological History of the Polar Oceans: Arctic Versus Antarctic. Kluwer Academic Publishers, pp. 131–161. doi: 10.1007/978-94-009-2029-3_8.

McKay, R., Naish, T., Carter, L., Riesselman, C., Dunbar, R., Sjunneskog, C., ... & Powell, R. D. (2012). Antarctic and Southern Ocean influences on Late Pliocene global cooling. *Proceedings of the National Academy of Sciences*, 109(17), 6423–6428.

Miller, K.G., Mountain, G.S., Wright, J.D., Browning, 2011. A 180-million-year record of sea level and ice volume variations from continental margin and deep-sea isotopic records. *Oceanography* 24 (2), 40–53.

Masson, D. G., Harbitz, C. B., Wynn, R. B., Pedersen, G., & Løvholt, F. (2006). Submarine landslides: processes, triggers and hazard prediction. *Philosophical Transactions of the Royal Society A: Mathematical, Physical and Engineering Sciences*, 364(1845), 2009–2039.

Maslin, M., Owen, M., Day, S., & Long, D. (2004). Linking continental-slope failures and climate change: Testing the clathrate gun hypothesis. *Geology*, 32(1), 53–56.

Maldonado, A., Barnolas, A., Bohoyo, F., Galindo-Zaldívar, J., Hernández-Molina, J., Lobo, F., ... & Vázquez, J. T. (2003). Contourite deposits in the central Scotia Sea: the importance of the Antarctic Circumpolar Current and the Weddell Gyre flows. *Palaeogeography, Palaeoclimatology, Palaeoecology*, 198(1), 187–221.

Maldonado, A., Barnolas, A., Bohoyo, F., Escutia, C., Galindo-Zaldívar, J., Hernández-Molina, J., ... & Vázquez, J. T. (2005). Miocene to recent contourite drifts development in the northern Weddell Sea (Antarctica). *Global and Planetary Change*, 45(1), 99–129.

Mulder, T., & Alexander, J. (2001). The physical character of subaqueous sedimentary density flows and their deposits. *Sedimentology*, 48(2), 269–299.

Nelson, C. H., Escutia, C. A. R. L. O. T. A., Damuth, J. E., Twichell, D. C., & David, C. (2011). Interplay of mass-transport and turbidite-system deposits in different active tectonic and passive continental margin settings: external and local controlling factors. *Mass-transport deposits in deepwater settings. SEPM Spec Publ*, 96, 39–66.

Naish, T., Powell, R., Levy, R., Wilson, G., Scherer, R., Talarico, F., ... & Schmitt, D. (2009). Obliquity-paced Pliocene West Antarctic ice sheet oscillations. *Nature*, 458(7236), 322–328.

Ohshima, K. I., Fukamachi, Y., Williams, G. D., Nihashi, S., Roquet, F., Kitade, Y., ... & Wakatsuchi, M. (2013). Antarctic Bottom Water production by intense sea-ice formation in the Cape Darnley polynya. *Nature Geoscience*, 6(3), 235–240.

Orsi, A. H., Nowlin, W. D., & Whitworth, T. (1993). On the circulation and stratification of the Weddell Gyre. *Deep Sea Research Part I: Oceanographic Research Papers*, 40(1), 169–203. Orsi, A., G. Johnson, and J. Bullister (1999), Circulation, mixing, and production of Antarctic Bottom Water, *Progress in Oceanography*, 43, 55–109.

O'Brien, P.E., Cooper, A.K., Florindo, F., Handwerker, D., Lavelle, M., Passchier, S., Pospichal, J.J., Quilty, P.G., Richter, C., Theissen, K.M., & Whitehead, J.M., (2004). Prydz Channel Fan and the History of Extreme Ice Advances in Prydz

Bay. In Cooper, A.K., O'Brien, P.E. & Shipboard Scientific Party. Prydz Bay–Cooperation Sea, Antarctica: Glacial History and Paleoceanography Sites 1165–1167. Proceedings of the Ocean Drilling Program, Scientific Results, 188.

Ó Cofaigh, C., Taylor, J., Dowdeswell, J.A., Pudsey, C.J., (2003). Palaeo-ice streams, trough mouth fans and high-latitude continental slope sedimentation. *Boreas* 32 (1), 37–55.

Passchier, S. (2011). Linkages between East Antarctic Ice Sheet extent and Southern Ocean temperatures based on a Pliocene high-resolution record of ice-rafted debris off Prydz Bay, East Antarctica. *Paleoceanography*, 26(4).

Patterson, M. O., McKay, R., Naish, T., Escutia, C., Jimenez-Espejo, F. J., Raymo, M. E., ... & Expedition, I. O. D. P. (2014). Orbital forcing of the East Antarctic ice sheet during the Pliocene and Early Pleistocene. *Nature Geoscience*, 7(11), 841-847.

Posamentier, H. W., & Kolla, V. (2003). Seismic geomorphology and stratigraphy of depositional elements in deep-water settings. *Journal of Sedimentary Research*, 73(3), 367-388.

Piper, D.J.W., Deptuck, M.E., Mosher, D.C., Hughes Clarke, J.E., Migeon, S., 2012. Erosional and depositional features of glacial meltwater discharges on the eastern Canadian continental margin. In: Prather, B., Deptuck, M.E., Mohrig, D., van Hoorn, B., Wynn, R. (Eds.), *Application of Seismic Geomorphological Principles to Continental Slope and Base-of Slope Systems: Case Studies from Seafloor and Near-seafloor Analogues*. SEPM. Special Publication.

Pollard, D., & DeConto, R. M. (2009). Modelling West Antarctic ice sheet growth and collapse through the past five million years. *Nature*, 458(7236), 329-332.

Rebesco, M., Camerlenghi, A., (2008). Late Pliocenemargin development and mega-debris flow deposits on the Antarctic continental margins: evidence of the onset of the modern Antarctic ice-sheet? *Palaeogeography, Palaeoclimatology, Palaeoecology* 260, 149–167.

Rebesco, M., Hernández-Molina, F. J., Van Rooij, D., & Wåhlin, A. (2014). Contourites and associated sediments controlled by deep-water circulation processes: State-of-the-art and future considerations. *Marine Geology*, 352, 111-154.

Rogenhagen, J., Jokat, W., Hinz, K., Kristoffersen, Y., (2004). Improved seismic stratigraphy of the Mesozoic Weddell Sea. *Marine Geophysical Research*, 25, 265–282. <http://dx.doi.org/10.1007/s11001-005-1335-y>.

Ruano, P., Bohoyo, F., Galindo-Zaldívar, J., Pérez, L. F., Hernández-Molina, F. J., Maldonado, A., ... & Medialdea, T. (2014). Mass transport processes in the southern Scotia Sea: Evidence of paleoearthquakes. *Global and Planetary Change*, 123, 374-391.

Reading, A. M. (2002). Antarctic seismicity and neotectonics (Doctoral dissertation, The Royal Society of New Zealand).

Shevenell, A.E., Kennett, J.P., and Lea, D.W., (2004). Middle Miocene Southern Ocean cooling and Antarctic cryosphere expansion. *Science*, 305(5691): 1766-70. doi: 10.1126/science.1100061.

Stow, D.A.V., Faugères, J.C., Howe, J.A., Pudsey, C.J., Viana, A.R., (2002). Bottomcurrents, contourites and deep-sea sediment drifts: current state-of-the-art. In: Stow, D.A.V., Pudsey, C.J., Howe, J.A., Faugeres, J.C., Viana, A.R. (Eds.), *Deep-water contourite systems: Modern drifts and ancient series*. Memoir. Geological Society of London, London, pp. 7–20.

Stow, D.A.V., Hernández-Molina, F.J., Llave, E., Sayago-Gil, M., Díaz-del Río, V., Branson, A., 2009. Bedform-velocity matrix: the estimation of bottom current

velocity from bedform observations. *Geology* 37, 327–330.

Straub, K. M. (2007). Quantifying turbidity current interactions with topography (Doctoral dissertation, Massachusetts Institute of Technology).

Shanmugam, G., 2006. Deep-water processes and facies models. Implications for Sandstone Petroleum Reservoirs, 5. Elsevier, Amsterdam.

Smellie, J. L., Rocchi, S., Gemelli, M., Di Vincenzo, G., & Armienti, P. (2011). A thin predominantly cold-based Late Miocene East Antarctic ice sheet inferred from glaciovolcanic sequences in northern Victoria Land, Antarctica. *Palaeogeography, Palaeoclimatology, Palaeoecology*, 307(1), 129-149.

Tripathi, A., Robert, C., Eagle, R., (2009). Coupling of CO₂ and Ice Sheet Stability Over Major Climate Transitions of the Last 20 Million Years. *Science*, 326, 1394-1397.

Uenzelmann-Neben, G. and Gohl, K. (2012): Amundsen Sea sediment drifts: Archives of modifications in oceanographic and climatic conditions, *Marine Geology*, 299-300, pp. 51-62. doi: 10.1016/j.margeo.2011.12.007. doi: 10.1016/j.margeo.2011.12.007.

Uenzelmann-Neben, G., (2006). Depositional patterns at Drift 7, Antarctic Peninsula: along-slope versus down-slope sediment transport as indicators for oceanic currents and climatic conditions. *Mar. Geol.* 233, 49–62.

Vorren, T. O., & Laberg, J. S. (1997). Trough mouth fans-palaeoclimate and ice-sheet monitors. *Quaternary Science Reviews*, 16(8), 865-881.

Vargas, C.A., Mann, P., Gómez, C., 2012. Morphologic expression of accretionary processes and recent submarine landslides along the southwestern Pacific margin of Colombia. In: Yamada, Y., Kawamura, K., Ikehara, K., Ogawa, Y., Urgeles, R., Mosher, D., Chaytor, J., Strasser, M. (Eds.), *Submarine Mass Movements and Their Consequences*. Springer, Netherlands, pp. 365–377.

Weber, M.E., Bonani, G., Fütterer, K.D., 1994. Sedimentation processes within channelridge systems, southern Weddell Sea, Antarctica. *Palaeoceanography* 9, 1027–1048.

Weppernig, R., Schlosser, P., Khatiwala, S., & Fairbanks, R. G. (1996). Isotope data from Ice Station Weddell: Implications for deep water formation in the Weddell Sea. *Journal of Geophysical Research: Oceans* (1978–2012), 101(C11), 25723-25739.

Yamane, M., Yokoyama, Y., Abe-Ouchi, A., Obrochta, S., Saito, F., Moriwaki, K., & Matsuzaki, H. (2015). Exposure age and ice-sheet model constraints on Pliocene East Antarctic ice sheet dynamics. *Nature communications*, 6.

Zachos, C.J., Dickens, R.G., Zeebe, E.R., (2008). An early Cenozoic perspective on greenhouse warming and carbon-cycle dynamics. *Nature*, 451, 279-283. doi:10.1038/nature06588.

7 Sedimentation and potential venting on the rifted continental margin of Dronning Maud Land

Xiaoxia Huang*, Wilfried Jokat
The manuscript is in preparation

7.1 Abstract

The topographic relief of Dronning Maud Land, formed by Middle and Late Mesozoic tectonic activity, had a strong spatial control on both early fluvial and subsequent glacial erosion and deposition. The sources, process, and products of sedimentation along the Dronning Maud Land (DML) margin and in the Lazarev Sea have been barely studied. The onshore mountain belt parallel to the coast of the DML margin acts as a barrier to the transport of terrigenous sediments from the east Antarctic interior to the margin and Lazarev Sea. The Jutul-Penck Graben system allows for local transport across the old mountain belt. Ice streams used this pre-existing tectonic fluvial system. Thus, this old topography controlled glacial sediment transport and deposition for parts of the DML. Offshore, we attribute repeated large-scale debris flow deposits to instability of sediments deposited locally on the steep gradient of the DML margin by high sediment flux ice streams. Two types of canyons are defined based on their axial dimensions and sedimentary processes. They arise from turbidity currents and slope failures during glacial/fluvial transport. In addition, we report pipe-like seismic structures in this region for the first time, and suggest that they occurred as consequences of volcanic processes.

Key words: Dronning Maud Land margin, debris flow deposits, canyons, ice streams, seismic chimneys

7.2 Introduction

The development of submarine canyons and debris flows are important geological factors in the transfer of large amounts of sediment onto the deeper parts of continental margins (Masson et al., 2006, Gee et al., 2006; Jobe et al., 2011). Various processes control the development of canyon system (Shepard, 1981). Gravity flows, including turbidity currents and debris flows, are thought to play an important role in sediment supply and erosion (Pratson and Coakley, 1996; Weaver et al., 2000, Straub and Mohrig, 2009).

The Dronning Maud Land (DML) continental slope is a rifted volcanic margin that is at present glaciated and strongly dissected by submarine canyons (Fig. 1). Processes related to the evolution of the margin by rifting have been intensively studied by the acquisition of seismic, gravity and magnetic data (BGR, AWI, PMGE, Univ. Bergen) over the past three decades. However, the origin of the canyons, surface sedimentary processes, and their relationship with the East Antarctic Ice Sheet (EAIS) are poorly understood.

The objective of this study is to improve understanding of sedimentation processes onshore and offshore in DML, from source to sink, by analyzing available seismic reflection data and drill sites on the margin. We focus on a number of erosional and depositional features such as submarine canyons, debris flow, and depocenters in sub basins on the slope, rise and abyssal plain off southwest DML and in the Lazarev Sea (Fig. 1). We link these features to processes of fluvial/glacial

erosion, transport, and deposition. Additionally, for the first time here, we report a set of pipe-like features that potentially indicate venting during the evolution of the volcanic margin. Our considerations of sedimentation patterns and the canyon system in relation to the evolution of the Lazarev Sea sheds light on dynamic interactions between the EAIS and sedimentary strata at its bed. We divide the study into four sections (A, B, C, D) and describe the sedimentary features in each section individually.

7.3 Geological setting

The continental margins of East Antarctica and East Africa experienced massive rift related volcanism (Jacobs et al., 1996; Jourdan et al., 2007). Such extrusive volcanism is thought to be caused by lithospheric extension above a mantle plume (White and McKenzie, 1989). Using seismic refraction data along the Explora Escarpment and the Lazarev Sea, Jokat et al. (2004) confirmed that the DML margin can be classified as a volcanic rifted continental margin that formed during the Mesozoic break-up of Gondwana (Jokat et al., 2003). Volcanic rifted continental margins are commonly characterized by thick wedges of volcanic flows, manifested in seismic reflection data as packages of seaward dipping reflectors (SDRs) with high seismic velocities (Franke, 2012). Two SDR sequences are known from seismic reflection data to occur along the Lazarev Sea margin, and have been interpreted to indicate two-phases of break-up (Hinz et al., 2004).

Plate tectonic reconstructions and seismic refraction data suggest that the final severance of continental connections between DML and SW Africa did not happen before 138 Ma, and that the continental margin off DML underwent a complex and long-lived rift history (Jokat et al., 2003; 2004, Eagles and König, 2006). In particular, the Lazarev Sea was an area of massive volcanism during and after the breakup. A late magmatic pulse built the Maud Rise large igneous province at 65 °S 3 °E. On the conjugate margin, the volcanic Mozambique Ridge formed in a stepwise manner (Jokat et al., 2004; Koenig and Jokat, 2010; Leinweber and Jokat, 2011). Volcanic processes and deposits have had a strong impact on the structure and geodynamic development of the DML margin and associated evolution of the Lazarev Sea.

The mountain range in central DML trends E-W, is 200 km wide and has average altitudes of 2000 m. This mountain belt has been cut by Jutul-Penck system, whose N-SE-originated branch is between 20 and 70 km wide and connects the interior of East Antarctic and Lazarev Sea (Riedel et al., 2012; Fretwell et al., 2013). The Jutul-penck Graben is thought to be a tectonic feature and reactivated during the Gondwana rift phase (Riedel et al., 2012). Thus, large volume sediments along the DML margin can be expected caused by long term erosion of the Antarctic continent and the DML mountain ranges.

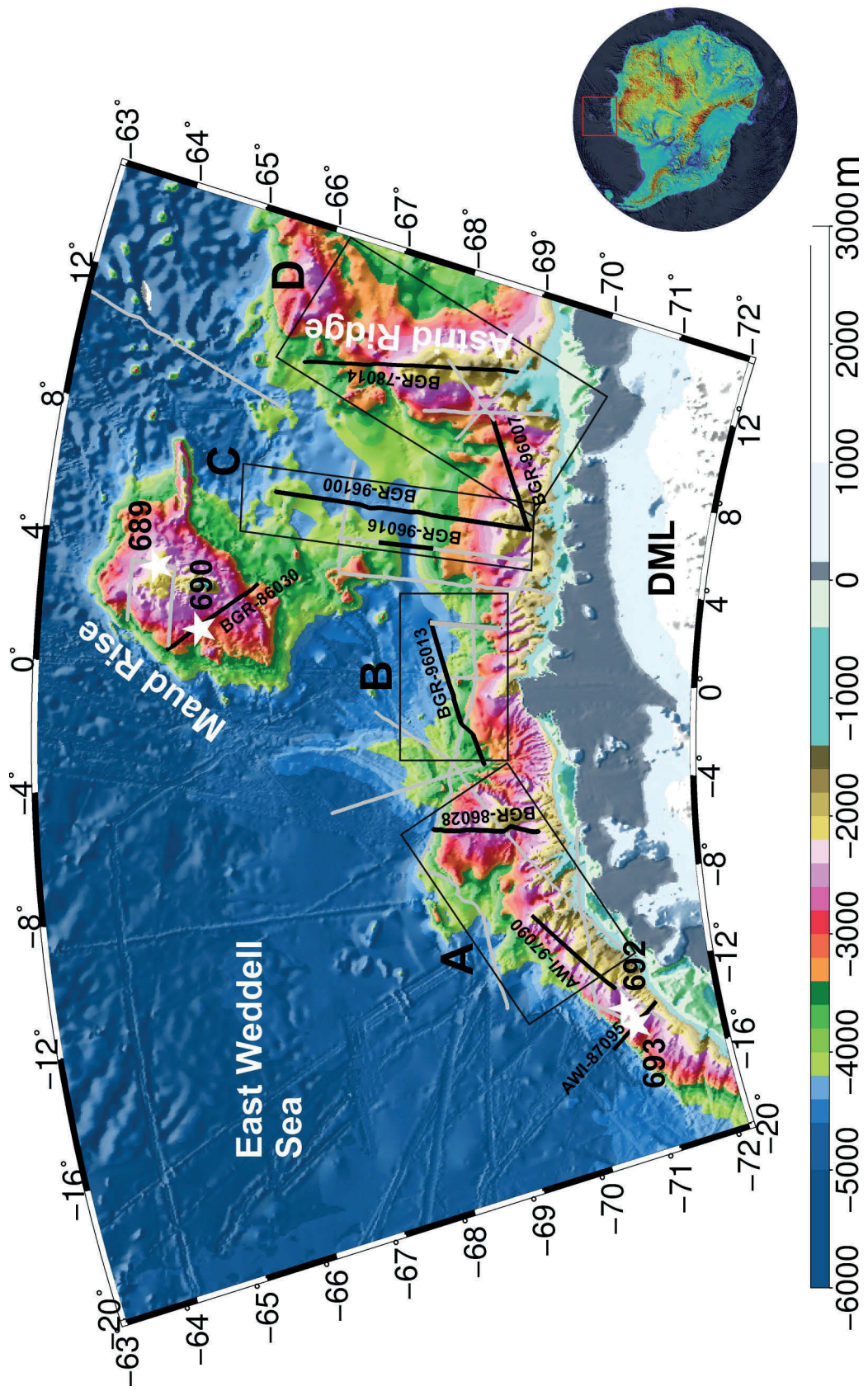


Fig. 7.1 Locations of multichannel seismic lines in the study region. The black lines in section A, B, C and D are presented in the study. The black stars represent the ODP drilling sites.

7.4 Data and interpretation constraints

The study ties the stratigraphic framework from a few drill sites into a multi-channel seismic (MCS) network acquired over the course of several RV Polarstern cruises, which were operated by AWI (in 1987, 1990, 1992 and 1997) and BGR (in 1978, 1986, and 1996) (Fig. 1). During ODP leg 113, two sites (692 and 693) were drilled on the mid-slope of the southern Weddell Sea margin. Site 693, near 71°S, 14° W, achieved penetration of 483.9 m (Fig. 2a) and recovered a Quaternary to Lower Cretaceous sedimentary sequence, which is largely rich in biosiliceous components. Cretaceous diatoms with Aptian-Albian age are well preserved. Above the Oligocene strata, diatom and clay muds are the dominant lithologies (Fig. 2b) (Barker and Kennett et al., 1990). Two more sites (689 and 690) are located on Maud Rise, a huge volcanic structure north of the margin. Site 690, with a penetration of 317.0 m, recovered pelagic, biogenic sediments that range in age from lowermost Maastrichtian through Pio-Pleistocene ages (Fig. 2). The recovered basalt from Maud Rise Site 690 was classified as olivine alkali ocean basalt (Barker and Kennett et al., 1990).

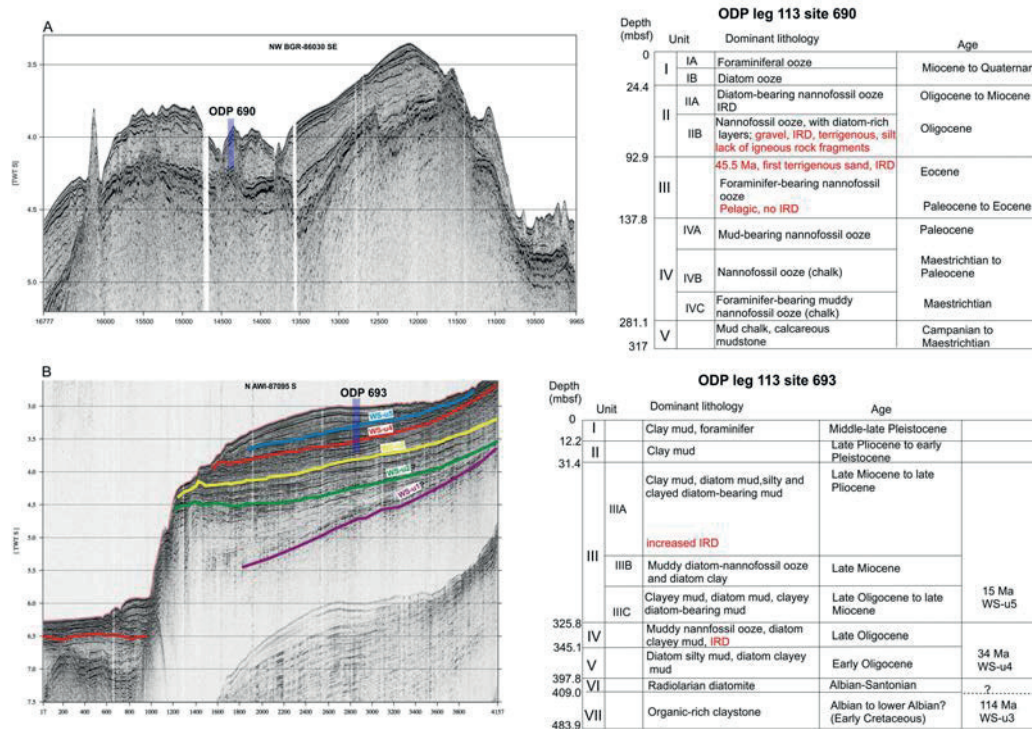


Fig. 7.2 The locations of ODP 690, 693 on the multichannel seismic lines from DML margin and Maud Rise. The tables at the right show the recovered dominant lithologies and accompanying age information from the two ODP samples.

Previous studies identified a number of prominent unconformities in the Weddell Sea (Miller et al., 1990, Rogenhagen et al., 2004, Huang et al., 2014) (Fig. 2). However, it is still a challenge to establish whether, and how, the changes responsible for their formation are manifested in the seismic stratigraphy of the Lazarev Sea and its Antarctic margin. More seriously, the existing stratigraphic model from the Riiser-Larsen Sea (Leitchenkov et al., 2008) is difficult to carry over to the study region because of the presence of a barrier to sedimentation between the two at the

prominent volcanic Astrid Ridge (Fig. 1). Interpretation of the sedimentary units in the Lazarev Sea is only possible by examination of the seismic reflection amplitude similarities and a jump correlation from ODP site 693 to section A, a distance of 100 km (Figs. 1, 3).

7.5 Results and interpretation

7.5.1 Seismic structures

Section A: Seismic chimneys

A number of vertical pipe-like zones of low seismic reflectivity cross the entire sedimentary section on the middle slope at 8~4 ° W (70~72° E) (Figs. 1, 3). The top reflector of each of these features is mound-shaped (Fig. 3 a and b). The internal reflection amplitudes within the feature are attenuated, and slightly arched. The pipes are not associated with noticeable relief on the seafloor. The flanks of the structures exhibit pull-up reflections (Fig. 3a, b). Such pipe-like features are commonly interpreted as seismic chimneys in seismic records (Planke et al., 2005). Abundant vertical faults are observed next to the seismic chimneys in the sedimentary sequence (Fig. 3a).

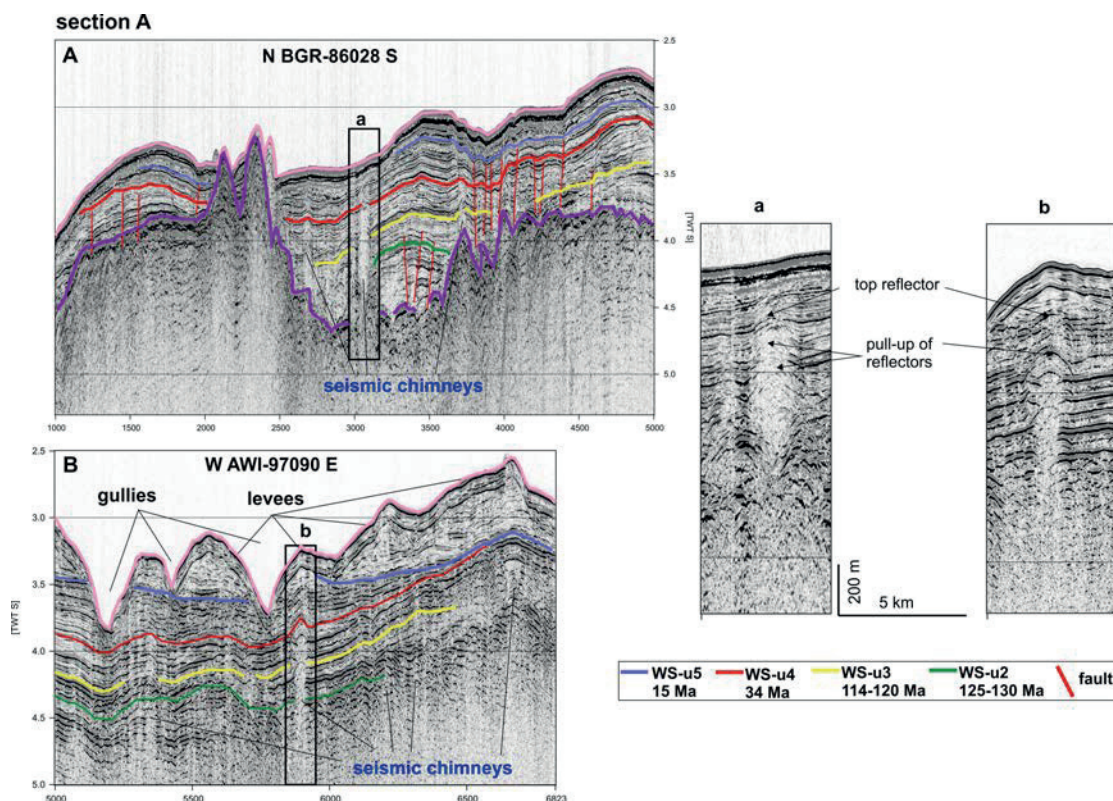


Fig. 7.3 Examples of pipe-like features, characterized by reflection-poor columns. The pipe-like features are interpreted as seismic chimneys in this study.

The seismic chimneys appear to be very narrow due to the vertical exaggeration of seismic profiles (Fig. 3). Assuming an average interval velocity of 1800 m/s, however, seismic chimney 'a' is about 1500 m wide and up to 800 m tall. Most of the seismic chimneys in the study region are similarly wider than they are tall. Another similar scale of seismic chimney is observed on the seismic line AWI-97090 (Fig.

3b); it terminates at a seismically chaotic unit. Several gullies and levee deposits modify the seafloor.

Section B: debris flows

The acoustic basement is identified as a strong reflector that can be traced throughout the entire seismic line (Fig. 4). Two chaotic units with weakly-reflective or reflection-free seismic facies are recognized across the upper continental slope between 0° and 4 ° E (Figs. 1, 4), and are referred to debris flow deposits. One buried debris flow deposit immediately overlies the moderately rugged basement at the upper slope (Fig. 4, CDP 6000-8836) and is clearly separated from the overlying units by a continuous reflector. This reflector may represent an erosional surface. In the north, the unit overlying this surface is another debris flow deposit (Fig. 4; CDP 4000-7000). The thicknesses of the debris flow deposits reach maxima of 200-300 m, and their downslope elongation is about 150-200 km (Fig. 4, BGR-96014). A slump-like feature is interpretable at the top of the debris flows (Fig. 4, CDP 4000-7000; 5 - 5.5 s TWT). This structure is characterized by its hummocky morphology with mound structures and internal irregular seismic facies deformed by growth faults (Fig. 4). The distal part of the slope of the line BGR-96014 (CDP 1-4000) is composed of sediments with moderate to well-developed layering depicted in high-amplitude reflections.

Section C sub-basins and valley

The 750 km long N-S trending seismic profile BGR-96100 runs across the continental shelf to the deep sea, terminating east of Maud Rise (Fig. 1, 5). Based on the seismic reflection characteristics and deep crustal structures, we divide the line into two zones. Zone I (Fig. 5, CDP 17000-30000) is characterized by relatively smooth, thick stretched continental crust (Jokat et al., 2004). The data show two packages of SDRs in Zone 1. The SDRs in the south have a steeper angle than those in the north. A thin sediment unit of 0.5 s TWT thickness is characterized by chaotic high amplitude seismic facies (Fig. 5, CDP 20000-26000, 'displaced mass') and lies over the upper slope of a moderately-rugged acoustic basement. The acoustic basement of Zone II (Fig. 5, CDP 1-17000) has a rough surface with strong amplitudes and is overlain by several distinct sedimentary features. Further to the north, we observe a sub-basin filled with more than 1 s TWT (Fig. 5, CDP 7800-11500) of sediments that return parallel and subparallel reflections. The topography becomes very complex towards Maud Rise in the north of the profile (Figs.1, 5). A seamount rises up from faulted basement to form a positive relief on the sea floor near CDP 2000. Younger sedimentary strata onlap at this structure (Fig. 5, CDP 2000-8000).

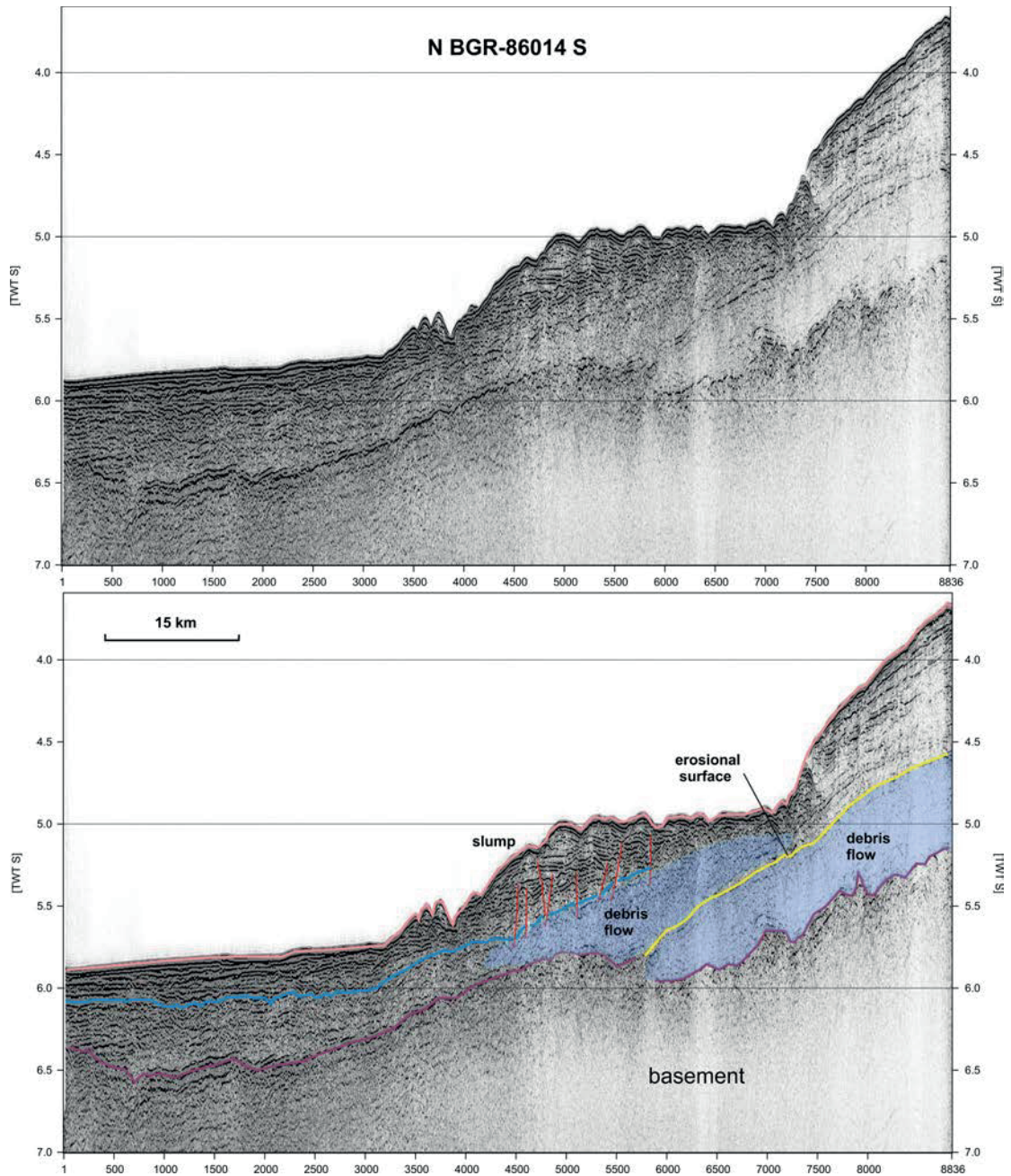


Fig. 7.4 Interpreted large-scale debris flow deposits and slumps in multichannel seismic data. Red lines signify interpreted growth faults.

A noticeable bathymetric and basement low, 75 km wide and 2 km deep, is bounded by the Antarctic margin and Maud Rise (Figs. 1, 5, 6). The basement valley is filled by 2s TWT of stratified sediments. The fill shows remarkable changes in the amplitude of its parallel reflections between three prominent unconformities, which may document the activities of oceanographic current and ice sheet changes.

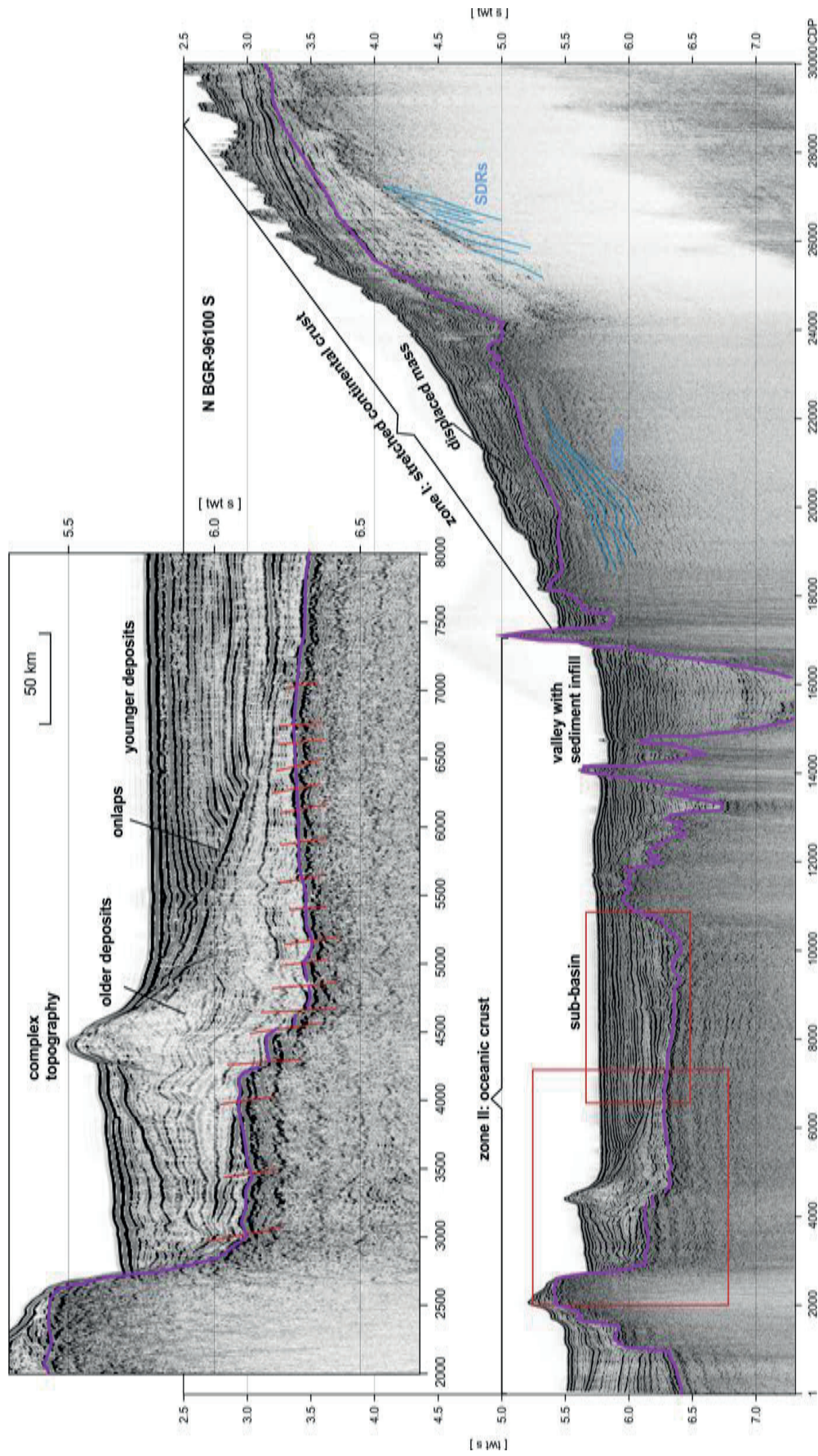


Fig. 7.5 Multichannel seismic line BGR-96100 from the continental slope to the eastern flank of Maud Rise in the Lazarev Sea. The long seismic profile demonstrates complex topography and sedimentation processes. Abundant normal faults are observed in the acoustic basement. SDRs = seaward dipping reflectors.

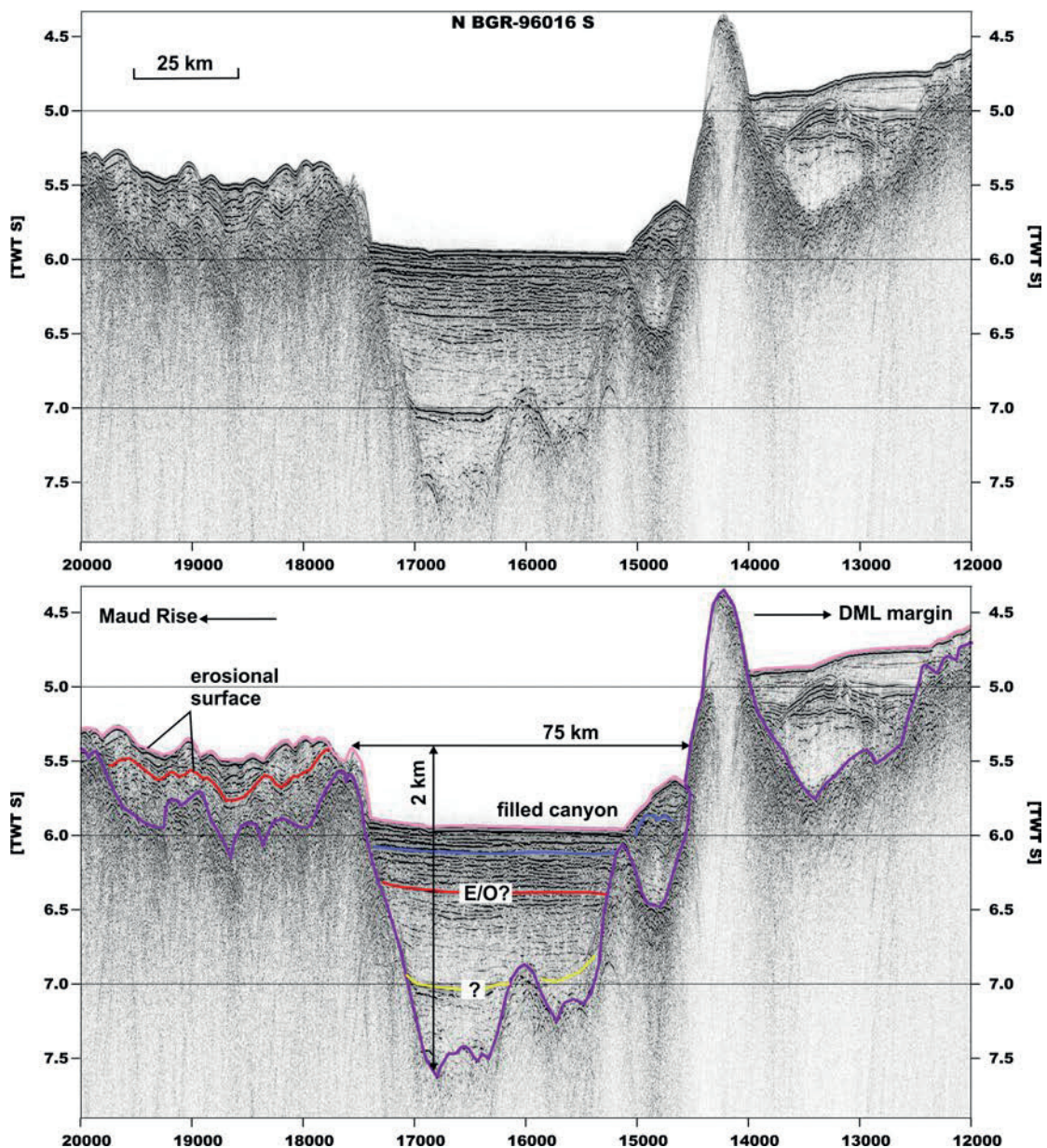


Fig. 7.6 A filled valley separating Maud Rise from Antarctica. Three unconformities are recognized in the fill sediment strata.

Section D, canyons at the Astrid Ridge

The N-S striking Astrid Ridge is located between 9°E and 15°E off the DML margin. It is characterized by a bathymetric high of 1500 m surrounded by deeper seafloor and has also a prominent, positive free-air gravity anomaly (Figs. 1, 7). The seismic line BGR-78014 provides an insight on the basement morphology and sedimentation from the ridge's southern end close to the continental margin towards its northern termination at the oceanic Astrid Fracture Zone. Near the southern end of the ridge, a deep fault-related graben has formed above the crystalline basement filled by sediments (Fig. 7, CDP 10500-13576). A channel levee complex is deposited over the top of the graben fill (Fig. 7; CDP 9000-13567). The seafloor depth of the southern part of the Astrid Ridge is about 1,500 m, and the sediment thickness can be as much as 1,000 m. Towards the north of the profile (Fig. 7 CDP 5000-8000), a strong distinct

reflector at 3.2-3.4 TWT clearly separates the stratified sediment drape (up to 200-300 meter thick) from the underlying unit, whose parallel reflectors are attributed to intra-basement layering. Little or no sediment is present over the rugged basement of the Astrid Fracture Zone (Fig.7, CDP 54-5000), in water that is about 3,700 m deep.

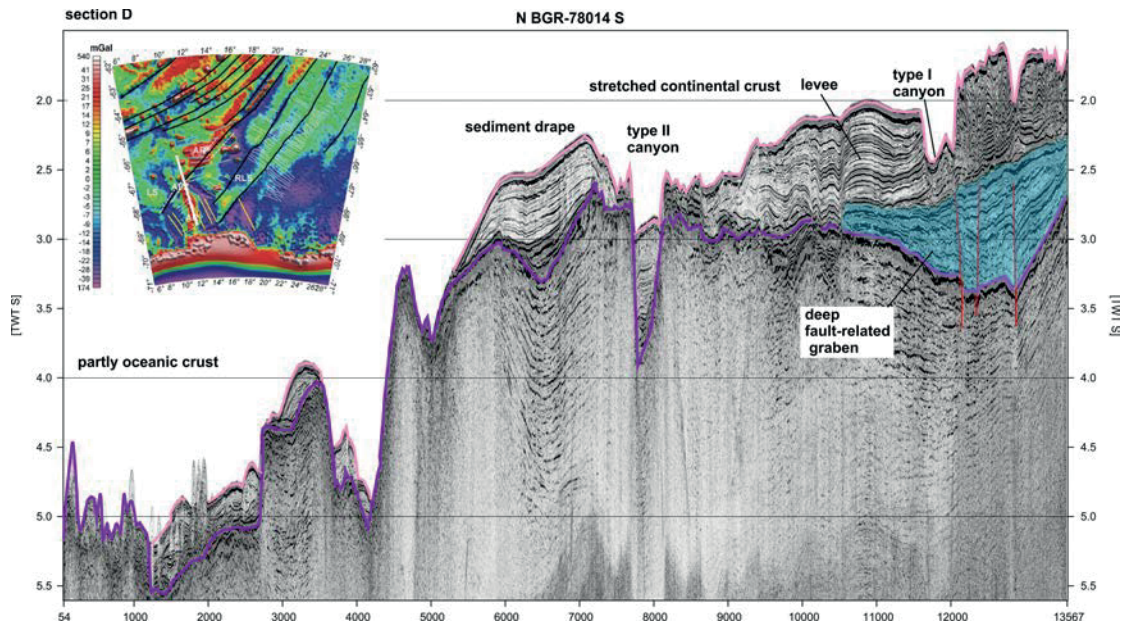


Fig. 7.7 The interpreted multichannel seismic line BGR-78014 crosses the Astrid Ridge. Astrid Ridge is also characterized by positive value on the free-air anomaly map (after Sandwell and Smith, 2009; Leinweber and Jokat, 2011).

Two types of canyons are present along the margin of the DML, near the Astrid Ridge (Figs. 1, 8). Type I canyons are of small size (less than 100 m high, variable width), with levees developed on their flanks (Fig. 8, CDP 2000-5000). The levees are internally stratified and thinning away from their crests. This canyon type exhibits smooth, highly aggradational morphologies without any infill. Type II canyons are larger (Fig. 8, CDP 10000-12000), reaching up to 50 km wide and 500 m high, and are bounded by pairs of prominent inter-canyon ridges (Fig. 8, CDP 8500-10500). The seismic facies within the inter-canyon ridges and canyon floor are characterized by very chaotic reflections with strong amplitudes. Slump-related terraces are often observed on the sidewalls of Type II canyons (Fig. 8, CDP 9800-10500).

7.5.2 Total sediment thickness variations and basement topography

Acoustic basement can be traced continuously throughout the entire study region (Fig. 8A). The depth of this basement and the thickness of sediments overlying it can be estimated using velocities determined from wide-angle data and drilling information (Jokat et al., 2004). Large uncertainties are to be expected in the area of sparse seismic coverage on the shelf.

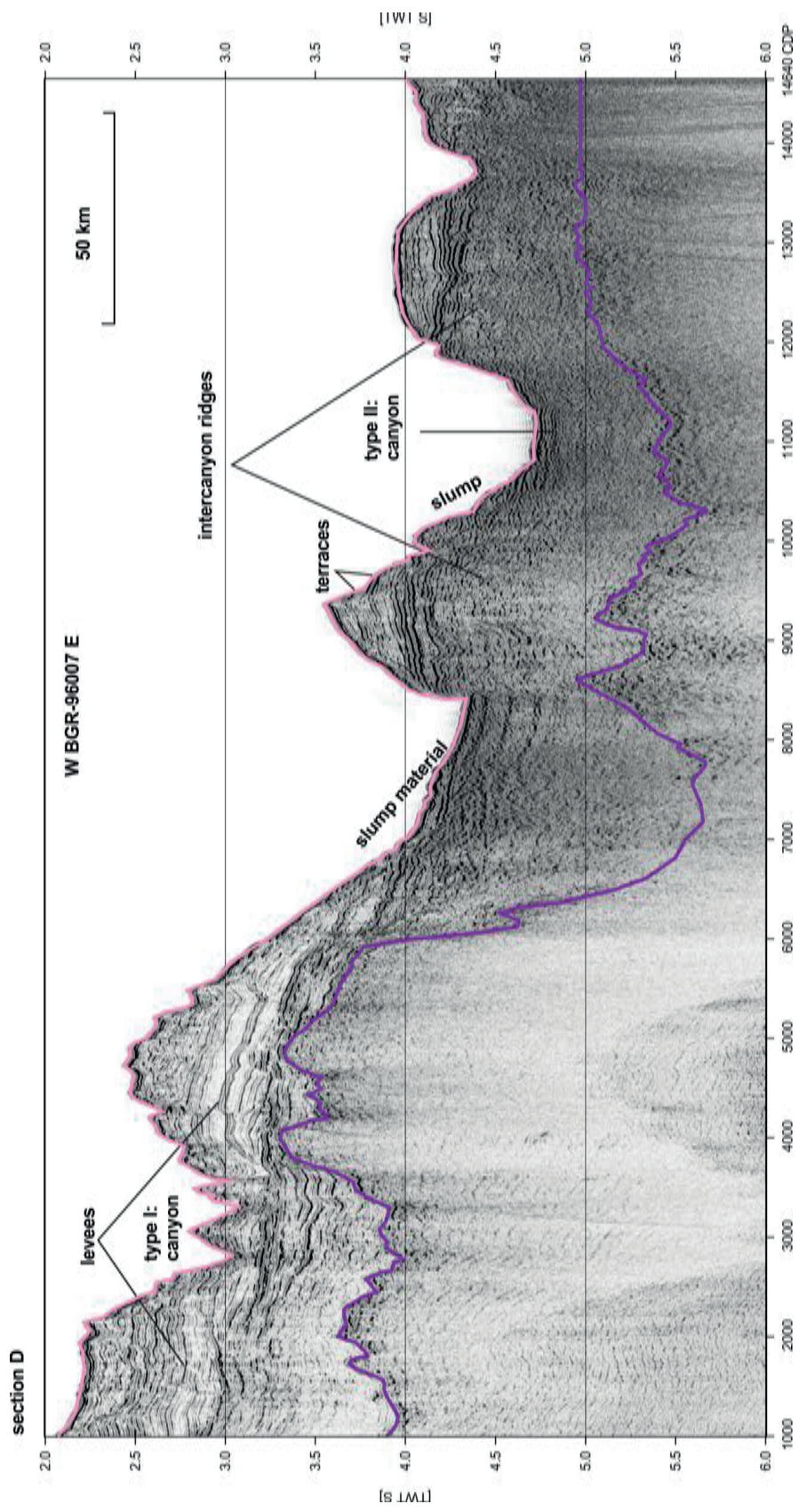


Fig. 7.8. Two types of canyons with different sizes and formation mechanisms are distinguished on the multichannel seismic line BGR-96007, next to the Astrid Ride.

In general, the seafloor topography varies along with the basement morphology, such that structural highs appear over basement highs and structural lows are centered over basement lows (Fig. 9). The total sediment thickness in the study region ranges from 50 to 2000 m. The volume of sediments in the study region is about $0.1 \cdot 10^6 \text{ km}^3$ (Fig. 10). Two pronounced depocenters are located to the west and east of Maud Rise. North and east of Maud rise, about $\sim 1300 \text{ m}$ of sediment is accumulated in a sub-basin (Figs. 1, 9). The sediment thickness overlying Maud Rise is in the range of 50-500 m. Drilling provided pelagic, biogenic sediments that range in age from lowermost Maastrichtian through to Plio-Pleistocene (Barker, Kennett et al., 1990, Florindo and Roberts, 2005). The valley between Maud Rise and the DML margin has been filled by up to 1.5 km thick sediment (Figs. 1, 9 and Fig. 5, CDP 15000-17000) (Fig. 9).

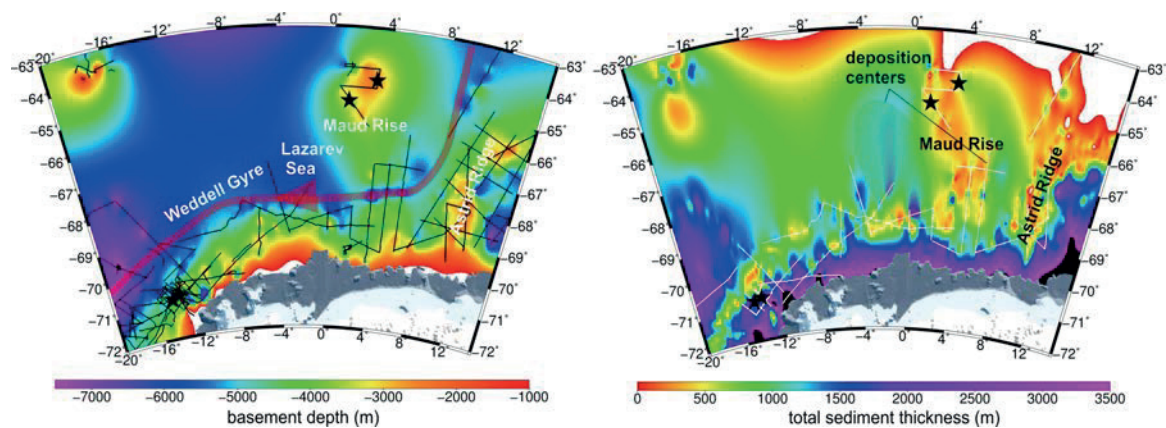


Fig. 7.9 A: The basement depth. The thick, dark red curve is a proposed Weddell Gyre pathway between Antarctica and Maud Rise. B: The total sediment thickness map of the Lazarev Sea and Dronning Maud Land margin. The thickness distribution appears to be constrained by basement morphology.

7.6 Discussion

7.6.1 Basin sedimentation processes

Antarctic marginal basins such as those in the Weddell and Riiser-Larsen seas, or off the Wilkes Land margin and in Prydz Bay, hold vast volumes of sediments delivered to them by (paleo) ice streams/rivers with huge drainage catchment areas (Kuvaas et al., 2004; Close et al., 2007; Leitchenkov et al., 2008; Huang et al., 2014) (Fig. 10, table). In strong contrast, only little sediments with a maximum thickness of just 1.8 km, are preserved in the Lazarev Sea and along the southwest DML margin since their formation (Figs. 8, 9). The limited sediment volume and debris flow deposits resolved by seismic reflection data (Fig. 4) indicate that the slope at the DML margin is sediment starved. Although the Jutul-Penck Graben system have cut the DML mountain belt and existed at the onset of glaciation, perhaps persisting there since its formation during Middle and Late Mesozoic tectonic activity. The absence of igneous and metamorphic rock fragments in the ODP 690 core from Maud Rise supports this view, by indicating that the terrestrial sediment flux from central parts of East Antarctica has been blocked at least since the rise formed in mid Cretaceous times (Ehrmann and Mackensen, 1992; Jacobs et al., 1996). However, fluvial

transport through the tectonic graben and expansion of the East Antarctic Ice sheet (EAIS) had strong spatial controls on erosion and offshore sedimentation.

7.6.1.1 fluvial transport in preglacial times

The Jutul-Penck Graben was formed most likely during the rifting of Gondwana (Näslund, 2001; Riedel et al., 2012). This tectonic graben system is thought to have developed large-scale, low-gradient bedrock surfaces through fluvial and later glacial erosion, transport, and deposition of poorly sorted material. Offshore, our data shows a large Type II canyons that indent the shelf edge west of Astrid Ridge (Figs. 1, 7 CDP 10000-12000). We attribute the erosive surface in the canyon floors and the numerous slumps and terraces on their sidewalls (Fig. 8) to slope failures. The continuously oversteepened canyon walls are probably the result of large gravitational flows that were fed from fluvial systems south of the mountain range and channeled through the Jutul-Penck graben (Fig. 8). The offshore canyons were eroded and locally filled by coarse-grained material from the interior of East Antarctica (Fig. 6). Later deposition might also have occurred when the canyon received hyperpycnal flows from the glaciated margin where ice sheets are most erosive. Such high-density flows eroded previously-deposited sediments and eventually redeposited them as turbidites further out in the basin.

7.6.1.2 Glacial transport

The ice drainage system is the source of locally derived coarse-grained glacial outwash at the onset of glaciation. Sediments deposited in this phase at ODP 690 (Late Eocene in East Antarctica, Barker et al., 1988; Ehrmann, 1992) consist mostly of terrigenous sand, gravel, diamicts, and ice rafted debris (IRD) (Fig. 2). Subglacial topography has been interpreted to play an important role in both present-day and paleo-ice stream flow (Laymon, 1992; Peters et al., 2006) and, therefore, for sediment transport. Paleo-ice streams can be expected to have followed the pre-existing Jutul-Penck Graben system, which cuts into the DML mountains (Fig. 10). Ice streams have acted as the major conduits for transporting terrigenous sediment from the Antarctic interior to the sediment-starved DML slope throughout glacial times.

Our results are in agreement with these concepts that paleo-ice streams played a major role in sediment transport. Packages of chaotic reflectors reaching hundreds of meters upslope indicate that the upper part of the margin experienced extensive slumps and debris flows (Figs. 1, 4). These debris flow deposits occurred at the continental slope as consequences of ice streams depositing their loads of sediment and meltwater at the shelf edge (Figs. 4 and 10), or of episodic ice sheet collapse at the shelf break. Large gravity flows can transport material over great distances as they accelerate down the continental slope, eroding earlier unstable sediment on the steeper basin-margin or upper slopes, and spawning new debris flow deposits and slumps (Fig. 4). The well-developed Type I canyons on the slope are interpreted to be related to downslope turbidity currents operating during glacial times (Figs. 1, 8). Debris flows and slumps can also produce turbidity currents (Vanneste and Larter, 1995), which are invoked to explain the formation of the lateral levee deposits along the canyon flanks (Fig. 8, at Type I).

7.6.2 Indication for potential venting?

This study documents the presence of seismic chimneys on the mid slope of the DML margin between 8~4 ° W for the first time (Fig. 3). We discuss their origin here. Seismic chimneys commonly occur in volcanic basins with significant gas hydrate accumulations, e.g. the Vøring and Møre margin basins, or the Ulleung Basin (Planke

et al., 2005; Horozal et al., 2009). Around Antarctica, seismic chimneys have also been observed in basins of the Amundsen Sea Embayment and Ross Sea (Geletti and Busetti, 2011; Weigelt et al., 2012). Geletti and Busetti (2011) related seismic chimneys to the presence of gas hydrates, whose presence they interpreted from Bottom-Simulating Reflectors (BSR) in their seismic records from the Ross Sea. In contrast, Weigelt et al. (2012) suggested that the reflection-poor vertical pipe-like structures in the sedimentary sequences on the middle shelf of the Amundsen Sea Embayment represent mud-diapirs rising from water-rich sediments, and suggested that their formation has been strongly influenced by glacial/interglacial cycles.

However, neither BSRs nor pockmarks, which are fed by fluids/gas seeping and migrating upward along faults, are observed in our seismic records. According to our stratigraphic model, the mound-shaped reflectors at the tops of the chimneys on the DML margin are overlain by glacial diatom-rich sediments above the glacial unconformities WS-u4 or WS-u5 (Fig. 2, 3). This may indicate that the process responsible for the chimneys, potentially venting, had ceased before the onset of the glacial regime. Thus, we may exclude the scenario that glacial dewatering resulted in these seismic chimneys at DML margin.

We suggest that the well-preserved and upward deformed vertical flanks and mounded top reflectors in the seismic chimneys are all evidence of venting. Taking into account the large (80 Myr) hiatus in ODP site 693 sampling (Barker et al., 1988) and its correlation with our stratigraphic age model (Fig. 2), the fact that the seismic chimneys seem to originate from the acoustic basement suggests that venting may have commenced around 120-130 Myr. In this context, they are most simply attributable to volcanic processes operating soon after the breakup of Gondwana (Fig. 3). This assumption is in agreement with Jacobs et al. (1996), who suggested that the continental crust of western DML was heated by regional melts from 180 Ma until the Early Cretaceous (140 Ma) when the lava they produced was eroded again. The scenario is consistent with the presence of two sequences of SDRs (Fig. 5), which Hinz et al. (2004) and Jokat et al. (2004), attributed to the presence of volcanic effusive rocks emplaced in a subaerial to shallow marine during two phases of break-up (at ~ 190 Ma during the initial stage, while the second, at 140 Ma). We conclude therefore, that the formation of the seismic chimneys is most probably linked to the intrusion of sills into the basement, prompting overpressure by heating pore fluids. The fault system acts as the migration pathways of venting (Fig. 3).

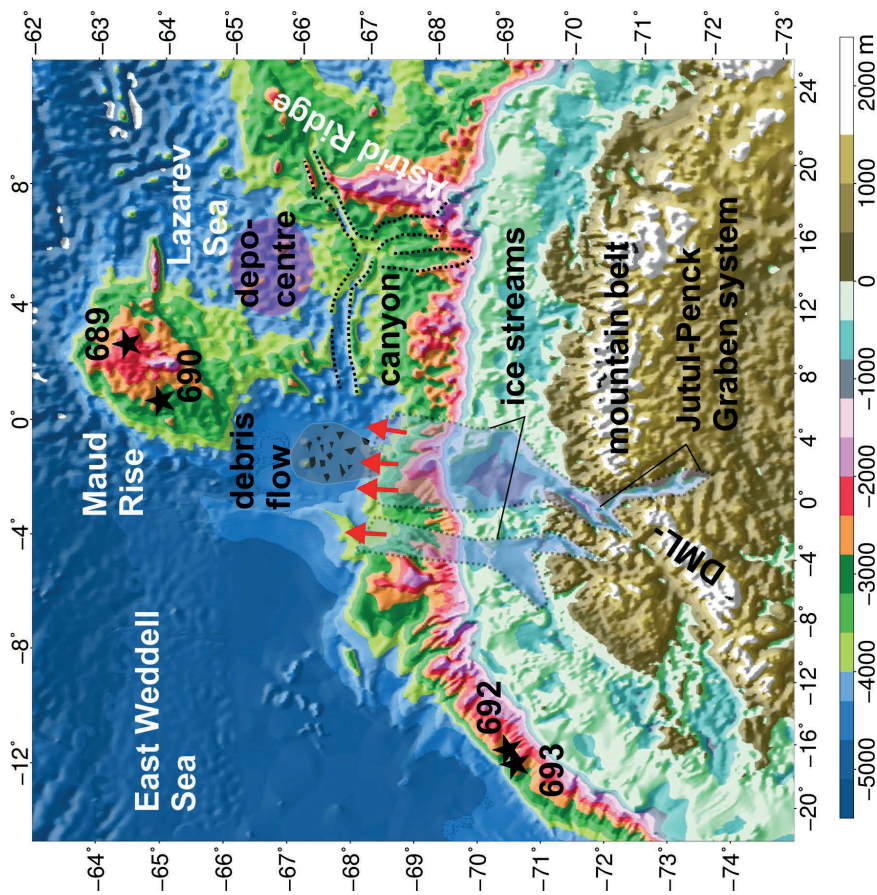


Table: glacial sediment thicknesses and volumes at different drainage basins

Sub-basins	Glacial sediment thickness (depo-center, km)	Glacial sediment volume (10^6 km ³)	Volume estimation based on ciation
Lazarev Sea	1.8	0.1	this study
WS	5.0	2.0	Huang et al., 2014
DML	2.0-4.0	0.6	Leitchenkov et al., 2008 Wilson et al., 2012
PB	2.0-3.0	1.3	Kuvaas et al., 2004 O'Brien et al., 2001
WL	4.0	0.6	Close et al., 2007 Escutia et al., 2004
RS	0.65	1.5	Bart et al., 2000 Hambrey et al., 2002
BS+AS	2.0	1.6	Scheuer et al., 2006 Nilsche et al., 2000

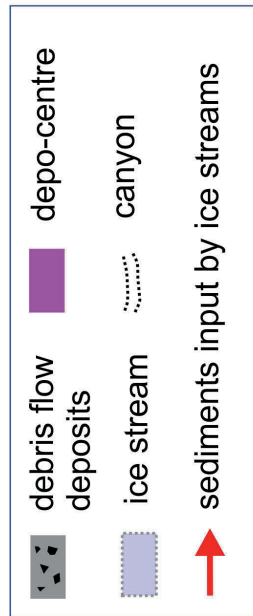


Fig. 7.10 Regional topographic changes along the DML margin (after Fretwell et al. (2013)) demonstrate several prominent tectonic and sedimentary features. Onshore, the DML-mountain belt and Jutul-Penck Graben system, with its ice streams, are observed. Ice streams are adopted from Rignot and Scheuchl (2011). Offshore, canyons, debris flow deposits and depocenters are recognized from the seismic reflection data. The table provides an overview of the glacial sediment thicknesses and volumes at the drainage basins around the Antarctic margin, along with relevant references.

7.7 Conclusions

1. Our seismic data document that the debris flow deposits at the continental slope and indicate as consequences of ice streams depositing their loads of sediment and meltwater at the shelf edge, or of episodic ice sheet collapse at the shelf break. Consequently, in comparison to other Antarctic sub basins with larger drainage areas, the total sediment thickness and volume observed in the study region are small and submarine fan deposits is not observed. The ice streams formed in the Jutul-Penck Graben system, which cuts across the DML mountain belt, is the most important conduit for delivery of sediments to the continental margin beyond the mountains. For the most part, however, the mountain belt acted as a barrier to terrigenous sediment transport from the east Antarctic interior to the Lazarev Sea. Therefore, we suggest that the major deposit in the Lazarev Sea probably not majorly originated from interior of East Antarctica.

2. Two types of canyon are defined based on their dimensions and axial sedimentation processes. Type I, of small size and with well developed levee deposits, resulted from turbidity current action during glacial times. Type II canyons are deeper and wider, and exhibit slumps and terraces on their sidewalls, which form the flanks of intercanyon ridges. These features may result from fluvial erosion or slope failure in preglacial times.

3. We reported the presence of pipe-like seismic chimneys at this margin for the first time. Tentatively, we attribute their formation to the intrusion of the melt during Mesozoic volcanism related to the margin's formation during the breakup of Gondwana.

7.8 Acknowledgements

The authors would like to thank the masters, crews and seismic teams of the many ship expeditions to the Weddell Sea, who made the acquisition of the data used in this study possible. The German Federal Institute of Geosciences and Resources (BGR) as well as research institutes in Norway are gratefully acknowledged for their contribution of the used seismic data to the Antarctic Seismic Data Library System (SDLS). X.H. has been receiving a PhD scholarship from the Chinese Scholarship Council (CSC).

7.9 References

- Anderson, J. B., Brake, C. F., & Myers, N. C. (1984). Sedimentation on the Ross Sea continental shelf, Antarctica. *Marine Geology*, 57(1), 295-333.
- Antobreh, A. A., & Krastel, S. (2007). Mauritania Slide Complex: morphology, seismic characterisation and processes of formation. *International Journal of Earth Sciences*, 96(3), 451-472. doi:10.1016/j.marpetgeo.2005.06.003.
- Barker, P.F., Kennett, J.P., et al, (1988). Proceedings of the Ocean Drilling Program, Scientific Results Leg 113. Ocean Drilling Program: 774. doi:10.2973/odp.proc.ir.113.1988.
- Bart, P. J., De Batist, M., & Jokat, W. (1999). Interglacial collapse of Crary trough-mouth fan, Weddell Sea, Antarctica: Implications for Antarctic glacial history. *Journal of Sedimentary Research*, 69(6).
- Bart, P. J., Anderson, J. B., Trincardi, F., & Shipp, S. S. (2000). Seismic data from the Northern basin, Ross Sea, record extreme expansions of the East Antarctic Ice

Sheet during the late Neogene. *Marine Geology*, 166(1), 31-50.

Close, D. I., Stagg, H. M. J., & O'Brien, P. E. (2007). Seismic stratigraphy and sediment distribution on the Wilkes Land and Terre Adélie margins, East Antarctica. *Marine geology*, 239(1), 33-57.

Donda, F., O'Brien, P. E., De Santis, L., Rebesco, M., & Brancolini, G. (2008). Mass wasting processes in the Western Wilkes Land margin: possible implications for East Antarctic glacial history. *Palaeogeography, Palaeoclimatology, Palaeoecology*, 260(1), 77-91. doi:10.1016/j.palaeo.2007.08.008

Eagles, G., & König, M. (2008). A model of plate kinematics in Gondwana breakup. *Geophysical Journal International*, 173(2), 703-717.

Ehrmann, W. U., & Mackensen, A. (1992). Sedimentological evidence for the formation of an East Antarctic ice sheet in Eocene/Oligocene time. *Palaeogeography, Palaeoclimatology, Palaeoecology*, 93(1), 85-112.

Escutia, C., De Santis, L., Donda, F., Dunbar, R. B., Cooper, A. K., Brancolini, G., & Eitrem, S. L. (2005). Cenozoic ice sheet history from East Antarctic Wilkes Land continental margin sediments. *Global and Planetary Change*, 45(1), 51-81.

Florindo, F., & Roberts, A. P. (2005). Eocene-Oligocene magnetobiochronology of ODP Sites 689 and 690, Maud Rise, Weddell Sea, Antarctica. *Geological Society of America Bulletin*, 117(1-2), 46-66.

Groenewald, P. B., Moyes, A. B., Grantham, G. H., & Krynauw, J. R. (1995). East Antarctic crustal evolution: geological constraints and modelling in western Dronning Maud Land. *Precambrian Research*, 75(3), 231-250. doi:10.1016/0301-9268(95)80008-6.

Geletti, R., & Busetti, M. (2011). A double bottom simulating reflector in the western Ross Sea, Antarctica. *Journal of Geophysical Research: Solid Earth* (1978–2012), 116(B4). DOI: 10.1029/2010JB007864

Gee, M. J. R., & Gawthorpe, R. L. (2006). Submarine channels controlled by salt tectonics: Examples from 3D seismic data offshore Angola. *Marine and Petroleum Geology*, 23(4), 443-458.

Hampton, M. A., Lee, H. J., & Locat, J. (1996). Submarine landslides. *Reviews of geophysics*, 34(1), 33-59. DOI: 10.1029/95RG03287.

Hinz, K., Neben, S., Gouseva, Y. B., & Kudryavtsev, G. A. (2004). A compilation of geophysical data from the Lazarev Sea and the Riiser-Larsen Sea, Antarctica. *Marine Geophysical Researches*, 25(3-4), 233-245.

Huang, X., Gohl, K., Jokat, W., (2014) Variability in Cenozoic sedimentation and paleo-water depths of the Weddell Sea basin related to pre-glacial and glacial conditions of Antarctica, *Global and Planetary Change*. DOI: 10.1016/j.gloplacha.2014.03.010.

Huang, X., & Gohl, K. (2015). Seismostratigraphic Analysis and Glacial History of the Weddell Sea Region, Antarctica. In *Towards an Interdisciplinary Approach in Earth System Science* (pp. 207-217). Springer International Publishing. doi: 10.1007/978-3-319-13865-7_22.

Huang, X., Jokat, W., (2014) Middle Miocene to present sediment transports and deposits in the southeast Weddell Sea, Antarctica, *Marine and Petroleum Geology*. in revision.

Horozal, S., Lee, G. H., Bo, Y. Y., Yoo, D. G., Park, K. P., Lee, H. Y., ... & Lee, K. (2009). Seismic indicators of gas hydrate and associated gas in the Ulleung Basin, East Sea (Japan Sea) and implications of heat flows derived from depths of the bottom-simulating reflector. *Marine Geology*, 258(1), 126-138. doi:10.1016/j.margeo.2008.12.004.

Hambrey, M. J., Barrett, P. J., & Powell, R. D. (2002). Late Oligocene and early Miocene glaciomarine sedimentation in the SW Ross Sea, Antarctica: the record from offshore drilling. *Geological Society, London, Special Publications*, 203(1), 105-128.

Jokat, W., Boebel, T., König, M., & Meyer, U. (2003). Timing and geometry of early Gondwana breakup. *Journal of Geophysical Research: Solid Earth* (1978–2012), 108(B9).

Hayes, D. E., Zhang, C., & Weissel, R. A. (2009). Modeling paleobathymetry in the Southern Ocean. *Eos, Transactions American Geophysical Union*, 90(19), 165-166.

Jokat, W., Ritzmann, O., Reichert, C., & Hinz, K. (2004). Deep crustal structure of the continental margin off the Explora Escarpment and in the Lazarev Sea, East Antarctica. *Marine Geophysical Researches*, 25(3-4), 283-304. doi: 10.1007/s11001-005-1337-9.

Jacobs, J., Kaul, N., & Weber, K. (1996). The history of denudation and resedimentation at the continental margin of western Dronning Maud Land, Antarctica, during break-up of Gondwana. *Geological Society, London, Special Publications*, 108(1), 191-199.

Jacobs, J., & Thomas, R. J. (2004). Himalayan-type indenter-escape tectonics model for the southern part of the late Neoproterozoic–early Paleozoic East African–Antarctic orogen. *Geology*, 32(8), 721-724.

Jobe, Z. R., Lowe, D. R., & Uchytel, S. J. (2011). Two fundamentally different types of submarine canyons along the continental margin of Equatorial Guinea. *Marine and Petroleum Geology*, 28(3), 843-860. doi:10.1016/j.marpetgeo.2010.07.012

Kuvaas, B., Kristoffersen, Y., Guseva, J., Leitchenkov, G., Gandjukhin, V., & Kudryavtsev, G. (2004). Input of glaciomarine sediments along the East Antarctic continental margin; depositional processes on the Cosmonaut Sea continental slope and rise and a regional acoustic stratigraphic correlation from 40 W to 80 E. *Marine Geophysical Researches*, 25(3-4), 247-263.

Kuvaas, B., & Kristoffersen, Y. (1991). The Crary Fan: a trough-mouth fan on the Weddell Sea continental margin, Antarctica. *Marine Geology*, 97(3), 345-362.

Leitchenkov, G., Guseva, J., Gandjukhin, V., Griukurov, G., Kristoffersen, Y., Sand, M., ... & Aleshkova, N. (2008). Crustal structure and tectonic provinces of the Riiser-Larsen Sea area (East Antarctica): results of geophysical studies. *Marine Geophysical Researches*, 29(2), 135-158. DOI: 10.1007/s11001-008-9051-z

Leinweber, V. T., & Jokat, W. (2012). The Jurassic history of the Africa–Antarctica corridor—new constraints from magnetic data on the conjugate continental margins. *Tectonophysics*, 530, 87-101. doi:10.1016/j.tecto.2011.11.008

Laymon, C. A. (1992). Glacial geology of western Hudson Strait, Canada, with reference to Laurentide Ice Sheet dynamics. *Geological Society of America Bulletin*, 104(9), 1169-1177.

Miller, H., Henriot, J.P., Kaul, N., Moons, A., (1990). A fine-scale stratigraphy of the eastern margin of the Weddell Sea. In: Bleil, U., Thiede, J. (Eds.), *Geological History of the Polar Oceans: Arctic Versus Antarctic*. Kluwer Academic Publishers, pp. 131–161. doi: 10.1007/978-94-009-2029-3_8.

Masson, D. G., Harbitz, C. B., Wynn, R. B., Pedersen, G., & Løvholt, F. (2006). Submarine landslides: processes, triggers and hazard prediction. *Philosophical Transactions of the Royal Society of London A: Mathematical, Physical and Engineering Sciences*, 364(1845), 2009-2039.

Näslund, J. O. (2001). Landscape development in western and central Dronning Maud Land, East Antarctica. *Antarctic Science*, 13(03), 302-311.

Nitsche, F. O., Cunningham, A. P., Larter, R. D., & Gohl, K. (2000). Geometry and development of glacial continental margin depositional systems in the

Bellingshausen Sea. *Marine Geology*, 162(2), 277-302.

O'Brien, P. E., Cooper, A. K., & Richter, C. (2001). Initial Report, Prydz Bay-Cooperation Sea, Antarctica: glacial history and paleoceanography: Proc. In ODP Init. Repts (Vol. 188).

Pritchard, H. D., Arthern, R. J., Vaughan, D. G., & Edwards, L. A. (2009). Extensive dynamic thinning on the margins of the Greenland and Antarctic ice sheets. *Nature*, 461(7266), 971-975. doi:10.1038/nature08471

Peters, L. E., Anandakrishnan, S., Alley, R. B., Winberry, J. P., Voigt, D. E., Smith, A. M., & Morse, D. L. (2006). Subglacial sediments as a control on the onset and location of two Siple Coast ice streams, West Antarctica. *Journal of Geophysical Research: Solid Earth* (1978–2012), 111(B1).

Planke, S., Rasmussen, T., Rey, S. S., & Myklebust, R. (2005, January). Seismic characteristics and distribution of volcanic intrusions and hydrothermal vent complexes in the Vøring and Møre basins. In Geological Society, London, Petroleum Geology Conference series (Vol. 6, pp. 833-844). Geological Society of London. doi: 10.1144/0060833.

Pratson, L. F. and Coakley, B. J.: A model for the headward erosion of submarine canyons induced by downslope-eroding sediment flows, *GSA Bull.*, 108, 2, 225–234, 1996.

Rogenhagen, J., Jokat, W., Hinz, K., & Kristoffersen, Y. (2004). Improved seismic stratigraphy of the Mesozoic Weddell Sea. *Marine Geophysical Researches*, 25(3-4), 265-282. DOI: 10.1007/s11001-005-1335-y.

Riedel, S., Jokat, W., & Steinhage, D. (2012). Mapping tectonic provinces with airborne gravity and radar data in Dronning Maud Land, East Antarctica. *Geophysical Journal International*, 189(1), 414-427. doi: 10.1111/j.1365-246X.2012.05363.x.

Rebesco, M., Domack, E., Zgur, F., Lavoie, C., Leventer, A., Brachfeld, S., ... & Pettit, E. (2014). Boundary condition of grounding lines prior to collapse, Larsen-B Ice Shelf, Antarctica. *Science*, 345(6202), 1354-1358. DOI: 10.1126/science.1256697.

Rignot, E., Mouginot, J., & Scheuchl, B. (2011). Ice flow of the Antarctic ice sheet. *Science*, 333(6048), 1427-1430.

Scheuer, C., Gohl, K., & Udintsev, G. (2006). Bottom-current control on sedimentation in the western Bellingshausen Sea, West Antarctica. *Geo-marine letters*, 26(2), 90-101.

Kanao, M., Suvorov, V. D., Yamashita, M., & Mishenkin, B. (2014). Crustal structure and tectonic evolution of Enderby Land, East Antarctica, as revealed by deep seismic surveys. *Tectonophysics*, 627, 38-47. doi:10.1016/j.tecto.2012.01.014.

Sultan, N., Cochonat, P., Canals, M., Cattaneo, A., Dennielou, B., Haflidason, H., ... & Wilson, C. (2004). Triggering mechanisms of slope instability processes and sediment failures on continental margins: a geotechnical approach. *Marine Geology*, 213(1), 291-321. doi:10.1016/j.margeo.2004.10.011.

Shepard, F. P. (1981). Submarine canyons: multiple causes and long-time persistence. *AAPG Bulletin*, 65(6), 1062-1077.

White, R. & McKenzie, D. 1989 Magmatism at rift zones: the generation of volcanic continental margins and flood basalts. *Journal of Geophysical Research*, 94, 7685-7729.

Weigelt, E., Uenzelmann-Neben, G., Gohl, K., & Larter, R. D. (2012). Did massive glacial dewatering modify sedimentary structures on the Amundsen Sea Embayment shelf, West Antarctica?. *Global and Planetary Change*, 92, 8-16. doi:10.1016/j.gloplacha.2012.04.006.

Weaver, P.E., Wynn, R.B., Kenyon, N.H., Evans, J., 2000. Continental margin

sedi- mentation, with special reference to the north-east Atlantic margin. *Sedimentology* 47 (s1), 239-256.

Wilson, D. S., Jamieson, S. S., Barrett, P. J., Leitchenkov, G., Gohl, K., & Larter, R. D. (2012). Antarctic topography at the Eocene–Oligocene boundary. *Palaeogeography, Palaeoclimatology, Palaeoecology*, 335, 24-34.

Young, D. A., Wright, A. P., Roberts, J. L., Warner, R. C., Young, N. W., Greenbaum, J. S., ... & Siegert, M. J. (2011). A dynamic early East Antarctic Ice Sheet suggested by ice-covered fjord landscapes. *Nature*, 474(7349), 72-75. doi:10.1038/nature10114.

8 Conclusions and Outlooks

8.1 Conclusions

This thesis has been focusing on all available multichannel seismic lines, ODP Sites, and SHADRILL sites in the Weddell Sea and provides detail information regarding paleobathymetry reconstruction, sedimentation history and modeled ocean circulation in the Weddell Sea basin. All the proposed questions are answered.

1. What is the distribution of sedimentary depocentres within the Weddell Sea basin, and how does it compare to the distribution of ice stream catchment areas on the adjacent Antarctic margins? **(Chapter 3)**

The Weddell Sea basin holds the largest volume of the sediments due to its huge ice stream catchment area. Two major seismic unconformities (WS-u4, WS-u5) and three seismic units (pre-glacial, transitional, full glacial) were mapped and served as a base to calculate for the first time basin-wide grids of sediment depths, thicknesses, rates and paleobathymetries. The distribution of the total sediment thickness shows a decreasing trend northward. The maximum sediment thickness of up to 12 km is found in the southern Weddell Sea in front of the Filchner-Ronne Ice Shelf. The pre-glacial unit has the thickest sediments owing to its long sedimentation period of 80 – 100 Myr, but was deposited with a relatively low rate. The tectonic evolution and seafloor spreading history of the Weddell Sea interacted with terrigenous sediment supply controlled its distribution. The transitional unit accumulated at a relatively high sedimentation rate. Its thickness varies in the range of 0 - 3 km. A relatively high sediment supply from a growing EAIS grounded to the coast or even inner shelf could be the main contributor to sedimentation on the continental rise. The high sedimentation rates during the full glacial period generated depocentres near the margins of the southern, southeastern and western Weddell Sea. Here, the maximum sediment thickness is 4-5 km for this period. Sedimentation rates varied from 0 to 200 m/myr. The large amount of sediments, and their deposition at high sedimentation rates in the southern Weddell Sea imply an increase of glacial advances of grounded EAIS, WAIS and APIS to the middle or outer shelf since the middle Miocene. Large sedimentary drifts and channel-levee complexes are abundant close to the continental margin, suggesting turbidity currents and other mass-flow processes redistributing the sediments.

2. How has the depth and shape of the Weddell Sea basin changed over the past 100 million of years, since the opening of the Southern Ocean gateways, since the onset of the Antarctic glaciations, and during the transition from the greenhouse to icehouse world? **(Chapter 3)**

I derived a grid series of the paleobathymetric evolution of the Weddell Sea basin for 120 Ma, 34 Ma and 15 Ma by using backstripping technique. The backstripping technique involves the stepwise removal of sediment loads and applies decompaction of the remaining underlying sequence as well as isostatic correction for the replacement of the sedimentary load by water or air. The models yield a consistent trend of deepening in the regional evolution of the Weddell Sea basin. This is consistent with the overall dominance of thermal subsidence effects. At 120 Ma, the

basement, which currently lies beneath as much as 12 km of sediments, is restored to a level of only ~3 km below seafloor. At the Eocene-Oligocene boundary (34 Ma), the grids show that the basin is about 0.5 - 1 km shallower compared with that of the present in the northwestern Weddell Sea, which is mainly due to the fact that relative young oceanic crust yields remarkable effect of the thermal subsidence. However, the paleowater depth of the central Weddell Sea is nearly consistent with today and the Middle Miocene. The small elevation difference is probably caused by the mantle rebound and decompaction of the remaining sediments after removal 5 - 6 km sediment layers, which were mostly deposited during glacial time. The effect of the thermal subsidence is nearly neglectable in the central Weddell Sea for the period from 15 Ma to present day. Possible sources of error in the paleobathymetric estimates are uncertainties in the modelled lithospheric thickness, stretching factor, porosity-depth relationship, and distributions of crustal nature and age are discussed. The predicted paleobathymetry will improve the testing of paleoceanographic and paleoclimatic scenarios through model simulations.

3. How did bathymetry influence ocean circulation in the Weddell Sea during the Middle Miocene? (**Chapter 4**)

In order to test sensitivity of the paleobathymetry as a boundary condition for the numerical climate models, several GCM runs have been simulated. The study provides robust evidence that paleo-ocean circulation is extremely sensitive to regional changes in paleobathymetry. The Weddell Gyre shifts poleward after applying an improved Mid-Miocene paleobathymetric grid. The higher-than present CO₂ level and the improved paleobathymetry together induce the warmest SSTs in the Weddell Sea as well as global climate associated to the MMCO. A low CO₂ level and with the improved paleobathymetry simulate the major AABW formation for the Atlantic sector. As a consequence, abundant AABW production and large sediment drifts developed and modified the margin geomorphology along the western and southern Weddell Sea continental rise and the regions with AABW flow. Globally, the dramatic deepening of the mixed layer may have influenced the evolution of deep ocean temperature and has potential consequences for carbon cycling by an increase in primary biomass production. Our study sheds light on how the shelf break significantly interacts with regional ocean circulation of the Weddell Sea. A similar test in the Ross Sea and other Antarctic embayment would therefore be of great interest to improve understanding of paleoclimate and the mechanisms of AABW formation in the Southern Ocean.

4. What factors control, or have controlled, glacial sedimentation patterns in the southeast Weddell Sea? (**Chapter 5**)

In the southeast Weddell Sea, two giant, sinuous, NE-SW-oriented sediment ridges are identified and their bathymetric expressions of the ridges are more than 150 km wide and 700 km long. Sediment thicknesses in the ridges reach as much as 2 km. We interpreted these ridges as turbidity-contourites, due to the complicated down-slope/along-slope processes occurring across their margins with channels at their flanks. The turbidity-contourites are formed by along slope process (e.g. AABW, WSBW), and significantly modified and conditioned by downslope process (turbidity flow) to form extensive levees in the study region. In addition, the seismic data allow

us to interpret the influences over time of the region's unique large catchment area, fast (paleo-) ice streams, abundant sediment supply, fluctuating sea level, and advancing and retreating ice sheets, on the development of the giant turbidity-contourites.

Other, related, changes in depositional style are visible in our offshore seismic data from the Late Miocene to Late Pliocene in this study. The remarkable increase in MTDs during the Late Miocene and Middle to Late Pliocene (between WS-u6 and WS-u7) is related to the build up of overpressure during rapid sediment accumulation, changing sea-level, and possibly also glacial-isostatic paleoearthquakes. Our stratigraphic studies may indicate that fluctuations of Antarctic ice sheets similar to those occurring during late Quaternary glacial cycles have been typical for the region during glacial periods since the Late Miocene or even earlier. However, the details of the ice sheet dynamics can only be constrained by deep scientific drilling.

5. What are and were the sources and transport patterns of sediment off the DML margin and in the Lazarev Sea? (**Chapter 6**).

My seismic data document that the debris flow deposits at the continental slope and indicate as consequences of ice streams depositing their loads of sediment and meltwater at the shelf edge, or of episodic ice sheet collapse at the shelf break. Consequently, in comparison to other Antarctic sub basins with larger drainage areas, the total sediment thickness and volume observed in the study region are small and submarine fan deposits is not observed. The ice streams formed in the Jutul-Penck Graben system, which cuts across the DML mountain belt, is the most important conduit for delivery of sediments to the continental margin beyond the mountains. For the most part, however, the mountain belt acted as a barrier to terrigenous sediment transport from the east Antarctic interior to the Lazarev Sea. Therefore, I suggest that the major deposit in the Lazarev Sea probably not majorly originated from interior of East Antarctica. Two types of canyon are defined based on their dimensions and axial sedimentation processes. Type I, of small size and with well developed levee deposits, resulted from turbidity current action during glacial times. Type II canyons are deeper and wider, and exhibit slumps and terraces on their sidewalls, which form the flanks of intercanyon ridges. These features may result from fluvial erosion or slope failure in preglacial times. I reported the presence of pipe-like seismic chimneys at this margin for the first time. Tentatively, I attribute their formation to the intrusion of the melt during Mesozoic volcanism related to the margin's formation during the breakup of Gondwana.

8.2 Outlooks

8.2.1 Paleobathymetry prospective

The first tempt of reconstructing the paleobathymetry of the Weddell Sea and implementing into the General Circulation Models (GCM) provide a series of evidences that the regional paleobathymetry changes can have profound influence on the regional paleocean circulation. The southerly-replaced shelf break of the Weddell Sea results in dramatic changes in simulated mixed layer depth and significant increase in AABW formation. Paleobathymetry manifests itself as a critical parameter for climate and circulation studies.

Our study also sheds light on how the shelf break significantly interacts with regional ocean circulation of the Weddell Sea, in a regional scale. Thus, similar

simulation experiments in the Ross Sea and other Antarctic embayment would therefore be of great interest to improve understanding of paleoclimate and the mechanisms of AABW formation in the Southern Ocean in future.

However, existing circum-Antarctica paleobathymetric grids either suffer from regional resolution and accuracy due to lack of recent seismic data used (Hayes et al., 2009) or have not included sediments at all (Brown et al., 2006). Thus, it is essential to set up a unified and precise circum-Antarctica Seismostratigraphic age model based on all available geophysical/geological records in order to reconstruct the paleobathymetry of the Southern Ocean.

In addition, the geometry and elevation of the continent and seafloor exerts a strong influence on climate and ocean circulation in response to more rapidly changing forcing agents. Multi-scale tectonic, geodynamic, seismostratigraphic, geomorphic and palaeoclimatic evidence must be combined to provide better boundary conditions for numerical models. The topography/paleobathymetry reconstruction will greatly reduce the gap between numerical climate models and geophysical/geological data. The possible challenges exist, particularly in Polar Regions, e.g. tectonic issue related to Gondwana Breakup in deeper time scales, the uniform seismostratigraphic model, continent-ocean boundaries.

8.2.2 stratigraphic age model prospective

Seismic stratigraphic and scientific drilling data from the Antarctic continental margins have provided much direct evidence concerning ice sheet evolution and sedimentation history. Understanding the transport and deposition of sediments along the Antarctic continental shelves helps to provide constraints on past ice sheet dynamics and Antarctic climate. Despite more than 1,400 seismic lines are available in the expanded Weddell Sea basin, it is still challenging to set up an accurate basin-wide stratigraphic age model due to sparse ODP and SHADRILL sites. Many of the cores are too shallow to date the basement, or not well recovered to evaluate the age of the important sedimentary elements.

In order to answer the questions related to Antarctic Ice Sheet stabilities, sea level changes and paleoclimate and paleocean circulations, more deep scientific drilling and necessary new seismic data is urgently needed in the Weddell Sea, particularly in the southeast Weddell Sea and Dronning Maud Land margins where sediment deposition is strongly influenced by ice sheet dynamics and sea level changes. The new drilling sites on the Weddell Sea margins will allow us to make a sufficient use of the existing seismic data.

Bibliography

- Anderson, J. B. (1999). Antarctic marine geology. Cambridge University Press.
- Anderson, J. B., Warny, S., Askin, R. A., Wellner, J. S., Bohaty, S. M., Kirshner, A. E., ... & Majewski, W. (2011). Progressive Cenozoic cooling and the demise of Antarctica's last refugium. *Proceedings of the National Academy of Sciences*, 108(28), 11356-11360.
- Allen, P. A., & Allen, J. R. (2013). Basin analysis: Principles and application to petroleum play assessment. John Wiley & Sons.
- Barker, P. F., Kennett, J. P., & And 23 others. (1990). Proceedings of the Ocean Drilling Program, Vol. 113, Scientific Results, Weddell Sea, Antarctica. Ocean Drilling Program.
- Barker, P. F., & Thomas, E. (2004). Origin, signature and palaeoclimatic influence of the Antarctic Circumpolar Current. *Earth-Science Reviews*, 66(1), 143-162.
- Bart, P. J. (2001). Did the Antarctic ice sheets expand during the early Pliocene? *Geology*, 29(1), 67-70.
- Barker, P. F., Filippelli, G. M., Florindo, F., Martin, E. E., & Scher, H. D. (2007). Onset and role of the Antarctic Circumpolar Current. *Deep Sea Research Part II: Topical Studies in Oceanography*, 54(21), 2388-2398.
- Brown, B., Gaina, C., & Müller, R. D. (2006). Circum-Antarctic palaeobathymetry: Illustrated examples from Cenozoic to recent times. *Palaeogeography, Palaeoclimatology, Palaeoecology*, 231(1), 158-168.
- Beckmann, A., Hellmer, H. H., & Timmermann, R. (1999). A numerical model of the Weddell Sea: Large-scale circulation and water mass distribution. *Journal of Geophysical Research: Oceans* (1978–2012), 104(C10), 23375-23391.
- Cooper, A.K., G. Brancolini, C. Escutia, Y. Kristoffersen, R. Larter, G. Leitchenkov, P. O'Brien, W. Jokat, 2008, Cenozoic climate history from seismic-reflection and drilling studies on the Antarctic continental margin, In: F. Florindo and M. Siebert (Eds). *Antarctic Climate Evolution, Developments in Earth and Environmental Sciences*, Vol. 8, Elsevier, 537p.
- Davies, B. J., Hambrey, M. J., Smellie, J. L., Carrivick, J. L., & Glasser, N. F. (2012). Antarctic Peninsula ice sheet evolution during the Cenozoic Era. *Quaternary Science Reviews*, 31, 30-66.
- DeConto, R. M., & Pollard, D. (2003). Rapid Cenozoic glaciation of Antarctica induced by declining atmospheric CO₂. *Nature*, 421(6920), 245-249.
- DeConto, R., Pollard, D., & Harwood, D. (2007). Sea ice feedback and Cenozoic evolution of Antarctic climate and ice sheets. *Paleoceanography*, 22(3).
- Dalziel, I. W. (2014). Drake Passage and the Scotia arc: A tortuous space-time gateway for the Antarctic Circumpolar Current. *Geology*, 42(4), 367-368.
- Eagles, G., & Jokat, W. (2014). Tectonic reconstructions for paleobathymetry in Drake Passage. *Tectonophysics*, 611, 28-50.
- Exon, N., Kennett, J., Malone, M., Brinkhuis, H., Chaproniere, G., Ennyu, A., ... & White, T. (2002). Drilling reveals climatic consequences of Tasmanian gateway opening. *Eos, Transactions American Geophysical Union*, 83(23), 253-259.
- Ehlers, B. M., & Jokat, W. (2013). Paleo-bathymetry of the northern North Atlantic and consequences for the opening of the Fram Strait. *Marine Geophysical Research*, 34(1), 25-43.

Foldvik, A., Gammelsrød, T., Østerhus, S., Fahrbach, E., Rohardt, G., Schröder, M., ... & Woodgate, R. A. (2004). Ice shelf water overflow and bottom water formation in the southern Weddell Sea. *Journal of Geophysical Research: Oceans* (1978–2012), 109(C2).

Fahrbach, E., Rohardt, G., Scheele, N., Schröder, M., Strass, V., & Wisotzki, A. (1995). Formation and discharge of deep and bottom water in the northwestern Weddell Sea. *Journal of Marine Research*, 53(4), 515-538.

Fahrbach, E., Hoppema, M., Rohardt, G., Boebel, O., Klatt, O., & Wisotzki, A. (2011). Warming of deep and abyssal water masses along the Greenwich meridian on decadal time scales: The Weddell gyre as a heat buffer. *Deep Sea Research Part II: Topical Studies in Oceanography*, 58(25), 2509-2523.

Faugères, J. C., & Stow, D. A. (1993). Bottom-current-controlled sedimentation: a synthesis of the contourite problem. *Sedimentary Geology*, 82(1), 287-297.

Grützner, J., Hillenbrand, C. D., & Rebesco, M. (2005). Terrigenous flux and biogenic silica deposition at the Antarctic continental rise during the late Miocene to early Pliocene: implications for ice sheet stability and sea ice coverage. *Global and Planetary Change*, 45(1), 131-149.

Lisiecki, L. E., & Raymo, M. E. (2005). A Pliocene–Pleistocene stack of 57 globally distributed benthic $\delta^{18}\text{O}$ records. *Paleoceanography*, 20(1).

Gordon, A. L. (1981). South Atlantic thermocline ventilation. *Deep Sea Research Part A. Oceanographic Research Papers*, 28(11), 1239-1264.

Halpern, B. S., Walbridge, S., Selkoe, K. A., Kappel, C. V., Micheli, F., D'Agrosa, C., ... & Watson, R. (2008). A global map of human impact on marine ecosystems. *Science*, 319(5865), 948-952.

Hinz, K., Neben, S., Gouseva, Y. B., & Kudryavtsev, G. A. (2004). A compilation of geophysical data from the Lazarev Sea and the Riiser-Larsen Sea, Antarctica. *Marine Geophysical Researches*, 25(3-4), 233-245.

Huber, M., & Nof, D. (2006). The ocean circulation in the southern hemisphere and its climatic impacts in the Eocene. *Palaeogeography, Palaeoclimatology, Palaeoecology*, 231(1), 9-28.

Hernández-Molina, F. J., Paterlini, M., Violante, R., Marshall, P., de Isasi, M., Somoza, L., & Rebesco, M. (2009). Contourite depositional system on the Argentine Slope: an exceptional record of the influence of Antarctic water masses. *Geology*, 37(6), 507-510.

Haq, B. U., Hardenbol, J., & Vail, P. R. (1987). Chronology of fluctuating sea levels since the Triassic. *Science*, 235(4793), 1156-1167.

Hübscher, C. (1994). Krustenstrukturen und Verlauf des Kontinentalrandes im Weddell-See/Antarktis= Crustal structures and location of the continental margin in the Weddell Sea/Antarctica. *Berichte zur Polarforschung (Reports on Polar Research)*, 147.

Herold, N., Seton, M., Müller, R. D., You, Y., & Huber, M. (2008). Middle Miocene tectonic boundary conditions for use in climate models. *Geochemistry, Geophysics, Geosystems*, 9(10).

Jokat, W., Miller, H., & Hübscher, C. (1996). Structure and origin of southern Weddell Sea crust: results and implications. Geological Society, London, Special Publications, 108(1), 201-211.

Jokat, W., Boebel, T., König, M., & Meyer, U. (2003). Timing and geometry of early Gondwana breakup. *Journal of Geophysical Research: Solid Earth* (1978–2012), 108(B9).

Jokat, W., Fechner, N., & Studinger, M. (1997). Geodynamic models of the Weddell Sea embayment in view of new geophysical data. *The Antarctic region: geological evolution and processes*, 453-460.

Jungclauss, J. H., Lorenz, S. J., Timmreck, C., Reick, C. H., Brovkin, V., Six, K., ... & Marotzke, J. (2010). Climate and carbon-cycle variability over the last millennium. *Climate of the Past*, 6, 723-737.

Katz, M. H. (2011). *Multivariable analysis: a practical guide for clinicians and public health researchers*. Cambridge university press.

Kennett, J. P., & Barker, P. F. (1990). Latest Cretaceous to Cenozoic climate and oceanographic developments in the Weddell Sea, Antarctica: an ocean-drilling perspective. In *Proceedings of the Ocean Drilling Program, Scientific Results (Vol. 113, pp. 937-960)*. Ocean Drilling Program College Station, TX. König, M., Jokat, W., (2006). The Mesozoic breakup of the Weddell Sea. *J. Geophys. Res.*, 111, B12102. doi: 10.1029/2005JB004035.

King, E. C. (2000). The crustal structure and sedimentation of the Weddell Sea embayment: implication for Gondwana reconstructions. *Tectonophysics* 327, 195-212.

Livermore, R. A., & Hunter, R. J. (1996). Mesozoic seafloor spreading in the southern Weddell Sea. *Geological Society, London, Special Publications*, 108(1), 227-241.

LaBrecque, J. L., & Barker, P. (1981). The age of the Weddell Basin.

Studinger, M., & Miller, H. (1999). Crustal structure of the Filchner-Ronne shelf and Coats Land, Antarctica, from gravity and magnetic data: implications for the breakup of Gondwana. *Journal of Geophysical Research*, 104(B9), 20379-20394.

Lawver, L. A., Gahagan, L. M., & Coffin, M. F. (1992). The development of paleoseaways around Antarctica. *Antarctic research series*, 56, 7-30.

Lawver, L. A., & Gahagan, L. M. (2003). Evolution of Cenozoic seaways in the circum-Antarctic region. *Palaeogeography, Palaeoclimatology, Palaeoecology*, 198(1), 11-37.

Lagabrielle, Y., & Bodinier, J. L. (2008). Submarine reworking of exhumed subcontinental mantle rocks: field evidence from the Lherz peridotites, French Pyrenees. *Terra Nova*, 20(1), 11-21.

Lawver, L. A., & Gahagan, L. M. (1998). Opening of Drake Passage and its impact on Cenozoic ocean circulation. *Oxford Monographs on Geology and Geophysics*, 39, 212-226.

Livermore, D. M., Canton, R., Gniadkowski, M., Nordmann, P., Rossolini, G. M., Arlet, G., ... & Woodford, N. (2007). CTX-M: changing the face of ESBLS in Europe. *Journal of Antimicrobial Chemotherapy*, 59(2), 165-174.

Livermore, R., Nankivell, A., Eagles, G., Morris, P., 2005. Paleogene opening of Drake Passage. *Earth Planet. Sci. Lett.*, 236, 459-470. <http://dx.doi.org/10.1016/j.epsl.2005.03.027>.

Lyle, M., Gibbs, S., Moore, T. C., & Rea, D. K. (2007). Late Oligocene initiation of the Antarctic circumpolar current: evidence from the South Pacific. *Geology*, 35(8), 691-694.

Lythe, M. B., Vaughan, D. G., Lambrecht, A., Miller, H., Nixdorf, U., Oerter, H., ... & Huybrechts, P. (2001). BEDMAP: A new ice thickness and subglacial topographic model of Antarctica. *Journal of Geophysical Research*, 106 (B6), 11, 335.

Lear, C. H., Elderfield, H., & Wilson, P. A. (2000). Cenozoic deep-sea temperatures and global ice volumes from Mg/Ca in benthic foraminiferal calcite. *science*, 287(5451), 269-272.

- Lewis, M. A., Neighbors, C., Oster-Aaland, L., Kirkeby, B. S., & Larimer, M. E. (2007). Indicated prevention for incoming freshmen: Personalized normative feedback and high-risk drinking. *Addictive behaviors*, 32(11), 2495-2508.
- McCave, I. N., & Tucholke, B. E. (1986). Deep current-controlled sedimentation in the western North Atlantic. *The Geology of North America*, 1000, 451-468.
- Matthews, R. K., & Poore, R. Z. (1980). Tertiary $\delta^{18}\text{O}$ record and glacio-eustatic sea-level fluctuations. *Geology*, 8(10), 501-504.
- Miller, K. G., Mountain, G. S., Wright, J. D., & Brownrigg, J. V. (2011). Sea level and ice Volume Variations. *Oceanography*, 24(2), 40-53.
- Maldonado, A., Bohoyo, F., Galindo-Zaldívar, J., Hernández-Molina, J., Jabaloy, A., Lobo, F. J., ... & Vázquez, J. T. (2006). Ocean basins near the Scotia–Antarctic plate boundary: influence of tectonics and paleoceanography on the Cenozoic deposits. *Marine Geophysical Researches*, 27(2), 83-107.
- Naish, T. R., Woolfe, K. J., Barrett, P. J., Wilson, G. S., Atkins, C., Bohaty, S. M., ... & Wonik, T. (2001). Orbitally induced oscillations in the East Antarctic ice sheet at the Oligocene/Miocene boundary. *Nature*, 413(6857), 719-723.
- Nicholls, K. W., Østerhus, S., Makinson, K., Gammelsrød, T., & Fahrbach, E. (2009). Ice–ocean processes over the continental shelf of the southern Weddell Sea, Antarctica: A review. *Reviews of Geophysics*, 47(3).
- Orsi, A. H., Johnson, G. C., & Bullister, J. L. (1999). Circulation, mixing, and production of Antarctic Bottom Water. *Progress in Oceanography*, 43(1), 55-109.
- Orsi, A. H., Nowlin, W. D., & Whitworth, T. (1993). On the circulation and stratification of the Weddell Gyre. *Deep Sea Research Part I: Oceanographic Research Papers*, 40(1), 169-203.
- Oszkó, L. (1997). Tectonic structures and glaciomarine sedimentation in the south-eastern Weddell Sea from seismic reflection data= Tektonischer Aufbau und glaziomarine Sedimentation im südöstlichen Weddellmeer nach reflexionsseismischen Untersuchungen. *Berichte zur Polarforschung (Reports on Polar Research)*, 222.
- Ohshima, K. I., Fukamachi, Y., Williams, G. D., Nishihashi, S., Roquet, F., Kitade, Y., ... & Wakatsuchi, M. (2013). Antarctic Bottom Water production by intense sea-ice formation in the Cape Darnley polynya. *Nature Geoscience*, 6(3), 235-240.
- Pfuhl, H. A., & McCave, I. N. (2005). Evidence for late Oligocene establishment of the Antarctic Circumpolar Current. *Earth and Planetary Science Letters*, 235(3), 715-728.
- Patterson, M. O., McKay, R., Naish, T., Escutia, C., Jimenez-Espejo, F. J., Raymo, M. E., ... & Expedition, I. O. D. P. (2014). Orbital forcing of the East Antarctic ice sheet during the Pliocene and Early Pleistocene. *Nature Geoscience*, 7(11), 841-847.
- Pearson, A. (2009). Global cooling during the Eocene-Oligocene climate transition. *Science*, 323(5918), 1187-1190.
- Rignot, E., Velicogna, I., Van den Broeke, M. R., Monaghan, A., & Lenaerts, J. T. M. (2011). Acceleration of the contribution of the Greenland and Antarctic ice sheets to sea level rise. *Geophysical Research Letters*, 38(5).
- Rebesco, M., Larter, R. D., Barker, P. F., Camerlenghi, A., & Vanneste, L. E. (1997). The history of sedimentation on the continental rise west of the Antarctic Peninsula (pp. 29-49). American Geophysical Union.
- Rahmstorf, S. (2002). Ocean circulation and climate during the past 120,000 years. *Nature*, 419(6903), 207-214.

Robert, C., & Kennett, J. P. (1997). Antarctic continental weathering changes during Eocene-Oligocene cryosphere expansion: Clay mineral and oxygen isotope evidence. *Geology*, 25(7), 587-590.

Rosaire, E. E., & Adler, J. L. (1934). Applications and limitations of dip shooting. *AAPG Bulletin*, 18(1), 119-132.

Rogenhagen, J. (2000). Interpretation seismischer und gravimetrischer Daten des Weddellmeeres, Antarktis= Interpretation of seismic and gravimetric data of the Weddell Sea, Antarctica. *Berichte zur Polarforschung (Reports on Polar Research)*, 369.

Shackleton, N. J., & Kennett, J. P. (1975). Paleotemperature history of the Cenozoic and the initiation of Antarctic glaciation: oxygen and carbon isotope analyses in DSDP Sites 277, 279, and 281. Initial reports of the deep sea drilling project, 29, 743-755.

Shevenell, A. E., Kennett, J. P., & Lea, D. W. (2008). Middle Miocene ice sheet dynamics, deep-sea temperatures, and carbon cycling: A Southern Ocean perspective. *Geochemistry, Geophysics, Geosystems*, 9(2).

Scher, H. D., & Martin, E. E. (2006). Timing and climatic consequences of the opening of Drake Passage. *Science*, 312(5772), 428-430.

Stow, D. A., Faugères, J. C., Howe, J. A., Pudsey, C. J., & Viana, A. R. (2002). Bottom currents, contourites and deep-sea sediment drifts: current state-of-the-art. *Geological Society, London, Memoirs*, 22(1), 7-20.

Stow, D. A., Hernández-Molina, F. J., Llave, E., Sayago-Gil, M., del Río, V. D., & Branson, A. (2009). Bedform-velocity matrix: the estimation of bottom current velocity from bedform observations. *Geology*, 37(4), 327-330.

Siegert, M. J., & Florindo, F. (2008). Antarctic climate evolution. *Developments in Earth and Environmental Sciences*, 8, 1-11.

Scher, H. D., Bohaty, S. M., Zachos, J. C., & Delaney, M. L. (2011). Two-stepping into the icehouse: East Antarctic weathering during progressive ice-sheet expansion at the Eocene–Oligocene transition. *Geology*, 39(4), 383-386.

Sheriff, R. E., & Geldart, L. P. (1995). *Exploration seismology*. Cambridge university press.

Smith, R. T., & Anderson, J. B. (2010). Ice-sheet evolution in James Ross Basin, Weddell Sea margin of the Antarctic Peninsula: The seismic stratigraphic record. *Geological Society of America Bulletin*, 122(5-6), 830-842.

Suckro, S. (2013). *Geodynamic and Palaeobathymetric Reconstruction between Canada and Greenland (Doctoral dissertation, Bremen, Universität Bremen, Diss., 2013)*.

Weppernig, R., Schlosser, P., Khatiwala, S., & Fairbanks, R. G. (1996). Isotope data from Ice Station Weddell: Implications for deep water formation in the Weddell Sea. *JOURNAL OF GEOPHYSICAL RESEARCH-ALL SERIES-*, 101, 25-723.

Wardell, N., Childs, J. R., & Cooper, A. K. (2007). Advances through collaboration: sharing seismic reflection data via the Antarctic Seismic Data Library System for Cooperative Research (SDLS) (No. 2007-1047-SRP-001). US Geological Survey.

Watts, A. B., & Ryan, W. B. F. (1976). Flexure of the lithosphere and continental margin basins. *Tectonophysics*, 36(1), 25-44.

Uenzelmann-Neben, G., & Gohl, K. (2012). Amundsen Sea sediment drifts: Archives of modifications in oceanographic and climatic conditions. *Marine Geology*, 299, 51-62.

ACKNOWLEDGEMENTS

I thank Prof. Dr. Cornelia Spiegel and Prof. Wilfried Jokat who agree to examine this thesis.

Many thanks to Dr. Karsten Gohl for his acceptance at the first place that I have the opportunity to do my PhD in AWI. I appreciate very much his help to start the idea of reconstruction paleobathymetry in the Weddell Sea and many discussions with him regarding the work. I also thank him for his patience to edit the two relevant manuscripts.

Many thanks to Prof. Wilfried Jokat for his supporting and inspiration. He suggested me to explore sedimentary processes on the Weddell Sea margin based on available seismic data and drilling sites after I finished my first manuscript. With his supervision, I obtain great experience and knowledge on seismic interpretation. I also appreciate very much that he supports me to present my PhD work on several international conferences and two times academic training programs in other countries.

Many thanks to Dr. Graeme Eagles. He read all of my manuscripts, my thesis, carefully edited them, provided important scientific input, and had countless discussions with me about my work. I deeply appreciate for his help.

Many thanks to Dr. Gabriele Uenzelmann-Neben for letting me join her Sonne expedition, which gave me a great opportunity to learn seismic data acquisition in the deep sea. I also thank that she continuously encourage me to speak more German and her critical, helpful suggestions about my work.

Many thanks to all my colleagues from geophysical section of AWI for providing a friendly work atmosphere. I particularly thank the office D-3170 (Dr. Michael Horn, Katharina Hochmuth, Ricarda Pietsch), their door is always open for tea, coffee, small talks or technical help. I would also like to thank Dr. Mechita Schmidt-Aursch, Dr. Karsten Gohl, and Tabea Altenbernd for their help to translate and edit the German summary in the thesis.

Special thanks to my family. My parents are the greatest parents I have ever met. They always encourage me to work hard, live independently, and chase my dreams. Many thanks to my boyfriend Mike Müller for his accompany to go through all of the ups and downs.

Curriculum Vitae

Xiaoxia Huang, Chinese, born in 08. 31. 1984

Education

- Ph.D. Geophysics, Oct. 2011- Sep. 2015. Alfred Wegener Institute for marine and polar research, Bremerhaven & Bremen University, Bremen, Germany
- MSc, Geophysics, 2008-2011. Ocean University of China, Qingdao, P.R. China
- MSc, Geoscience, Sep.2009-Aug.2010. Bremen University, Bremen, Germany, Double MSc degrees in geoscience, Bremen University, and in geophysics, Ocean University of China, 2011.
- B.S., Geology, Sep. 2004-Jul. 2008. Northwest University, Xi'an, P.R. China, B.S., Geology, 2008
-

Expeditions:

- Heincke cruise, Germany, 12-14 April 2012
- R/V SONNE (So 224), SW Pacific, 5th. Oct-23rd Nov. 2012

Peer Reviewed Publications:

- [1] **Huang, X.**, Gohl, K., Jokat, W., (2014), Variability in Cenozoic sedimentation and paleo-water depths of the Weddell Sea basin related to pre-glacial and glacial conditions of Antarctica, *Global and Planetary Change*, 118, 25-41. Doi:10.1016/j.gloplacha.2014.03.010.
- [2] **Huang, X.**, Gohl, K., (2015) Earth System Science-Seismostratigraphic analysis and glacial history of the Weddell Sea region, Antarctica. In: G. Lohmann, H. Meggers, V. Unnithan, D. Wolf-Gladrow, J. Notholt, A. Bracher (eds.), *Towards an Interdisciplinary Approach in Earth System Science*, SpringerBriefs in Earth System Sciences, Springer, Heidelberg, Germany. ISBN 978-3-319-13864-0, Doi: 10.1007/978-3-319-13865-7, pages 207-217.
- [3] **Huang, X.**, Jokat, W., Gohl, K. (2014) Bottom current-controlled sedimentary archives in the southeast Weddell Sea/ Van Rooij, D. and Rueggeberg, A. (editors), In: *Book of Abstracts. 2nd Deep-Water Circulation Congress: The Contourite Log-book*. Ghent, Belgium, 10-12 September 2014, (VLIZ Special Publication ; 69), Oostende, Belgium, Flanders Marine Institute (VLIZ), 152 p., ISBN: 1377-0950.
- [4] **Huang, X.**, Jokat, W., (2014), Middle Miocene to present sediment transport and deposits in the southeast Weddell Sea, Antarctica, submitted to *Global and Planetary Change*, revision version under review.
- [5] **Huang, X.**, Starz, M., Gohl, K., Lohmann, G., Weddell Sea circulation and its paleoclimatic consequences in the Middle Miocene: evidences from modeled results and seismic records, submitted to *Geophysical Research Letter*, under review.
- [6] **Huang, X.**, Jokat, W., Sedimentation and potential venting on the rifted continental margin of Dronning Maud Land (in prep.)
- [7] **Michael E Weber**, Gerhard Kuhn, Peter U. Clark, Trevor Williams, James E.T. Channell, James Smith, Wilfried Jokat, Xiaoxia Huang, Simon Belt, Jerry X. Mitrovica (Pre-848, 2014), Late Neogene ice-sheet and sea-level history of the Weddell Sea, Antarctica.

Conferences Contributions as First Author

- [1] **Huang, X.**, and Gohl, K. (2013), Seismostratigraphic analysis and paleobathymetry mapping of the Weddell Sea region, Antarctica, for paleocurrent and paleoclimate simulations, European Geoscience Union (EGU) General Assembly, Vienna, 8 April 2013 - 12 April 2013.
- [2] **Huang, X.**, and Gohl, K., Expanded and integrated seismostratigraphic analysis of the Weddell Sea region, Antarctica, Workshop on The Scotia Arc - Geodynamic Evolution and Global Implications, Granada, Spain, 14 May 2013 - 16 May 2013.
- [3] **Huang, X.**, (2013) Cenozoic sedimentation, paleo-water depths, seismic interpretation of the Weddell Sea, Antarctica. Elite PhD course on Tectonics, University of Copenhagen, 11-15 Nov. 2013.
- [4] **Huang, X.**, Jokat, W., and Gohl, K., Sedimentation pattern of the southeastern Weddell Sea, EGU conference, Vienna, 28 April 2014 - 2 May 2014.
- [5] **Huang, X.**, Jokat, W., and Gohl, K., (2014), Bottom current-controlled sedimentary archives in the southeast Weddell Sea. 2nd Deep-Water Circulation Congress: 'The Contourite Log-Book', Ghent, Belgium, 10 Sep. 2014 - 12 Sep. 2014.
- [6] **Huang, X.**, Jokat, W., Stürz, M., Gohl, K., Lohmann, G., Seismostratigraphy, paleobathymetry, and simulated Middle Miocene ocean circulation in the Weddell Sea, San Francisco, 15-19 December, 2014.
- [7] **Huang, X.**, Jokat, W., Glacial erosion, transport, and deposition on the rifted continental margin of Dronning Maud Land, EGU conference, Vienna, 12-17 April 2015.